Investigation of systemic inflammation in aneurysmal subarachnoid hemorrhage (aSAH) and its impact on post-aSAH complications

Dissertation

zur

Erlangung des Doktorgrades (Dr. rer. nat.)

der

Mathematisch-Naturwissenschaftlichen Fakultät

der

Rheinischen Friedrich-Wilhelms-Universität Bonn

vorgelegt von

Shafqat Rasul Chaudhry

aus

Mianwali, Pakistan

Bonn, 2018

Angefertigt mit Genehmigung der Mathematisch-Naturwissenschaftlichen Fakultät der Rheinischen Friedrich-Wilhelms-Universität Bonn

1. Gutachter: Prof. Dr. Dirk Dietrich

2. Gutachter: Prof. Dr. Alf Lamprecht

Tag der Promotion: 23.04.2018

Erscheinungsjahr: 2018

List of Contents

Abbreviations

aSAH	Aneurysmal Subarachnoid Hemorrhage
SAH	Subarachnoid Hemorrhage
CVS	Cerebral Vasospasm
DIND	Delayed Ischemic Neurological Deficits
CI	Cerebral Ischemia
Intervent-ional CI	Intervention related Cerebral Ischemia
DCI	Delayed Cerebral Ischemia
PRRs	Pattern Recognition Receptors
PAMPs	Pathogen Associated Molecular Pattern
DAMPs	Damage Associated Molecular Pattern
DCs	Dendritic cells
NK cells	Natural Killer Cells
T cells	T lymphocytes
Th cells	$CD4^+$ Helper T Lymphocytes
Th 1	$CD4^+$ Helper T Lymphocytes subtype 1
Th 2	$CD4^+$ Helper T Lymphocytes subtype 2
Th 17	$CD4^+$ Helper T Lymphocytes subtype secreting IL-17
Tregs	CD4+ Regulatory T Lymphocytes
CD	Cluster of differentiation
T-bet	T-box transcription factor
GATA3	G-A-T-A nucleotide sequence binding transcription factor
ROR-γt	Retinoic acid receptor related orphan nuclear receptor γt
IL	Interleukin
IL-1α	Interleukin 1α
IL-1β	Interleukin 1β
TNF-α	Tumor Necrosis Factor α
IFN-γ	Interferon gamma
IL-6	Interleukin 6
IL-17	Interleukin 17
IL-23	Interleukin 23

IL-33	Interleukin 33
ST2	Suppressor of Tumorogenicity receptor 2
HMGB1	High Mobility Group Box 1
B cells	B Lymphocytes
NFκB	Nuclear factor κ-light chain enhancer of activated B cells
MAPK	Mitogen Activated Protein Kinase
C/EBP	CCAAT/ enhancer-binding proteins
RANTES	Regulated upon activation, normal T cell expressed and secreted
STAT	Signal Transducer and Activator of Transcription
JNK	c-jun N-terminal kinase
MyD88	Myeloid differentiation primary response protein 88
NLRs	NOD like receptors
mtDNA	Mitochondrial DNA
CytB	Mitochondrial Cytochrome B
COX-1	Mitochondrial cytochrome c oxidase subunit-1
GPCRs	G-protein coupled receptors
ADAM17	A disintegrin and metalloproteinase 17
SNPs	Single Nucleotide Polymorphisms
GWAS	Genome Wide Association Studies
MS	Multiple Sclerosis
mins	Minutes
secs	Seconds
ANS	Autonomic Nervous System

Dedication

“Dedicated to my beloved parents and my respected teachers”

Acknowledgements

First of all, I would like to express my heartiest gratitude to Prof. Dr. Dirk Dietrich for allowing me to pursue my PhD study under his supervision and his continuous support. I am immensely impressed by his foresightedness, critical realization of the matters and his discipline. I am also grateful to Prof. Alf Lamprecht for being my co-supervisor and providing me the opportunity to regularly present and discus my progress reports in his group. I am very grateful to him for his nice and constructive comments which led to significant improvements in my progress reports and publications. I am also highly indebted to Prof. Dr. Karl G. Wagner and Prof. Dr. Andreas Schieber for their willingness to review my thesis and being the part of examination committee.

I am also thankful to PD Dr. Sajjad Muhammad for giving me the opportunity to work on this clinical project and his continuous support, guidance and encouragement during the project. My sincere thanks are extended to Dr. Elmar Endl and Mr. Andreas Dolf for their excellent support and mentorship for flow cytometry experiments at FACS Core facility, Bonn. Additionally, I would also like to thank Mr. Peter Wurst at FACS Core facility. I am also highly indebted to PD Dr. Stilla Frede, department of Anesthesiology and PD Dr. Gerald Seifert, IZN for their kind support in serum mitochondrial DNA quantification. I would also like to thank Mr. Frank Splettstoesser for his technical support during mitochondrial DNA standard curves generation. I am also thankful to Prof. Dr. Stoffel Wagner and Anke Carstensen for their collaboration and support for IL-6 measurements at the department of Clinical Chemistry and Clinical Pharmacology. I am also thankful to PD Dr. Thomas Kinfe for providing me the opportunity to investigate the cytokine response in neuromodulation studies. Finally, I would like to thank director Prof. Dr. Hartmut Vatter, for his kind support and allowing me to work in his institute. Indeed, I would also like to acknowledge the funding sources ‘Stiftung Neurochirurgische Forschung’ and ‘BONFOR Programm Instrument V’ to Prof. Dr. Dirk Dietrich and PD. Dr. Sajjad Muhammad for the project and a kind support from HEC-DAAD scholarship programe.

Additionally, I would like to thank the technical staff namely Ralph Mahlberg, Pia Stausberg and Julia Kaspari. I am also thankful to my lab colleagues for their excellent support namely Sabrina, Pia, Vicky, Oliver, Dilshad, Natascha, Monika, Sara, Isabelle and Hyunte. My deepest gratitude to my beloved parents who have despite of all their chronic ailments and sufferings supported and encouraged me to pursue my education and allowed me to study

abroad. The support of my sisters to compensate for my absence and look after my parents also requires a special mention. Finally, I would also like to thank Associate Prof. Dr. Qaiser Jabeen Khan who has been excellent mentor during my master research and all my respected teachers throughout my education career.

1. Introduction

1.1. Stroke

It is estimated that around 15 million people become victim of this deadly disease every year all around the world, with one third destined to death and another one third left with lifelong disabilities (Corbyn, 2014). Strokes can be broadly classified as ischemic stroke and hemorrhagic stroke. Approximately 80% of the strokes are ischemic and are characterized by blockage of the cerebral blood vessels supplying brain, while remaining 20% are hemorrhagic, involving rupture of the blood vessels, with two major subcategories, i.e., intracerebral hemorrhage and subarachnoid hemorrhage (Murray et al., 2015).

1.2. Subarachnoid hemorrhage

Subarachnoid hemorrhage is a specific subtype of hemorrhagic stroke that is characterized by extravasation of the blood from a ruptured aneurysm into the subarachnoid space and also sometimes involves ventricles and deeper brain parenchyma (Suarez et al., 2006; Macdonald, 2014). Although it accounts for only 5% of all the stroke events, but the mortality inflicted by it is around 50% (32% to 67%) and affects at relatively younger age compared to ischemic stroke with 27.3% of stroke related years of productive life lost (van Gijn et al., 2007; Macdonald, 2014; Fanizzi et al., 2017; Grasso et al., 2017). The incidence is estimated around 10.5 per 100,000 persons per year, but varies geographically with higher incidence in Japan (22.7) and Finland (19.7) (de Rooij et al., 2007; Grasso et al., 2017). In approximately 85% of the cases, rupture of the intracranial aneurysm is the underlying cause of subarachnoid hemorrhage (Macdonald and Schweizer, 2017), while the remaining cases with relatively good clinical outcome belong to non-aneurysmal SAH. The fatality of the disease is reflected by 20% deaths occurring before any medical attention, 30% within 24 hours of onset and 40% - 60% within a month after subarachnoid hemorrhage (Korja and Kaprio, 2016; Grasso et al., 2017). Among the survivors, one third remains lifelong dependent and those with good recovery still have neurological and/or cognitive deficits (Suarez et al., 2006; van Dijk et al., 2016).

1.3. Intracranial aneurysms and risk factors

Aneurysms are the weak bulging lesions or abnormal dilatations present in almost 3.2% of our population. Aneurysms are formed due to the hemodynamic shear stress in the arterial wall at the bifurcation of arteries and are marked by chronic inflammation and degeneration

in the arterial wall (Etminan and Rinkel, 2016; Aoki et al., 2017). Majority of the aneurysms have a saccular or berry morphology (90%) and fusiform aneurysms occurring in posterior circulation account for only 10% (Drake and Peerless, 1997). The risk factors for the aneurysm development are hypertension, smoking, chronic alcohol consumption, aging, female gender, and family history of aneurysmal subarachnoid hemorrhage (aSAH) in first degree relatives (D'Souza, 2015). A few genetic disorders such as autosomal dominant polycystic kidney disease, Marfan syndrome, Ehlers-Danlos syndrome type IV, neurofibromatosis type 1, and fibromuscular dysplasia have been found to be associated with intracranial aneurysms formation (D'Souza, 2015) . Single nucleotide gene polymorphisms (SNPs) in or near the genes *CDKN2B-AS1*, *SOX17* transcription regulator gene, endothelin receptor gene, *HDAC9* and the gene encoding elastin have been revealed in genome wide association studies (GWAS) and linkage analysis to be strongly associated with intracranial aneurysms (Etminan and Rinkel, 2016). An exome wide association study has identified SNP of collagen type XVIIα1 chain gene to be significantly associated with aneurysmal subarachnoid hemorrhage (aSAH) (Yamada et al., 2017).

1.4. Aneurysm treatment and post-aSAH complications

The obliteration of the bleeding aneurysm from the arterial circulation is achieved by neurosurgical clipping and endovascular coiling in majority of the cases (Cahill and Zhang, 2009), but still outcome of the patients is not improved. This is mainly due to the post-aSAH complications occurring mainly over the first two weeks after initial bleed (Macdonald and Schweizer, 2017). The brain injury following aSAH occurs in two phases. An early brain injury occurring within initial 72 hours of the insult results from transient global cerebral ischemia and toxic effects of the extravasated blood (Cahill et al., 2006; Cahill and Zhang, 2009; Macdonald and Schweizer, 2017). This may be followed by a secondary delayed phase of brain damage over a period of 3 – 14 days and is the time frame where post-aSAH complications can develop and cause neurological deterioration (Macdonald and Schweizer, 2017). The major post-aSAH complications include rebleeding, cerebral vasospasm (CVS), hydrocephalus, seizures, delayed ischemic neurological deficits (DIND), cortical spreading depression, delayed cerebral ischemia (DCI), infections, cardiomyopathy and pulmonary edema (Suarez et al., 2006). The research in the past was maligned by a sole focus on cerebral vasospasm and strategies aimed at its reversal were developed. The failure of the endothelin antagonists to improve the outcome despite reversing the cerebral vasospasm has

recognized that clinical outcome after aSAH is determined by multiple factors. These conflicting results led to change the direction of aSAH research to early brain injury with profound stress laid on the role of inflammation that plays crucial and central role in the development of post aSAH complications (Macdonald, 2014; Savarraj et al., 2017a; Savarraj et al., 2017b).

1.5. Inflammation and subarachnoid hemorrhage

Acute inflammation is the sentinel host defense response for protection against infection or injury and has been historically defined by the cardinal features such as redness (rubor), swelling (tumor), pain (dolor), heat (calor) and loss of function (functio laesa) (Galea and Brough, 2013; Murray et al., 2015; Basil and Levy, 2016). However, prolonged and dysregulated inflammation could be devastating and even detrimental following CNS insult (Murray et al., 2015). Inflammation occurring in the absence of pathogens (as in case of aSAH) is usually ascribed as sterile inflammation, however, involves similar cascades of mechanisms mounted against pathogens (Chen and Nuñez, 2010). This is owing to the pattern recognition receptors (PRRs) which respond to the evolutionarily conserved danger molecular motifs, which may either be exogenous 'pathogen associated molecular patterns (PAMPs)' derived from pathogens or endogenous 'damage associated molecular patterns (DAMPs)' molecules derived from injured, stressed and necrotic cells (Matzinger, 1994; Chen and Nuñez, 2010; Takeuchi and Akira, 2010). Immediately after acute brain injury, local and systemic inflammatory response leads to trigger inflammatory signaling cascades accompanied by the activation and infiltration of immune cells at the site of injury (Murray et al., 2015). A great body of evidence supports the critical role of inflammation in the aSAH (Provencio, 2013; Lucke-Wold et al., 2016; Savarraj et al., 2017a; Savarraj et al., 2017b). Moreover, evidence support that early inflammation after aSAH leads to poor outcomes (Provencio, 2013). Release of DAMPS might be critical to initiate and sustain the inflammation.

1.6. Damage associated molecular patterns (DAMPs) and aSAH

Any type of injury either ischemic or traumatic can potentially release damage associated molecular patterns from injured or stressed cells leading to inflammation without presence of any pathogens. During sterile inflammation DAMPs bind to the PRRs on immune cells, lead to activation of subcellular signaling pathways including NFκB and finally, upregulate the

expression of multiple genes including the transcription and release of pro-inflammatory mediators (Chen and Nuñez, 2010; Takeuchi and Akira, 2010; O'Neill et al., 2013). Over the past years, an ever expanding list of DAMPs along with their cognate receptors has been identified including HMGB1, HSPs (Heat Shock Proteins), S100 proteins, SAP130, ATP, mitochondrial DNA, formyl peptides, heparan sulphate, β-amyloid, biglycan, versican, IL-1α, IL-33, cholesterol and uric acid crystals (Chen and Nuñez, 2010). There is sufficient evidence that support the involvement of DAMPs in the pathophysiology of SAH.

1.6.1. High mobility group box 1 (HMGB1) and aSAH

HMGB1 (High mobility group box 1) is a well characterized prototypical protein DAMP. HMGB1 is expressed in all eukaryotic cells as a non-histone DNA binding nuclear transcription factor, but signifies danger upon its extracellular release from necrotic cells (Bianchi and Manfredi, 2009). Extracellularly released HMGB1 is then recognized by TLR-2, TLR-4, TLR-9 and receptor for advanced glycation end products (RAGE) (Bianchi and Manfredi, 2009). Evidence on the role of HMGB1 after aSAH is increasing continuously in the recent years. Release of HMGB1 in cerebrospinal fluid of patients after aSAH was found by Nakahara et al. (2009). Interestingly, the elevated HMGB1 levels were higher in the CSF of patients with a poor clinical outcome after aSAH and HMGB1 levels correlated with TNF-α, IL-6 and IL-8, suggesting an indispensable role of HMGB1 in ongoing inflammation (Nakahara et al., 2009). King and colleagues also found significant associations of CSF HMGB1 levels with poor Hunt and Hess (H&H) grades and the disability and dependence among aSAH patients (King et al., 2010). A subsequent study employing a rabbit model of SAH has shown that HMGB1 was upregulated and translocated in the cytosol of the microglia for active secretion (Murakami et al., 2011). Zhu et al. (2012a) evaluated HMGB1 levels in systemic circulation and demonstrated an association with CVS, poor functional outcomes and mortality after one year of aSAH, highlighting the prognostic value of on admission plasma HMGB1 determination.

Sun et al. (2014b) found as early as 2 h post SAH release of HMGB1 from the neurons and intraventricular injection of recombinant HMGB1 upregulated the inflammation as assessed by upregulation of TLR-4, NF-κB, IL-1β and cleaved Caspase-3. Furthermore, in-vitro application of hemoglobin (Hb) led to the upregulation and translocation of HMGB1 from nucleus to cytoplasm in neuronal cultures. Interestingly, application of Glycyrrhizic acid, a

natural inhibitor of HMGB1, downregulated IL-1β and thus, prevented activation of glial cells upon conditioned medium application from Hb primed neurons (Sun et al., 2014b). Thereafter, two other natural compounds, Purpurogallin, a natural phenol and 4′-O-β-d-glucosyl-5-O-methylvisamminol were demonstrated to attenuate HMGB1 expression in double hemorrhagic SAH rat model and intriguingly, were also effective in decreasing the cerebral vasospasm and its associated changes in basilar arteries (Chang et al., 2014; Chang et al., 2015a). A similar study employing Rhinacanthin-C, an extract from *Rhinacanthus nasutus*, ameliorated SAH associated increase in HMGB1 mRNA and protein as well as pro-inflammatory cytokines and cleavage of Caspase-3 and Caspase 9 (Chang et al., 2016).

Another clinical study described elevated CSF HMGB1 levels in acute hydrocephalus after aSAH and strong correlations with H&H score, WFNS (World Federation of Neurological Surgeons) score, GCS (Glasgow Coma Scale), days on intensive care unit and poor outcome after 3 months (Sokol et al., 2015). Wang and colleagues confirmed the association of CSF HMGB1 levels and poor outcome after 3 months in a relatively larger cohort of aSAH patients. Further, they revealed in SAH rat model that both HMGB1 and its receptor RAGE are upregulated and application of post-SAH CSF either from patients or rats induced RAGE expression and reduced viability of neuronal cultures. Interestingly, administration of recombinant soluble form of RAGE to interfere with RAGE and HMGB1 signaling reduced the neuronal cell death both in-vitro and in-vivo (Wang et al., 2016). The first evidence that HMGB1 may be involved in the inflammatory response leading to CVS, the most feared complication after aSAH, came from the observations of Zhao and colleagues. They observed increased expression of HMGB1 in the vasospastic rat basilar arteries at day 3, 5 and 7 after SAH (Zhao et al., 2016). Li et al. (2017) have shown increased basilar artery thickness and reduced luminal diameter with increased expression of HMGB1 protein and mRNA of pro-inflammatory cytokines, and all these changes were ameliorated after glycyrrhizic acid supplementation for 3 days (Li et al., 2017). Finally, administration of anti-HMGB1 antibody prevented basilar artery vasospasm, decreased extracellular translocation and expression of HMGB1 in smooth muscle cells, decreased the expression of contractile and inflammation associated molecules, decreased plasma HMGB1 levels, improved the morphology and decreased the number of cerebral cortex microglia, and lastly recovery from the neurological deficits (Haruma et al., 2016).

Delayed cerebral ischemia (DCI) is seen in approximately 30% of the aSAH patients (Francoeur and Mayer, 2016). A case series of three aSAH patients with DCI has shown significant elevation of HMGB1 compared to controls, but did not show significant changes in both CSF and plasma HMGB1 levels as compared to baseline. Interestingly, there was a trend towards increase in plasma and decrease in CSF HMGB1 levels (Bell et al., 2017). Another study defined DCI as cerebral infarction and interestingly, found the presence of minor allele G of rs2249825 as an independent predictor of DCI. This single nucleotide polymorphism (SNP) of HMGB1 (C/G at 3814) may lead to enhanced HMGB1 expression and consequently result in DCI (Hendrix et al., 2017). The above discussed evidence suggests that HMGB1 not only plays a distinct role during early brain injury, but also in post aSAH sequelae with prominent involvement in CVS, DCI and thereby, impact the clinical outcome.

1.6.2. IL-1α and IL-33

IL-1α and IL-33 are both members of the IL-1 family of cytokines and are synthesized as pro-forms requiring cleavage of around 100 amino acid residues at the N-terminal to give mature forms (Kim et al., 2013). IL-1α and IL-33 share a unique feature that they have a dual role as intracellular transcriptional regulators and as extracellular potent regulators of inflammation (Hirsiger et al., 2012). Interestingly, both pro- and mature forms of IL-1α are active in inducing inflammation, whereas pro-IL-33 not and probably requires processing by serine proteases extracellularly into mature form (Kim et al., 2013). IL-1α, signaling via IL-1R, is constitutively expressed in endothelial cells, keratinocytes and fibroblasts, but in monocytes/macrophages its synthesis occurs de novo (Hirsiger et al., 2012). IL-1α binds not only to cellular receptors, but also functions as a transcription factor in the presence of pro-inflammatory stimuli such as LPS or TNF and promotes production of NF-κB (p65), IL-6 and IL-8 (Buryskova et al., 2004; Werman et al., 2004). Moreover, IL-1α can mediate recruitment of neutrophils via increased secretion of CXCL-1 by mesenchymal cells (Eigenbrod et al., 2008).

As discussed above, in a rat filament model of SAH, IL-1α was expressed mainly in microglia/macrophages after 12 hours with higher expression in basal structures adjacent to hemorrhage site in addition to cortex, striatum and hippocampus and co-localize with HO-1 in activated microglia (Greenhalgh et al., 2012). Moreover, application of heme upregulated the secretion of active form of IL-1α from organotypic slice cultures and mixed glial cell

cultures and the administration of IL-1R antagonist reduced BBB breakdown and brain damage (Greenhalgh et al., 2012). Interestingly, IL-1α gene expression was highest at day 7 and correlated with decreased vessel caliber in canine vasospastic basilar arteries isolated at different days after intracisternal blood injections (Aihara et al., 2001). Inhibition of p38-MAPK signaling reduced IL-1α gene and protein expression in human VSMCs in vitro and downregulated IL-1α mRNA expression in canine basilar arteries showing reversal of vasospasm (Sasaki et al., 2004). Bowman et al. (2004) showed increased IL-1α levels in rat femoral arteries displaying vasospasm.

IL-33 is known to have anti-inflammatory activity via promoting Th2 type response. IL-33 can stimulate cells of innate and adaptive immunity via binding to ST2 membrane receptors (Chackerian et al., 2007). ST2 receptor is a member of TLR/IL-1R superfamily and its heteromer with IL-1R accessory protein (IL-1RAcP) is responsible for IL-33 signaling, while soluble ST2 (sST2) act as a decoy receptor (Jiang et al., 2012a). Interestingly, monocytes/ macrophages are polarized towards alternate type (M2) phenotype in the presence of IL-33 (Kurowska-Stolarska et al., 2009). However, IL-33 has been assigned to play an inflammatory role in CNS reflecting its pleiotropic nature (Hudson et al., 2008; Jiang et al., 2012a). Huang et al. (2014) have observed an increased expression of IL-33 mRNA and protein in the cerebral cortex of the rats after experimental SAH. Intriguingly, IL-33 expression co-localized with neuronal and astrocytic markers and mRNA expression of IL-33 correlated with that of IL-1β after SAH (Huang et al., 2014). So, IL-1α and IL-33 represent important DAMPs implicated in neuroinflammation after experimental SAH and therefore, needs further investigations.

1.6.3. Mitochondrial DAMPs

In recent years, mitochondria have been recognized as a host of different DAMPs including TFAM (mitochondrial transcription factor A), N-formyl peptides, cardiolipin and hypomethylated/non-methylated mitochondrial DNA which are released upon cell stress, injury and necrosis (Galluzzi et al., 2012). Mitochondrial DNA (mtDNA) has been identified a long time ago to induce TNF secretion from splenocytes and arthritis in mice joints (Collins et al., 2004). Zhang et al. (2010) have shown that circulating mtDNA, acting via TLR-9, elicits MAPK-signaling based migration and degranulation of neutrophils leading to organ injury. There are now evidences that mtDNA can upregulate innate immune responses

through several PRRs, most importantly TLR-9, NLRP3-, NLRC4-, AIM2-inflammasome complex and cGAS-STING (West and Shadel, 2017). Several studies have shown elevated circulating cell free mtDNA and its biomarker and prognostic potential in connection to diseases involving CNS pathology (Lu et al., 2010; Mathew et al., 2012; Podlesniy et al., 2013; Sondheimer et al., 2014; Perez-Santiago et al., 2016; Podlesniy et al., 2016b; Podlesniy et al., 2016a; Varhaug et al., 2016). Wang and colleagues have evaluated plasma and CSF mtDNA levels from 21 aSAH patients and found significant elevation of mtDNA in the CSF on admission, which was associated with poor clinical outcome. However, plasma mtDNA levels showed a delayed elevation at day 8 in poor clinical outcome patients (Wang et al., 2013).

1.6.4. Hemoglobin and its derivatives

The extravasated blood and its degradation products acutely trigger neuroinflammation in addition to global ischemic insult in aSAH (Macdonald, 2014; Miller et al., 2014). Erythrocyte hemolysate degradation yields methemoglobin, heme, hemin and oxyhemoglobin, which are described as TLR-4 ligands and as DAMPs (Piazza et al., 2011; Gladwin and Ofori-Acquah, 2014; David B. Kurland, 2015; Kwon et al., 2015). Methemoglobin leads to increased TNF-α secretion through its interaction with not only TLR-4 homodimers, but also TLR-2/TLR-4 heterodimers (Kwon et al., 2015). Heme promotes increased formation of Neutrophil Extracellular Traps (NETs) from neutrophils and heme activated TLR-4 only upregulates MyD88 dependent substream pathway leading to NFκB and MAPK activation with resultant TNF-α secretion (Gladwin and Ofori-Acquah, 2014). Hemin (iron (III)-protoporphyrin IX) acts additively to endotoxin with a mechanism of TLR-4 activation distinct from endotoxin (Piazza et al., 2011). Oxyhemoglobin, which might spontaneously oxidize to methemoglobin, leads to increased TNF-α secretion from vascular smooth muscle cells (VSMCs) via increased TLR-4 expression and activation (Wu et al., 2010; David B. Kurland, 2015).

It is well established that the degree of bleeding on initial CT scan correlates with poor clinical outcome (Suarez et al., 2006). Hemoglobin and its derivatives released after erythrocyte hemolysis can induce contraction of cerebral arteries both *in-vitro* and *in-vivo* (Macdonald and Weir, 1991). Induction of basilar artery vasospasm by application of either LPS (TLR-4 ligand) or blood in the subarachnoid space indicated a common shared pathway

upregulating inflammation after SAH (Recinos et al., 2006). Furthermore, intra-subarachnoid administration of methemoglobin activates microglia with enhanced TNF-α and TLR-4 upregulation (Kwon et al., 2015). Heme has demonstrated cytotoxic effects on macrophages, microglia, astrocytes and brain endothelial cells (Dutra and Bozza, 2014). It has also been shown that heme has the potential to induce IL-1β secretion via NLRP3 inflammasome in macrophages (Dutra et al., 2014). However, in a rat filament model of SAH, it was shown that heme upregulated the expression of HO-1 around the hemorrhage site and IL-1α, which was confirmed *in-vitro* by application of heme to organotypic slice cultures preferentially releasing IL-1α over IL-1β (Greenhalgh et al., 2012). So, hemoglobin and its degradation products play a role of DAMPs and strategies aimed at their early removal or neutralization may help to reduce the pathophysiological events triggered by subarachnoid blood hemolysis to prevent complications and improve clinical outcome.

1.6.5. S100B

S100B is the founding member of calgranulins, a family of small intracellular calcium binding proteins and is majorly expressed in astrocytes, with limited expression in neurons (Bianchi, 2007; Sorci et al., 2010). Passively released S100B by necrotic and damaged cells, has diagnostic and prognostic value in different CNS pathologies (Sen and Belli, 2007). At higher micromolar concentrations, extracellular S100B behaves as DAMP with neurotoxic effects mediated by RAGE and is involved in many neurodegenerative and inflammatory brain diseases (Bianchi et al., 2011). It can induce neuronal death, pro-inflammatory cytokines (IL-1β) and stress related inflammatory enzymes such as inducible nitric oxide synthase (iNOS) (Huang et al., 2010).

S100B measured on admission or on various days post aSAH at both CNS and systemic levels has been shown to significantly rise after aSAH and found to be associated with severity of aSAH (H&H, WFNS grades), hematoma on CT (Fischer grades), neurosurgical clipping, CVS, intracranial hypertension, hydrocephalus and VP-shunt placement, cerebral infarcts, size of ischemic lesions, short-term survival and mortality, neuropsychological evaluation tests, and functional outcome assessed at various intervals after aSAH (Masakazu Takayasu et al., 1985; Persson et al., 1987; Hardemark et al., 1989; Wiesmann et al., 1997; Petzold et al., 2003; Weiss et al., 2006; Pereira et al., 2007; Stranjalis et al., 2007; Sanchez-Pena et al., 2008; Moritz et al., 2010; Brandner et al., 2012; Jung et al., 2013; de Azua Lopez et al., 2015; Kellermann et al., 2016; Lai and Du, 2016).

S100B release in the periphery has been found to be independent of BBB dysfunction and higher S100B serum/CSF ratio associated with better neurological function highlight a repair role for active stimulated release of S100B (Kleindienst et al., 2010). Lower serum levels of S100B observed after administration of magnesium sulphate and atorvastatin signifies its potential to monitor the therapeutic efficacy in aSAH patients (Hassan et al., 2012; Sanchez-Pena et al., 2012). These lines of evidence clearly highlight the DAMP role of S100B in aSAH pathophysiology.

1.6.6. Other DAMPs

Components of the extracellular matrix (ECM), released upon proteolysis following tissue injury in soluble form can act as DAMPs (Schaefer, 2014). These normally ECM sequestered components such as biglycan, decorin, versican, tenascin-C, hyaluronan, and heparan sulfate are recently recognized as rapid activators of innate immune response by interacting with PRRs after their release (Moreth et al., 2012; Schaefer, 2014). Among these several of ECM released DAMPs have been investigated in preclinical and clinical investigations both at CNS and systemic levels after SAH and include hyaluronic acid, syndecan-1 (SDC-1, a heparan sulfate proteoglycan), sCD44 (hyaluronan receptor), Tenascin-C, Periostin, Fibronectin and Galectin-3 (Heula et al., 2015).

Heat shock proteins (HSP) are highly conserved chaperones aiding in protein folding and represent another potential subgroup of DAMPs which can activate PRRs such as TLR-2 and TLR-4 leading to MyD88 dependent upregulation of NFκB (Kang et al., 2015). Numerous heat shock proteins such as HSP10, HSP20, HSP27, HSP32 (HO-1), HSP47, HSP60, HSP70, HSP72, and HSP90α have been shown to be implicated in SAH pathophysiology (Satoh et al., 2003; Matz et al., 1996b; Matz et al., 1996a; Turner et al., 1999; Macomson et al., 2002; Nikaido et al., 2004). Table 1 below represents some important DAMPs with their receptors.

1.6.7. Significance of DAMPs investigation

All the evidences described above suggest the involvement and importance of DAMPs in the context of aSAH pathophysiology. Since, DAMPs are the initiators of inflammation and therefore, their early blockage or sequestration may be helpful to reduce the ongoing inflammation and reduce the severity of the disease with protection against ensuing complications and poor outcomes. HMGB1 represent an excellent example, where pre-

clinical approaches to neutralize HMGB1 by administering anti-HMGB1 monoclonal antibody or other molecules (ethyl pyruvate, glycyrrhizic acid, ghrelin, purpurogallin, siRNA) that inhibit the release of HMGB1 have been shown to be beneficial (Sun et al., 2014b). Recombinant soluble form of RAGE to interfere with RAGE and HMGB1 signaling has been shown to be neuroprotective in experimental SAH (Wang et al., 2016). RAGE is implicated in the signaling of multiple DAMPs and represents a potential therapeutic target. Similarly, sST-2 administration to abrogate IL-33 signaling in SAH needs to be investigated (Boyapati et al., 2016). Since TLRs are implicated in the signaling of numerous DAMPs, therefore, they represent important modulatable targets to culminate DAMP signaling during brain injury (Downes and Crack, 2010). Furthermore, the other DAMP receptors and the downstream signaling pathways represent potential modulatable targets.

Finally, investigation of the time course of various DAMPs may have a diagnostic and prognostic potential and will be helpful for early identification of the patients at increased risk of developing different complications and achieving poor clinical outcome. Therefore, it will aid in addressing early and aggressive treatment and management in these patients. Further, DAMPs may be used as treatment response markers. Systemic S100B and HMGB1 represent interesting DAMP molecules that have been investigated in aSAH associated complications and may serve as potential biomarkers. Our knowledge, regarding DAMPs and their implication in complex pathophysiological events triggered after brain injury is still in infancy and further investigations aimed at combined multifaceted role of DAMPs in brain injury after aSAH are required.

Table 1. List of some important DAMPs members and their receptors (Boyapati et al., 2016)

Sr. #	DAMPs	Receptors
1.	HMGB1	TLR-2, TLR-4, TLR-9, RAGE
2.	IL-1α	IL-1R
3.	IL-33	ST2 (IL-1RL1)
4.	Heme, Hemin, Oxyhemoglobin, methemoglobin	TLR-4
5.	mtDNA	TLR-9, NLRP3, NLRC4, AIM-2, cGAS-STING
6.	TFAM	RAGE, TLR-9
7.	N-formyl peptides	FPR1, FPRL1
8.	S-100 proteins	TLR-4, RAGE

9.	Fibrinogen	TLR-4
10.	Fibronectin	TLR-2, TLR-4
11.	Hyaluronan	TLR-2, TLR-4
12.	Biglycan	TLR-2, TLR-4, P2X4, P2X7, NLRP3
13.	Versican	TLR-2, TLR-6, CD14
14.	Heparan sulfate	TLR-4
15.	Tenascin C	TLR-4
16.	Galectin-3	TLR-2, TLR-4

1.7. Cytokine response and aSAH

Interactions between the nervous system and immune system are becoming increasingly an important concern to be further explored in recent years and have been known to take place not only during homeostasis, rather during acute or chronic inflammation as well (Veiga-Fernandes and Mucida, 2016). Apart from cell to cell contacts, soluble mediators such as cytokines and chemokines represent an important mode of communication at proximal and distal sites (Ordovas-Montanes et al., 2015). Circulating cytokines play an important role in determining the status of health in individuals and due to their involvement in immuno-inflammatory responses after injury, they are increasingly implicated in potential immuno-neuromodulatory effects in CNS diseases (Osuka et al., 1998; Oke and Tracey, 2009). As already mentioned above, the interest in the role of inflammation after aSAH has been fueled after the failure of endothelin antagonists to improve outcome despite successful reversal of vasospasm (Macdonald, 2014). Inflammation during early brain injury after aSAH is associated with secondary brain injury (Helbok et al., 2015). A great body of evidence supports the upregulation of different cytokines at both CNS and systemic levels (Kwon and Jeon, 2001; Takizawa et al., 2001; Niwa and Osuka, 2016; Chaudhry et al., 2017; Savarraj et al., 2017a; Savarraj et al., 2017b). Increased cytokines after aSAH mediate damage to the brain tissue and also upregulate the recruitment of inflammatory cells in a complex and vicious cycle (Macdonald, 2014). Pro-inflammatory cytokines have been known to contribute to early brain injury via increasing brain edema due to BBB disruption and inducing neuronal apoptosis (Ostrowski et al., 2006; Sozen et al., 2009). Systemic inflammatory response occurring in 75% of the cases after aSAH may have its roots in elevated levels of cytokines (Macdonald et al., 2014). The section below briefly reviews some important cytokines in the context of aSAH, post-aSAH complications and outcome.

1.7.1. IL-1β

IL-1β represents one of the leading cytokines that remained the subject of intensive investigation in the context of CNS diseases as it is considered as a master cytokine regulating inflammation locally and systemically (Allan et al., 2005; Dinarello et al., 2012; Murray et al., 2015). IL-1 was identified as potent endogenous pyrogen and is known to be comprised of IL-1α and IL-1β as products of different genes (Allan et al., 2005; Murray et al., 2015). Both are secreted as pro-forms, only IL-1α is active in pro-form, but pro-IL-1β is inactive and requires caspase-1 mediated activation to a 17 kDa mature form (Thornberry et al., 1992; Allan et al., 2005). IL-1β signals via engaging type-I IL-1 receptor (IL-1R1) and IL-1 receptor accessory protein (IL-1RAcP), while type-II IL-1R (IL-1R2) acts as a decoy receptor, devoid of any intracellular signaling domain (Sims et al., 1988; Korherr et al., 1997; Subramaniam et al., 2004; Boraschi and Tagliabue, 2013). All of these three receptors can be shed from the membrane and are also present as soluble forms (Subramaniam et al., 2004). A third ligand of IL-1 receptor acts as an antagonist (IL-1RA) and antagonizes the effects of IL-1 competitively at IL-1R1 (Allan et al., 2005; Murray et al., 2015).

Preclinical and clinical studies in the setting of ischemic stroke have shown elevation of IL-1β (Allan et al., 2005; Murray et al., 2015). Similarly, several preclinical studies have shown upregulation of IL-1β in the cerebral cortex, basilar arteries and in the peripheral circulation after SAH (Keiichi Iseda et al., 2007; Sozen et al., 2009; Kooijman et al., 2014b; Zhou et al., 2015; Chen et al., 2016; Wu et al., 2016b; You et al., 2016; Huang et al., 2017). IL-1β levels have been shown to increase at both CNS and systemic levels in aSAH patients (Hirashima et al., 1997; Kwon and Jeon, 2001; Muroi et al., 2008; Hopkins et al., 2012; Zhou et al., 2015). A significant upregulation of IL-1β was seen in CSF of aSAH patients with higher H&H grades and non-significant 3 folds higher levels were observed in patients developing DIND (Kwon and Jeon, 2001). However, IL-1β levels were found to be non-significantly very low in CSF of aSAH patients either with higher Fischer grades or poor clinical outcome (Kwon and Jeon, 2001). IL-1β levels were found to be higher in CSF of aSAH patients showing CVS and poor clinical outcomes and levels in plasma were low, suggesting an intrathecal origin (Fassbender et al., 2001). IL-1β is known to induce toxicity in cerebral endothelial cells in-vitro and preclinical studies also show an upregulation of IL-1β during CVS (Kimura et al., 2003; Keiichi Iseda et al., 2007). Moreover, LPS stimulation of monocytes showed increased IL-1β activation index in aSAH patients who later on developed CVS (Nam et al., 2001). In a

rat-SAH model, administration of intracerebroventricular anti-IL-1β antibody conferred protection against vasospasm (Jedrzejowska-Szypułka et al., 2009).

Interestingly, serum levels of soluble form of IL-1RA have been found to be upregulated after aSAH (Gruber et al., 2000). Elevation of IL-1RA in CSF has been shown to associate with DCI and poor clinical outcome (Mathiesen et al., 1997). Administration of sIL-1RA to interfere with IL-1 signaling has shown neuroprotective effects in SAH model (Greenhalgh et al., 2012). Administration of Anakinra, a recombinant form of IL-1RA has shown decreased levels of neutrophils, CRP and IL-6 with improvement of clinical scores during 6 hours of ischemic stroke. A similar phase II clinical study investigating twice a day subcutaneous administration of Anakinra for 21 days after aSAH found reduction of systemic inflammation reflected by reduced IL-6 levels and improved functional outcome at 6 months, though non-significant (Galea et al., 2017a). Due to better tolerance and desirable effects of IL-1RA, currently a phase III clinical study in aSAH is underway (Galea et al., 2017a).

1.7.2. TNF-α

TNF-α, also called cachectin, was identified to be a factor in blood capable of inducing hemorrhagic necrosis in tumors and a macrophage mediator linked to disease associated wasting and shock (Probert, 2015). TNF-α is synthesized as a 26 kDa transmembrane protein, which is cleaved by metaloprotease, TNF-α converting enzyme (TACE)/ADAM17 to liberate soluble trimeric TNF-α (17 kDa), which binds TNF receptor I (TNFR1 – also known as p55/p60 and a death domain containing protein) constitutively expressed at low levels or TNFR2 (p75/p80); initiating a complex substream signaling, also involving NFκB mediated expression of cytokines and chemokines (Sedger and McDermott, 2014; Probert, 2015). TNF-α is an acute phase reactant cytokine released by a variety of cells under inflammatory clues (Hong et al., 2014). Besides IL-6 and IL-1β, TNF-α is one of the principal cytokines secreted by microglia and astrocytes and has also been shown in preclinical SAH studies to be released by glial cells (McKeating and Andrews, 1998; van Dijk et al., 2016). TNF-α has been known to recruit inflammatory cells and mediate cellular injury (Mathiesen et al., 1997). In the CSF of aSAH patients, the $CD16^{+}$ monocytes may be a source of TNF-α (Moraes et al., 2015). This pro-inflammatory cytokine is linked with both homeostatic and pathophysiological roles and is one of the leading cytokines mediating neuroinflammation. The effects of TNF-α are not only restricted to immune cells, but can also mediate excitotoxicity by impairing astrocytic glutamate transport and upregulation of Ca^{2+}

permeability associated AMPA and NMDA receptors and downregulation of inhibitory $GABA_A$ receptors in neurons (Olmos et al., 2014).

TNF-α plays a critical role in intracranial aneurysm formation and their rupture which results in SAH (Jayaraman et al., 2005; Jayaraman et al., 2008; Starke et al., 2014).TNF-α has been demonstrated in a number of preclinical studies to be upregulated to play an inflammatory role and involved in disruption of blood brain barrier (BBB) after SAH (Chen et al., 2016; Haruma et al., 2016; Wu et al., 2016a). TNF-α release after aSAH in interstitial fluid has been determined by microdialysis (Hanafy et al., 2010b). Increased levels of TNF-α have been detected after aSAH, which were correlated with the severity of aSAH assessed by H&H grade (Schallner et al., 2015; Zhou et al., 2015; Wu et al., 2016a). Elevated levels of TNF-α in CSF have been shown to be associated with CVS (Fassbender et al., 2001; Wu et al., 2016a). Interstitial levels of TNF-α well correlated with angiographic vasospasm in poor grade aSAH patients (Hanafy et al., 2010a). TNF-α has been shown to mediate vasoconstrictive properties of hemolyzed blood and is responsible for causing CVS (Vecchione et al., 2009). Moreover, TNF-α has shown toxicity in cerebral endothelial cells through cleavage of caspase-3 and inducing apoptosis in them (Kimura et al., 2003). A non-significant two fold higher CSF levels of TNF-α were found in aSAH patients presenting with DIND (Kwon and Jeon, 2001). Interestingly, a study evaluating the effect of hypothermia and barbiturates on inflammatory cytokines has found elevated levels of TNF-α in combined therapy group compared to the other without combined therapy at both CSF and plasma level (Muroi et al., 2008). Mathiesen and co-authors (1997) have found a significant elevation of CSF TNF-α level during 4 – 10 days after aSAH in patients with poor clinical outcome (Mathiesen et al., 1997). Early systemic levels of TNF-α are associated with poor functional outcomes (Chou et al., 2012). In a rat SAH model, pretreatment with TNF-α blocking antibody significantly protected the hippocampus neuronal loss due to apoptosis (Jiang et al., 2012b). So, all these evidences suggest that TNF-α plays an important role in inflammation induced after aSAH.

1.7.3. IL-6

IL-6 is a pleiotropic cytokine with hormone like activity that can influence vascular and metabolic diseases (Bethin et al., 2000; Hodes et al., 2014; Kraakman et al., 2015). IL-6 signals via IL-6R (CD126, type 1 cytokine α-receptor subunit) and gp130 (CD130, β-receptor subunit) and involves downstream pathways such as GTPase Ras-Raf, MAPK and JAK-

STAT (Scheller et al., 2011; Hunter and Jones, 2015). Three modes of IL-6 signaling have been identified: classical involving membrane bound IL-6R and gp130; trans-signaling dependent on soluble IL-6R whereby only gp130 expressing cells can gain response to IL-6-sIL-6R complex; and recently identified cluster signaling in which dendritic cells harboring IL-6-IL-6R complex in their membranes engage gp130 on the target cell membranes (Scheller et al., 2011; Hunter and Jones, 2015; Quintana, 2017). Depending on the context of disease, IL-6 has both pro-inflammatory and anti-inflammatory effects (Hunter and Jones, 2015).

In acute pathological conditions including aSAH, IL-6 stimulates the neuro-inflammatory response that may contribute to the disease progression (Suzuki et al., 2009). Both TNF-α and IL-1β are elevated in CSF during early inflammatory cascade and induce IL-6 after aSAH (Mathiesen et al., 1997). Increased CSF levels of IL-6 correlate with the severity of aSAH (Gruber et al., 2000; Kwon and Jeon, 2001; Kiiski et al., 2017). IL-6 levels in cerebrospinal fluid (CSF) of patients after aSAH have been shown to be associated with occurrence of cerebral vasospasm and poor clinical outcome (Gaetani et al., 1998; Osuka et al., 1998; Gruber et al., 2000; Fassbender et al., 2001; Nam et al., 2001; Schoch et al., 2007; Sarrafzadeh et al., 2010; Helbok et al., 2015; Niwa and Osuka, 2016; Wu et al., 2016a; Zeiler et al., 2017). Increased expression of IL-6 mRNA was observed in canine vasospastic basilar arteries at day 7 (Aihara et al., 2001). Patients presenting with DIND post-aSAH display significantly higher IL-6 levels, both at CSF and systemic levels (Kwon and Jeon, 2001; Muroi et al., 2013). IL-6 measured in CSF has also been shown to predict infection and shunt-dependency due to chronic hydrocephalus after aSAH (Hopkins et al., 2012; Wostrack et al., 2014; Kiiski et al., 2017). Gruber et al. (2000) have shown a trend towards raised IL-6 in the CSF of aSAH patients who developed cerebral infarction. Serum IL-6 levels after aSAH were associated with the development of DCI, and DCI is a major factor leading to poor clinical outcomes (McMahon et al., 2013). Moreover, elevated early serum IL-6 levels predict the unfavourable clinical outcome (Muroi et al., 2013; Hollig et al., 2015b; Hollig et al., 2015a; Kao et al., 2015).

IL-6 represents also one of the extensively investigated cytokines in the CSF of aSAH patients and development of point of care testing at the patient bedside after aSAH highlight its importance in ongoing inflammation (Dengler et al., 2008). IL-6 has also been shown to represent a surrogate measure of response monitoring after administration of various

therapeutic agents to aSAH patients (Muroi et al., 2008; Kawaguchi et al., 2010; Muroi et al., 2012; Muroi et al., 2014; Singh et al., 2014; Galea et al., 2017a). Above evidence also suggests that IL-6 has an important prognostic potential for aSAH associated complications and clinical outcomes and represents an important cytokine in aSAH associated inflammation.

1.7.4. IL-23

IL-23 is a heterodimeric cytokine composed of p40 (shared with IL-12 p40) and p19 subunits and signals by binding to IL-23R and IL-12Rβ1 (Oppmann et al.; Parham et al., 2002). The p19 subunit of IL-23 shares structural homology with IL-6 and TNF-α (Oppmann et al., 2000). The exogenous and endogenous stimuli trigger the release of IL-23 from activated dendritic cells and activated macrophages (Uhlig et al., 2006; Lyakh et al., 2008). IL-23 can drive the polarization of T helper cells into Th17 cells producing a pro-inflammatory cytokine IL-17 and expressing IL-23R (Lyakh et al., 2008; Ghoreschi et al., 2010). Systemic IL-23 levels are found to be elevated in a number of diseases including systemic lupus erythematosus, psoriasis, urticaria, asthma, rheumatoid arthritis, multiple sclerosis, schizophrenia, and Alzheimer's disease (Ciprandi et al., 2012; Wen et al., 2012; Atwa et al., 2014; Chen et al., 2014; Du et al., 2014; Borovcanin et al., 2015; Fotiadou et al., 2015; Wendling et al., 2015). In a mouse model of ischemic stroke, serum IL-23 as well as IL-23 mRNA and protein levels in the brain tissue were raised and contributed to evolution of infarct volume (Ma et al., 2013). Mice deficient in IL-23 p19 displayed protection against ischemia/ reperfusion injury (I/R) and better behavioural outcomes (Shichita et al., 2009). Interestingly, the source of IL-23 were infiltrating macrophages from the peripheral circulation (Shichita et al., 2009). Moreover, serum IL-23 levels has been shown to be increased in patients with carotid atherosclerosis, which accounts for 20 – 30% of ischemic stroke events (Abbas et al., 2015).

1.7.5. IL-17

IL-17 or IL-17A is a signature cytokine for Th17 cells which express transcription factor RORγt (retinoic acid receptor-related orphan receptor-γt) and require IL-23 for maturation to an inflammatory phenotype (Gaffen et al., 2014). In addition to Th17 cells, IL-17 is also secreted by other innate immune cells such as γδ T cells, NK T cells and innate lymphoid cells (Gaffen et al., 2014). IL-17 signals mainly through heterodimeric complex of IL-17RA

and IL-17RC and activates downstream pro-inflammatory pathways NFκB, MAPK and C/EBP (Korn et al., 2009; Gaffen et al., 2014). IL-17 can upregulate inflammation by inducing secretion of pro-inflammatory cytokines such as TNF-α, IL-1β, IL-6 and chemokines for recruiting neutrophils and macrophages (Mills, 2008). IL-17 plays a key role in many inflammatory autoimmune diseases such as psoriasis, inflammatory bowel disease, multiple sclerosis, rheumatoid arthritis and asthma (Korn et al., 2009; Gu et al., 2013). Shichita and co-authors have shown that IL-17 producing cells (mainly γδ T cells) mediate ischemic-reperfusion injury (Shichita et al., 2009). IL-17 positive lymphocytes were also detected in post stroke autopsies and antibody mediated neutralization of IL-17 in experimental stroke reduced infarction and improved outcome (Gelderblom et al., 2012). However, detailed investigations of IL-17 in the context of aSAH at both clinical and preclinical level are scarce. Very recently, a study investigating network analysis of cytokines in the peripheral circulation after aSAH has shown that IL-17A is detectable after aSAH and IL-17A was correlated with IFN-γ under different conditions associated with aSAH (Savarraj et al., 2017a; Savarraj et al., 2017b).

1.7.6. IL-10

IL-10 represents an important anti-inflammatory cytokine that is co-induced with pro-inflammatory cytokines via pathways which have negative regulatory feedback impact to limit damage to the host (Wang et al., 2017). IL-10 is secreted by almost all types of immune cells under different conditions including Th cells, Tregs, CD8+ T cells, B cells, DCs, macrophages, eosinophils, neutrophils and NK cells (Wang et al., 2017). Interleukin-10 was shown to be produced by Th2 cells (anti-inflammatory) and inhibit the pro-inflammatory Th1 response (Moore et al., 2001; Couper et al., 2008). However, IL-10 has been shown to regulate Th2 responses induced by Schistosoma infestation, Aspergillus infection or allergens (Wang et al., 2017). IL-10 also limits pro-inflammatory cytokine secretion from macrophages and DCs (Moore et al., 2001; Couper et al., 2008). IL-10 inhibits production of pro-inflammatory cytokines such as IL-1α, IL-1β, IL-6, IL-12, IL-18, G-CSF, TNF-α, PAF, LIF and chemokines such as MCP-1, MCP-5, MIP-1α, MIP-1β, RANTES, CXCL8, IP-10, MIP-2, KC etc. from monocytes/macrophages (Moore et al., 2001). Interestingly, IL-10 promotes differentiation of IL-10 secreting Treg cells with immunosuppressive properties (Hawrylowicz and O'Garra, 2005). Human IL-10, a homodimer of 35kDa, is encoded by chromosome 1 and is secreted after cleavage of an 18 amino acids long signal peptide from a

protein comprising 178 amino acids (Sabat et al., 2010). IL-10 signaling is mediated by binding to IL-10 receptor (IL-10R) through downstream pathway dependent upon STAT3 (Sabat et al., 2010; Wang et al., 2017).

IL-10 has been shown to be upregulated in different CNS pathologies and limit inflammation via reduction of pro-inflammatory cytokine synthesis, decreasing cytokine receptor expression and also inhibiting receptor activation with a promotion of neuronal and glial cell survival (Strle et al., 2001). Pre-clinical studies employing SAH models have shown non-significant upregulation of IL-10 in the CNS and basilar arteries and it was associated with a rise in pro-inflammatory cytokines (Aihara et al., 2001; Kooijman et al., 2014b; Song et al., 2014; Li et al., 2017). In ruptured intracranial aneurysms, reduction in IL-10 expression has been seen with upregulated expression of TNF-α and some SNPs in IL-10 gene have been identified to be associated with the formation of intracranial aneurysms (Jayaraman et al., 2005; Sathyan et al., 2015). In clinical studies, IL-10 levels have been shown to follow a constant pattern when present in detectable amounts when determined in extracellular fluid by microdialysis or in CSF (Mellergård et al., 2008; Mellergard et al., 2011; Hopkins et al., 2012). Systemic levels of IL-10 were also shown to reflect similar pattern as observed at CNS level (Hopkins et al., 2012). In a study comparing systemic IL-10 levels among endovascularly based normothermia and conventional temperature management in aSAH patients has not shown any significant difference (Broessner et al., 2010). Serum IL-10 levels have been shown to follow a significant decrease after initial rise in SAH patients (Dziurdzik et al., 2004). Most of the studies investigating IL-10 levels after aSAH are without comparative controls (Dziurdzik et al., 2004; Mellergård et al., 2008; Mellergard et al., 2011; Hopkins et al., 2012; Savarraj et al., 2017a; Savarraj et al., 2017b). A study investigating plasma IL-10 levels in aSAH patients in comparison to patients with unruptured intracranial aneurysms has not shown any significant difference (Chamling et al., 2017). Only a small single study has recruited healthy control group and found a significant elevation at day 1 and non-significant elevation at day 3 after aSAH of plasma IL-10 levels and furthermore, found significant IL-10 release from PBMCs from aSAH patients on LPS stimulation (Kinoshita et al., 2007). Systemic IL-10 levels have been found to be significantly higher in aSAH patients with poor Hunt and Hess grades (H&H $\geq$ 4), higher Fischer grades, and contracting pneumonia infection (Chamling et al., 2017; Savarraj et al., 2017a; Savarraj et al., 2017b). Recently, IL-10 levels measured within 48 hours after aSAH have shown to be elevated

significantly in patients with general cerebral edema and higher subarachnoid hemorrhage early brain edema score (Savarraj et al., 2017a). The same study with slightly different dichotomization of the mRS has shown significantly higher serum IL-10 levels after aSAH in patients with poor clinical outcome at discharge (Savarraj et al., 2017a). Previous studies investigating IL-10 levels after ischemic stroke, intracerebral hemorrhage and traumatic brain injury have shown association of elevated IL-10 levels with poor functional outcomes (Garcia et al., 2017). Pre-clinical and clinical studies investigating serum IL-10 levels in detail after aSAH are still lacking (Garcia et al., 2017).

1.7.7. CCL5/RANTES

Chemokines represent small 8 – 14 kDa soluble cytokines which play a major role in chemotaxis and the recruitment of leucocytes (Zlotnik and Yoshie, 2000; Dorner et al., 2002). Based on the arrangement of the cysteine residues in the conserved structure from N-terminal, different chemokine families such as C, CC, CXC and CX3C have been identified (Mantovani, 1999; Zlotnik and Yoshie, 2000). In humans, around 50 chemokines are known to exist (Rollins, 1997; Mantovani, 1999). Some chemokines are known to be constitutively expressed with homeostatic roles in many physiological processes, while several others are induced during inflammation in response to inflammatory stimuli with critical role in innate and adaptive immune responses (Mantovani, 1999; Dorner et al., 2002; Raman et al., 2011). Regulated on activation, normal T cell expressed and secreted (RANTES) or CCL5 is a pro-inflammatory chemokine from class CC of chemokines and binds several of seven transmembrane GPCRs such as CCR5, CCR4, CCR3, CCR1, Syndecan (SDC)-1, SDC-4, and CD44 (Rollins, 1997; Xia and Hyman, 1999; Zlotnik and Yoshie, 2000; Suffee et al., 2017). CCL5 is secreted by T-lymphocytes, endothelial cells, epithelial cells, endometrial cells, smooth muscle cells, platelets, eosinophils, fibroblasts, glial cells and neurons (Appay and Rowland-Jones, 2001; Terao et al., 2008; Levy, 2009; Tokami et al., 2013). In vitro, RANTES is known to be as potent as MCP-1 for monocytes and has also been known to act as chemoattractant for $CD4^+$ T cells, $CD8^+$ T cells, eosinophils, NK cells, and basophils (Rollins, 1997).

In numerous CNS related pathologies, CCL5 has been known to play an inflammatory role (Simpson et al., 2000; Bartosik-Psujek and Stelmasiak, 2005; Cartier et al., 2005; Zaremba et al., 2006; Tang et al., 2014; Cerri et al., 2017). Elevated CCL5 has been regarded as a risk

factor for stroke in asymptomatic subjects (Canouï-Poitrine et al., 2011). Increased plasma levels of CCL5 have been observed after traumatic brain injury and ischemic stroke (Tokami et al., 2013; Albert et al., 2017). In a cerebral ischemia model, knockout of RANTES was associated with relatively lower infarct volume and reduced plasma levels of IL-6, IL-10 and IL-12 and furthermore, circulating blood cells were identified as a potential source of RANTES that mediates BBB disruption, cerebral inflammation and infarction (Terao et al., 2008). In contrast to this, CCR5 knockouts had larger infarcts (Woiciechowsky et al., 1998). Tokami et al. (2013) has suggested an autocrine or paracrine role of neuron derived CCL5 which upregulates neuroprotective growth factors such as BDNF, EGF and VEGF and downregulates Caspase-3 in neurons through CCR5 and CCR3 ligation on neurons. Furthermore, they speculate that CCR1 expression by endothelial cells and by circulating blood cells may underlie the acute detrimental effects of RANTES (Tokami et al., 2013). Pedrazzi et al. (2007) have shown that HMGB1 could lead to secretion of CCL5 from astrocytes and due to localization of astrocytes in close proximity to BBB, secreted CCL5 may play an important role in microglial and blood monocyte migration and activation, thus enhancing the brain damage. Promotion of leucocyte infiltration at the inflammation site is a well established effect of RANTES (Appay and Rowland-Jones, 2001). CCL5 has been shown to mediate the brain damage through increasing the infiltration of mononuclear cells through BBB and lead to secondary brain injury via induction of potent inflammatory cytokines (Mirabelli-Badenier et al., 2011). Furthermore, CCL5 produced by DCs lead to a Th1 polarized response (Lebre et al., 2005; Ma et al., 2007). Interestingly, monoclonal antibody targeting of CCL5 has shown reduced leucocyte infiltration in CNS and also prevented neurological deficits in MS mouse model (Chang et al., 2015b).

CCL5 expression has been shown to be upregulated in the rat cerebral aneurysm arterial walls (Aoki et al., 2008). In a study focused on identifying expression of long non-coding (lnc)-RNAs identified 17 lnc-RNAs targeting CCL5 in cerebral aneurysms on resections (Li et al., 2016). Recent preclinical investigations in the context of SAH have demonstrated the involvement of CCL5 in ongoing inflammation (Smithason et al., 2012; Chang et al., 2015b). Analysis of multiple systemic cytokines after aSAH has already shown that CCL5 levels peaked 6-8 days after aSAH, but were the part of the cluster of platelet associated cytokines that were correlated at all the times of assessment after aSAH and included platelet derived growth factor (PDGF)-AA, PDGF-AB/BB, sCD40L, CXCL1P1 and TNF-α (Savarraj et al.,

2017b). Interestingly, the CCL5 levels were shown to be negatively correlated with FLTL3 in less severe grade aSAH patients (Savarraj et al., 2017b).

1.8. Immune cell response after aSAH

1.8.1. Monocyte response

Monocytes represent important members of the mononuclear phagocyte system comprised of myeloid derived cells (Jakubzick et al., 2017). Increased infiltration of monocytes has been observed in the stem and frontal parts of the brain at 90 minutes and 24 hours after experimental SAH, which was significantly reduced after antibody mediated IL-1β neutralization (Jedrzejowska-Szypułka et al., 2009). It was interesting to note that application of CSF from aSAH patients led to increased monocyte transmigration through human endothelial cell layers in in-vitro migration assay (Schneider et al., 2012). Monocytes have been regarded as a source of IL-1β and IL-6 in CSF of aSAH patients (Takizawa et al., 2001). Rat basilar arteries showing vasospasm highly express CD34 after SAH and play a major role in monocyte/ macrophage recruitment in addition to others (Wang et al., 2010). Increased adventitial infiltration of monocytes was seen after SAH in rat basilar arteries and that was abrogated by 6-mercaptopurine supplementation (Chang et al., 2010). Chang and colleagues have described increased perivascular MCP-1^{+} (Monocyte Chemoattractant Protein-1/ CCL2) monocytes in double hemorrhagic SAH model (Chang et al., 2015a). Mice carrying negative mutations of PPARγ in smooth muscle cells express increased monocyte/macrophage marker CD68 in cerebral arteries along with CXCL1, MCP-1 and TNF-α and increased incidence of aneurysm formation and rupture (Hasan et al., 2015). Aoki et al. (2017) have demonstrated that macrophage infiltration led by MCP-1 and activation of NFκB involving PGE_2-PGEP2 (PGE receptor subtype 2) signaling in arterial wall leads to aneurysm formation, suggesting that inflammation is not only present after aneurysm rupture, rather also drives aneurysm formation.

Yang and co-authors have found a significant increase in blood monocytes after aSAH and increased expression of leucocyte adhesion molecules PSGL-1 and Mac-1 (Yang et al., 2012). Interestingly, PSGL-1 expression on admission was significantly associated with the development of DCI (Yang et al., 2012). Monocytes harvested from aSAH patients showing vasospasm when stimulated with LPS ex-vivo has shown increased IL-1β release (Nam et al., 2001). Another compelling evidence for the role of monocytes in post-aSAH inflammation

came from the findings of Ma et al., (2015), who found increased TLR-4 expression on monocytes after aSAH. TLR-4 expression on PBMCs was highest on day1 and low on day 7. Furthermore, it was associated with aSAH severity (H&H IV-V), Fischer score, CVS, DCI, infarction and poor clinical outcome (Ma et al., 2015). Transcriptomic analysis of the peripheral blood revealed upregulation of genes pertinent to monocytes after aSAH (Pera et al., 2013). Intriguingly, decreased HLA-DR expression on monocytes and reduced TNF-α secretion from monocytes in LPS stimulation ex-vivo functional assay was seen in aSAH patients presenting with DIND and contracting pneumonia infection, implicating an impairment of immune cell function (Sarrafzadeh et al., 2011).

Mills et al. (2000) described for the first time M1/M2 paradigm similar to Th1/Th2, where M1 represent pro-inflammatory monocytes/macrophages, whereas M2 as anti-inflammatory ones. Ruptured intracerebral aneurysms from patients were shown to possess increased M1 ($HLA\text{-}DR^{+}$) cells opposed to M2 ($CD163^{+}$) cells as revealed by immunohistochemical analysis of aneurysm dome resections (Hasan et al., 2012). However, human monocytes have been characterized into three subgroups based on differential cell surface expression of CD14 and CD16 as classical $CD14^{++}CD16^{-}$, intermediate $CD14^{+}CD16^{+}$ and non-classical $CD14^{+}CD16^{++}$ (Ziegler-Heitbrock et al., 2010; Ziegler-Heitbrock and Hofer, 2013; Guilliams et al., 2014). A flow cytometric analysis from aSAH patients showed increased $CD14^{++}CD16^{+}$ monocytes in CSF compared to peripheral blood, but their reduced counts in the peripheral blood of aSAH patients compared to healthy controls (Moraes et al., 2015). CD16+ monocytes have already been described as pro-inflammatory, since they represent activated state owing to CD16 expression, upregulated expression of pro-inflammatory cytokines, and enhanced antigen presentation potency (Moraes et al., 2015).

1.8.2. T cell response

Lymphocytes upon activation also release different cytokines mediating damaged cells clearance, infected cell killing and microbial neutralization (Zhou et al., 2017). Lymphocyte infiltrations have been observed in CVS affected arteries on autopsies (Hughes and Schianchi, 1978). Aneurysmal tissue harvested during aneurysm clipping contained numerous T cells, while B cells were rare (Chyatte et al., 1999). Increased infiltration of T cells has been observed in subarachnoid space in close proximity to cerebral blood vessels after experimental SAH and numbers of T cells and helper T cells (CD4+) have been shown

to peak after two days of SAH induction and persist significantly in higher numbers till day 7 compared to shams (Kubota et al., 1993). Of note, peripheral T cells showed significant elevation at day 3, but not the helper T cells (Kubota et al., 1993). Moreover, T cells expressing IL-1β were also detected in the CSF from aSAH patients (Takizawa et al., 2001). Impairments in proliferative properties of suppressor lymphocytes (now known as Treg cells) were documented in the peripheral blood of aSAH patients and later on, (Chrapusta et al., 2000) have shown significant decrease in CD4+ T cells in dexamethasone treated aSAH patients compared to controls and decreased proliferative response, while enhanced T cell adhesion and T cell co-stimulatory properties in the peripheral blood of aSAH patients (Ryba et al., 1993). Interestingly, patients presenting with CVS had increased CD4+ T helper cells in the peripheral blood and more aggressive T cell adhesion and co-stimulatory properties (Chrapusta et al., 2000).

Several studies have investigated CD4+ T helper cells in the peripheral blood after aSAH (Chrapusta et al., 2000; Sarrafzadeh et al., 2011; Moraes et al., 2015; Zhang et al., 2015; Zhou et al., 2017). Over the past different subsets of CD4+ T helper cells have been characterized, more importantly Th1, Th2, Th17 and Treg cells. Naïve CD4+ T helper cells can differentiate into interferon (IFN)-γ secreting, expressing T-bet signature transcription factor Th1 cells in response to IL-12 induced STAT4 signaling and mediate cell based response against intracellular pathogens (Chrapusta et al., 2000; Sarrafzadeh et al., 2011; Moraes et al., 2015; Zhang et al., 2015; Zhou et al., 2017). Th2 cell polarization occurs under the influence of IL-4 upregulated STAT6 signaling and expression of master transcription factor GATA3 and these cells produce cytokines such as IL-4, IL-5 and IL-13 and mediate extracellular immune responses against parasitic infestations and contribute to allergic responses (Murphy and Reiner, 2002). Th17 cells secrete IL-17, express master transcription factor RORγt and involve STAT3 signaling in response to various cytokines such as IL-6, TGF-β and IL-23; and play critical role in antibacterial, antifungal responses and autoimmune diseases (Acosta-Rodriguez et al., 2007; Gaffen et al., 2014). T regulatory (reg) cells express FOXP3 as a signature transcription factor and secrete immunosuppressive cytokines such as IL-10, TGF-β and IL-35 and have the capability to suppress nearly all immune cell subtypes. Therefore, they play an indispensable role in immune tolerance and prevention against autoimmune diseases (Sakaguchi et al., 2010).

A lymphopenic response has been observed after aSAH, but interestingly it was shown to be associated with increased CD4+ T cells expressing transient activation marker CD69 (Moraes et al., 2015). Acute focal neurological deficits in aSAH patients can lead to an early significant reduction in CD4+ T cells, which may underlie the observed immunosuppression after aSAH (Sarrafzadeh et al., 2011). A very recent study has shown significant reduction of CD4+ T cells and Treg cells after aneurysmal obliteration surgery and even in patients presenting with fever and poor prognosis (Zhou et al., 2017). Regarding CD4+ T cell subsets, only limited studies have been done so far. A preclinical study investigated the polarization of Th1 cells to Th2 upon administration of statins in endovascular puncture model of SAH (Ayer et al., 2013). A single clinical study has investigated T helper cell subsets in patients with both ruptured and unruptured intracranial aneurysms and has found significant elevation of Th17 cells and reduction of Th2 cells compared to controls (Zhang et al., 2015). Detailed studies investigating the dynamics of these different CD4+ T cell subsets along with their activation states after aSAH are lacking. These studies are highly encouraged as they would not only help in understanding the interplay between different T helper cell subtypes during the course of the disease, but would be advantageous from biomarker and therapeutic point of view.

1.9. Role of systemic inflammation after aSAH

A systemic inflammatory response has been observed in 75% of the aSAH patients presenting with pyrexia, tachypnea, tachycardia and leucocytosis and the inflammatory cytokines have been blamed for this response (Macdonald et al., 2014). Cytokines released as a consequence of intrathecal inflammation after aSAH may eventually enter the systemic circulation owing to post-aSAH compromised BBB and upregulate systemic inflammatory cascades and may explain peripheral organ system failures (Gruber et al., 2000). Interestingly, development of systemic inflammatory response syndrome and extracerebral organ-system damage after aSAH is accompanied by a significant systemic upregulation of sTNFR1 and sIL-1RA (Gruber et al., 2000). Blockage of IL-1 signaling via sIL-1RA has been shown to abrogate the brain injury (Greenhalgh et al., 2012). Systemic levels of different pro-inflammatory molecules such as CRP, TNF-α, IL-1β and IL-6 have been shown to be upregulated and associated with DCI or poor clinical outcome (McMahon et al., 2013; Muroi et al., 2013; Miller et al., 2014; Ma et al., 2015; Da Silva et al., 2017). Inflammation plays a crucial role in determining the clinical outcome and cognitive function after aSAH

(Muroi et al., 2013; Hong et al., 2014; Da Silva et al., 2017). Therefore, investigation of systemic inflammation after aSAH represent a potential target that seems promising to uncover and provide with not only new therapeutic options, but also with new biomarkers and prognostic markers of post-aSAH complications and clinical outcome. A schematic representation of the role of inflammation mediated by DAMPs and cytokines after aSAH is represented in Fig. 1.

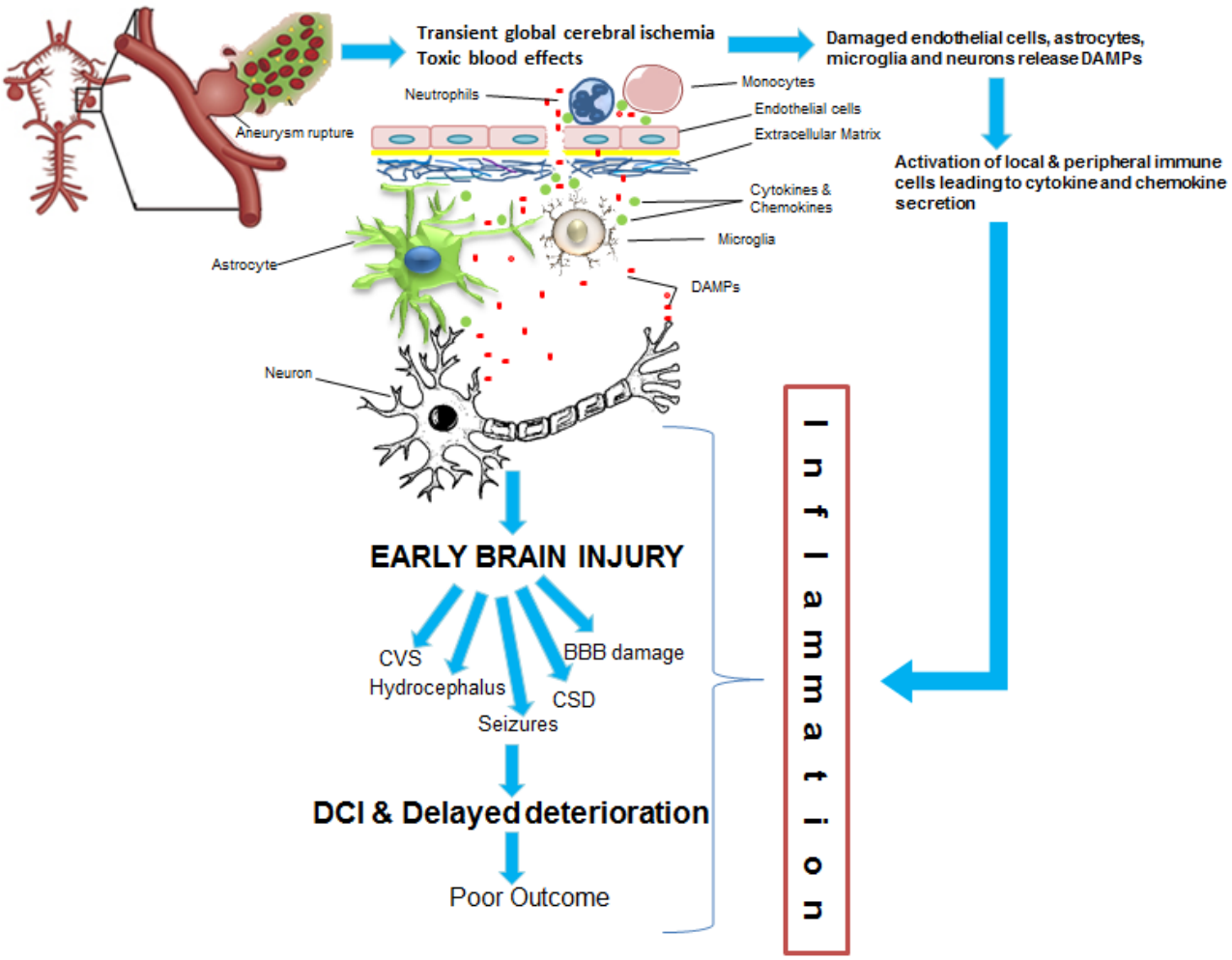

Figure 1: Schematic representation of the role of inflammation mediated by DAMPs and cytokines after aSAH and their possible association with post-aSAH complications and clinical outcome (modified from: https://www.nature.com/articles/cddis201663)

2. Aims of the study

Since, inflammation is known to play a major role in aSAH and post-aSAH complications and can affect the clinical outcome of the aSAH patients. Therefore, the aim of this study was to investigate the role of molecules that can initiate and drive inflammation after aSAH, during post-aSAH complications and its impact on clinical outcome of the aSAH patients. The inflammation driven by aSAH is sterile in nature, hence, we aimed to characterize DAMPs after aSAH, their association with post-aSAH complications and their impact on clinical outcome. We investigated the role of main DAMPs such as HMGB1, IL-1α, IL-33 and mitochondrial DNA in the systemic circulation of patients after aSAH, post-aSAH complications and their impact on clinical outcome.

To characterize the mediators of systemic inflammation after aSAH, this study aimed to investigate some selective cytokines which are either not previously investigated or lack comprehensive and detailed investigations. We selected pro-inflammatory molecules including IL-6 and RANTES, anti-inflammatory molecule IL-10 and Th17 response molecules including IL-23 and IL-17. The secondary aim of the study was to highlight the diagnostic or prognostic potential of these DAMPs molecules and cytokines for aSAH, post-aSAH complications and clinical outcome.

Additionally, the aim of the study was to characterize monocyte and CD4+ T cell subsets response during early and delayed brain injury phases after aSAH.

3. Materials and Methods

3.1. Ethics statement

This study was performed according to the guidelines of the Helsinki declaration and was approved by the local ethics committee of the medical faculty of the University of Bonn, Germany (Reference Number: LfD 138/ 2011). Informed consent was obtained by the treating neurosurgeon.

3.2. Patient population

This retrospective study included 80 consecutive patients unless otherwise stated after aneurysmal SAH with Hunt and Hess grade I – V, who were admitted to the department of Neurosurgery, University Hospital Bonn, the University of Bonn, Germany. The patients presenting to our neurosurgery unit within 24 hours of aSAH were considered for sampling. Patients with age ≤ 18 years, ischemic stroke, traumatic brain injury, onset of symptoms beyond 24 hours, SAH due to arteriovenous malformations or vasculitis, pregnancy, signs of eminent death and those who did not provide informed consent were excluded from the study. Blood samples were collected at seven different time points including on day 1 (within the first 24 hours), day 3, 5, 7, 9, 11 and 13. Patients whose blood samples were available less than four time points (due to death etc.) were excluded from analysis. Twenty-eight control patients with spinal stenosis without any known cerebral pathology were enrolled in the study unless otherwise stated.

3.3. Clinical monitoring and aneurysm treatment

Institutional standardized diagnostic and treatment regimen was followed. SAH was ascertained by computed tomography (CT) scan. CT angiography (CT-A) and digital subtraction angiography (DSA) were performed for further evaluation of the aneurysm. The aneurysm treatment decision (neurosurgical clipping or endovascular coiling) was based on an interdisciplinary approach. An early treatment strategy (within 24 hours of admission) was followed. The treatment protocol at the neuro-intensive care unit (NICU) included hourly neurological monitoring, continuous invasive blood pressure and body temperature measurements, daily transcranial Doppler (TCD) and the administration of nimodipine for 21 days starting from the day of admission. Generally, patients who were not clinically assessable were screened for vasospasm by daily TCD and DSA on day 7 after ictus. CT-A

and CT perfusion (CT-P) were performed upon suspicion of CVS to confirm the presence of the latter. The patients having significant perfusion deficits with a difference in mean transient time (MTT) above 2 seconds in comparison to the contralateral hemisphere in CT-P were considered to be treated. CVS patients were treated with induced hypertension using catecholamines, maintaining a target mean arterial blood pressure (MAP) at around 110 mm Hg until resolution of CVS. Hypertensive treatment was stopped after final CT-A and CT-P showed no further evidence of CVS with perfusion deficits.

3.4. Assessment of clinical severity and degree of bleeding

The clinical severity of aSAH patients was assessed by Hunt and Hess grades (H&H grades) with dichotomization into two groups: aSAH patients with H&H I-II grades were considered to be having less severe aSAH or good grades, whereas patients presenting with H&H grades III-V were considered to be having severe aSAH and poor grades (Mathiesen et al., 1997). The degree of bleeding after aSAH was assessed by the volume of hematoma on CT-scans as according to Fischer scale.

3.5. Clinical outcome assessment

The clinical outcome of the patients was assessed at discharge by well known and commonly used clinical outcome assessment scales i.e., Glasgow Outcome Scale (GOS) and Modified Rankin Scale (mRS). In order to characterize the patients into good outcome and poor outcome patients for the ease of comparison, both the scales were dichotomized to represent poor outcomes and good outcomes at discharge. Glasgow Outcome Scale scores were dichotomized as GOS score 1 – 3 represented poor clinical outcome and GOS score 4 – 5 represented good clinical outcome as described previously (Chaudhry et al., 2017). Patients presenting with a mRS 0 – 2 were grouped into good outcome, while those with a score of 3 – 6 were regarded as with a poor outcome as described by others (Broessner et al., 2010).

3.6. Peripheral blood sampling and retrieval of serum

Blood samples of aSAH patients were collected on days 1, 3, 5, 7, 9, 11 and 13 after aSAH. Blood samples from spinal stenosis control patients or healthy controls were available at a single time point. The peripheral venous blood was withdrawn in monovette serum gel tubes (Sarstedt, Germany), allowed to clot for 15 minutes at room temperature and then, spun at 3500 rpm in a benchtop centrifuge (Sigma Laborzentrifugen, Osterode am Harz, Germany)

for 10 minutes to obtain serum. The serum was aliquoted into 500 µl clean polypropylene microtubes (Axygen™, USA) and they were immediately frozen at -80 °C until analysis. Peripheral blood leukocytes count and other hematological parameters were recorded from daily laboratory tests.

3.7. Analysis of serum DAMPs and cytokines

In order to investigate the questions posed by the proposed hypothesis, we have adopted the two well known molecular and cell biology techniques including ELISA and qPCR to quantify DAMPs and cytokines in aSAH patients and controls. The details of these are given below:

3.7.1. Enzyme Linked Immunosorbent Assays (ELISAs)

HMGB1 and selective cytokines were quantified using pre-coated sandwich ELISA kits by following the instructions of the manufacturers. The detailed procedures for every ELISA kit are mentioned in section 3.7.1.1 below. Serum HMGB1 was analyzed using Shino test ELISA kit obtained from IBL International (Catalog no. ST51011, Hamburg, Germany). Serum IL-17 and IL-23 levels were quantified using pre-coated Platinum ELISA kits purchased from eBioscience (Catalog no. BMS2017 and BMS2023/3, Bender MedSystems GmbH, Vienna, Austria). For serum IL-10 determination, pre-coated BD OptEIA Human IL-10 ELISA Kit II was purchased from BD (Catalog no. 550613, Becton Dickinson Biosciences, San Jose, CA, USA). Quantikine ELISA kits purchased from R&D Systems were used for the measurement of IL-1α and IL-33 (Catalog no. DLA50 and D3300, R&D Systems, Minneapolis, USA). RANTES/CCL5 ELISA kit was also purchased from R&D Systems (Catalog no. DRN00B, R&D Systems, Minneapolis, MN, USA). Serum IL-6 levels were measured using Immulite immunoassay as a part of routine diagnostics service available at the central lab. facility of the department of Clinical Chemistry and Clinical Pharmacology, University of Bonn. The detailed procedures of the ELISAs are presented as following:

3.7.1.1. HMGB1 ELISA

All the components of the kit were brought to the room temperature before use. Lyophilized standard was diluted with an appropriate amount of the provided standard diluent to yield a final concentration of 320 ng/mL. Seven microcentrifuge tubes were labeled as 80 ng/mL, 40 ng/mL, 20 ng/mL, 10 ng/mL, 5 ng/mL, 2.5 ng/mL and 0 ng/mL. In the first tube 300 µL

while in the rest of the tubes 100 µL of the diluent buffer was dispensed. The standard stock solution was left for at least 10 minutes at room temperature to allow complete reconstitution. The stock solution was gently swirled and 100 µL of it was added to the tube labeled 80 ng/mL. After a brief vortex mixing, 100 µL was transferred to the next tube labeled 40 ng/mL. In this way, serial dilutions were made up to 2.5 ng/mL and last tube labeled 0 ng/mL contained only diluent buffer and served as blank. The wash buffer was diluted 1:5 with the deionized distilled water.

A volume of 100 µL of diluent buffer was added to the wells of the microtiter plate. Blank wells were supplied with 10 µL of the diluent buffer (0 ng/mL). Then, 10 µL of the standards, positive control and the samples were pipetted into the respective wells and the microplate was shaken briefly for 30 secs. The plate was sealed with an adhesive foil and incubated at 37°C for 20 – 24 hours. Afterwards the adhesive foil was removed and the contents of the wells were discarded. Each well was washed 5 times with 400 µL of the diluted wash buffer using an automatic washer (HydroFlex^{TM} microplate washer, Tecan, Groedig, Austria). Enzyme conjugate diluted with an enzyme conjugate diluent was added into the wells in a volume of 100 µL. The plate was sealed again and incubated for 2 hrs at +25°C. Later on, plate was washed again as mentioned above and 100 µL of the colour solution consisting of colouring reagent A and B was added in each well. The plate was again incubated at room temperature for 30 minutes covered with an aluminium foil to protect it from the light. Afterwards, 100 µL stop solution was added and after cleaning the back of the wells, optical density of each well at 450 nm was determined with the help of a multiwellplate reader (Thermoscientific Multiskan^{TM} Go, microtiterplate spectrophotometer, Vantaa, Finland). The results were then computed from the calibration curve generated from the standards. The limit of detection of the assay was 1 ng/mL.

3.7.1.2. IL-1α ELISA

The components of the kit were brought to the room temperature. The washing buffer was prepared by adding 20 mL of wash buffer concentrate to deionized distilled water to prepare 500 mL of wash buffer. The human IL-1α standard was reconstituted with calibrator diluent RD6C to produce a stock solution of 250 pg/mL. The standard was allowed to equilibrate for a minimum of 15 minutes with gentle agitation prior to making dilutions. Then, 6 microcentrifuge tubes were labelled as 125 pg/mL, 62.5 pg/mL, 31.3 pg/mL, 15.6 pg/mL, 7.8

pg/mL, and 3.9 pg/mL, respectively. Each tube was supplemented with 500 µL of the calibrator diluent RD6C. Then, 1:2 serial dilutions were prepared by pipetting 500 µL of the reconstituted standard stock solution to the first tube labelled as 125 pg/mL. After gently vortexing, 500 µL from 125 pg/mL tube was transfered to the 2nd tube labelled as 62.5 pg/mL and the same process was repeated until the last tube labelled as 3.9 pg/mL. The undiluted human IL-1α standard stock solution (250 pg/mL) served as the highest standard. The calibrator diluent RD6C served as the blank.

The microplate was removed from the sealed pouch and 50 µL of assay diluent RD1-83 was pipetted into each well. About 200 µL of the calibrator diluent RD6C was added to each of the blank wells. An aliquot of 200 µL of standards, controls, or samples were added to the appropriate wells of the microplate. After covering with the adhesive strip provided, the microplate was incubated for 2 hours at room temperature. The contents of the microplate were decanted or aspirated after 2 hours of incubation. The wells of the microplate were then washed 3 times with approximately 400 µL of wash buffer per well with thorough aspiration of microwell contents between washes using an automatic washer (HydroFlex^{TM} microplate washer, Tecan, Groedig, Austria). Care was taken not to scratch the surface of the microwells. After the last wash step, the wells were emptied and microplate was tapped on absorbent pad or paper towel to remove excess wash buffer. Added 200 µL of human IL-1α conjugate to each well and covered with a new adhesive film for incubation for 2 hours at room temperature. After repeating the washing step as described above, 200 µL of substrate solution consisting of equal volumes of colouring reagents A and B, was added to each well and incubated the microplate for 20 minutes at room temperature protected from light. After adding 50 µL of stop solution to each well, the optical density was measured at 450 nm as primary wavelength and 540 nm or 570 nm as reference wavelength using Thermoscientific Multiskan^{TM} Go, microtiterplate spectrophotometer (Vantaa, Finland). The absorbance values were then corrected by subtracting the reference wavelength (540 nm or 570 nm) values from primary wavelength (450 nm) absorbance values. The results were then computed from the standard curve obtained from standards. The sensitivity of the assay kit was 1 pg/mL.

3.7.1.3. IL-33 ELISA

The components of the kit were brought to the room temperature. The calibrator diluent RD5-26 was diluted 1:5 by adding 4 mL of calibrator diluent RD5-26 to 16 mL of deionized

distilled water to prepare 20 mL of calibrator diluent RD5-26. The washing buffer was prepared by adding 20 mL of wash buffer concentrate to deionized distilled water to prepare 500 mL of wash buffer. The human IL-33 standard was reconstituted with deionized distilled water to produce a stock solution of 4000 pg/mL. The standard was allowed to equilibrate for a minimum of 15 minutes with gentle agitation prior to making dilutions. Then, 7 microcentrifuge tubes were labelled as 400 pg/mL, 200 pg/mL, 100 pg/mL, 50 pg/mL, 25 pg/mL, 12.5 pg/mL, and 6.25 pg/ml respectively. In the first tube 900 µL of the calibrator diluent RD5-26 (1:5 diluted) was added, while in remaining tubes 500 µL of the calibrator diluent RD5-26 (1:5) was pipetted. In the first tube labelled as 400 pg/mL, 100 µL of the stock solution was added and briefly vortexed. Then, 1:2 serial dilutions were prepared for the rest of the tubes by pipetting 500 µL from the first tube to the next tube labelled as 200 pg/mL. After gently vortexing, 500 µL from 200 pg/mL tube was transfered to the 3rd tube labelled as 100 pg/mL and the same process was repeated until the last tube labelled as 6.25 pg/mL. The calibrator diluent RD5-26 (1:5) served as zero standard.

The microplate was removed from the sealed pouch and 100 µL of assay diluent RD1-77 was pipetted into each well. About 200 µL of the calibrator diluent RD5-26 (1:5) was added to each of the blank wells. Approximately, 200 µL volumes of standards, controls, or samples were added to the appropriate wells of the microplate. After covering with the adhesive strip provided, the microplate was incubated for 2 hours at room temperature on an orbital microplate shaker set at 500 rpm ± 50 rpm. The contents of the microplate were decanted or aspirated after 2 hours of incubation. The wells of the microplate were then washed 4 times with approximately 400 µL of wash buffer per well with thorough aspiration of microwell contents between washes using an automatic washer (HydroFlex^{TM} microplate washer, Tecan, Groedig, Austria). Care was taken not to scratch the surface of the microwells. After the last wash step, the wells were emptied and microplate was tapped on absorbent pad or paper towel to remove excess wash buffer. Added 200 µL of human IL-33 conjugate to each well and covered with a new adhesive film for incubation for 2 hours at room temperature on the shaker. After repeating the washing step as described above, 200 µL of substrate solution consisting of equal volumes of colouring reagents A and B, was added to each well and incubated the microplate for 30 minutes at room temperature protected from light. After adding 50 µL of stop solution to each well, the optical density was measured at 450 nm as primary wavelength and 540 nm or 570 nm as reference wavelength using Thermoscientific

Multiskan^{TM} Go, microtiterplate spectrophotometer (Vantaa, Finland). The absorbance values were then corrected by subtracting the reference wavelength (540 nm or 570 nm) values from primary wavelength (450 nm) absorbance values. The results were then computed from the standard curve obtained from standards. The sensitivity of the assay kit was 1 pg/mL.

3.7.1.4. IL-23 ELISA

The components of the kit were brought to the room temperature. The wash buffer concentrate (50 mL) was diluted 20 times with deionized distilled water to a final volume of 1000 mL in a volumetric flask. Similarly, assay buffer concentrate (5 mL) was diluted 20 times with deionized distilled water to a final volume of 100 mL. Human IL-23 standard was reconstituted with a sample diluent volume specified on the vial to provide a concentration of 4000 pg/mL. The vial was gently swirled and the mixture was allowed to stand for 10 – 30 minutes. Then, 8 microcentrifuge tubes were labelled as 2000 pg/mL, 1000 pg/mL, 500 pg/mL, 250 pg/mL, 125 pg/mL, 62.5 pg/mL, 31.3 pg/mL, and 15.6 pg/mL respectively. Each tube was supplemented with 225 µL of the sample diluent. Then, 1:2 serial dilutions were prepared by pipetting 225 µL of the reconstituted standard to the first tube labelled as 2000 pg/mL. After gently vortexing, 225 µL from 2000 pg/mL tube was transferred to the 2nd tube labelled as 1000 pg/mL and the same process was repeated until the last tube labelled as 15.6 pg/mL. The sample diluent served as the blank.

The microwell strips were washed twice with approximately 400 µL of wash buffer per well with thorough aspiration of microwell contents between washes using an automatic washer (HydroFlex^{TM} microplate washer, Tecan, Groedig, Austria). The wash buffer was allowed to sit in the wells for about 10 – 15 seconds before aspiration. Care was taken not to scratch the surface of the microwells. After the last wash step, the wells were emptied and microwell strips were tapped on absorbent pad or paper towel to remove excess wash buffer. The microwell strips were then used immediately after washing.

The blank wells were then pipetted in with 100 µL of the sample diluent and 100 µL of each standard was added in duplicate to the standard wells. The sample wells were supplemented with 50 µL of sample diluent followed by addition of 50 µL of each serum sample into respective sample wells. The plate was covered with an adhesive film and incubated at room temperature (18° to 25°C) for 2 hours. A 1:250 dilution of the concentrated biotin-conjugate solution (48 µL) with 11.952 mL of assay buffer (1x) was prepared in a clean plastic tube

immediately before use. After 2 hours of incubation, adhesive film was removed and wells were emptied. The microwell strips were washed 5 times as described above. A volume of 100 µL of biotin-conjugate (1x) prepared as described above was added to all the wells and the microplate was covered with an adhesive film and incubated at room temperature (18° to 25°C) for 1 hour. Similar to biotin-conjugate, a 1:250 dilution of the concentrated avidin-horse reddish peroxidase (HRP) solution (48 µL) with 11.952 mL of assay buffer (1x) was prepared in a clean plastic tube. After 1 hour of incubation, the adhesive film was removed and the emptied wells were washed 5 times as described above. A volume of 100 µl of diluted avidin-HRP was supplied to all the wells and the microplate was covered with an adhesive film and incubated at room temperature (18° to 25°C) for 30 minutes. The incubation was followed by adhesive film removal, emptying of the wells and washing for 5 times as described above. After washing, 100 µL of the tetramethyl benzidine (TMB) substrate solution was immediately added to the microplate wells and incubated in dark at room temperature (18° to 25°C) for about 15 minutes. The enzyme reaction was then stopped by quickly pipetting 100 µl of the stop solution into each well. It was made sure that the stop solution was spread quickly and uniformly throughout the microwells to completely inactivate the enzyme. The absorbance of each microwell was read on a spectrophotometer using 450 nm as the primary wavelength and 620 nm as the reference wavelength Thermoscientific Multiskan^{TM} Go, microtiterplate spectrophotometer (Vantaa, Finland). The absorbance values were then corrected by subtracting the reference wavelength (620 nm) values from primary wavelength (450 nm) absorbance values. The results were then computed from the standard curve obtained from standards and since, the samples were diluted 1:2, therefore, the concentration values of the samples were multiplied by a dilution factor of 2 to yield final serum IL-23 concentrations in the samples. The sensitivity of the assay kit was 4 pg/mL.

3.7.1.5. IL-17 ELISA

The components of the kit were brought to the room temperature. The wash buffer concentrate (50 mL) was diluted 20 times with deionized distilled water to a final volume of 1000 mL in a volumetric flask. Similarly, assay buffer concentrate (5 mL) was diluted 20 times with deionized distilled water to a final volume of 100 mL. Human IL-17 standard was reconstituted with a volume of deionized distilled water specified on the vial to provide a concentration of 200 pg/mL. The vial was gently swirled and the mixture was allowed to

stand for 10 – 30 minutes. Then, 7 microcentrifuge tubes were labelled as 100 pg/mL, 50 pg/mL, 25 pg/mL, 12.5 pg/mL, 6.3 pg/mL, 3.1 pg/mL, and 1.6 pg/mL, respectively. Each tube was supplemented with 225 µL of the sample diluent. Then, 1:2 serial dilutions were prepared by pipetting 225 µL of the reconstituted standard to the first tube labelled as 100 pg/mL. After gently vortexing, 225 µL from 100 pg/mL tube was transferred to the 2nd tube labelled as 50 pg/mL and the same process was repeated until the last tube labelled as 1.6 pg/mL. The sample diluent served as the blank.

The microwell strips were washed twice with approximately 400 µL of wash buffer per well with thorough aspiration of microwell contents between washes using an automatic washer (HydroFlex^{TM} microplate washer, Tecan, Groedig, Austria). The wash buffer was allowed to sit in the wells for about 10 – 15 seconds before aspiration. Care was taken not to scratch the surface of the microwells. After the last wash step, the wells were emptied and microwell strips were tapped on absorbent pad or paper towel to remove excess wash buffer. The microwell strips were then used immediately after washing.

The blank wells were then pipetted in with 100 µL of the sample diluent and 100 µL of each standard was added in duplicate to the standard wells. The sample wells were supplemented with 50 µL of sample diluent followed by addition of 50 µL of each serum sample into respective sample wells. A 1:100 dilution of the concentrated biotin-conjugate solution (60 µL) with 5.94 mL of assay buffer (1x) was prepared in a clean plastic tube immediately. A volume of 50 µL of biotin-conjugate (1x) was added to all the wells and the microplate was covered with an adhesive film and incubated at room temperature (18° to 25°C) for 2 hours on a microplate shaker set at 400 rpm. Similar to biotin-conjugate, a 1:200 dilution of the concentrated streptavidin-horse reddish peroxidase (HRP) solution (60 µL) with 11.94 mL of assay buffer (1x) was prepared in a clean plastic tube in order to be used within 30 minutes following preparation. After 2 hours of incubation, adhesive film was removed and wells were emptied. The microwell strips were washed 4 times as described above. A volume of 100 µl of diluted streptavidin-HRP (1x) was supplied to all the wells and the microplate was covered with an adhesive film and incubated at room temperature (18° to 25°C) for 1 hour on a microplate shaker set at 400 rpm. The incubation was followed by adhesive film removal, emptying of the wells and washing for 4 times as described above. After washing, 100 µL of the tetramethyl benzidine (TMB) substrate solution was immediately added to the microplate wells and incubated in dark at room temperature (18° to 25°C) for about 10 minutes. The

enzyme reaction was then stopped by quickly pipetting 100 µl of the stop solution into each well. It was made sure that the stop solution was spread quickly and uniformly throughout the microwells to completely inactivate the enzyme. The absorbance of each microwell was read on a spectrophotometer using 450 nm as the primary wavelength and 620 nm as the reference wavelength Thermoscientific Multiskan^{TM} Go, microtiterplate spectrophotometer (Vantaa, Finland). The absorbance values were then corrected by subtracting the reference wavelength (620 nm) values from primary wavelength (450 nm) absorbance values. The results were then computed from the standard curve obtained from standards and since, the samples were diluted 1:2, therefore, the concentration values of the samples were multiplied by a dilution factor of 2 to yield final serum IL-17 concentrations in the samples. The sensitivity of the assay kit was 0.5 pg/mL.

3.7.1.6. IL-10 ELISA

The components of the kit were brought to the room temperature. The wash buffer concentrate (25 mL) was diluted 20 times with deionized distilled water to a final volume of 500 mL in a volumetric flask. Lyophilized IL-10 standard was reconstituted with a volume of standard/sample diluent specified on the vial to prepare a 500 pg/mL stock standard. The vial was gently swirled and the stock standard was allowed to equilibrate for 15 minutes followed by a gentle vortex mixing. Then, 6 microcentrifuge tubes were labelled as 250 pg/mL, 125 pg/mL, 62.5 pg/mL, 31.3 pg/mL, 15.6 pg/mL, and 7.8 pg/mL, respectively. Each tube was supplemented with 300 µL of the standard/sample diluent. Then, 1:2 serial dilutions were prepared by pipetting 300 µL of the reconstituted stock standard to the first tube labelled as 250 pg/mL. After gently vortexing, 300 µL from 250 pg/mL tube was transferred to the 2nd tube labelled as 125 pg/mL and the same process was repeated until the last tube labelled as 7.8 pg/mL. The standard stock solution served as the highest standard. The standard/sample diluent served as the blank.

A volume of 50 µL of elisa diluent was pipetted into each well of the microplate. The blank wells were then pipetted in with 100 µL of the standard/sample diluent. About 100 µL of each standard and sample was added to the appropriate wells. The microplate was gently shaken or tapped for 5 seconds to mix and then, was covered with a plate sealer and incubated at room temperature (18° to 25°C) for 2 hours. Within 15 minutes prior to use, working detector was prepared by pipetting 12 mL of the detection antibody to a clean plastic

tube and adding in 48 µL of the enzyme concentrate. The contents of the microwell strips were decanted or aspirated after 2 hours of incubation. The wells were then washed 5 times with approximately 300 µL of wash buffer per well with thorough aspiration of microwell contents between washes using an automatic washer (HydroFlex^{TM} microplate washer, Tecan, Groedig, Austria). Care was taken not to scratch the surface of the microwells. After the last wash step, the wells were emptied and microwell strips were tapped on absorbent pad or paper towel to remove excess wash buffer. The microwell strips were then used immediately after washing. Afterwards, 100 µL of working detector was added to each well and the microplate was covered with a plate sealer and incubated at room temperature for 1 hour. After incubation, adhesive plate sealer was removed and wells were emptied. The microwell strips were washed 7 times as described above with an additional soaking step for 1 minute. After washing, 100 µL of the tetramethyl benzidine (TMB) one step substrate reagent was immediately added to the microplate wells and incubated in dark at room temperature (18° to 25°C) for about 30 minutes. The enzyme reaction was then stopped by quickly pipetting 50 µl of the stop solution into each well. The absorbance of each microwell was read on a spectrophotometer using 450 nm as the primary wavelength and 570 nm as the reference wavelength Thermoscientific Multiskan^{TM} Go, microtiterplate spectrophotometer (Vantaa, Finland). The absorbance values were then corrected by subtracting the reference wavelength (570 nm) values from primary wavelength (450 nm) absorbance values. The results were then computed from the standard curve obtained from standards. The sensitivity of the assay kit was 2 pg/mL.

3.7.1.7. RANTES/CCL5 ELISA

The components of the kit were brought to the room temperature. The calibrator diluent RD6-11 was diluted 1:5 by adding 20 mL of calibrator diluent RD6-11 to 80 mL of deionized or distilled water to prepare 100 mL of calibrator diluent RD6-11. For this assay, serum samples required a 100-fold dilution and were diluted by adding 10 µL of each serum sample into 990 µL of calibrator diluent RD6-11 in the clean 1.5 mL microcentrifuge tubes. The washing buffer was prepared by adding 20 mL of wash buffer concentrate to deionized distilled water to prepare 500 mL of wash buffer. The human RANTES standard was reconstituted with calibrator diluent RD6-11 (1:5 diluted) to produce a stock solution of 2000 pg/mL. The standard was allowed to equilibrate for a minimum of 15 minutes with gentle agitation prior to making dilutions. Then, 6 microcentrifuge tubes were labelled as 1000 pg/mL, 500 pg/mL,

250 pg/mL, 125 pg/mL, 62.5 pg/mL, and 31.3 pg/mL, respectively. Each tube was supplemented with 500 µL of the calibrator diluent RD6-11 (1:5 diluted). Then, 1:2 serial dilutions were prepared by pipetting 500 µL of the reconstituted stock standard to the first tube labelled as 1000 pg/mL. After gently vortexing, 500 µL from 1000 pg/mL tube was transferred to the 2nd tube labelled as 500 pg/mL and the same process was repeated until the last tube labelled as 31.3 pg/mL. The undiluted human RANTES standard stock solution (2000 pg/mL) served as the highest standard. The calibrator diluent RD6-11 (1:5 diluted) served as the blank.

The microplate was removed from the sealed pouch and 100 µL of assay diluent RD1W was pipetted into each well. About 100 µL of the calibrator diluent RD6-11 (1:5 diluted) was added to each of the blank wells. About 100 µL volumes of standards, controls, or samples were added to the appropriate wells of the microplate. After covering with the adhesive strip provided, the microplate was incubated for 2 hours at room temperature. The contents of the microplate were decanted or aspirated after 2 hours of incubation. The wells of the microplate were then washed 3 times with approximately 400 µL of wash buffer per well with thorough aspiration of microwell contents between washes using an automatic washer (HydroFlex^{TM} microplate washer, Tecan, Groedig, Austria). Care was taken not to scratch the surface of the microwells. After the last wash step, the wells were emptied and microplate was tapped on absorbent pad or paper towel to remove excess wash buffer. Afterwards, added 200 µL of human RANTES conjugate to each well and covered with a new adhesive film for another incubation of 1 hour at room temperature. After repeating the washing step as described above, 200 µL of substrate solution consisting of equal volumes of colouring reagents A and B, was added to each well and incubated the microplate for 20 minutes at room temperature protected from light. After adding 50 µL of stop solution to each well, the optical density was measured at 450 nm as primary wavelength and 540 nm or 570 nm as reference wavelength using Thermoscientific Multiskan^{TM} Go, microtiterplate spectrophotometer (Vantaa, Finland). The absorbance values were then corrected by subtracting the reference wavelength (540 nm or 570 nm) values from primary wavelength (450 nm) absorbance values. The results were then computed from the standard curve obtained from standards. The sensitivity of the assay kit was 2 pg/mL.

3.7.2. Real time quantitative Polymerase Chain Reaction (qPCR)

The second DAMP member, mtDNA from the healthy controls and aSAH patients was quantified using a real time quantitative PCR. Before qPCR quantification, DNA was isolated from the serum and mtDNA for standard curves was generated as described below:

3.7.2.1. Isolation of serum DNA

Cell free circulating DNA in the serum of aSAH patients and controls was isolated using QIAMP DNA mini kit (Catalog no. 51306, QIAGEN, Germany) by following the manufacturer's instructions with slight modifications. Briefly, the serum samples were centrifuged for 2-3 mins at 6000 rpm (Eppendorf, Germany) to get rid of any contaminating cellular debris and obtain cell free DNA. A 200 µl aliquot of serum was applied to 20 µl proteinase K and 200 µl lysis buffer and incubated for 20 mins at 56 °C. Afterwards, 230 µl of absolute alcohol was added and the mixture was applied to the provided columns after a brief spin down. The columns were washed twice sequentially with the provided washing buffers and finally, DNA was eluted from the column using 50 µl of elution buffer. The extracted DNA was stored at -80 °C until qPCR quantification.

3.7.2.2. Generation of mtDNA for standard curves

3.7.2.2. A. Normal PCR amplification of mtDNA

The mtDNA was kindly provided by Dr. Stilla Frede, Department of Anesthesiology, University of Bonn. This mtDNA was extracted from the mitochondria that were isolated from HepG2 cells as described previously (Schafer et al., 2016). This mtDNA was then used as a template to amplify different mitochondrial gene fragments i.e., mt Cytochrome B (mt CytB), mt D-Loop (mt D-Loop) and mt Cytochrome c oxidase subunit I (mt COX-1) by using following primers: mtCytB Fwd: 5'- CCT CCA AAT CAC CAC AGG A -3', Rev: 5'- TGA GTA GAG AAA TGA TCC GTA ATA -3' (Eurogentec, Belgium); mtD-Loop Fwd: 5'- ATC AAC CCT CAA CTA TCA -3', Rev: 5'- ACT GTA ATG TGC TAT GTA -3'; and mt COX-1 Fwd: 5'- TCA TCT GTA GGC TCA TTC -3', Rev: 5'- GGC ATC CAT ATA GTC ACT -3' (Invitrogen, Germany). A 2 µL of mtDNA template was applied to a 50 µL PCR reaction volume containing 40 nM concentrations of the above mentioned primers. The PCR profile was initial denaturation at 95 °C for 5 mins followed by 40 cycles of 95 °C for 1 min, 55 °C

for 1 min and 72 °C for 1.5 min (Bimoetra T3000 Thermocycler, Biometra GmbH, Goettingen, Germany).

3.7.2.2. B. Gel electrophoresis of mtDNA amplicons

The amplicons amplified by the above PCR were confirmed by gel electrophoresis on a 2% agarose gel. A 2 g amount of agarose (Catalog # 35-1020, PeqGold Universal Agarose, VWR, Germany) in 100 mL of the TAE buffer was heated for 2 minutes in a microwave oven. Then, 10 µL of the ethidium bromide was added to 100 mL of the gel solution. After a brief heating (30 secs) and mixing, the gel solution was poured into the gel casting chamber and combs (PEQLAB Biotechnologie GmbH, Erlangen, Germany) were placed to allow the formation of wells. Approximately after 20 minutes, when the gel was polymerized and combs were removed, TAE buffer was added into the chamber until it reaches the edges of the gel. A prestained DNA ladder (15 µL) was loaded into the wells before each mtDNA gene fragment and 25 µL of PCR amplicons were loaded into the respective wells. The chamber was connected to the power supply (BioRad Power PAC 3000, Munich, Germany) and the gel was run for 2 minutes at 100 V. Then, the surface of the gel was completely submerged under the additional TAE buffer and the gel was allowed to run further for 45 minutes at 100 V. After the gel run was complete, the gel was photographed under UV illumination (Bio Doc-IT^{TM} Imaging System, Upland, CA, USA) to confirm the PCR amplification of the respective mtDNA fragments.

3.7.2.2. C. mtDNA PCR product purification

Since for each mt gene fragment, 6 microcentrifuge tubes containing 50 µL of the PCR reaction volumes were prepared and 25 µL of the PCR product was loaded onto the gel and the remaining was pooled for purification. A volume of 100 µL of the pooled PCR product for each mt gene fragment was then purified by High Pure PCR Product Purification Kit (Catalog no. 11732668001, Roche, Germany) by following the manufacturer's instructions. A 100 µL aliquot of the pooled PCR product was mixed with 500 µL of the binding buffer and applied to a high pure filter tube followed by centrifugation at maximum speed for 60 secs. The flow through was discarded and 500 µL of the washing buffer was applied to the filter tube and centrifuged at 13000 g for 1 min. The flow through was again discarded and a similar subsequent wash with 200 µL of the washing buffer was done. The filter tube was connected to a clean 1.5 mL microcentrifuge tube and 50 µL of elution buffer was applied.

After centrifugation for 1 minute at maximum speed, the highly purified DNA product was obtained in the microcentrifuge tube.

3.7.2.2. D. Preparation of mtDNA standard dilutions

Purified mitochondrial gene fragments were then quantified by applying 1 µL of the respective mtDNA to the nanodrop (Thermoscientific NanoDrop 2000 Spectrophotometer, Wilmington, USA) and finally serial dilutions were prepared using sterilized TE buffer (pH 7.4) ranging from 100 ng/mL to 1 pg/mL. The serially diluted mtDNA standard dilutions were then confirmed through normal PCR and gel electrophoresis.

3.7.3. Real time PCR quantification of mtDNA

A real time PCR approach based on Taqman probes labelled with 6-carboxyflourescein (6-FAM) on their 5' end and a non-fluorescent minor groove binder (MGB) on their 3' end was established to quantify serum mtDNA levels. The following primers were employed for qPCR: mt CytB Fwd: 5'- AACCGCCTTTTCATCAATCG -3', Rev: 5'-TAGCGGATGATTCAGCCATAATT -3'; mt D-Loop Fwd: 5'-TCAACTATCACACATCAACTGCAACT 3', Rev: 5'-GGGTAGGTTTGTTGGTATCCTAGTG -3', and mt COX-1 Fwd: 5'-TCATCTGTAGGCTCATTCATTTCTCT -3', Rev: 5'-TCTACTATTAGGACTTTTCGCTTCGA -3'. The sequences of Taqman Probes used were as follows: mt CytB 5'-6-FAM-CCACATCACTCGAGACGT-MGB-Eclipse-3', mt D-Loop: 5'- 6-FAM-CAAAGCCACCCCTCA-MGB-Eclipse-3' and mt COX-1: 5'-6-FAM-TTTTCATGATTTGAGAAGCC-MGB-Eclipse-3'. Both the primers and probes were purchased from Eurogentec, Belgium. A qPCR was carried out using a reaction volume of 12.5 µL consisting of Taqman Universal qPCR mastermix (Life Technologies, Germany), 900 nM of each primer and 100 nM of the respective probes. All the samples and standards were run in triplicates on a 384 microwell plate in a CFX384 Touch^{TM} Real-Time PCR detection system (Bio-Rad Laboratries, Inc.). The qPCR conditions were initial heating at 50 °C for 2 mins, then at 95 °C for 10 mins to activate the Taq Polymerase and finally 50 cycles of 95 °C for 15 sec and 60 °C for 1 min. The data was acquired at the end of each cycle. The serum mtDNA levels were then computed from the respective standard curves for each mitochondrial gene fragment.

3.8. Polychromatic cell surface based flow cytometric immunophenotyping

In addition to DAMPs and cytokine response, we also assessed systemic immune cell response by analyzing peripheral blood of 15 aSAH patients at day 1 and day 7, while once from 10 healthy volunteers by flow cytometry. Different subsets of monocytes and CD4+ T cells were investigated by following the approach described by Maecker et al. (2012) by establishing two flow cytometry panels.

Briefly, the peripheral EDTA anticoagulated blood (3 ml) was lysed with erythrocyte lysis buffer (eBioscience, Germany) at room temperature. After erythrocyte lysis, cells were centrifuged at 350 g for 5 minutes at 4° C and washed with 2 mL of an ice cold FCS flow cytometry buffer (BD Biosciences, Germany) after discarding the supernatant. After washing the cells, cells were resuspended in 1 mL of FCS buffer, counted using countess cell counting slides (Catalog # C10283, Eugene, Oregon, USA) through Countess^{TM} automated cell counter (ThermoFischer scientific, Germany) and adjusted to a final concentration of 1 million cells per 100 µL with FCS buffer. Then, 100 µL aliquots of the cells were dispensed into 5 ml flow cytometry tubes (Catalog # 55.1578, Sarstedt, Germany) after labelling them for stained cells and fluorescence minus one (FMO) controls. For acquisition of single stained compensation controls, one drop of Ultracomp eBeads (eBioscience, Germany) was suspended in 100 µL of FCS buffer. The cells were incubated with Human Fc block pure (Catalog # 564220, BD Biosciences, Germany) for 10 minutes on ice. The panel of anti-human antibodies for monocytes consisted of CD45 APC-H7, CD14 FITC, CD15 PerCP-Cy5.5, CD16 APC, CCR2 BV421, HLA-DR PE-Cy7 (BD Biosciences, USA) and CX3CR1 PE (eBioscience, CA, USA). The panel of anti-human T cell antibodies was comprised of CD45 APC-H7, CD3 PE-Cy7, CD4 BV605, CD25 PerCP-Cy5.5, CD127 FITC, CXCR3 APC, CCR6 BUV737, HLA-DR BV421 and CD38 PE (BD Biosciences, USA). The cells were then sequentially stained for chemokine receptors at room temperature allowing at least 5 minutes interval before next antibody addition as suggested by Jalbert et al. (2013) for both the panels. Afterwards, the cells for both stained samples and FMO controls were stained on ice for 20 minutes using respective master mixes of antibodies prepared in Brilliant Violet Staining buffer (BV Buffer, BD Biosciences, Germany). The list of antibodies used for both panels along with their catalog numbers and clones are given in appendix 10.4. After incubation, cells were washed with 2 mL of FCS buffer and resuspended in approximately 500 µL of the FCS buffer. Live and dead cells discrimination was made using water soluble

Hoechst 33258 dye (Sigma Aldrich, Germany) added (0.1 µg/10 µL) approximately 1 minute before acquisition of each tube.

The cells were then analyzed on LSR Fortessa™ cell analyzer (BD Biosciences, CA, USA) at the Flow Cytometry Core Facility at the Institute of Molecular Medicine, University of Bonn. The flow cytometer settings were validated using 8 peaks SPHERO™ Calibration Particles (Catalog # 559123, BD Biosciences, CA, USA). For both panels, around 350 – 400 thousand CD45+ leucocyte events were acquired for stained cells and 100 thousand CD45+ events for FMO controls. About 10000 all events were acquired for single stained compensation controls. The gating strategy for both the panels is given in appendices 10.5 and 10.6. BD FACSDiva™ v6.2 for windows 7 (BD Biosciences, USA) software was used during acquisition on LSR Fortessa, while the data was analyzed afterwards using FlowJo software version 10.2 for Microsoft Windows 7 (Treestar, Ashland, OR).

3.9. Statistical analysis

The normality of the data was assessed by Shapiro-Wilk test or Kolmogrov-Smirnov test. Normally distributed data were expressed as mean ± SEM, whereas non-normally distributed data was displayed using box plots with whiskers representing median, interquartile range and minimum and maximum values. Student's t test or Mann Whitney *U* test was used for comparison between controls and aSAH patients depending upon the data distribution. For subgroup analysis, the data was dichotomized into two groups and compared by using appropriate test as described by Mathiesen et al., 1997 and Faasbender et al., 2000. Correlations between different measured analytes and aSAH associated characters were assessed by Pearson correlation or Spearmann's rho depending on data distribution. A p value less than 0.05 was considered as a significant difference between the two groups being compared. The data was analyzed by using GraphPad Prism 5.00 for windows (CA, USA) and SPSS 21 (IBM, NY, USA).

4. Results

4.1. Role of DAMPs after aSAH

We have determined the following selective DAMPs members including HMGB1, IL-1α, IL-33 and mtDNA in the systemic circulation of the patients after aSAH.

4.1.1. HMGB1 in systemic circulation

High mobility group box-1 (HMGB1), a non-histone DNA binding protein, is expressed in almost all nucleated cells where it stabilizes DNA and facilitates transcription (Andersson and Tracey, 2011). However, extracellular HMGB1, released either passively from necrotic cells or actively from immune cells, serves as a damage-associated molecular pattern molecule (DAMP) and triggers inflammation via binding to toll-like receptor 4 (TLR4), TLR2 and receptor for advanced glycation end products (RAGE) (Wang et al., 1999; Muhammad et al., 2008; Qiu et al., 2008). HMGB1 is an early mediator of inflammation in experimental cerebral ischemia and its interaction with RAGE contributes to brain damage (Muhammad et al., 2008). HMGB1 is expressed in brain tissue and released early after experimental SAH (Murakami et al., 2011; Sun et al., 2014b). Here, we have investigated the temporal profile of systemic release of HMGB1 over a period of two weeks in aSAH patients.

4.1.1.1. Temporal profile of serum HMGB1 release

This study included 79 consecutive patients with a mean age of 57 years, 37% males and 63% females, who were admitted to hospital after aneurysmal SAH with Hunt and Hess grade I – V. Twenty-eight control patients with spinal stenosis undergoing myelographic examination were enrolled in the study. The detailed characters of these patients are presented in Table 2. The time course of HMGB1 release over 13 days after aSAH is represented in Figure 2. The HMGB1 serum levels were significantly increased from day 1 after aSAH until day 13 when compared to non-SAH controls (Fig. 2). HMGB1 concentration was initially strongly elevated and reached almost double the level found in controls. However, it dropped slowly, but remained significantly high compared to controls until day 13. Up till now, no study showing elevated serum HMGB1 levels over almost two weeks in patients after aSAH covering the peak interval of CVS development has been conducted.

4.1.1.2. HMGB1 is differentially expressed in patients developing CVS

To analyze the time course of HMGB1 release and its association with CVS, we compared HMGB1 concentration of patients who developed CVS with non-CVS on different days after aSAH. HMGB1 concentrations were significantly increased on day 1 in patients who developed CVS compared to patients from the non-CVS group (Fig. 4F). HMGB1 concentrations remained significantly higher until day 13, showing a significant association of HMGB1 with development of CVS starting from day 1 to day 13 (Fig. 4F). However, we did not find any significant difference in a group of patients who developed chronic hydrocephalus except on day 13 (Fig. 4D). Serum HMGB1 concentration showed some significant elevation in patients with DIND only at day 11 and day 13 (Fig. 4E). Similarly, HMGB1 serum concentration in patients who suffered from seizures did not differ significantly than those without seizures (Fig. 4C). There was also no significant increase in HMGB1 concentration in patients who had cerebral ischemia or contracted infections (Fig. 5A, D). Further dichotomization of the cerebral ischemia into interventional cerebral ischemia (interventional CI) or delayed cerebral ischemia (DCI) also revealed no significant difference in serum HMGB1 concentration (Fig. 5B, C). However, such a dichotomy in infections group showed only significant increase of HMGB1 concentration at day 13 in other infections group (presence of UTI, osteomyelitis or in combination with Pneumonia or Meningitis, Fig. 6A), but no significant increase was associated with Pneumonia or Meningitis (Fig. 5E, F). Interestingly, comparison of aSAH patients with Pneumonia and other infections, although showed only at day 1 a significant increase in HMGB1 concentration in Pneumonia patients, represented a non-significant gradual fading pattern of HMGB1 concentration in patients with Pneumonia and a non-significant gradual rise in patients with other infections (Fig. 6B). Intriguingly, different parameters, including sex, aneurysm localization and presence of intracerebral and/ or intraventricular bleeding, in addition to aSAH did not influence serum HMGB1 concentrations (Fig. 3A, C, E, F, 4A). Furthermore, patients with less severe aSAH grades (H&H grades I-II, good grade) differed in HMGB1 levels only on day 11 (Fig. 3D). Interestingly, treatment modality also did not influence serum HMGB1 levels (Fig. 3B). A previous study has shown a correlation of serum HMGB1 on admission with clinical outcome after one year (Zhu et al., 2012b). We, however, did not find any association of serum HGMB1 with clinical outcome at discharge (Fig. 6C, D, 7A, B).

4.1.1.3. Correlation of systemic HMGB1 with leukocytes and IL-6

The source of serum HMGB1 might be peripheral leukocytes or brain via disrupted blood-brain barrier. Hence, we quantified peripheral leukocytes to analyze association with serum HMGB1. Interestingly, serum HMGB1 concentrations significantly correlated with peripheral leukocytes (Fig. 7D) indicating the leukocytes as possible source of systemic HMGB1. Systemic HMGB1 can potentially induce release of other cytokines including IL-6. We quantified IL-6 serum levels to analyze its correlation with HMGB1. Serum IL-6 levels showed a significant correlation with HMGB1 (Fig. 7C), indicating the possibility of a pleiotropic effect of HMGB1.

4.1.1.4. ROC Curve analysis of peripheral HMGB1 for CVS prediction

As serum HMGB1 levels displayed a significant association with CVS, we performed an ROC curve analysis for the prediction of CVS using serum HMGB1 levels. The ROC curves showed significant area under the curve (AUC) almost approaching to 70% on day 1, 3, 5 and 7 (Fig. 8). ROC analysis revealed that serum HMGB1 on day 1, with a cutoff value of 4.8 ng/ml, could predict CVS with a sensitivity of 55% and a specificity of 72%. This suggests that systemic HMGB1 levels may be a predictor of CVS after aneurysmal subarachnoid hemorrhage.

Table 2. Baseline characteristics of the control and aSAH patients

Spinal stenosis control patients (n)	**28**
Age (mean ± SD)	67.42 ± 13.68
Female gender, n (%)	15 (53.57%)
aSAH patients (n)	**79**
Age (mean ± SD)	56.72 ± 11.84
Female gender, n (%)	50 (63.29%)
Aneurysm treatment modality	
Surgical clipping, n (%)	39 (49.37%)
Endovascular coiling, n (%)	40 (50.63%)
Intracerebral bleed (ICB), n (%)	15 (18.99%)
Intraventricular hemorrhage (IVH), n (%)	10 (12.66%)
IVH+ICB, n (%)	11 (13.92%)
Cerebrovascularspasm, n (%)	44 (55.70%)
Delayed Ischemic Neurological Deficits, n (%)	28 (35.44%)
Infarcts (Cerebral Ischemia, CI), n (%)	32 (40.51%)
Interventional CI, n (%)	16 (20.25%)
Delayed Cerebral Ischemia (DCI), n (%)	16 (20.25%)
VP shunt dependent hydrocephalus, n (%)	25 (31.65%)
Seizures, n (%)	23 (29.11%)
Infections, n (%)	28 (35.44%)
Pneumonia, n (%)	15 (18.99%)
Meningitis, n (%)	7 (8.86%)
Others (UTI, Osteomyelitis etc), n (%)	6 (7.59%)
Hess and Hunt Grade, median	**3**
1: Asymptomatic/mild headache, n (%)	5 (6.33%)
2: Moderate/severe headache, n (%)	24 (30.38%)
3: Drowsiness/confusion, n (%)	22 (27.85%)
4: Stupor, n (%)	13 (16.46%)
5: Coma/decerebrate posturing, n (%)	15 (18.99%)
Fischer Grade, median	**3**
1: No blood detected, n (%)	1 (1.27%)
2: Diffuse SAH, <1 mm thick, n (%)	2 (2.53%)

3: Diffuse SAH, ≥1 mm thick, n (%)	67 (84.81%)
4: Clot in ventricle/parenchyma, n (%)	9 (11.39%)
Glasgow outcome scale (GOS), median	**3**
5: Good recovery, n (%)	33 (41.77%)
4: Moderate disability, n (%)	6 (7.59%)
3: Severe disability, n (%)	24 (30.38%)
2: Vegetative state, n (%)	10 (12.66%)
1: Death, n (%)	6 (7.59%)
Modified Rankin scale (mRS), median	**3**
0: No symptoms at all, n (%)	2 (2.53%)
1: No significant disability, n (%)	25 (31.65%)
2: Slight disability, n (%)	8 (10.13%)
3: Moderate disability, n (%)	7 (8.86%)
4: Moderately severe disability, n (%)	17 (21.52%)
5: Severe disability, n (%)	14 (17.72%)
6: Death, n (%)	6 (7.59%)

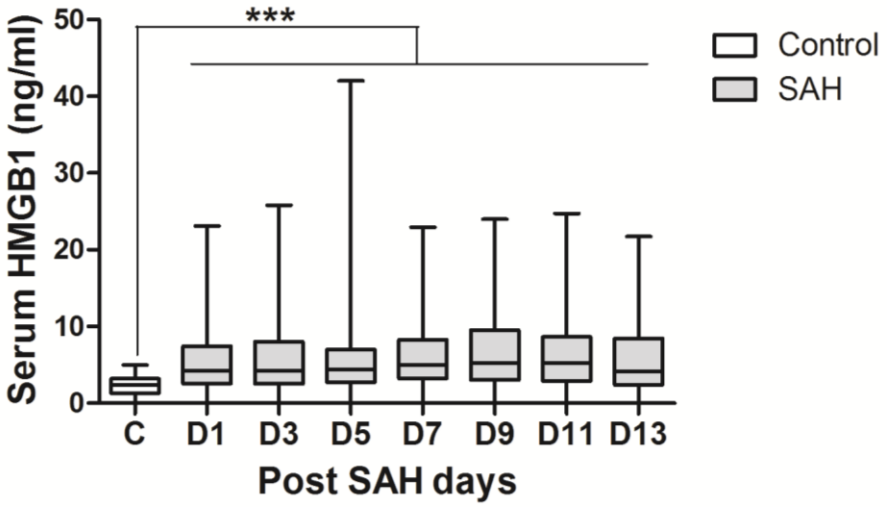

Figure 2: Elevated serum HMGB1 levels in patients over two weeks after aSAH when compared to controls, Mann Whitney *U* test, $p < 0.05$ was considered as a significant difference, controls n = 28, aSAH n = 79.

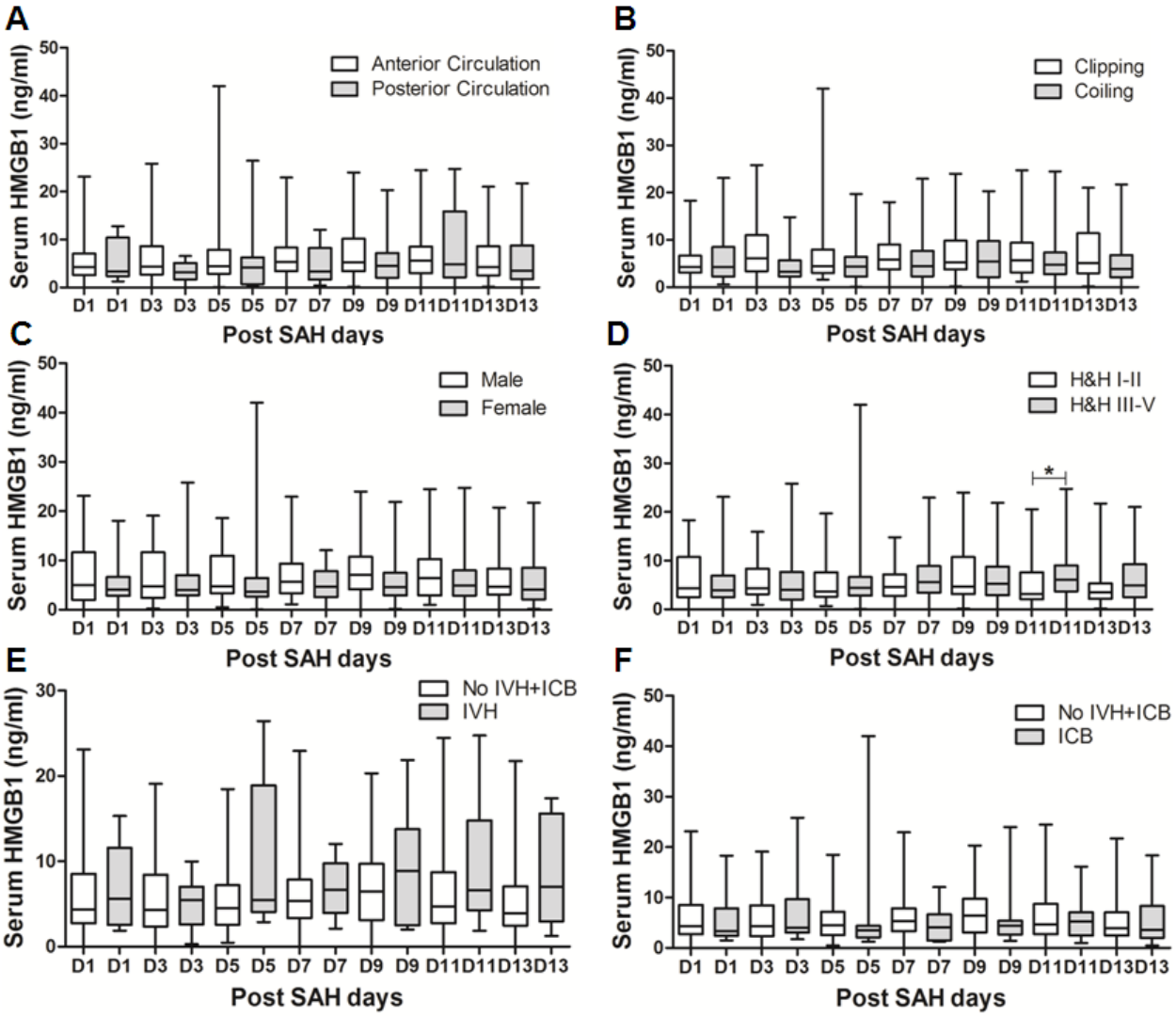

Figure 3: A. Comparison of serum HMGB1 levels in patients with localization of aneurysm in anterior (n = 68) vs. posterior circulation (n = 11); **B.** clipping (n = 39) vs. coiling (n = 40); **C.** males (n=29) vs. females (n=50); **D.** good aSAH grade (H&H I-II, n = 29) vs. poor grade (H&H III-V, n = 50); **E.** no intraventricular hemorrhage and intracerebral bleeding (No IVH+ICB, n = 43) vs. intraventricular hemorrhage (IVH, n = 10); **F.** No IVH+ICB (n = 43) vs. intracerebral bleeding (ICB, n = 15); Mann Whitney *U* test, $p < 0.05$ was considered as a significant difference.

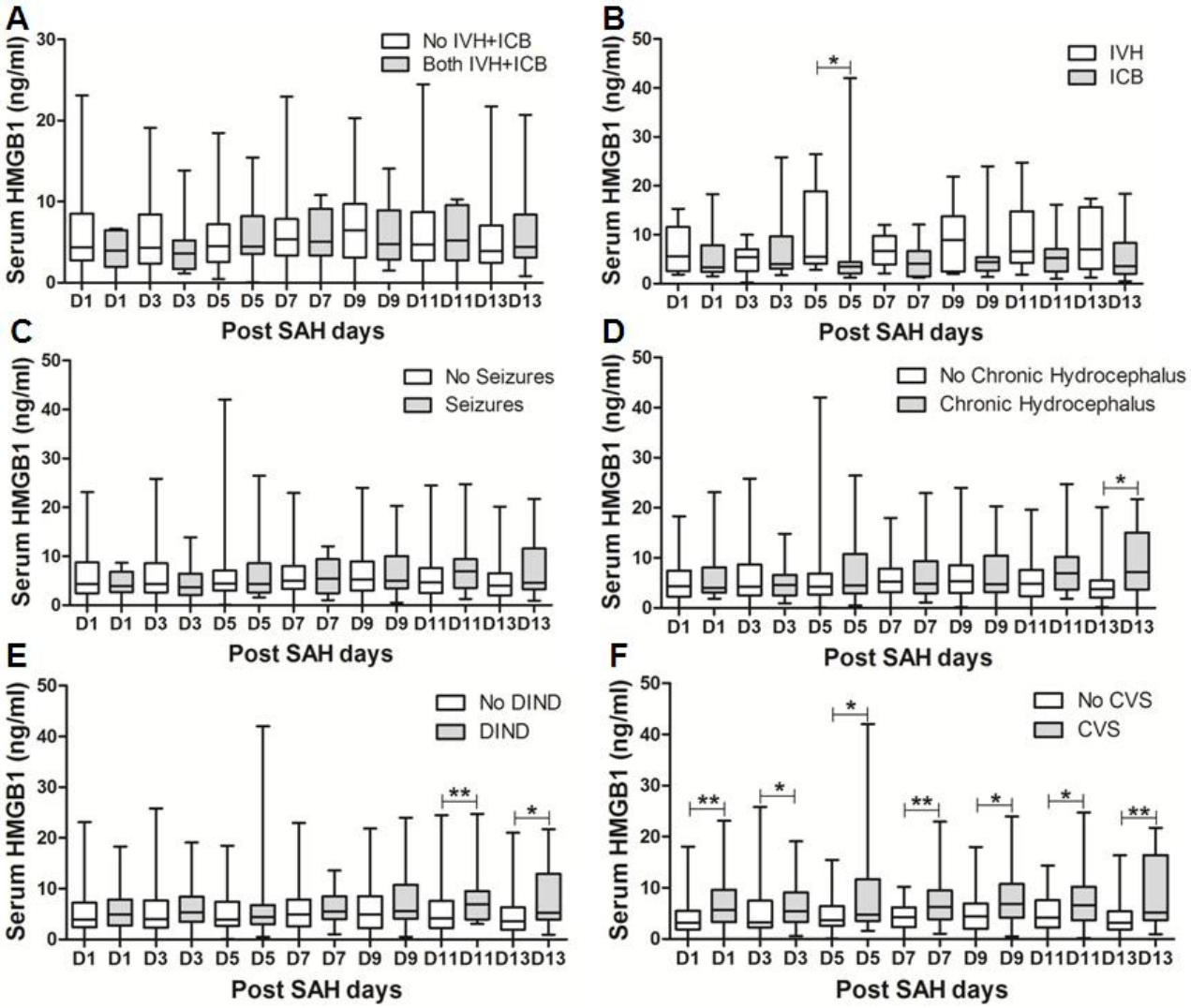

Figure 4: A. Comparison of serum HMGB1 levels in patients with: No IVH+ICB (n = 43) vs. both intraventricular hemorrhage and intracerebral bleeding (ICB, n = 11); **B.** IVH (n = 10) vs. ICB (n = 15); **C.** no seizures (n = 56) vs. seizures (n = 23); **D.** no ventriculoperitoneal-shunt dependent chronic hydrocephalus (n = 54) vs. ventriculoperitoneal-shunt dependent chronic hydrocephalus (n = 25); **E.** no delayed ischemic neurological deficits (DIND, n = 51) vs. DIND (n = 28); **F.** no cerebral vasospasm (CVS, n = 35) vs. CVS (n = 44); Mann Whitney *U* test, $p < 0.05$ was considered as a significant difference.

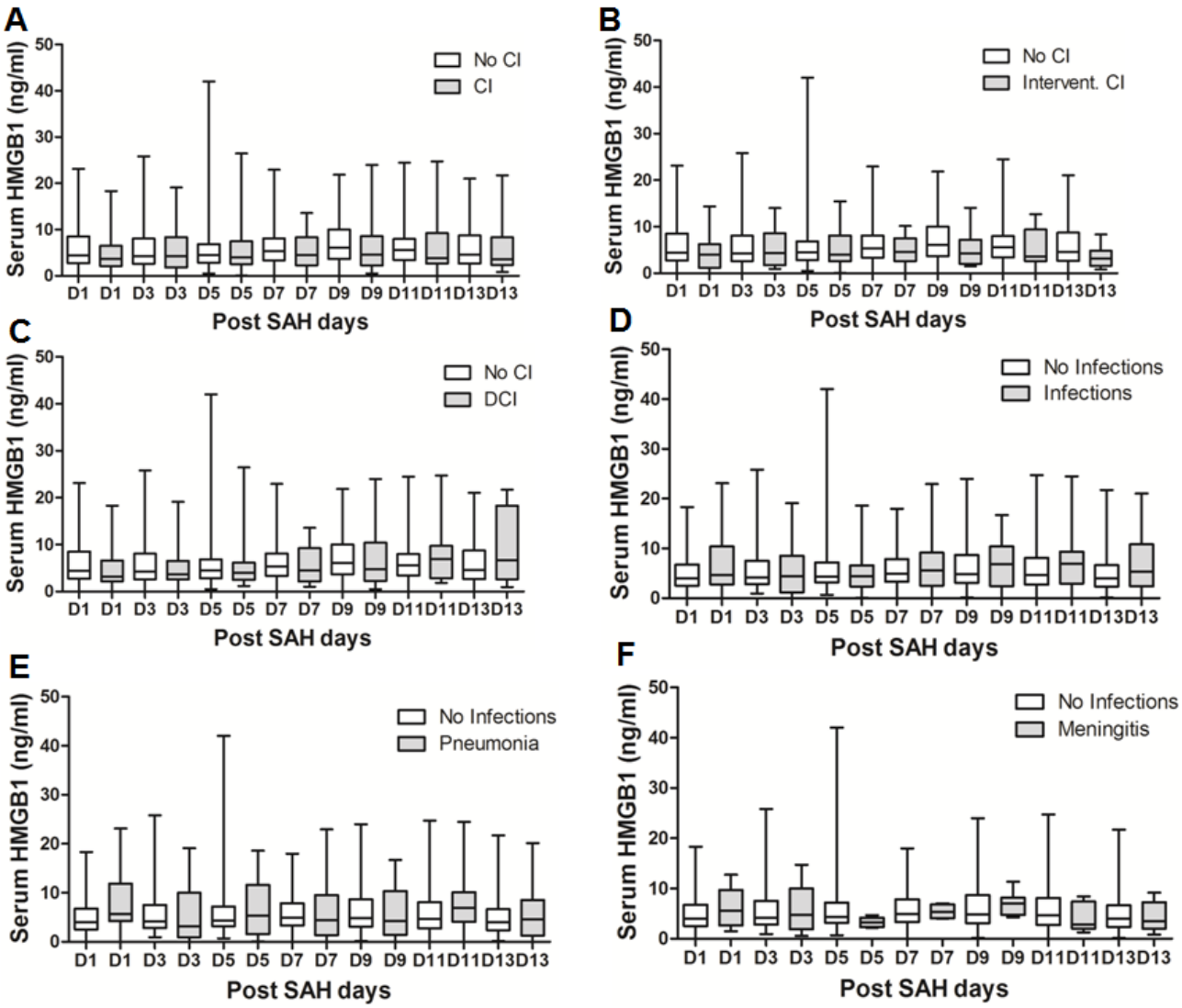

Figure 5: A. Comparison of serum HMGB1 levels in patients with no cerebral infarction/ischemia (CI, n = 47) vs. CI (n = 32); **B.** no CI (n = 47) vs. interventional CI (n = 16); **C.** no CI (n = 47) vs. delayed cerebral ischemia (DCI, n = 16); **D.** no infections (n = 51) vs. infections (n = 28); **E.** no infections (n = 51) vs. pneumonia (n = 15); **F.** no infections (n = 51) vs. meningitis (n = 7); Mann Whitney *U* test, $p < 0.05$ was considered as a significant difference.

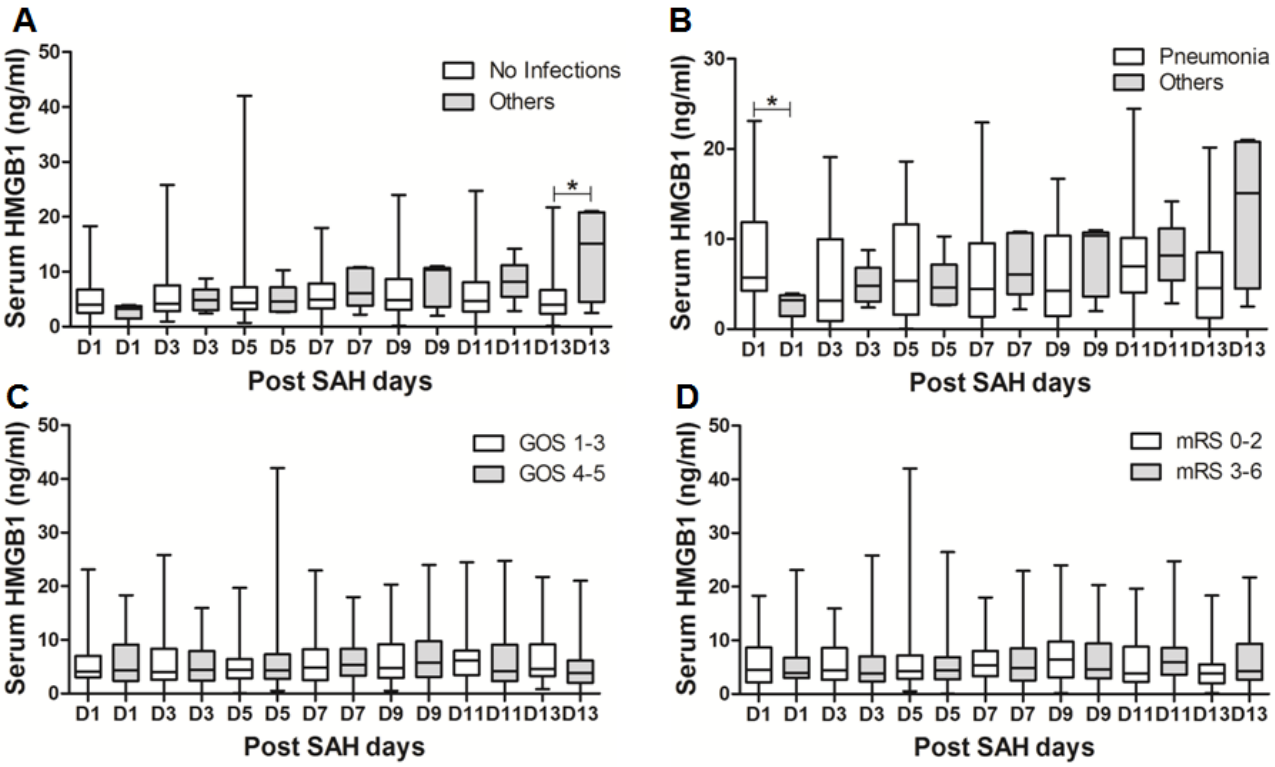

Figure 6: A. Comparison of serum HMGB1 levels in patients with no infections (n = 51) vs. others (other infections either in combination with pneumonia, meningitis or alone such as UTI, osteomyelitis etc., n = 6); **B.** pneumonia (n = 15) vs. others (n = 6); **C.** poor clinical outcome (GOS 1-3, n = 40) vs. good clinical outcome (GOS 4-5, n = 39) as assessed by Glasgow Outcome Scale (GOS); **D.** good clinical outcome (mRS 0-2, n = 35) vs. poor clinical outcome (mRS 3-6, n = 44) as assessed by modified Rankin Scale (mRS); Mann Whitney *U* test, $p < 0.05$ was considered as a significant difference.

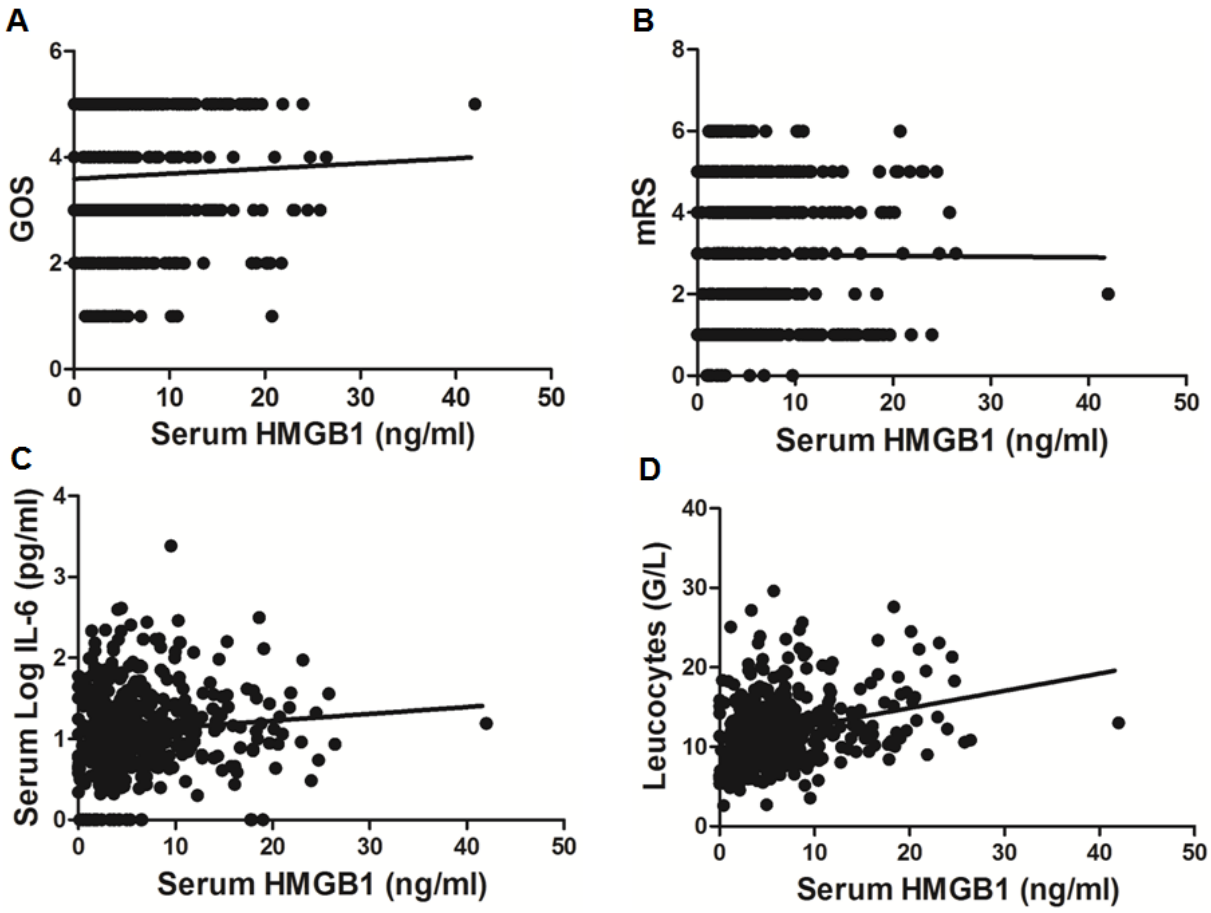

Figure 7: A. Correlation of cumulative serum HMGB1 levels vs. Glasgow Outcome Scale (GOS) (Spearman's rho = 0.006, p = 0.896, n = 524); **B.** Correlation of cumulative serum HMGB1 levels vs. modified Rankin Scale (mRS) (Spearman's rho = 0.025, p = 0.572, n = 524); **C.** Correlation of cumulative serum HMGB1 levels vs. serum log IL-6 levels (Spearman's rho = 0.105, p < 0.017, n = 517); **D.** Correlation of cumulative serum HMGB1 levels vs. leucocyte counts (Spearman's rho = 0.288, p < 0.000, n = 461).

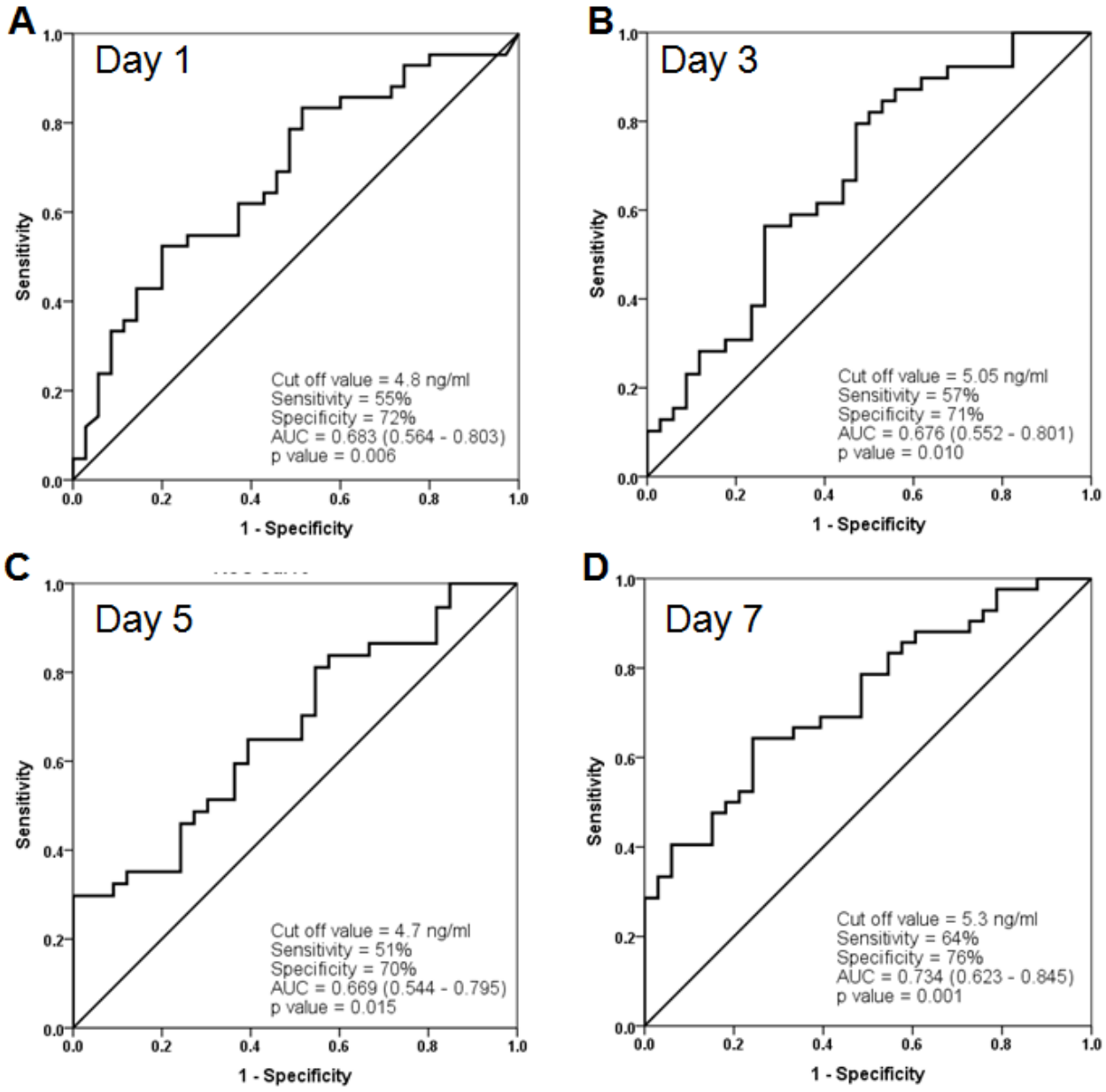

Figure 8: ROC curves for predicting CVS on day 1, 3, 5 and 7 after aSAH.

4.1.2. Serum IL-1α and IL-33

Both IL-1α and IL-33 are dual action cytokines with transcriptional properties inside cellular milieu, while DAMPs activity in the extracellular environment. We have initially screened both serum IL-1α and IL-33 in the sera from 10 aSAH patients at days 1, 3, 5, 7, 9, 11 and 13 and in controls as well. Both the cytokines were either non-detectable or measured below the lowest standard of the standard curve standards ran during the ELISAs. This prompted us to precluded further analysis of the sera from remaining patients. Savarraj et al. (2017a) have also shown that serum levels of IL-33 are non-detectable after aSAH.

4.1.3. Mitochondrial DNA

Tissue damage during early brain injury may lead to release of damage associated molecular pattern molecules (DAMPs) that may play a key role to initiate and sustain inflammation during the course of aSAH. Mitochondrial DNA (mtDNA) shares homology to bacterial DNA owing to unmethylated CpG motifs and acts as a DAMP (Zhang et al., 2010). Mitochondrial DNA can bind to TLR 9 on immune cells and upregulate systemic inflammation (Zhang et al., 2010). In this part of the study, we investigated the cell free circulating mtDNA in the peripheral blood of aSAH patients and its association with post aSAH complications and clinical outcome. Systemic levels of cell free circulating mtDNA fragments such as mt Cytochrome B (mt CytB), mt Cytochrome c oxidase subunit-1 (mt COX-1) and mt D-Loop were quantified in the DNA isolated from the serum of aSAH and control patients by real time PCR using Taqman probes. The baseline characters of aSAH patients are represented in Table 3.

4.1.3.1. Mitochondrial Cytochrome B (mt CytB)

The mt CytB levels were higher initially at day 1, 3, and 5, but did not reach significance as compared to healthy controls (HC) (Fig. 9A). However, at day 7 mt CytB levels were significantly raised in aSAH patients as compared to HC and remained significantly high till day 13 (1.4, 1.4, 1.6, 1.7, 2.1, 1.9, and 1.8 folds at days 1, 3, 5, 7, 9, 11 and 13, respectively). The mt CytB DNA appeared to be slowly released into systemic circulation, peaking at day 9 and then started to decline (Fig. 9A).

For further analysis, mt CytB levels were dichotomized based on gender, severity of aSAH, treatment modality, location of aneurysms, development of different complications and clinical outcome. Serum levels of mt CytB tended to be higher in male patients with occasional significant differences seen on day1, day 3 and day 9 (Fig. 10A). A significant difference existed only on day 1 between the patients who have ICB as compared to No IVH+ICB and on day 3, although the levels were still high, but did not reach significance ($p = 0.075$, Fig. 10B). There was no impact of infections on mt CytB levels and further, subgrouping based on the development of pneumonia, meningitis, and other infections (presence of other infections such as UTI or in combination with pneumonia or meningitis) revealed only significant difference at day 9 between aSAH patients with pneumonia (Fig. 10D). Similarly, patients who developed cerebral infarction, here referred to as cerebral

ischemia (CI), did not display any significant changes in mt CytB levels. However, upon further subgrouping into interventional CI (aSAH patients who developed CI due to aneurysm repair) or DCI (aSAH patients where CI cause can be ascribed to CVS) showed significant difference between patients with Interventional CI compared to No CI at day 3, day 9 and day 13, while on day 11 p value was 0.05. This suggests that mt CytB levels are sensitive to CI resulting from neurosurgical clipping or endovascular coiling.

4.1.3.2. Mitochondrial D-Loop (mt D-Loop)

A region of mitochondrial D-Loop approximately 132 bp was amplified. The levels of mt D-Loop were significantly higher from day 1 and remained high till day 13 in aSAH group as compared to HC (2.2, 2.2, 2.4, 2.3, 3.1, 2.7, and 2.4 folds on days 1, 3, 5, 7, 9, 11 and 13, respectively) (Fig. 9B).

An analysis analogous to mt CytB was performed with serum mt D-Loop levels. Serum mt D-Loop levels were only significantly high on day 9 in males and on day 13 in patients with severe aSAH (H&H III-V) (Fig. 11A, B). Like mt CytB, serum mt D-Loop levels were only downregulated in patients with pneumonia on day 9 compared to patients without infections and on day 1 there was a non-significant difference ($p = 0.088$) (Fig. 11C). Patients who experienced post aSAH seizures have lower levels of mt D-Loop DNA levels with significant differences on day 3 and day 7 (Fig. 11D). A similar trend was seen in patients who required ventriculoperitoneal shunt (VP-Shunt) placement due to development of chronic hydrocephalus on day 1 and day 9 (Fig. 11E). Interestingly, mt D-Loop DNA levels seem to be higher with significance difference only on day 9 in patients with good clinical outcome (mRS 0-2) (Fig. 11F).

4.1.3.3. Mitochondrial Cytochrome c oxidase subunit-1 (mt COX-1)

A third mitochondrial gene fragment about 136 bp was selected from mtDNA encoding mt COX-1. Similar to mt D-Loop, mt COX-1 levels were significantly increased after aSAH compared to HC early at day 1 and remained elevated till day 13 (2.3, 1.8, 2.1, 2.5, 3.2, 3.2, 2.7 folds on days 1, 3, 5, 7, 9, 11 and 13, respectively) (Fig. 9C). The release pattern of mt COX-1 in systemic circulation after aSAH was almost identical to mt D-Loop, however, all the gene fragments reached peak levels at day 9 and then, started to decline. Interestingly, this

represents an important time period during which complications arise and lead to deterioration of aSAH patients.

Patients with ICB and who have DIND showed significantly higher mt COX-1 levels on day 1 and day 11, respectively (Fig. 12A & B). Seizures have a similar impact on mt COX-1 levels as was evident with mt D-Loop, however, only significant difference existed at a single time point (day 7) (Fig. 12C). Levels of mt COX-1 were significantly downregulated at day 3 and day 9 in patients developing CI and further, dichotomy of CI patients revealed significant downregulation of mt COX-1 levels in patients with interventional CI compared to No CI at day 3, day 9 – 13 (Fig. 12D, E).

4.1.3.4. Correlations

Some significant correlations were observed for serum mtDNA genes measured at different days with aSAH patient associated characters, ensuing complications and clinical outcome at discharge (Table 4). Cumulative levels measured over two weeks of mt CytB, mt D-Loop and mt COX-1 DNA showed some weak, but significant correlations with different aSAH patient characters, complications and clinical outcome represented in table 5.

Table 3. Baseline characters of aSAH patients recruited for mtDNA quantification

aSAH (n)	80
Age (years) (mean±SD)	56.97 (±12.00)
Females (%)	62.5%
Treatment modality	
Neurosurgical clipping (%)	48.8%
Endovascular coiling (%)	51.3%
Intraventricular hemorrhage: IVH (%)	12.5%
Intracerebral bleeding: ICB (%)	20.0%
ICB and IVH (%)	13.8%
Hunt and Hess grade (median)	3
1 (%)	6.3%
2 (%)	30.0%
3 (%)	28.8%
4 (%)	16.3%
5 (%)	18.8%
Fischer grade (median)	3
1 (%)	1.3%
2 (%)	2.5%
3 (%)	85.0%
4 (%)	12.5%
CVS (%)	55.0%
Cerebral Ischemia (%)	41.3%
Intervention related CI (%)	21.3%
DCI (%)	20.0%
Seizures (%)	30.0%
VP-Shunt dependent hydrocephalus (%)	31.3%
Infections (%)	36.3%
Pneumonia (%)	18.8%
Meningitis (%)	8.8%
Others (%)	8.8%
Pneumonia+Meningitis (%)	2.5%
Pneumonia+UTI (%)	2.5%
Meningitis+UTI (%)	1.3%
Misc. (Osteomyelitis, sepsis) (%)	2.5%
DIND (%)	35.0%
Aneurysm location	
Anterior circulation (%)	86.3%
Posterior circulation (%)	13.8%
GOS (median)	3
1 (%)	8.8%
2 (%)	12.5%
3 (%)	30.0%
4 (%)	7.5%
5 (%)	41.3%
mRS (median)	3

0 (%)	2.5%
1 (%)	31.3%
2 (%)	10.0%
3 (%)	8.8%
4 (%)	21.3%
5 (%)	17.5%
6 (%)	8.8%

Table 4. Correlations of different mtDNA genes (mt CytB, mt D-Loop and mt COX-1) with different aSAH associated parameters

Sr. #	Log mtDNA	aSAH characters	No. of XY pairs	Spearman rho	P value	95% CI
1	CytB D1	Female	80	-0.254	0.023	-0.454 to 0.030
2	CytB D1	Leucocytes D13	61	-0.315	0.014	-0.531 to -0.061
3	CytB D3	Female	79	-0.221	0.051	-0.427 to 0.007
4	CytB D3	Leucocytes D5	76	0.323	0.005	0.098 to 0.516
5	CytB D5	Female	77	-0.243	0.033	-0.448 to -0.014
6	CytB D5	CRP D13	32	-0.381	0.031	-0.650 to -0.027
7	CytB D7	Female	79	-0.225	0.046	-0.431 to 0.002
8	CytB D9	Female	78	-0.2316	0.041	-0.437 to -0.003
9	CytB D9	CI	78	-0.239	0.035	-0.444 to -0.011
10	CytB D3	Interventional CI	79	-0.243	0.031	-0.446 to -0.017
11	CytB D9	Interventional CI	78	-0.326	0.004	-0.517 to -0.105
12	CytB D9	Leucocytes D11	57	0.306	0.020	0.042 to 0.531
13	CytB D9	β-Blockers	78	0.240	0.034	0.012 to 0.444
14	CytB D11	β-Blockers	73	0.237	0.044	0.000 to 0.448
15	CytB D11	CaCBs	73	0.264	0.024	0.029 to 0.471
16	CytB D11	Leucocytes D11	55	0.375	0.005	0.114 to 0.588
17	CytB D13	β-Blockers	70	0.257	0.032	0.016 to 0.470
18	CytB D13	Interventional CI	70	-0.284	0.017	-0.492 to -0.045
19	CytB D13	CRP D1	36	-0.392	0.018	-0.645 to -0.063
20	CytB D13	CRP D13	28	-0.426	0.024	-0.696 to -0.052
21	D-Loop D1	Chronic Hydrocephalus	80	-0.280	0.012	-0.476 to -0.058
22	D-Loop D1	CRP D1	43	-0.309	0.044	-0.564 to 0.000
23	D-Loop D1	Leucocytes D13	61	-0.278	0.030	-0.501 to -0.020
24	D-Loop D5	CRP D9	38	-0.337	0.038	-0.599 to -0.010
25	D-Loop D7	CRP D11	33	0.360	0.040	0.008 to 0.632
26	D-Loop D9	Chronic	78	-0.289	0.010	-0.486 to -0.065

		Hydrocephalus				
27	D-Loop D9	GOS	78	0.288	0.011	0.063 to 0.485
28	D-Loop D9	mRS	78	-0.274	0.015	-0.473 to -0.048
29	D-Loop D9	Leucocytes D1	77	0.230	0.045	-0.001 to 0.437
30	D-Loop D11	CaCBs	73	0.240	0.041	0.003 to 0.451
31	D-Loop D13	CRP D1	35	-0.405	0.016	-0.656 to -0.073
32	COX1 D1	Leucocytes D13	61	-0.276	0.032	-0.499 to -0.018
33	COX1 D3	CRP D3	41	-0.328	0.036	-0.584 to -0.013
34	COX1 D3	Seizures	79	-0.224	0.047	-0.430 to 0.003
35	COX1 D5	CRP D1	41	-0.319	0.042	-0.577 to -0.003
36	COX1 D7	Seizures	79	-0.246	0.029	-0.448 to -0.019
37	COX1 D9	CI	78	-0.234	0.039	-0.439 to -0.005
38	COX1 D3	Interventional CI	79	-0.297	0.008	-0.491 to -0.075
39	COX1 D9	Interventional CI	78	-0.323	0.004	-0.514 to -0.101
40	COX1 D11	Interventional CI	73	-0.336	0.004	-0.531 to -0.108
41	COX1 D11	DIND	73	0.242	0.039	0.006 to 0.453
42	COX1 D11	Leucocytes D11	55	0.305	0.024	0.0353 to 0.534
43	COX1 D13	Interventional CI	70	-0.335	0.005	-0.534 to -0.102
44	COX1 D13	CRP D1	36	-0.351	0.036	-0.616 to -0.016

Table 5. Correlations of cumulative mtDNA levels of mt CytB, D-Loop and COX-1 measured over two weeks with different aSAH patient associated characters, complications and clinical outcome.

Log mt DNA	Complications & outcome	Spearman r	P value	95% CI
D-Loop	GOS	0.113	0.010	0.024 to 0.200
D-Loop	mRS	-0.104	0.019	-0.191 to -0.015
D-Loop	Female Gender	-0.152	0.001	-0.238 to -0.064
D-Loop	Pneumonia	-0.1330	0.003	-0.219 to -0.044

D-Loop	Chronic hydrocephalus	-0.128	0.004	-0.215 to -0.039
D-Loop	Seizures	-0.152	0.001	-0.238 to -0.064
D-Loop	Leucocytes	0.120	0.0110	0.025 to 0.212
CytB	CVS	0.101	0.019	0.014 to 0.187
CytB	CI	-0.105	0.020	-0.190 to -0.018
CytB	Interventional CI	-0.179	<0.000	-0.262 to -0.094
CytB	Pneumonia	-0.149	0.001	-0.233 to -0.062
CytB	Others	0.1013	0.019	0.014 to 0.186
CytB	Fischer	0.113	0.009	0.026 to 0.198
CytB	Female Gender	-0.2012	<0.000	-0.283 to -0.116
CytB	Leucocytes	0.123	0.008	0.030 to 0.213
COX-1	CI	-0.150	0.000	-0.232 to -0.066
COX-1	Interventional CI	-0.208	<0.000	-0.288 to -0.125
COX-1	Fischer	0.100	0.018	0.015 to 0.183
COX-1	Infections	-0.117	0.005	-0.201 to -0.033
COX-1	Pneumonia	-0.107	0.011	-0.191 to -0.022
COX-1	Meningitis	-0.0834	0.049	-0.168 to 0.002
COX-1	Seizures	-0.094	0.026	-0.178 to -0.009

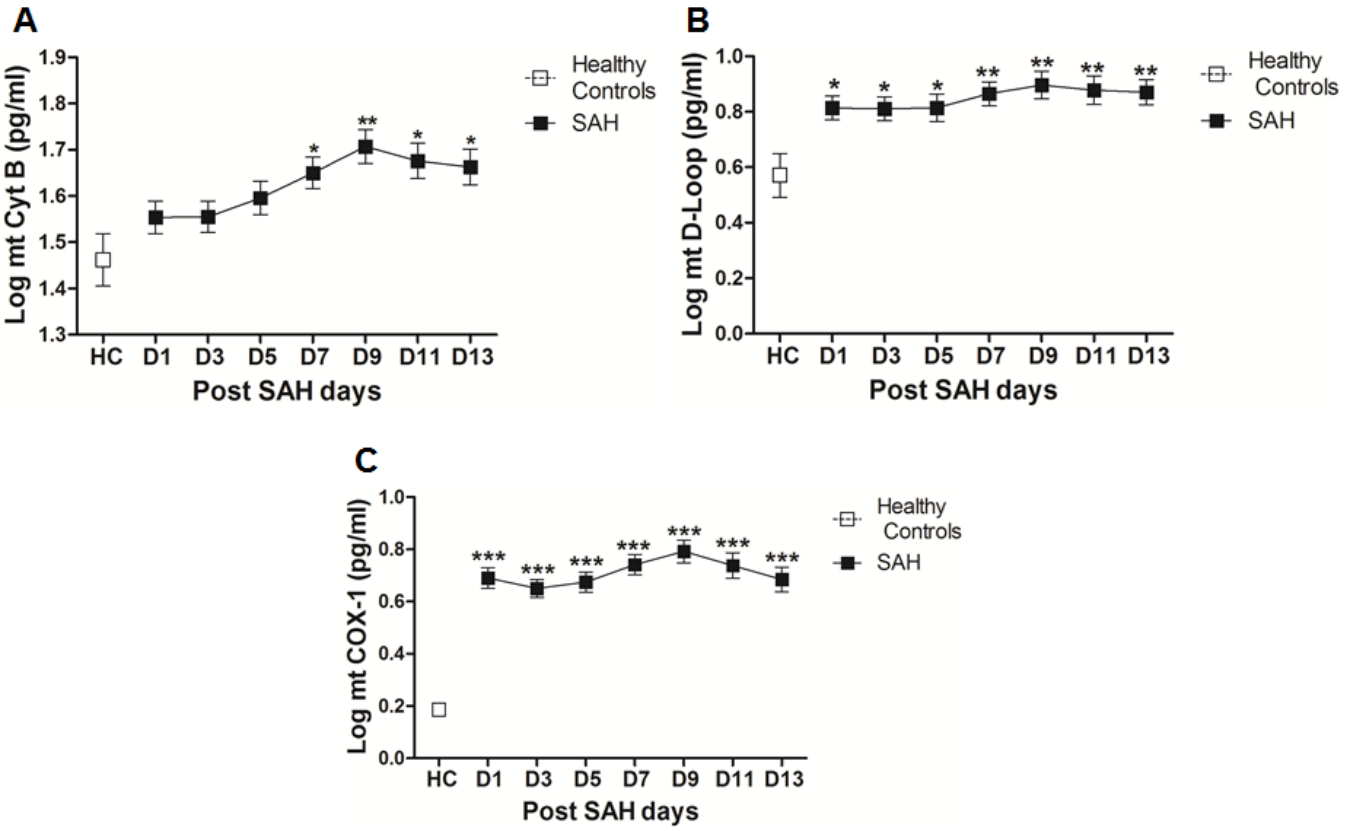

Figure 9: Comparison of serum mtDNA among healthy controls (HC, n =18) and aSAH patients (n = 80). **A.** Serum mt CytB levels among healthy controls and aSAH patients. **B.** Serum mt D-Loop levels among healthy controls and aSAH patients. **C.** Serum mt COX-1 levels among healthy controls and aSAH patients. Student's t test, $p < 0.05$ was considered as a significant difference.

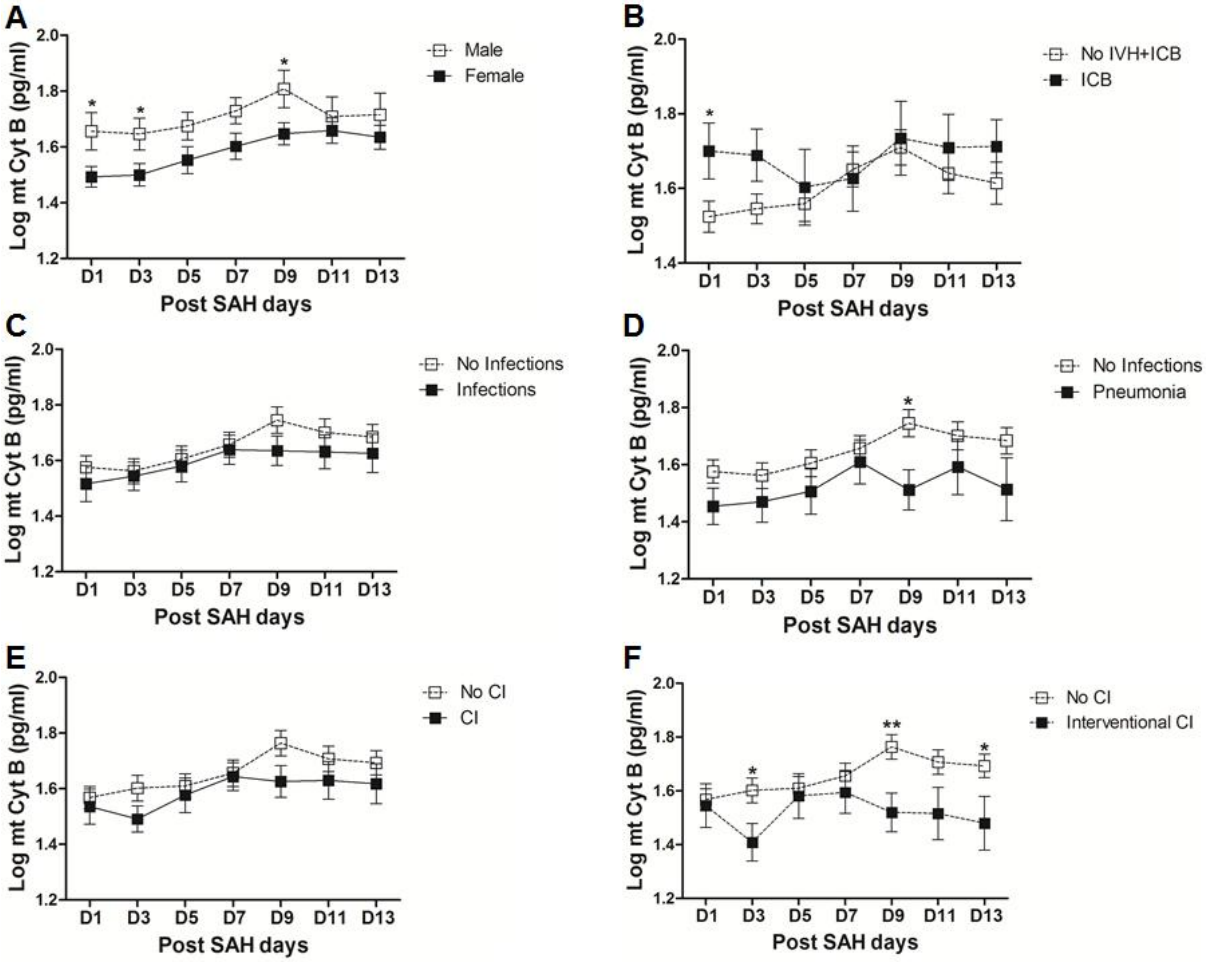

Figure 10: Comparison of mt CytB levels among different aSAH subgroups. **A.** Comparison of mt CytB levels among male (n = 30) and female (n = 50) aSAH patients. **B.** Comparison of mt CytB levels in patients showing No IVH+ICB (n = 43) and only ICB (n = 16). **C.** Comparison of mt CytB levels among patients developing infections (n = 29) and no infections (n = 51). **D.** Comparison of mt CytB levels among patients with no infections (n = 51) and Pneumonia (n = 15). **E.** Comparison of mt CytB levels in aSAH patients showing CI (n = 33). **F.** Comparison of mt CytB levels among patients who have no CI (n = 47) and interventional CI (n = 17). Unpaired t test, $p < 0.05$ was considered as a significant difference.

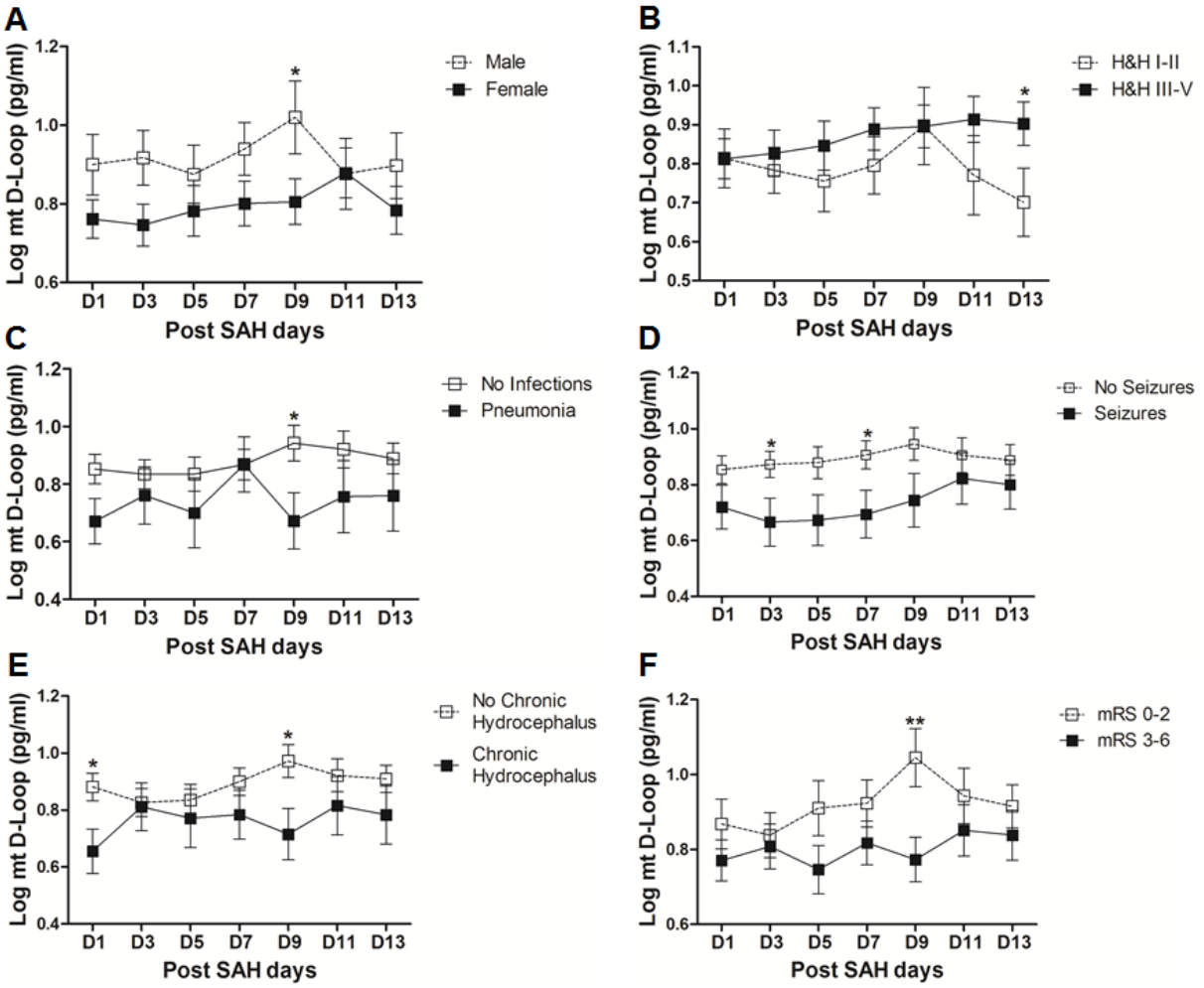

Figure 11: Comparison of mt D-Loop levels among different aSAH subgroups. **A.** Comparison of mt D-Loop levels among male (n = 30) and female (n = 50) aSAH patients. **B.** Comparison of mt D-Loop levels among patients with severe aSAH (H&H III-V, n = 51) and less severe aSAH (H&H I-II, n = 29). **C.** Comparison of mt D-Loop levels among patients with no infections (n = 51) and Pneumonia (n = 15). **D.** Comparison of mt D-Loop levels among patients who developed seizures (n = 24) and no seizures (n = 56). **E.** Comparison of mt D-Loop levels among patients who developed chronic hydrocephalus (n = 25) and who do not (n = 55). **F.** Comparison of mt D-Loop levels among patients with good clinical outcome (mRS 0-2, n = 35) and poor outcome (mRS 3-6, n = 45). Unpaired t test, $p < 0.05$ was considered as a significant difference.

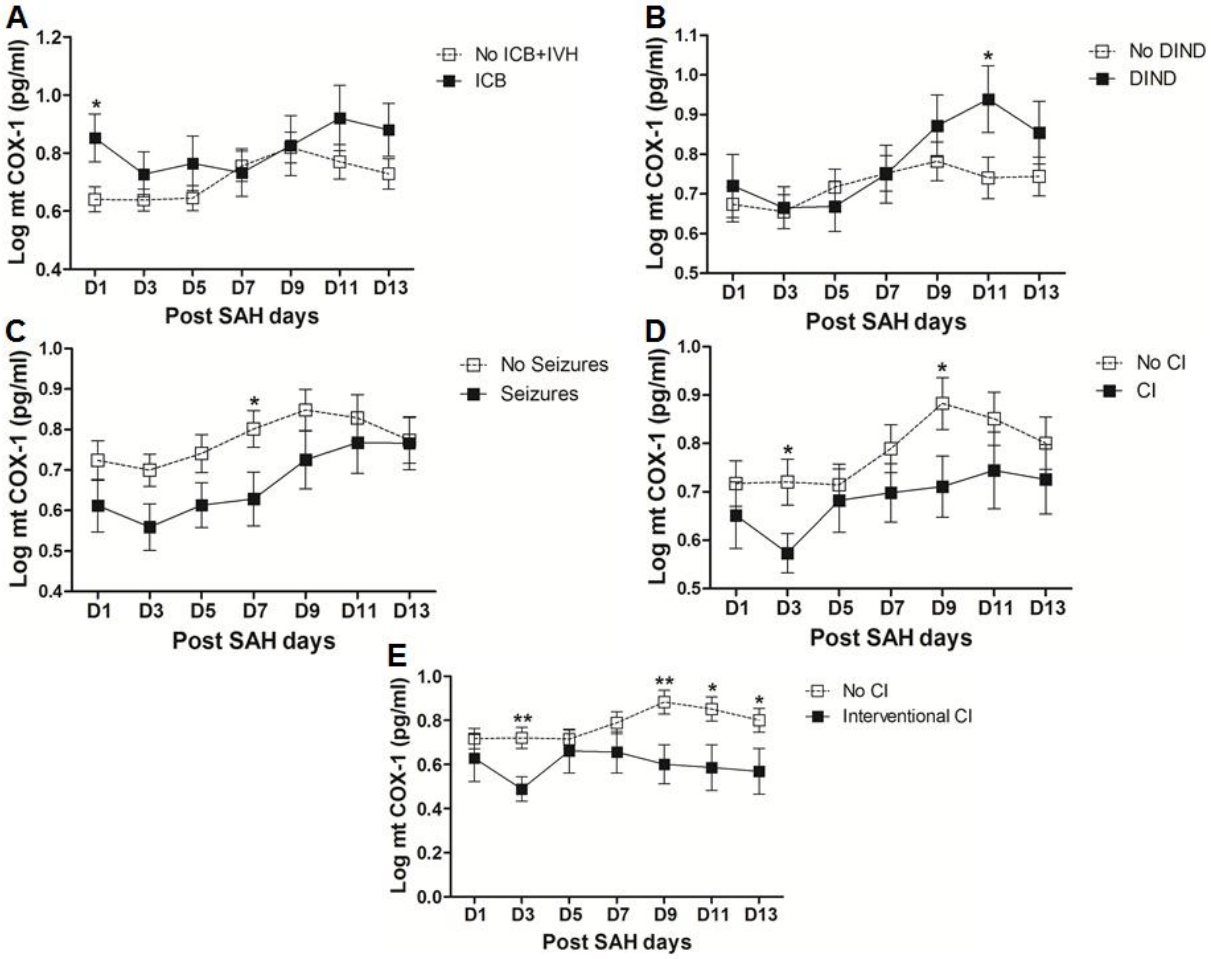

Figure 12: Comparison of mt COX-1 levels among different aSAH subgroups. **A.** Comparison of mt COX-1 levels in aSAH patients with No IVH+ICB (n = 43) and only ICB (n = 16). **B.** Comparison of mt COX-1 levels among patients with No DIND (n = 52) and with DIND (n = 28). **C.** Comparison of mt COX-1 levels among aSAH patients developing seizures (n = 24) and no seizures (n = 56). **D.** Comparison of mt COX-1 levels in aSAH patients showing CI (n = 33) and no CI (n = 47). **E.** Comparison of mt COX-1 levels among patients who have no CI (n = 47) and interventional CI (n = 17). Unpaired t test, $p < 0.05$ was considered as a significant difference.

4.2. Investigation of systemic cytokines after aSAH

Selected cytokines that were either not previously investigated or scarce information was available relating to their association with post-aSAH complications and clinical outcome were also included in this study. We have determined the systemic levels of IL-23, IL-17, IL-10, and CXCL5 at day 1 and at day 7 post aSAH, while IL-6 levels determination was carried out on days similar to HMGB1 and mtDNA.

4.2.1. Serum IL-23

The baseline characters of aSAH patients whose sera were employed for IL-23, IL-17 and CCL5 determination are represented in table 6. We analyzed serum IL-23 levels in aSAH patients at two different time points, at day 1 as an early time point and at day 7 as a late time point during the course of the disease. Serum IL-23 levels were significantly raised in aSAH patients on both time points as compared to control patients (Fig. 13). The mean (±SEM) serum IL-23 levels among controls, aSAH patients at day 1 and day 7 were 8.23 (± 1.99) pg/ml, 28.07 (± 3.40) pg/ml and 31.70 (± 3.83) pg/ml respectively.

4.2.1.1. Serum IL-23 in post-aSAH complications

For further analysis, we dichotomized the aSAH patients based on their clinical severity (Hunt and Hess grade), treatment modality (clipping and coiling), aneurysm location (anterior or posterior circulation), and post-aSAH complications. There was no significant difference in IL-23 levels between good grade (Hunt and Hess I-II) vs poor grade (Hunt and Hess grade III-V) aSAH patients at day 1, but serum IL-23 levels were significantly raised at day 7 in good grade aSAH patients (Fig. 14A). Serum IL-23 levels were raised significantly at day 1 in aSAH patients presenting with intracerebral bleeding and this difference non-significantly persisted at day 7 compared to aSAH patients without ICB (Fig. 14B). Serum IL-23 levels were significantly higher in patients who were treated with neurosurgical clipping compared to endovascular coiling at day 7 (Fig. 14C) showing the possibility that craniotomy and operative manipulation may induce the IL-23. Serum IL-23 levels were slightly lower in patients who developed seizures at day 1, however, at day 7 serum IL-23 levels were significantly lowered in aSAH patients with seizures (Fig. 14D). In other post-aSAH complications such as CVS, DIND, CI, and infections, no significant changes in serum IL-23 levels were observed (data not shown). Further subcategorizing the patients who developed

CI into interventional CI and DCI groups showed that serum IL-23 levels were significantly higher early at day 1 in DCI group compared to interventional CI, whereas serum IL-23 levels at day 7 were non-significantly higher in DCI group (Fig. 14E). Similarly, we subcategorized the patients who developed infections into pneumonia, meningitis and others (other infections or a co-occurrence with pneumonia and meningitis). Serum IL-23 levels were significantly reduced in patients who developed other infections or their co-occurrence with pneumonia and meningitis at both days of assessment (Fig. 14F).

4.2.1.2. Serum IL-23 and post-aSAH clinical outcome

Assessment of clinical outcome using Glasgow outcome scale (GOS) and modified Rankin scale (mRS) at discharge from the hospital showed no difference in serum IL-23 levels in patients with good clinical outcome (GOS 5-4; mRS 0-2) as compared to patients with poor clinical outcomes (GOS 3-1; mRS 3-6) (Fig. 15). However, at day 7, serum IL-23 levels were inclined to non-significantly rise in good outcome patients.

Table 6. Characteristics of control and aSAH patients

Controls (n)	24
Age (years) (mean±SD)	67.06 (±13.54)
Females (%)	45.8%
aSAH (n)	80
Age (years) (mean±SD)	58.29 (±11.8)
Females (%)	61.3%
Treatment modality	
Neurosurgical clipping (%)	48.8%
Endovascular coiling (%)	51.3%
Intraventricular hemorrhage: IVH (%)	13.8%
Intracerebral bleeding: ICB (%)	18.8%
ICB and IVH (%)	13.8%
Hunt and Hess grade (median)	3
1 (%)	7.5%
2 (%)	30.0%
3 (%)	28.8%
4 (%)	16.3%
5 (%)	17.5%
Fischer grade (median)	3
1 (%)	1.3%
2 (%)	2.5%
3 (%)	83.8%
4 (%)	12.5%
CVS (%)	56.3%
Cerebral Ischemia (%)	42.5%
Intervention related CI (%)	21.3%
DCI (%)	21.3%
Seizures (%)	28.8%
VP-Shunt dependent hydrocephalus (%)	31.3%
Infections (%)	36.3%
Pneumonia (%)	18.8%
Meningitis (%)	10.0%
Others (%)	7.5%
Pneumonia+Meningitis (%)	2.5%
Pneumonia+UTI (%)	2.5%
Meningitis+UTI (%)	1.3%
Misc. (Osteomyelitis) (%)	1.3%
DIND (%)	35.0%
Aneurysm location	
Anterior circulation (%)	86.3%
Posterior circulation (%)	13.8%
GOS (median)	3.5
1 (%)	8.8%
2 (%)	11.3%
3 (%)	30.0%
4 (%)	7.5%
5 (%)	42.5%
mRS (median)	3

0 (%)	2.5%
1 (%)	32.5%
2 (%)	10.0%
3 (%)	8.8%
4 (%)	21.3%
5 (%)	16.3%
6 (%)	8.8%

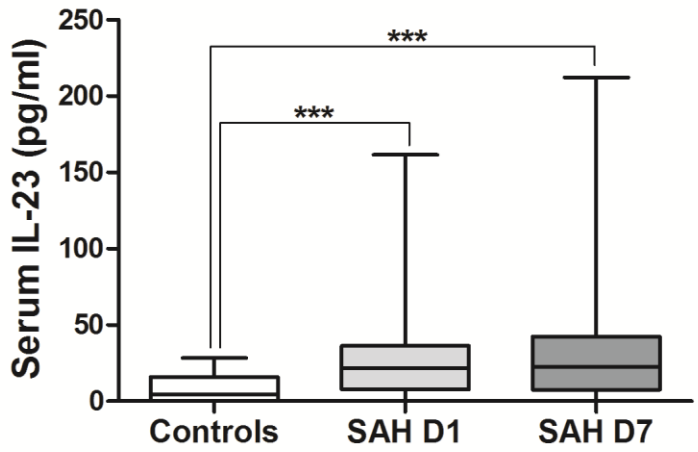

Figure 13: Serum IL-23 levels in control patients (n = 24) and aSAH patients (n = 80) at day 1 and day 7. Mann-Whitney *U* test; *p* value <0.0001 at day 1 and <0.0001 at day 7. SAH D1= Subarachnoid hemorrhage at day one, SAH D7= Subarachnoid hemorrhage at day seven.

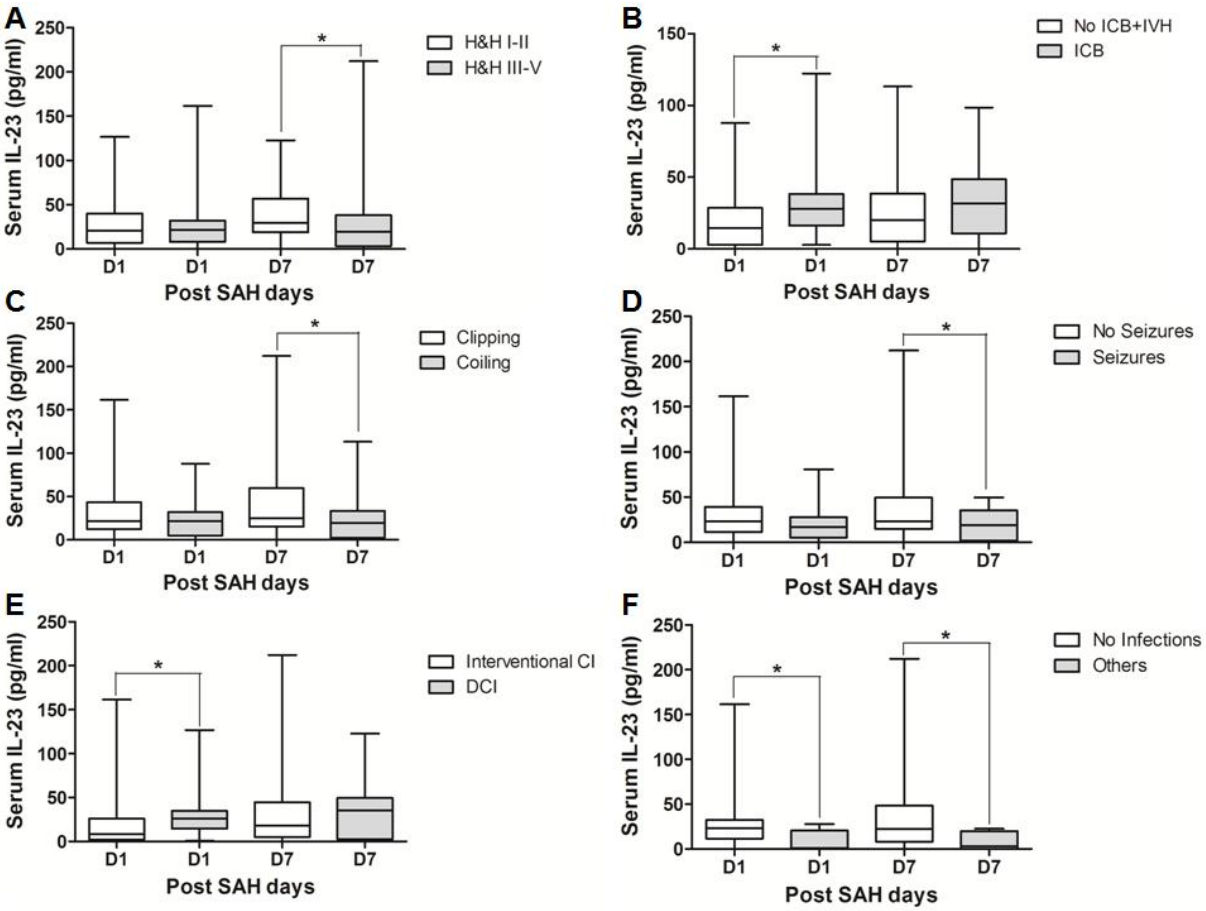

Figure 14: A. Serum IL-23 levels at day 1 and day 7 after aSAH in patients: with good grade aSAH (Hunt and Hess I-II, n = 30) and poor grade aSAH (Hunt and Hess III-V, n = 50); **B.** with Intracerebral bleeding (ICB, n = 15) compared to who had no intraventicular and intracerebral bleeding (No ICB+IVH, n = 43); **C.** treated by neurosurgical clipping (n = 39) and endovascular coiling (n = 41); **D.** developing seizures (n = 23) and no seizures (n = 57); **E.** who had interventional CI (n = 17) and DCI (n = 17); **F.** with other infections (n = 6) compared to no infections (n = 51); Mann-Whitney *U* test; **p* value < 0.05 was considered as significant difference.

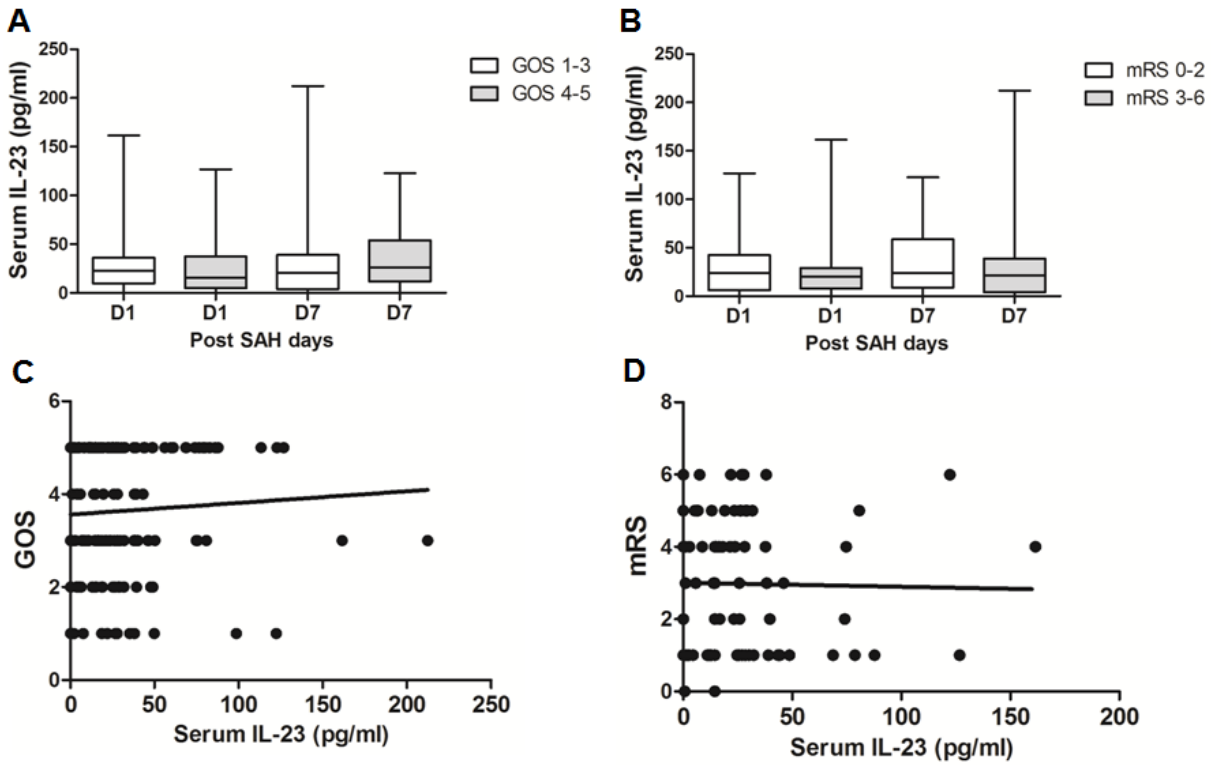

Figure 15: A. Serum IL-23 levels at day 1 and day 7 after aSAH in patients presenting with good outcome (GOS 4-5, n = 40) and poor outcome (GOS 1-3, n = 40) as assessed by GOS; **B.** Serum IL-23 levels at day 1 and day 7 after aSAH in patients presenting with good outcome (mRS 0-2, n = 36) and poor outcome (3-6, n = 44) as assessed by mRS; Mann-Whitney *U* test, **p* value <0.05 was considered as significant difference. **C and D.** No significant Spearman correlation of serum IL-23 (pg/ml) with GOS (n = 160, Spearman's rho = 0.063, $p = 0.429$) and mRS (n = 160, Spearman's rho = -0.006, $p = 0.955$) was observed.

4.2.2. Serum IL-17

Serum IL-17 levels were significantly raised in aSAH patients on day 1 and day 7 as compared to control patients (Fig. 16). Serum IL-17 levels among control and aSAH patients at day 1 and day 7 were found to be 1.33 (±0.27) pg/ml, 3.23 (±0.20) pg/ml and 4.54 (±0.43) pg/ml respectively. Serum IL-17 levels, unlike serum IL-23 levels, were significantly higher at day 7 as compared to day 1 (Fig. 16).

4.2.2.1. Serum IL-17 in post-aSAH complications

An analysis of serum IL-17 after dichotomy in different subgroups showed some significant differences (Fig. 17). Serum IL-17 levels were non-significantly higher at day 7 in poor grade aSAH (H&H III-V, Fig. 17A). Serum IL-17 levels were also significantly higher at day 1 in aSAH patients involving aneurysms of anterior circulation compared to posterior circulation aneurysm rupture (Fig. 17B). Interestingly, serum IL-17 levels were significantly reduced at day 1 in patients having additional intracerebral bleeding and intraventricular hemorrhage, but at day 7 they were significantly higher compared to patients without ICB and IVH (Fig. 17C). The patients who developed CVS, chronic hydrocephalus and seizures did not show any significant difference in serum IL-17 levels (data not shown). Interestingly, serum IL-17 levels were significantly decreased at day 7 in patients who developed delayed ischemic neurological deficits (DIND, Fig. 17D). Furthermore, serum IL-17 levels were significantly elevated in aSAH patients who had interventional CI compared to DCI later on day 7 (Fig. 17E). In contrast to serum IL-23 levels, serum IL-17 levels were significantly elevated in other infections group at both day 1 and day 7 as compared to patients who did not contract any infections (Fig. 17F). Further dissection of the data revealed that serum IL-17 levels were also significantly higher in patients who developed other infections compared to those with pneumonia at day 1 and day 7 and with meningitis at day 7 (Fig. 18A, B).

4.2.2.2. Serum IL-17 and post-aSAH clinical outcome

To analyze if serum IL-17 has a correlation with clinical outcome, we evaluated clinical outcome with two well known scales including Glasgow outcome scale and modified Rankin scale. The dichotomy of patients in good outcome and poor outcome showed no difference in serum IL-17 levels among the patients with good clinical outcome (GOS = 4–5; mRS = 0–2) and poor outcome (GOS = 1–3; mRS = 3–6) as shown in Fig. 18C, D. Pooled serum IL-17

levels did not show any significant correlation with GOS and mRS (Fig. 18E, F, respectively). However, at day 7, serum IL-17 levels tended to non-significantly decrease in patients with good clinical outcome and vice versa.

4.2.2.3. Correlations between serum IL-23 and IL-17 with different baseline characteristics of aSAH patients and post-aSAH complications

The significant correlations of serum IL-23 and serum IL-17 with different aSAH associated parameters at day 1 and day 7 were assessed by non-parametric Spearman's correlation and are shown in Table 7.

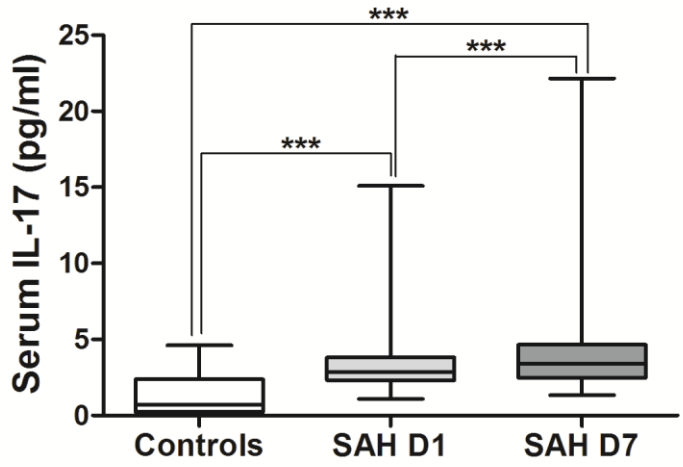

Figure 16: Serum IL-17 levels in control patients (n = 24) and aSAH patients (n = 80) at day 1 and (n = 79) day 7. Mann-Whitney *U* test, *p* value <0.0001 at day 1 and <0.0001 at day 7. Wilcoxon signed rank test for comparison at day 1 and day 7, *p* value <0.0001. SAH D1= Aneurysmal Subarachnoid hemorrhage at day one, SAH D7= Aneurysmal Subarachnoid hemorrhage at day seven.

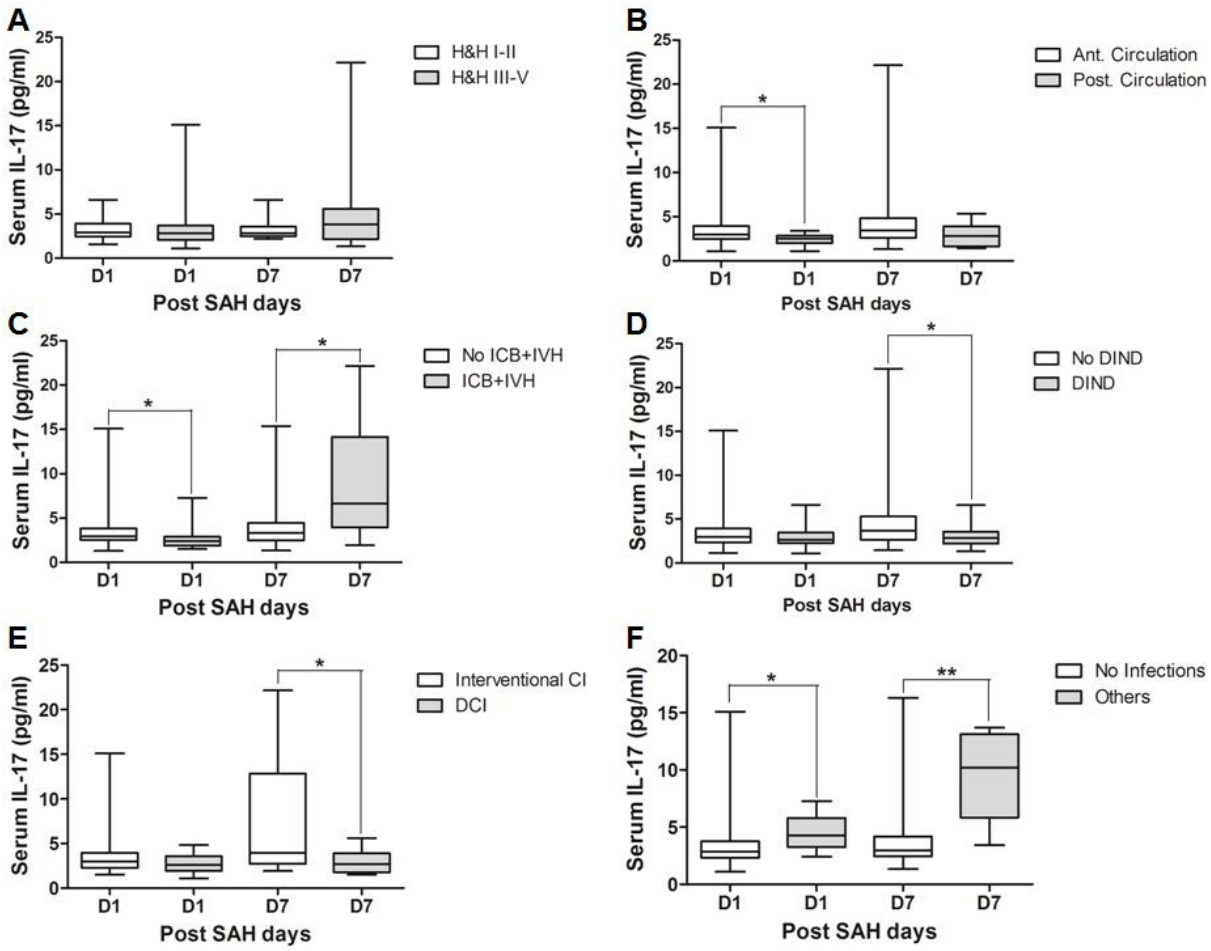

Figure 17: A. Serum IL-17 levels at day 1 and day 7 after aSAH in patients with: good grade SAH (Hunt and Hess I-II, n = 29) and poor grade SAH (Hunt and Hess III-V, n = 50); **B.** anterior circulation aneurysms (n = 68) vs. posterior circulation aneurysms (n = 11); **C.** No ICB+IVH (n = 43) and IVH+ICB (n = 11); **D.** DIND (n = 27) and no DIND (n = 52); **E.** interventional CI (n = 17) and DCI (n = 16); **F.** other infections (n = 6) compared to no infections (n = 51); Mann-Whitney *U* test, **p* value <0.05 was considered as significant difference.

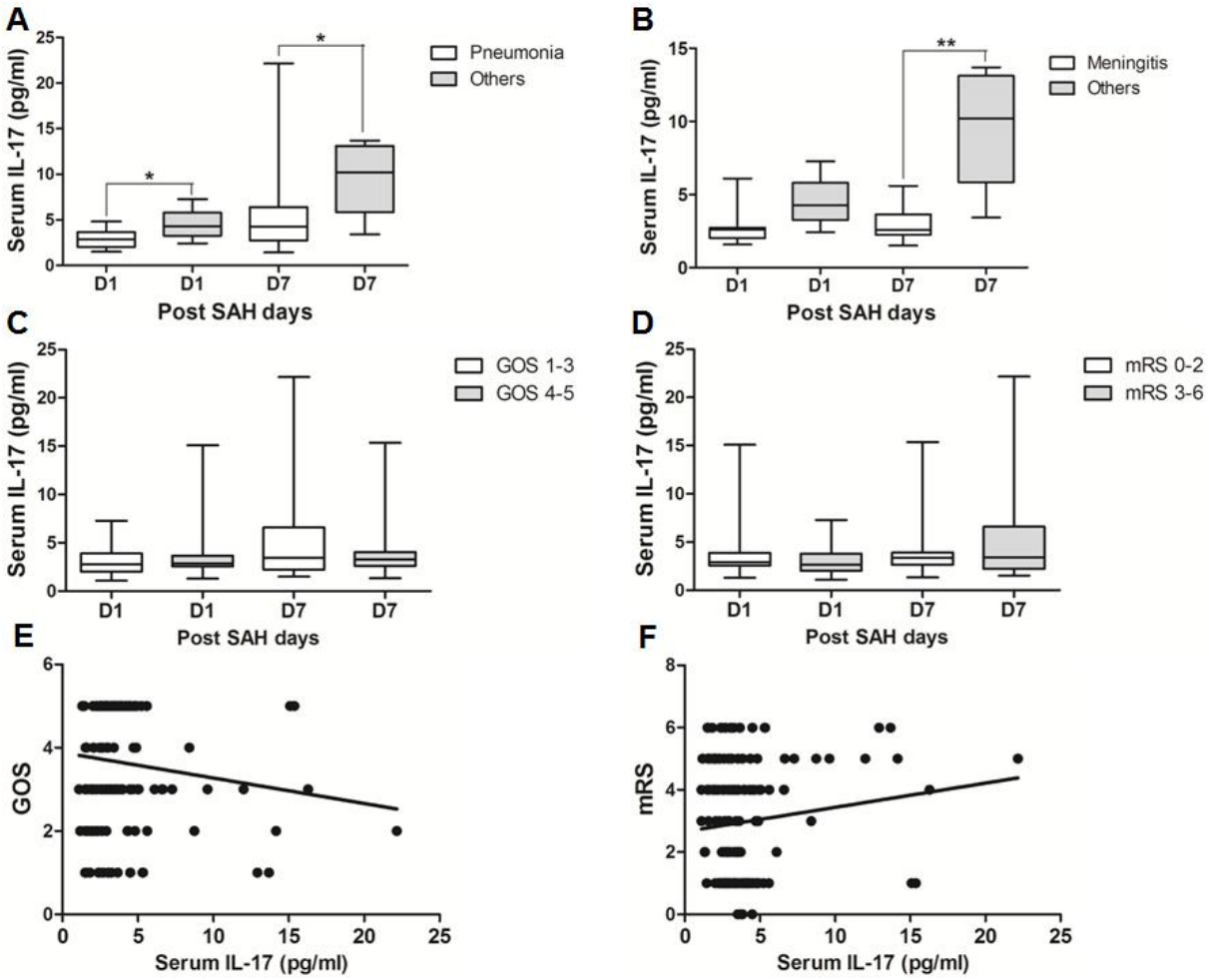

Figure 18: A. Serum IL-17 levels at day 1 and day 7 after aSAH in patients with: Pneumonia (n = 15) compared to other infections (n = 6); **B.** Meningitis (n = 8) compared to other infections (n = 6); **C.** good outcome (GOS 4-5, n = 40) and poor outcome (GOS 1-3, n = 40) as assessed by GOS; **D.** good outcome (mRS 0-2, n = 36) and poor outcome (mRS 3-6, n = 44) as assessed by mRS. Mann-Whitney *U* test, **p* value <0.05 was considered as significant difference. **E and F.** No significant Spearman correlation of serum IL-17 (pg/ml) with GOS (n = 159, Spearman's rho = 0.007, *p* = 0.932) and mRS (n = 159, Spearman's rho = -0.03, *p* = 0.710) was observed.

Table 7. Correlations of different aSAH associated parameters with serum IL-23 and IL-17 levels

Sr. #	Serum IL-23/IL-17 at Day 1 & Day 7	aSAH characters	No. of XY pairs	Spearman's rho	P value
1	Serum IL-23 day 1	Interventional CI	80	-0.238	0.033
2	Serum IL-23 day 7	H&H grade	80	-0.256	0.022
3	Serum IL-23 day 7	Fischer grade	80	-0.313	0.005
4	Serum IL-23 day 7	Age	80	-0.268	0.016
5	Serum IL-23 day 7	Endovascular coiling	80	-0.245	0.028
6	Serum IL-23 day 7	Seizures	80	-0.222	0.048
7	Serum IL-17 day 1	Posterior circulation	80	-0.249	0.026
8	Serum IL-17 day 7	H&H grade	79	0.261	0.020
9	Serum IL-17 day 7	DIND	79	-0.292	0.009
10	Serum IL-17 day 7	Interventional CI	79	0.236	0.036
11	Serum IL-17 day 7	DCI	79	-0.229	0.042

4.2.3. Serum IL-6

IL-6 is a well-known pro-inflammatory cytokine that is secreted early after aSAH (Helbok et al., 2015; Niwa and Osuka, 2016). IL-6 levels in cerebrospinal fluid (CSF) of patients after aSAH have been shown to be associated with occurrence of cerebral vasospasm and clinical outcome (Osuka et al., 1998; Schoch et al., 2007; Sarrafzadeh et al., 2010; Helbok et al., 2015; Niwa and Osuka, 2016; Wu et al., 2016a; Zeiler et al., 2017). Moreover, elevated early serum IL-6 levels predict the unfavourable clinical outcome (Muroi et al., 2013; Hollig et al., 2015b; Hollig et al., 2015a; Kao et al., 2015). However, detailed studies exploring the kinetics of IL-6 release in systemic circulation over the 2 weeks after aSAH and its association with post-aSAH complications and its impact on early clinical outcome prediction are lacking. Here, we analyzed the systemic IL-6 levels over two weeks (covering the peak time to develop the post-aSAH complications) after bleeding and its role in post-aSAH complications. We have determined the serum IL-6 levels in aSAH patients and healthy controls. The detailed characters of aSAH patients are shown in Table 8. Serum IL-6 levels were significantly raised in systemic circulation after aSAH as compared to healthy controls and remained persistently high till day 13 of assessment (Fig. 19). For further analysis, the data was dichotomized as described above for other cytokines. Serum IL-6 levels remained significantly raised in patients presenting with poor H&H grade, reflecting severity of aSAH (Fig. 20E). There was no significant difference in IL-6 levels among patients undergoing neurosurgical clipping or endovascular coiling (Fig. 20A) and same was true for gender comparison reflecting the fact that gender and craniotomy do not alter the systemic IL-6 levels (Fig. 20B). Serum IL-6 levels, only at day 1 and day 5, were significantly higher in patients having anterior circulation aneurysms (Fig. 20C). Most of the studies describe mean age of aSAH patients around 55 years (Fassbender et al., 2001; Macedo et al., 2010; Galea et al., 2017b). So, we have dichotomized patients above or below 55 years of age and found that serum IL-6 levels tend to be higher in patients with age above 55 years. This tendency reached to a significant difference at day 5 – day 7 reflecting the possibility of more severe systemic inflammation at higher age (Fig. 20D). Serum IL-6 levels were significantly raised in aSAH patients who present with additional intraventricular or intracerebral bleeding or both simultaneously at several days in comparison to patients who only had subarachnoid bleed (Fig. 20F, 21A, B).

4.2.3.1. Serum IL-6 in post-aSAH complications

To analyze the influence of systemic IL-6 levels on the occurrence of post-aSAH complications, we dichotomized the patients into groups who developed the complications and those without these complications. Serum IL-6 levels were found to be significantly raised after aSAH in patients who displayed DIND (delayed ischemic neurological deficits) throughout the assessment days (Fig. 21C). Similarly, patients who were diagnosed with angiographic vasospasm had significantly elevated serum IL-6 levels (Fig. 21D). Except at day 1 and day 5, serum IL-6 levels were significantly increased in patients who developed seizures as compared to those who didn't (Fig. 21E). Similarly, IL-6 levels were upregulated in patients who developed chronic hydrocephalus and required ventriculoperiotoneal shunt placement (Fig. 21F). A significant proportion of aSAH patients confront with nosocomial infections after the initial bleeding showing the possibility of immunosupression after SAH (Frontera et al., 2008; Sarrafzadeh et al., 2011). We found that serum IL-6 levels were significantly raised in aSAH patients who contracted infections (Fig. 22A). Further, dissecting the data into pneumonia, meningitis and other infections (having other infections such as UTI or in addition to pneumonia or meningitis) groups revealed distinct differences in serum IL-6 levels among these groups. Interestingly, aSAH patients contracting pneumonia infection or other infections had significantly higher serum IL-6 levels as compared to non-infectious aSAH patients (Fig. 22B&D). However, presence of meningitis did not elevate serum IL-6 and the levels remained parallel to aSAH patients without infections (Fig. 22B). Finally, we have evaluated serum IL-6 levels among patients who developed cerebral infarction and found a delayed significant elevation of serum IL-6 at day 9 – day 13 (Fig. 22E). Further dichotomy of CI group into interventional CI and DCI showed that serum IL-6 levels were non-significantly raised lately in interventional CI group. However, interestingly serum IL-6 levels were significantly lower at day 1 in DCI group compared to No CI group, but were impaired early at day 3 and remained elevated with occasional significant difference existing only at day 9 (Fig. 22D).

4.2.3.2. Serum IL-6 and post-aSAH clinical outcome

The clinical outcome of the aSAH patients at discharge was assessed by GOS and mRS. Dichotomy into good clinical outcome and poor clinical outcome by both scores revealed a significant difference in serum IL-6 levels. Serum IL-6 levels were significantly higher early

at day 1 till day 13 in aSAH patients with poor clinical outcome (GOS 1-3) as assessed by GOS (Fig. 23A). Although, there was no significant difference at day 1, but later on till last day of assessment was marked with significant elevation of serum IL-6 levels in patients with poor clinical outcome (mRS 3-6) assessed by mRS compared to good outcome patients (mRS 0-2, Fig. 23B).

Table 8. Clinical characteristics of aSAH patients whose serum IL-6 levels were determined

Number of aSAH patients	80
Age (years) (mean±SD)	56.97 (±12.00)
Females (%)	62.5%
Treatment modality	
Neurosurgical clipping (%)	48.8%
Endovascular coiling (%)	51.3%
Intraventricular hemorrhage: IVH (%)	12.5%
Intracerebral bleeding: ICB (%)	20.0%
ICB and IVH (%)	13.8%
Hunt and Hess grade (median)	**3**
1 (%)	6.3%
2 (%)	30.0%
3 (%)	28.8%
4 (%)	16.3%
5 (%)	18.8%
Fischer grade (median)	**3**
1 (%)	1.3%
2 (%)	2.5%
3 (%)	83.8%
4 (%)	12.5%
CVS (%)	55.0%
Cerebral Ischemia (%)	41.3%
Intervention related CI (%)	21.3%
DCI (%)	20.0%
Seizures (%)	30.0%
VP-Shunt dependent hydrocephalus (%)	31.3%
Infections (%)	37.5%
Pneumonia (%)	18.8%
Meningitis (%)	8.8%
Others (%)	10.0%
Pneumonia+Meningitis (%)	2.5%
Pneumonia+UTI (%)	3.8%
Meningitis+UTI (%)	1.3%
Misc. (Osteomyelitis, wound infection) (%)	2.5%
DIND (%)	35.0%
Aneurysm location	
Anterior circulation (%)	86.3%
Posterior circulation (%)	13.8%
GOS (median)	**3**
1 (%)	8.8%
2 (%)	12.5%
3 (%)	30.0%
4 (%)	5.0%
5 (%)	41.3%
mRS (median)	**3**
0 (%)	2.5%
1 (%)	31.3%

2 (%)	10.0%
3 (%)	8.8%
4 (%)	21.3%
5 (%)	17.5%
6 (%)	8.8%

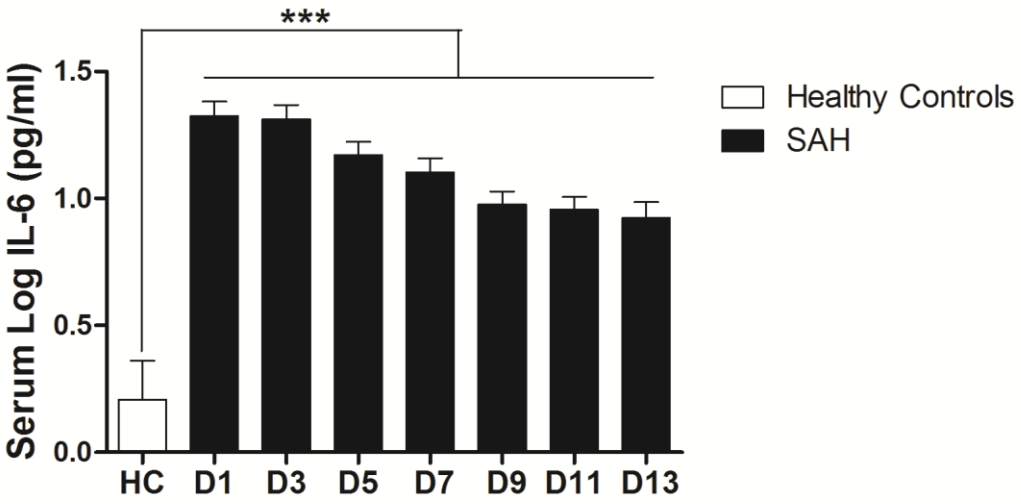

Figure 19: Comparison of serum IL-6 levels among healthy controls and aSAH patients. HC = Healthy controls (n = 10) SAH = Aneurysmal Subarachnoid hemorrhage (n = 80), D1 – D13 = Day 1 – Day 13, Unpaired t test, $p < 0.05$ was considered as a significant difference.

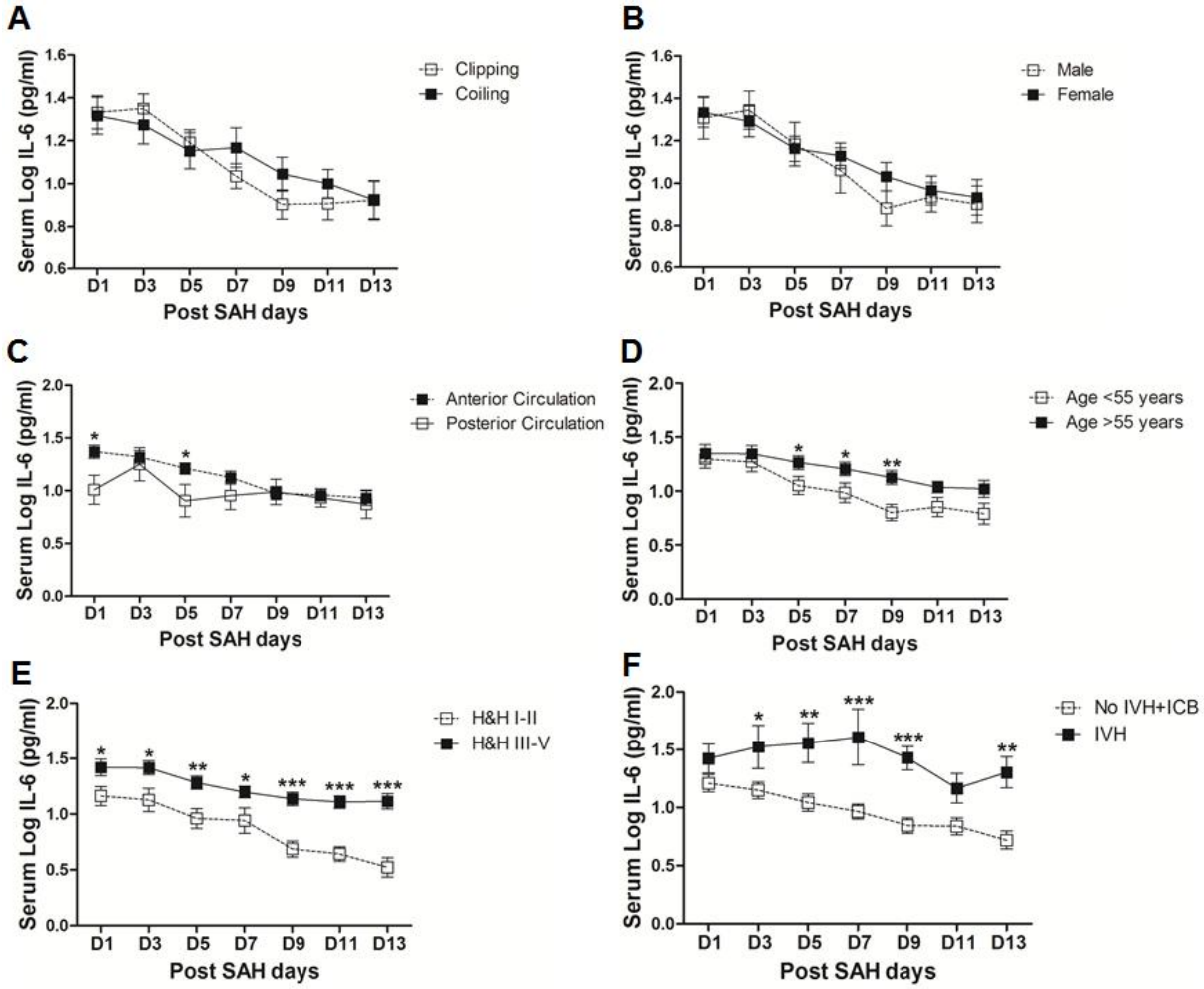

Figure 20: A. Comparison of serum IL-6 levels among aSAH patients with: aneurysm repair by neurosurgical clipping (n = 39) or by endovascular coiling (n = 41); **B.** male sex (n = 30) and female sex (n = 50); **C.** anterior circulation aneurysms (n = 69) and posterior circulation aneurysms (n = 11); **D.** age below 55 years (n = 37) and equal to/above 55 years (n = 43); **E.** with good H&H grades (n = 29) and poor H&H grades (n = 51). **F.** no IVH+ICB (n = 43) vs. IVH (n = 10). Unpaired t test, $p < 0.05$ was considered as a significant difference.

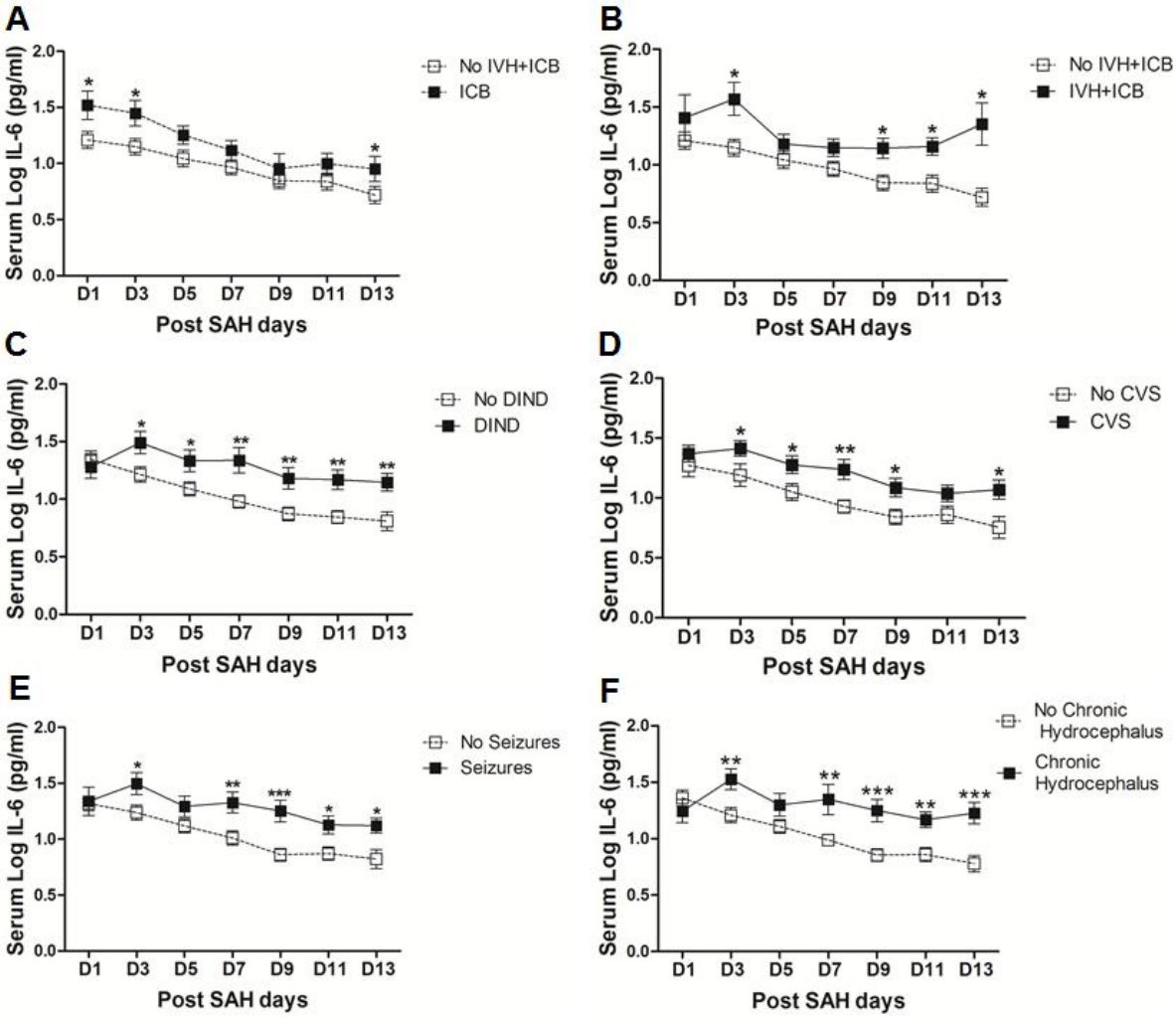

Figure 21: A. Comparison of serum IL-6 levels among aSAH patients with: no IVH+ICB (n = 43) and ICB (n = 16); **B.** no IVH+ICB (n = 43) and both IVH+ICB (n = 11); **C.** DIND (n = 28) and No DIND (n = 52); **D.** CVS (n = 44) and No CVS (n = 36); **E.** seizures (n = 24) and no seizures (n = 56); **F.** chronic hydrocephalus (n = 25) and no chronic hydrocephalus (n = 55). Unpaired t test, $p < 0.05$ was considered as a significant difference.

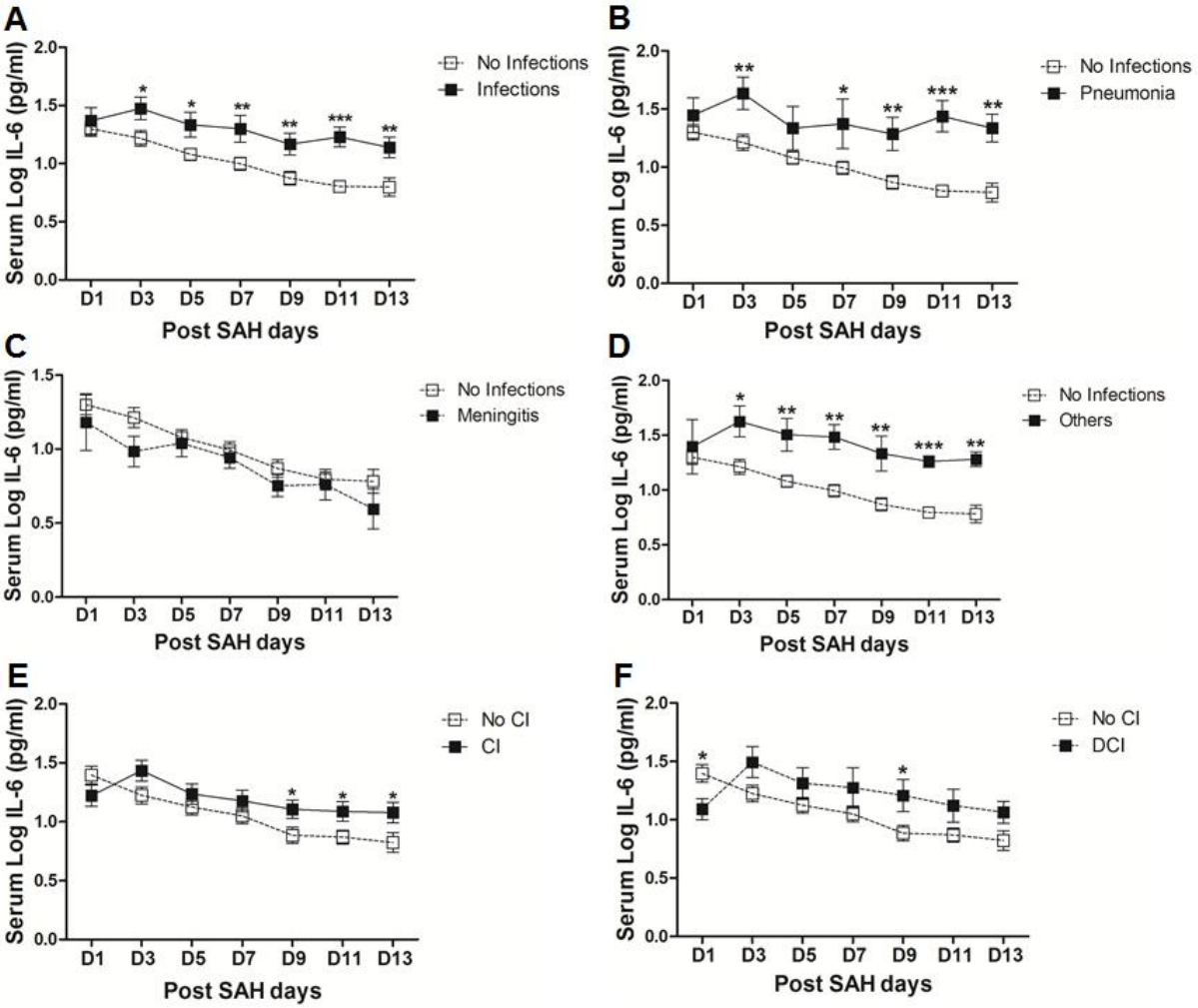

Figure 22: A. Comparison of serum IL-6 levels in aSAH patients with: infections (n = 30) and without infections (50); **B.** only pneumonia (n = 14) and no infections (n = 50). **C.** only meningitis (n = 7) and no infections (n = 50); **D.** other infections (n = 9) and no infections (n = 50); **E.** cerebral ischemia (CI = 33) and no CI (n = 47); **F.** DCI (n = 16) and no CI (n = 47). Unpaired t test to compare the two groups, $p < 0.05$ was considered as a significant difference.

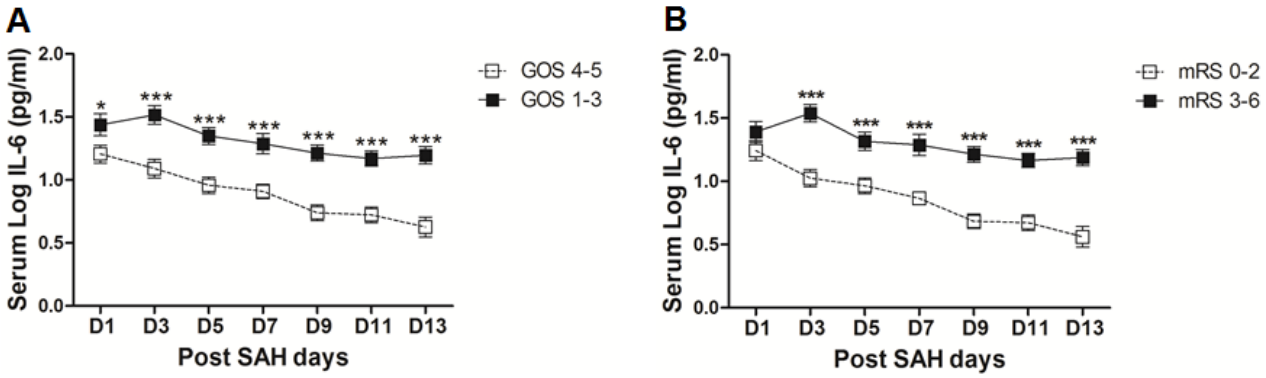

Figure 23: A. Comparison of serum IL-6 levels among aSAH patients with: good clinical outcome (GOS 4-5, n = 39) and poor clinical outcome (GOS 1-3, n = 41) as assessed by GOS; **B.** good clinical outcome (mRS 0-2, n =35) and poor clinical outcome (mRS 3-6, n = 45) as assessed by modified Rankin scale. Unpaired t test, $p < 0.05$ was considered as a significant difference.

4.2.4. Serum IL-10

The baseline characters of aSAH patients whose serum IL-10 levels were determined are shown in Table 9. The median H&H and Fischer scores were 3, while median GOS score was 4 and mRS score was 3. Serum IL-10 levels were significantly raised after aSAH at day 1 as compared to controls (Fig. 24). Determination of serum IL-10 levels at day 7 after aSAH showed significant elevation of serum IL-10 levels as was obvious on day 1, while there was no significant difference between day 1 and day 7 serum IL-10 levels in aSAH patients (Fig. 24).

The dichotomization of the data into two groups for the analysis of aSAH patients with a specific character and without that character was carried out as described above for other cytokines and revealed some interesting differences in serum IL-10 levels. There was no significant difference in serum IL-10 levels based on gender, aneurysm location, or treatment modality based dichotomy (data not shown). Serum IL-10 levels were non-significantly elevated in poor grade aSAH (H&H III-V) patients at both days compared to less severe grade aSAH (H&H I-II), (Fig. 25B). Serum IL-10 levels were non-significantly elevated at day 1 in patients older than 55 years of age and reached to a significant difference at day 7 compared to their younger counterparts (Fig. 25A). Patients presenting with additional intraventricular hemorrhage (IVH) showed significantly elevated serum IL-10 levels at day 7 (Fig. 25C). Presence of intracerebral bleeding alone did not lead to significant elevation of serum IL-10 levels unless accompanied by IVH simultaneously (Fig. 25D).

4.2.4.1. Serum IL-10 in post-aSAH complications

Dichotomy of the patients presenting with different aSAH associated complications and those without these complications revealed some intriguing findings. Aneurysmal SAH patients who developed delayed ischemic neurological deficits (DIND) did not show any significant difference in serum IL-10 levels and same was true for patients experiencing seizures although serum IL-10 levels tend to be higher at both days in patients with seizures (data not shown). However, patients who developed cerebral vasospasm (CVS) and shunt-dependent chronic hydrocephalus showed significant elevation in serum IL-10 levels at day 7 post-aSAH respectively (Fig. 25E, F). There was no significant difference among the patients who developed cerebral ischemia/infarction (CI) compared to those who did not. Although levels of IL-10 did not differ significantly, however, serum IL-10 levels tended to be higher in

patients with delayed cerebral ischemia (DCI) compared to no CI or interventional CI (Fig. 26E, F). Serum IL-10 levels were significantly increased at day 7 in aSAH patients who contracted different infections (Fig. 26A). Further exploration based on the type of contracted infections showed that serum IL-10 levels were significantly raised at day 7 in patients who developed pneumonia and other infections compared to no infections, respectively (Fig. 26B, C). Comparison among different infections only showed significantly elevated serum IL-10 levels at day 1 after pneumonia compared to meningitis (Fig. 26D).

4.2.4.2. Serum IL-10 and post-aSAH clinical outcome

The most interesting finding was the existence of difference in serum IL-10 levels in patients achieving good clinical outcome and poor clinical outcome at discharge as assessed by Glasgow outcome scale and modified Rankin scale. Serum IL-10 levels measured on day 1 and day 7 were significantly higher in aSAH patients with poor outcome (GOS 1-3) as compared to good clinical outcome (GOS 4-5) as assessed by GOS (Fig. 27A). Assessment of clinical outcome by mRS also revealed similar results with higher serum IL-10 levels at both days in patients with poor clinical outcome (mRS 3-6) compared to those ones with good outcome (mRS 0-2) (Fig. 27B).

Table 9. Characters of aSAH patients whose serum IL-10 levels were determined

Number of aSAH patients	76
Age (years) (mean±SD)	59.14 (±11.93)
Females (%)	60.53%
Treatment modality	
Neurosurgical clipping (%)	48.7%
Endovascular coiling (%)	51.3%
Intraventricular hemorrhage: IVH (%)	13.2%
Intracerebral bleeding: ICB (%)	18.4%
ICB and IVH (%)	14.5%
Hunt and Hess grade (median)	**3**
1 (%)	7.9%
2 (%)	31.6%
3 (%)	28.9%
4 (%)	15.8%
5 (%)	15.8%
Fischer grade (median)	**3**
1 (%)	1.3%
2 (%)	2.6%
3 (%)	82.9%
4 (%)	13.2%
CVS (%)	57.9%
Cerebral Ischemia (%)	43.4%
Intervention related CI (%)	22.4%
DCI (%)	21.1%
Seizures (%)	28.9%
VP-Shunt dependent hydrocephalus (%)	30.3%
Infections (%)	35.5%
Pneumonia (%)	19.7%
Meningitis (%)	7.9%
Others (Pneumonia, Meningitis in combination with UTI, or Osteomyelitis, wound infection) (%)	7.9%
DIND (%)	34.2%
Aneurysm location	
Anterior circulation (%)	85.5%
Posterior circulation (%)	14.5%
GOS (median)	**4**
1 (%)	7.9%
2 (%)	11.8%
3 (%)	27.6%
4 (%)	7.9%
5 (%)	44.7%
mRS (median)	**3**
0 (%)	2.6%
1 (%)	34.2%
2 (%)	9.2%
3 (%)	9.2%
4 (%)	19.7%
5 (%)	17.1%
6 (%)	7.9%

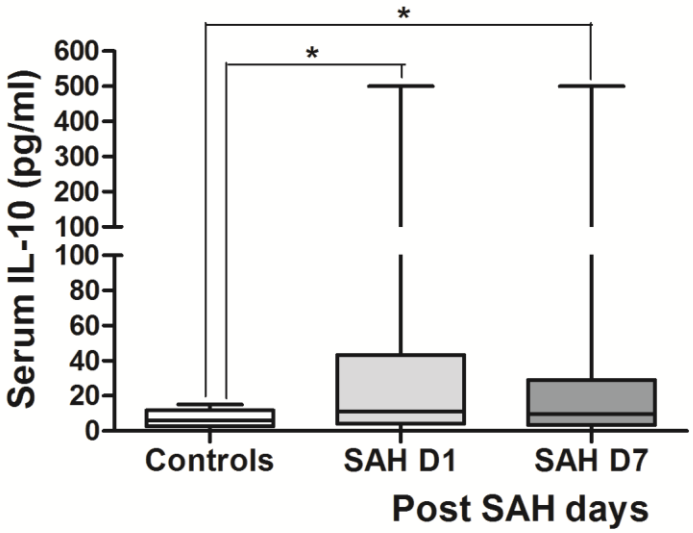

Figure 24: Serum IL-10 levels in control patients (n = 24) and aSAH patients (n = 76) at day 1 and day 7. Mann-Whitney *U* test; *p* value = 0.011 at day 1 and 0.037 at day 7. SAH D1= Aneurysmal Subarachnoid hemorrhage at day one, SAH D7= Aneurysmal Subarachnoid hemorrhage at day seven.

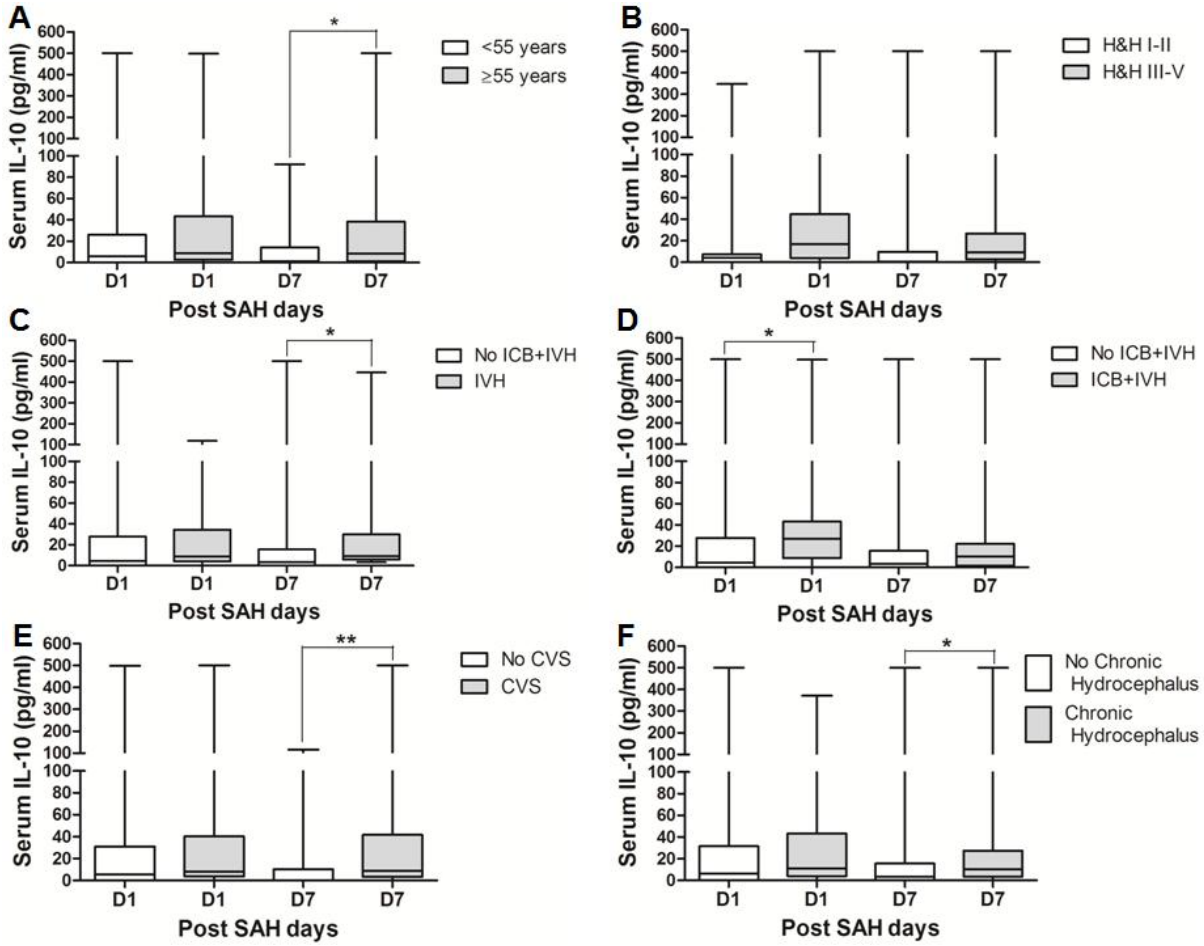

Figure 25: A. Comparison of serum IL-10 levels in aSAH patients with: age <55 years (n = 29) and ≥ 55 years (n = 47); **B.** less severe aSAH (H&H I-II, n = 30) and severe aSAH (H&H III-V, n = 46); **C.** no intracerebral bleeding and intraventricular hemorrhage (No ICB+IVH, n = 41) vs. IVH (n = 10); **D.** no ICB+IVH (n = 41) vs. ICB+IVH (n = 11); **E.** no CVS (n = 32) and CVS (n = 44); **F.** no VP-Shunt dependent chronic hydrocephalus (n = 53) and VP-Shunt dependent chronic hydrocephalus (n = 23). Mann Whitney *U* test; *p* value < 0.05 was considered as a significant difference.

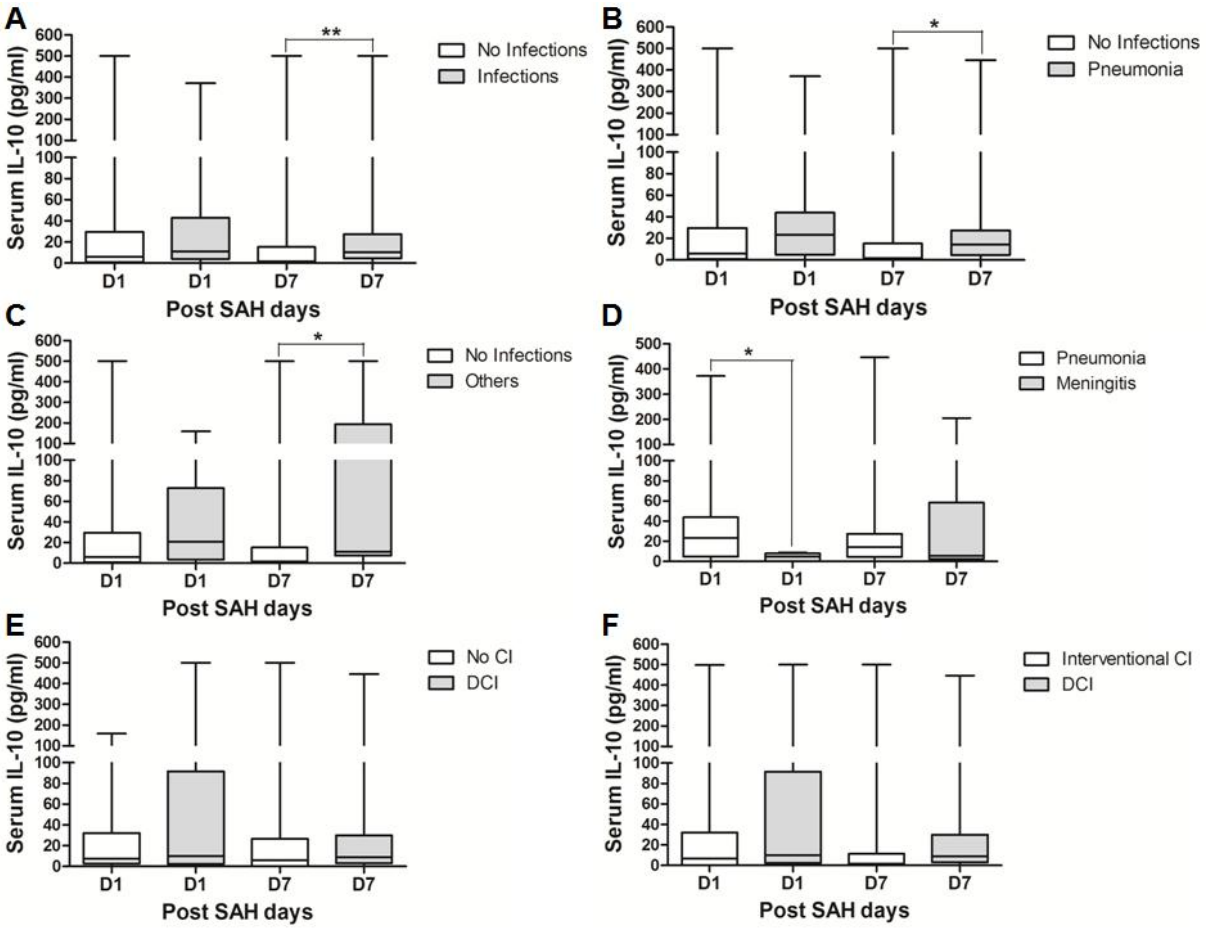

Figure 26: A. Comparison of serum IL-10 levels in aSAH patients with: no infections (n = 49) and infections (n = 27); **B.** no infections (n = 49) and pneumonia (n = 15); **C.** no infections (n = 49) and others (n = 6); **D.** pneumonia (n = 15) and meningitis (n = 6); **E.** no CI (n = 43) and DCI (n = 16); **F.** interventional CI (n = 17) and DCI (n = 16). Mann Whitney *U* test; *p* value < 0.05 was considered as a significant difference.

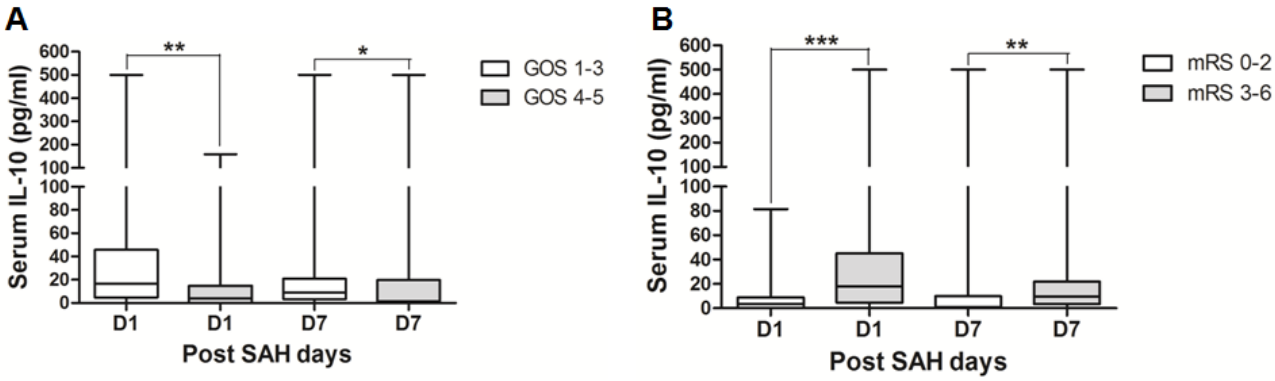

Figure 27: A. Comparison of serum IL-10 levels in aSAH patients with: good clinical outcome (GOS 4-5, n = 40) vs. poor outcome (GOS 1-3, n = 36) as assessed by GOS; **B.** good clinical outcome (mRS 0-2, n = 35) vs. poor outcome (mRS 3-6, n = 41) as assessed by mRS. Mann Whitney *U* test; *p* value < 0.05 was considered as a significant difference.

4.3. Chemokine response after aSAH

4.3.1. Serum CCL5 (RANTES)

Serum CCL5 levels were quantified in aSAH patients at day 1 and day 7 and were compared to a control group of spinal stenosis patients undergoing diagnostic myelography. Serum CCL5 levels were significantly increased early after aSAH on day 1 compared to controls (Fig. 28). Similarly on day 7 after aSAH, serum CCL5 levels were still significantly high compared to the controls (Fig. 28). The median CCL5 levels at day 7 appeared to be slightly higher than day 1 in aSAH patients, nevertheless did not reach significant difference (Fig. 28).

Further subgrouping for detailed analysis of serum CCL5 in different aSAH patient associated characters was carried out. Serum CCL5 levels did not show any significant difference in aSAH patients based on gender, age, aneurysm location, aneurysm treatment modality or the severity of aSAH as assessed by H&H grades (data not shown). However, serum CCL5 levels tended to be lower in aSAH patients with age $\geq$ 55 years (Fig. 29A). Serum CCL5 levels were significantly decreased at day 7 in patients with intracerebral bleeding (ICB) compared to those without any additional bleed except aSAH (Fig. 29B).

4.3.2. Serum CCL5 and post-aSAH complications

Similar analysis for aSAH associated complications was performed. There was no significant impact of the development of CVS, DIND or seizures on serum CCL5 levels (data not shown). However, serum CCL5 levels were significantly lower in aSAH patients who developed chronic hydrocephalus and required the placement of ventriculoperitoneal shunt as compared to who did not develop this complication (Fig. 29C). Serum CCL5 levels at both day 1 and day 7 tended to be lower in aSAH patients who contracted infections (data not shown), however, on further dichotomization, only serum CCL5 levels were shown to be significantly reduced at day 7 in patients contracting pneumonia compared to those without any infection (Fig. 29D). Similarly, there existed no significant difference in aSAH patients who developed cerebral ischemia and further dissection into intervention related cerebral ischemia or DCI also revealed no any significant difference (data not shown).

4.3.3. Serum CCL5 and post-aSAH clinical outcome

Serum CCL5 levels were analyzed in aSAH patients with dichotomy into good and poor clinical outcome at discharge as assessed by both GOS and mRS. Interestingly, serum CCL5 levels were non-significantly higher at day 1 in patients with good clinical outcome (GOS 4-5) and further, on day 7 they were significantly higher compared to poor clinical outcome (GOS 1-3) patients as assessed by GOS on discharge (Fig. 29E). Assessment of clinical outcome by mRS reflected the same trend as observed with GOS, i.e., non-significantly higher serum CCL5 levels at day1 and significantly higher serum CCL5 levels on day 7 (Fig. 29F).

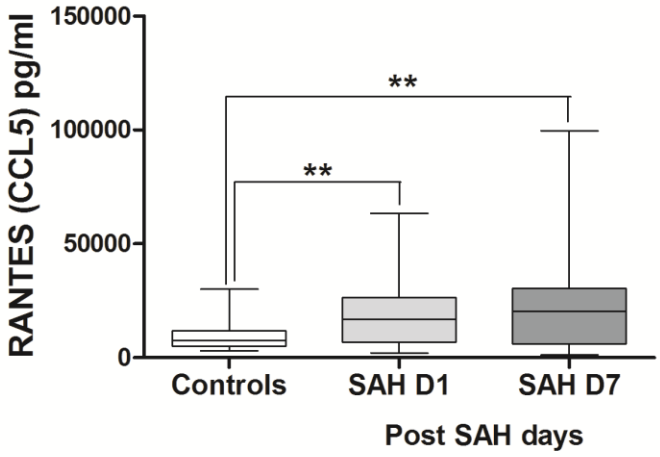

Figure 28: Comparison of serum RANTES/CCL5 levels among controls (n = 24) and aSAH patients (n = 80). Mann Whitney *U* test; *p* value = 0.004 at post SAH day 1 and *p* = 0.003 at post SAH day 7.

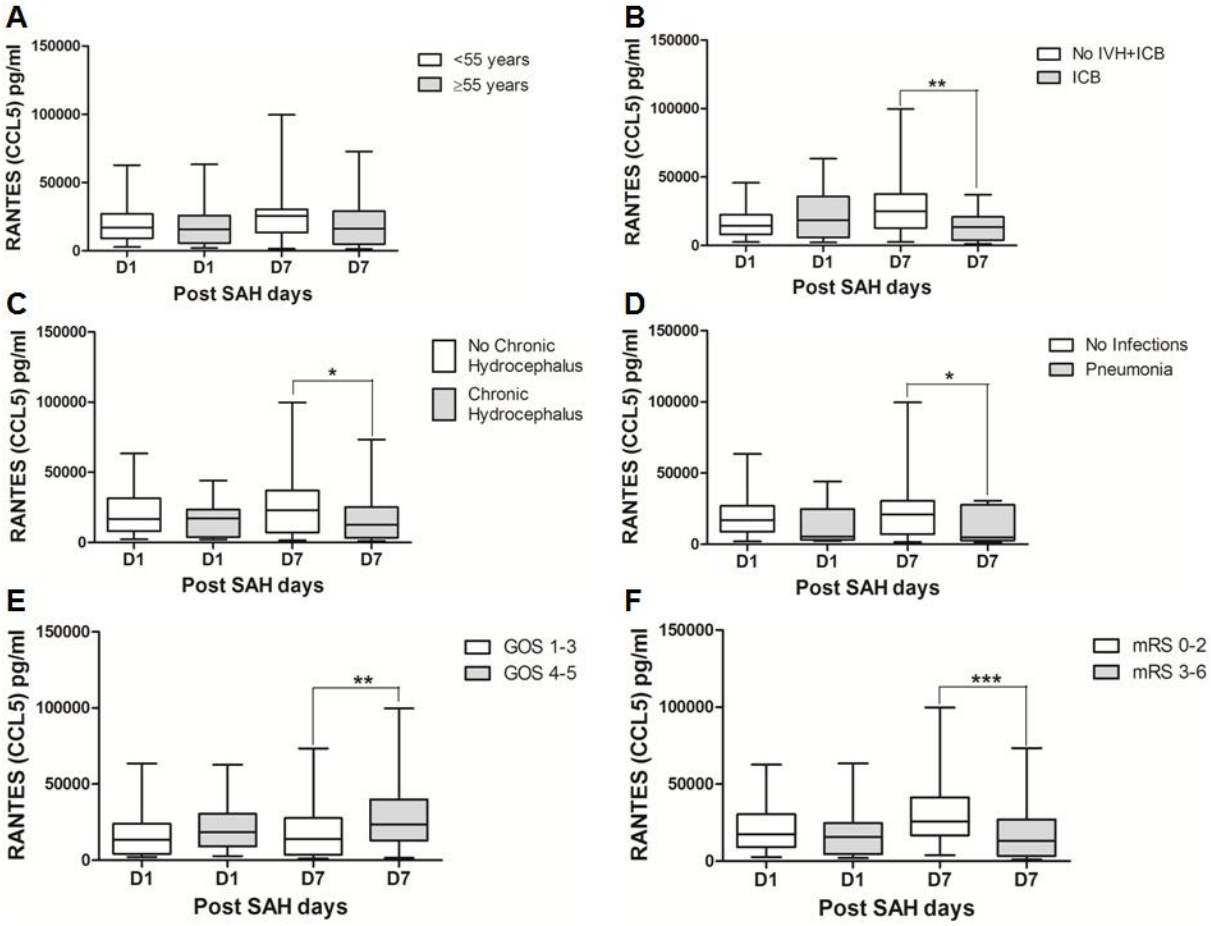

Figure 29: A. Comparison of serum RANTES (CCL5) levels in aSAH patients with: <55 years of age (n = 31) and ≥55 years of age (n = 49); **B.** only intracerebral bleeding (ICB; n = 15) compared to patients without intracerebral and intraventricular hemorrhage (No IVH+ICB; n = 43); **C.** no chronic hydrocephalus (n = 55) and with chronic hydrocephalus (n = 25) requiring VP-Shunt placement; **D.** no infections (n = 51) and Pneumonia (n = 15); **E.** good clinical outcome GOS 4-5 (n = 40) and with poor clinical outcome GOS 1-3 (n = 40) as assessed by Glasgow Outcome Scale; **F**. good clinical outcome (mRS 0-2; n = 36) and with poor clinical outcome (mRS 3-6; n = 44) as assessed by modified Rankin scale. Mann Whitney *U* test; *p* value <0.05 was considered as a significant difference.

4.4. Cellular immune response after aSAH

The elevated levels of DAMPs (HMGB1, mtDNA) and different cytokines may involve the activation and polarization of immune cells. Therefore, we have characterized the different subsets of peripheral blood monocytes and CD4+ T helper cells during first 72 hours (hereafter represented as day 1) covering the time course of early brain injury and at day 7 during the phase of delayed brain injury by polychromatic cell surface based flow cytometric immunophenotyping.

4.4.1. Monocyte response after aSAH

Monocytes were identified based on their intermediate side scatter (SSC) and CD45 expression, and expressed as percentage of CD45+ leucocytes and were non-significantly higher at day 1 and at day 7 in aSAH patients in comparison to healthy controls. Interestingly, monocyte number was significantly increased at day 7 as compared to day 1 in aSAH patients (Fig. 30A). However, monocytes recognized as CD14+ CD15- cells when expressed as frequency of CD45+ leucocytes showed a non-significant increasing trend after aSAH as compared to healthy controls (Fig. 30B). Monocytes can be categorized into three subsets based on differential expression of CD14 and CD16 into classical (CD14++ CD16-), intermediate (CD14+ CD16+), and nonclassical (CD14-CD16++). There was no significant difference in classical monocytes among healthy controls and aSAH patients at both times of assessment (Fig. 30C). There was no significant difference in intermediate monocytes among controls and aSAH patients at day 1. Interestingly, a significant decrease in the frequency of intermediate monocytes was observed at day 7 as compared to day 1 in aSAH patients (Fig. 30D). Intriguingly, nonclassical monocytes were significantly lower at day 1 in aSAH patients compared to healthy controls, but this significance did not persist at day 7 due to slight increase in nonclassical monocytes (Fig. 30E).

Additionally, we have assessed the chemokine markers such as CX3CR1, CCR2, and activation and maturation marker HLA-DR on these subsets of monocytes. The CX3CR1+ classical monocytes remained unaltered among controls and aSAH patients (Fig. 31A). The frequency of intermediate CX3CR1+ monocytes was non-significantly higher at day 1 and then, non-significantly reduced at day 7 in aSAH patients compared to healthy controls. Interestingly, a significant reduction in intermediate CX3CR1+ monocytes was seen on day 7 after initial rise at day 1 in aSAH patients (Fig. 31B). The proportion of nonclassical

CX3CR1+ monocytes was reduced significantly at day 1 and non-significantly at day 7 in aSAH patients as compared to controls (Fig. 31C). It was interesting to note that the classical CCR2+ monocytes were significantly increased early after aSAH compared to healthy controls, but later on at day 7, no significant difference persisted (Fig. 31D). The frequency of intermediate CCR2+ monocytes was significantly increased early at day 1 as compared to day 7 in aSAH patients (Fig. 31E) and no significant difference was observed in nonclassical CCR2+ monocytes among controls and aSAH patients (Fig. 31 F). It was noteworthy to observe that the classical HLA-DR+ monocytes were significantly reduced at day 1 and day 7 in aSAH patients in comparison with healthy controls (Fig. 31G). However, a significant decrease in intermediate HLA-DR+ monocytes occurred at day 7 compared to day 1 in only aSAH patients (Fig. 31H). Finally, HLA-DR+ nonclassical monocytes were significantly reduced at day 1 after aSAH and at day 7 an upsurge resulted in a non-significant difference compared to healthy volunteers (Fig. 31I).

4.4.2. CD4+ T cell response after aSAH

Lymphocytes in the peripheral blood of aSAH patients and healthy controls were identified by their low SSC and high CD45 expression and were expressed as percentage of CD45+ leucocytes. A lymphopenic response was observed in aSAH patients at both days of assessment compared to healthy controls (Fig. 32A). The same was reflected for CD4+ T cells when expressed as percentage of CD45+ leucocytes (Fig. 32B). However, a significant increase in CD4+ T cells was observed at day 1 and day 7 after aSAH compared to healthy controls when expressed as frequency of lymphocytes (Fig. 32C). Further, we investigated Tregs ($CD25^{hi}$ $CD127^{lo}$) and different subsets of CD4+ T cells (Th1, Th2 and Th17) based on differential surface expression of chemokine receptors CXCR3 and CCR6 as described by Maecker et al., (2012).

Th1 (CXCR3+ CCR6-) cells were non-significantly reduced at day 1 after aSAH compared to healthy controls and were non-significantly higher at day 7 compared to day 1 in aSAH patients (Fig. 33A). There was no significant difference among healthy controls and aSAH patients in Th2 (CXCR3- CCR6-) cells response, however, Th2 cells were significantly decreased at day 7 in comparison to day 1 after aSAH (Fig. 33B). Interestingly, no significant difference was present in Th17 (CXCR3- CCR6+) cells among healthy controls and aSAH patients, but a significant increase in Th17 cells was observed at day 7 compared to day 1 in

aSAH patients (Fig. 33C). The most striking finding was the increase in Treg cells at both days of assessment in aSAH patients as opposed to healthy volunteers and Treg cells were even significantly higher at day 7 compared to day 1 in aSAH patients (Fig. 33D).

Like monocytes, we have investigated the activation markers HLA-DR and CD38 on these different CD4+ T cell subsets. Among Th1 cells, only HLA-DR- CD38+ Th1 cells were significantly reduced at day 1 after aSAH compared to healthy controls, but at day 7 no significant difference was observed (Fig. 34A). Similarly, HLA-DR- CD38+ Th2 cells were also reduced significantly at day 1 after aSAH compared to healthy controls (Fig. 34C). Interestingly, HLA-DR- CD38- Th2 cells were significantly increased at day 1 after aSAH compared to healthy controls and this was followed by a significant decrease at day 7 compared to day 1 (Fig. 34B). The frequency of HLA-DR+ CD38- Th2 cells was also significantly reduced at day 7 compared to day 1 in only aSAH patients (Fig. 34D). A significant increase in HLA-DR- CD38+ Th17 cells was revealed on day 7 compared to day 1 in aSAH patients (Fig. 34E). Analysis of CD38 and HLA-DR activation markers on Treg cells also revealed some interesting significant differences. The HLA-DR- CD38- subset of Treg cells was significantly outnumbered at day 1 and day 7 after aSAH compared to healthy controls (Fig. 34F). Similarly, Treg cells showing the simultaneous expression of CD38 and HLA-DR were also significantly increased at day 1 and day 7 after aSAH compared to healthy controls (Fig. 34I). Treg cells expressing only HLA-DR (HLA-DR+ CD38-) were significantly raised at day 1 after aSAH compared to healthy controls, but at day 7 decrease in their number led to a non-significant difference (Fig. 34H). Finally, HLA-DR- CD38+ Treg cells were significantly increased after aSAH at both days compared to healthy controls and there existed a significant increase also at day 7 compared to day 1 in aSAH patients (Fig. G).

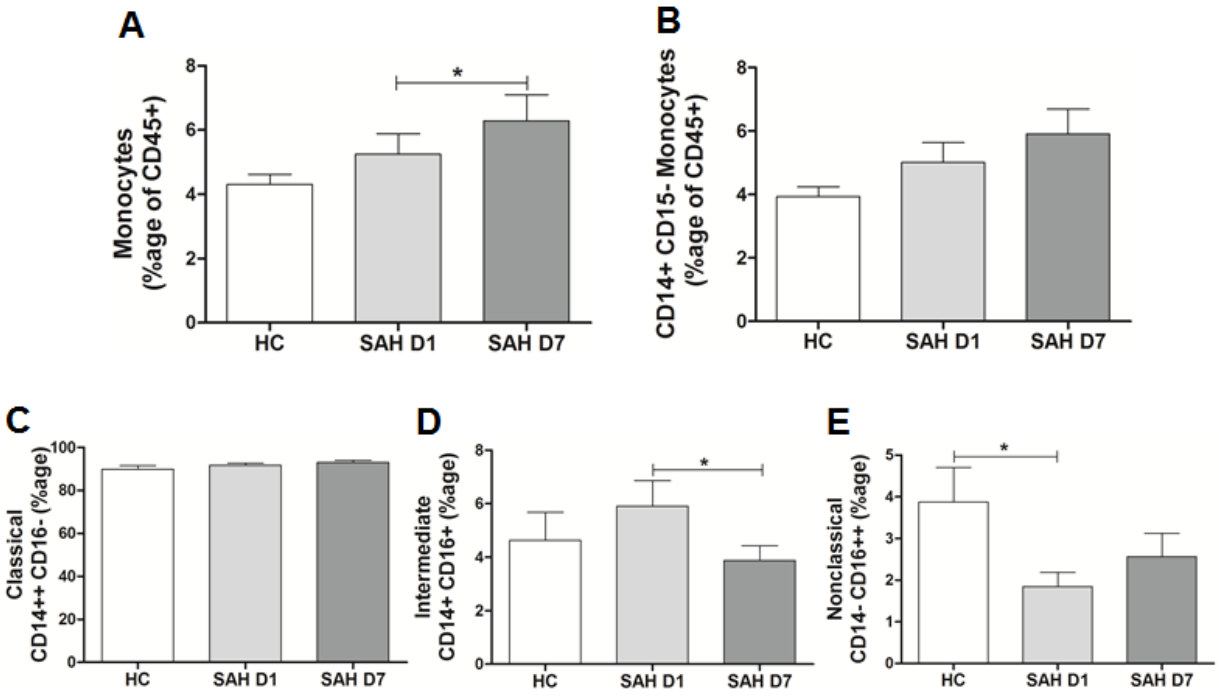

Figure 30: A. Comparison of peripheral blood monocytes (intermediate SSC and CD45 expressing cells) expressed as percentage of CD45+ leucocytes after aSAH with healthy controls; **B.** Comparison of peripheral blood monocytes (CD14+ CD15- cells) expressed as percentage of CD45+ leucocytes after aSAH with healthy controls. **C.** Comparison of: classical (CD14++ CD16-) monocytes expressed as percentage of CD14+ CD15- monocytes after aSAH with healthy controls; **D.** intermediate (CD14+ CD16+) monocytes expressed as percentage of CD14+ CD15- monocytes after aSAH with healthy controls; **E.** nonclassical (CD14- CD16++) monocytes expressed as percentage of CD14+ CD15- monocytes after aSAH with healthy controls (n = 10). Unpaired t test for comparison among healthy controls and aSAH patients, paired t test for comparison at day 1 and day 7 in aSAH patients; *p* value <0.05 was considered as a significant difference. HC = Healthy controls (n = 10), SAH = aSAH (n = 15), D1 = day 1 post-aSAH; D7 = day 7 post-aSAH.

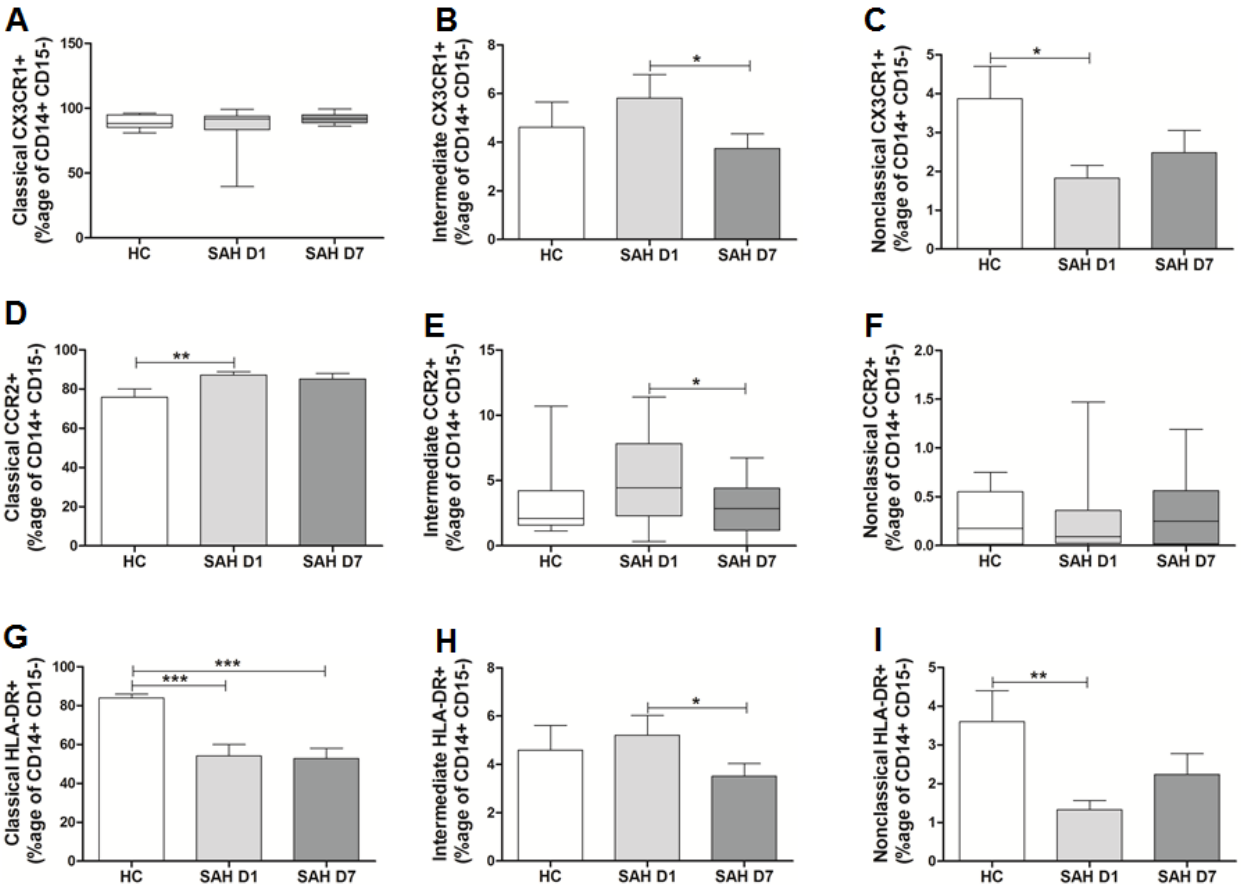

Figure 31: A. Comparison of peripheral blood CX3CR1+: classical monocytes after aSAH with healthy controls; **B.** intermediate monocytes after aSAH with healthy controls; **C.** nonclassical monocytes after aSAH with healthy controls. **D.** Comparison of peripheral blood CCR2+: classical monocytes after aSAH with healthy controls; **E.** intermediate monocytes after aSAH with healthy controls; **F.** nonclassical monocytes after aSAH with healthy controls. **G.** Comparison of peripheral blood HLA-DR+: classical monocytes after aSAH with healthy controls; **H.** intermediate monocytes after aSAH with healthy controls; **I.** nonclassical monocytes after aSAH with healthy controls. Unpaired t test or Mann Whitney *U* test for comparison among healthy controls and aSAH patients, paired t test or Wilcoxon signed rank test for comparison at day 1 and day 7 in aSAH patients; *p* value <0.05 was considered as a significant difference. HC = Healthy controls (n = 10), SAH = aSAH (n = 15), D1 = day 1 post-aSAH; D7 = day 7 post-aSAH.

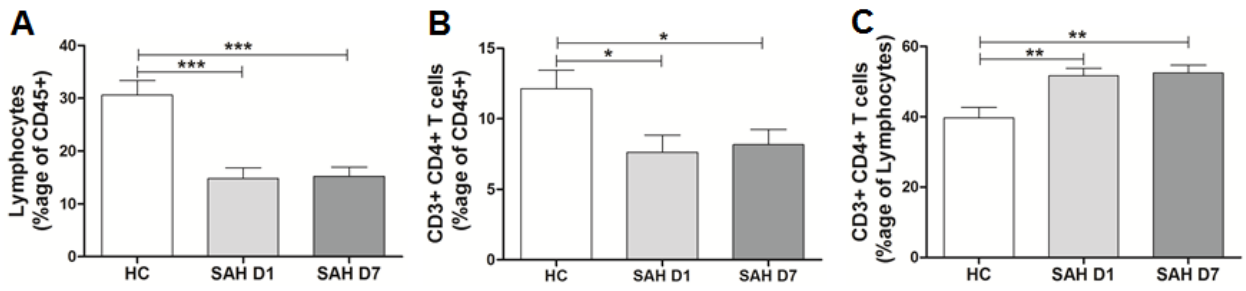

Figure 32: A. Comparison of peripheral blood: lymphocytes (low SSC and high CD45 expressing cells) after aSAH with healthy controls; **B.** CD4+ T cells after aSAH with healthy controls; **C.** CD4+ T cells expressed as percentage of lymphocytes after aSAH with healthy controls. Unpaired t test for comparison among healthy controls and aSAH patients, paired t test for comparison at day 1 and day 7 in aSAH patients; *p* value <0.05 was considered as a significant difference. HC = Healthy controls (n = 10), SAH = aSAH (n = 15), D1 = day 1 post-aSAH; D7 = day 7 post-aSAH.

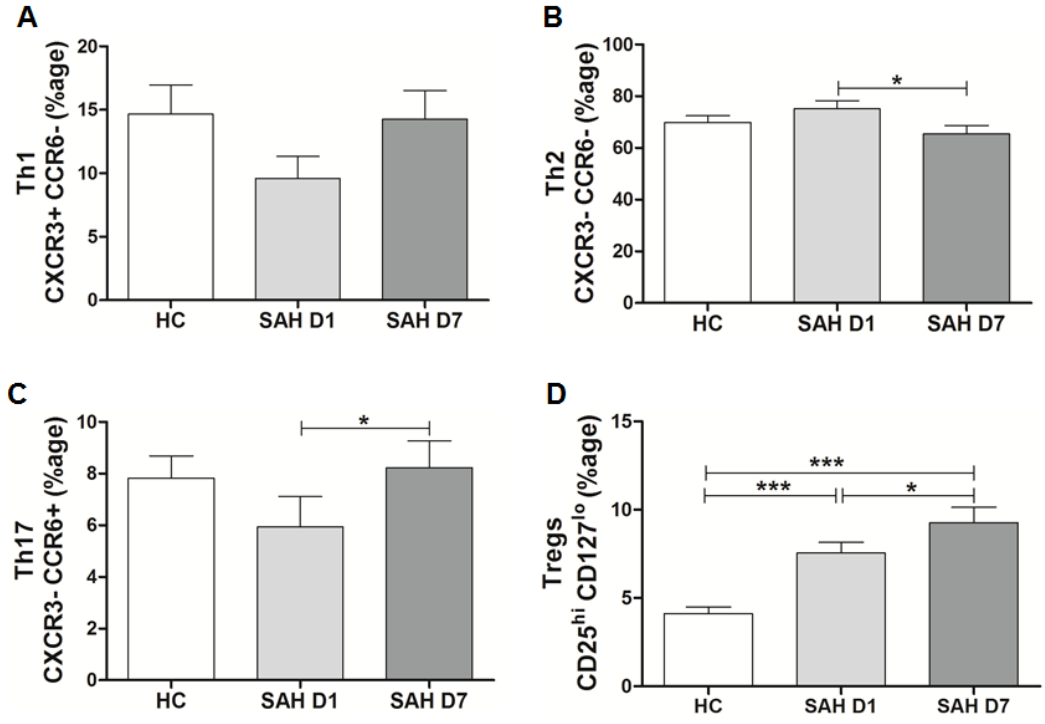

Figure 33: A. Comparison of peripheral blood CD3+ CD4+ T cell subset: Th1 (CXCR3+ CCR6-) cells after aSAH with healthy controls; **B.** Th2 (CXCR3- CCR6-) cells after aSAH with healthy controls; **C.** Th17 (CXCR3- CCR6+) cells after aSAH with healthy controls. **D.** Treg ($CD25^{hi}$ $CD127^{lo}$) cells after aSAH with healthy controls. Unpaired t test for comparison among healthy controls and aSAH patients, paired t test for comparison at day 1 and day 7 in

aSAH patients; *p* value <0.05 was considered as a significant difference. HC = Healthy controls (n = 10), SAH = aSAH (n = 15), D1 = day 1 post-aSAH; D7 = day 7 post-aSAH. All subsets were expressed as percentage of CD4+ T cells.

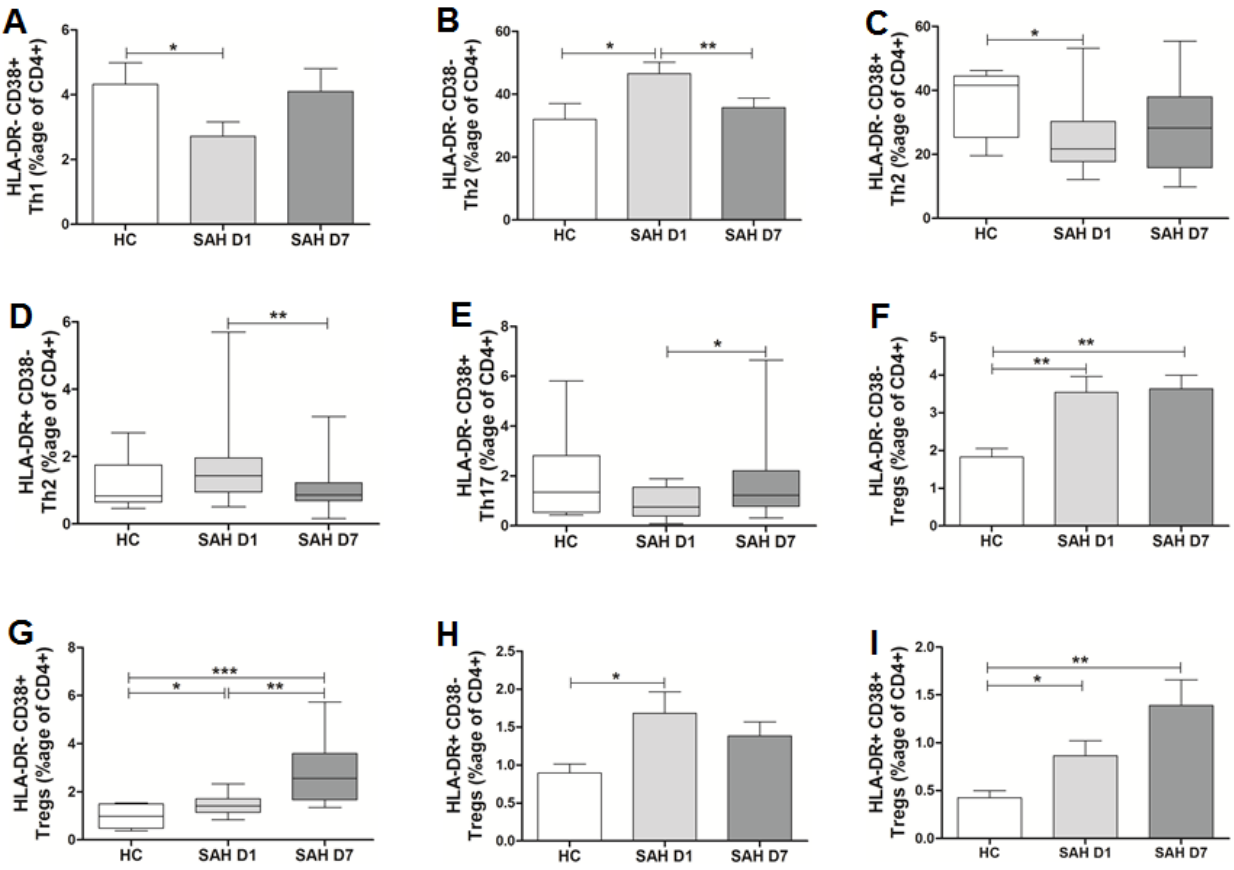

Figure 34: A. Comparison of peripheral blood: Th1 HLA-DR- CD38+ cells after aSAH with healthy controls; **B.** Th2 HLA-DR- CD38- cells after aSAH with healthy controls; **C.** Th2 HLA-DR- CD38+ cells after aSAH with healthy controls; **D.** Th2 HLA-DR+ CD38- cells after aSAH with healthy controls; **E.** Th17 HLA-DR- CD38+ cells after aSAH with healthy controls; **F.** Tregs HLA-DR- CD38- cells after aSAH with healthy controls; **G.** Tregs HLA-DR- CD38+ cells after aSAH with healthy controls; **H.** Tregs HLA-DR+ CD38- cells after aSAH with healthy controls; **I.** Tregs HLA-DR+ CD38+ cells after aSAH with healthy controls. Unpaired t test or Mann Whitney *U* test for comparison among healthy controls and aSAH patients, paired t test or Wilcoxon signed rank test for comparison at day 1 and day 7 in aSAH patients; *p* value <0.05 was considered as a significant difference. HC = Healthy controls (n = 10), SAH = aSAH (n = 15), D1 = day 1 post-aSAH; D7 = day 7 post-aSAH. All subsets were expressed as percentage of CD4+ T cells.

4.5. Modulation of systemic inflammation with spinal cord stimulation

In another study, we determined the effects of burst spinal cord stimulation (Burst SCS) on modulation of systemic cytokines in Failed Back Surgery Syndrome (FBSS) patients. Interestingly, Burst SCS increased systemic circulating anti-inflammatory IL-10, in addition to improvements in FBSS back pain and back pain associated co-morbidities like disrupted sleep architecture and depressive symptoms in FBSS patients. Thus, suggesting a possible relationship between burst SCS and burst-evoked modulation of peripheral anti-inflammatory cytokine IL-10 in chronic back pain (Fig. 35A).

Potential associations among refractory chronic lower back pain and metabolic disorders such as obesity, diabetes, hypertension and metabolic syndrome have been sought and these metabolic disorders are characterized by a low grade systemic inflammation (Muhammad et al., 2017). Further investigations for obesity and metabolic disorder related adipokines/cytokines such as adiponectin, ghrelin and leptin were also carried out in FBSS patients. Non-significant lower levels of Ghrelin were found in pre-SCS compared to healthy controls, which were slightly increased after 3 months of Burst SCS comparable to that of controls, but non-significantly (Fig. 35B). Systemically elevated leptin levels have been implicated in low grade chronic inflammation (Iikuni et al., 2008). Interestingly, leptin levels were significantly high in pre-SCS compared to controls and even after post-SCS, but it was interesting to note that the Burst SCS led to non-significantly decrease leptin levels compared to pre-SCS (Fig. 35C). These pieces of evidence suggest that spinal cord stimulation may be used as a potential therapeutic intervention to modulate the systemic inflammatory response after aSAH. A recent study sought the feasibility to manage CVS in aSAH patients after cervical spinal cord stimulation (Slavin et al., 2011).

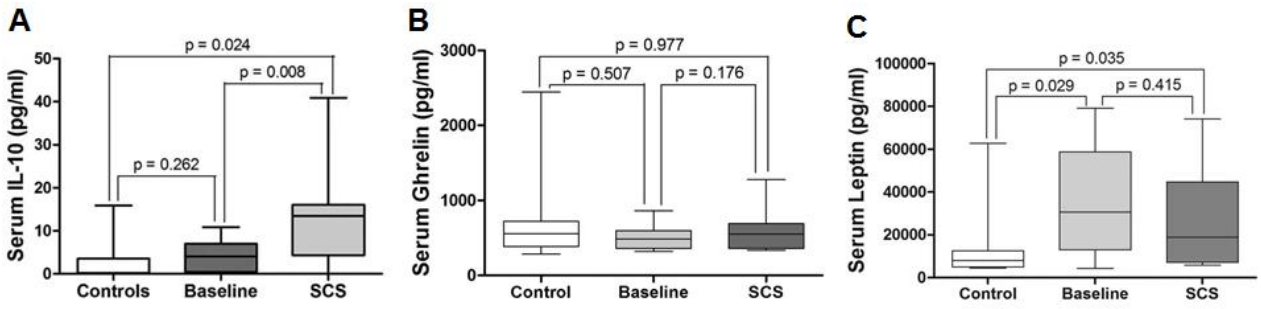

Figure 35: A. Anti-inflammatory cytokine IL-10 serum levels in FBSS patients (n = 12) at baseline, after three months of Burst spinal cord stimulation (SCS) and in healthy controls (n = 10). **B.** Anti-obesity ghrelin serum levels in FBSS (n = 12) patients at baseline, after three months of Burst spinal cord stimulation (SCS) and in healthy controls (n = 10). **C.** Pro-obesity adipokine serum levels in FBSS patients (n = 12) at baseline, after three months of Burst spinal cord stimulation (SCS) and in healthy controls (n = 10). Unpaired t test or Mann Whitney *U* test for comparison among healthy controls and aSAH patients, paired t test or Wilcoxon signed rank test for comparison at day 1 and day 7 in aSAH patients; *p* value <0.05 was considered as a significant difference.

5. Discussion

Aneurysmal subarachnoid hemorrhage, a morbid and lethal subtype of hemorrhagic stroke, is characterized by an intracranial bleed into subarachnoid space due to rupture of an intracranial aneurysm usually located at bifurcation of cerebral arteries (Suarez et al., 2006; Macdonald, 2014). The consequent transient global cerebral ischemia and extravasated blood toxicity leads to early brain injury that comprise all the events occurring within 72 hours of aSAH (Cahill and Zhang, 2009; Munoz-Guillen et al., 2013). Since the bleeding aneurysm can be obliterated from circulation by microsurgical clipping or endovascular coiling, but majority of the aSAH patients experience a delayed deterioration phase after surviving the initial ictus (Macdonald, 2014). This delayed deterioration is the result of post-aSAH complications such as cerebral vasospasm (CVS), hydrocephalus, rebleeding from the ruptured aneurysm, seizures, cortical spreading depression (CSD), and most importantly delayed cerebral ischemia (DCI) (Suarez et al., 2006; Iadecola, 2009; Macdonald, 2014). The failure of the past aSAH research focused solely on the reversal of CVS (a major contributor to DCI) to improve clinical outcome, led to explore additional mechanisms of brain injury. In the recent decade, there is renewed interest in the role of inflammation both at CNS and systemic levels after aSAH. A great body of evidence suggests that aSAH is characterized by a systemic inflammatory response (Yoshimoto et al., 2001; Smithason et al., 2012; McMahon et al., 2013; Chaudhry et al., 2017; Da Silva et al., 2017; Savarraj et al., 2017a; Savarraj et al., 2017b).

Inflammation is the consequence of recognition of danger signal molecules or alarmins by the pattern recognition receptors (PRRs) on the immune cells. Such danger signal molecules are referred to as damage associated molecular patterns (DAMPs) or pathogen associated molecular patterns (PAMPs) depending on whether they are derived from stressed, injured and necrotic cells or from invading pathogens, respectively (Chen and Nuñez, 2010; Takeuchi and Akira, 2010). Here, we have investigated two prototypical DAMPs molecules (HMGB1 as a prototype for DAMP proteins and mtDNA, a classical DAMP from nucleic acid family) to identify possible associations with post-aSAH complications and clinical outcome at discharge.

5.1. DAMPs

5.1.1. High mobility group box 1 (HMGB1)

We have showed elevated serum concentrations of the danger signal molecule HMGB1 over the two weeks following aSAH in humans. Importantly, our analysis covered the peak interval of CVS development. Our findings show that the nuclear protein HMGB1 was detectable early after aSAH and remained high over the peak time period of CVS when compared to non-SAH controls (Fig. 2). Interestingly, HMGB1 levels in patients who developed CVS were significantly higher than those found in aSAH patients without CVS (Fig. 4F). HMGB1 was already higher on day 1 (Fig. 4F) and the divergence between the CVS and the non-CVS group started very early on day 1, peaked over days 5, 7, 9, 11 and was still higher at day 13 covering the peak time of the development of CVS (Fig. 4F). Interleukin-6 has been intensively investigated in aSAH and it is known to be a prognostic marker for clinical outcome after aSAH (Muroi et al., 2013; Helbok et al., 2015; Hollig et al., 2015b). We quantified plasma IL-6 concentrations in the serum of our patients on day 1 until day 13. Interestingly, serum HMGB1 concentrations showed a significant correlation with serum IL-6 concentrations (Fig. 7C). Although a recent report demonstrated serum HMGB1 increase on admission that correlated with clinical outcome after one year (Zhu et al., 2012b), our data over the two weeks did not show any correlation with clinical outcome at discharge from hospital (Fig. 6C, D, 7A, B).

HMGB1 is a non-histone DNA binding protein that can be released either during cell death by damaged cells or actively by immune cells. Cell death occurs as early as 10 minutes after SAH favouring the possibility of passive release of HMGB1 (Friedrich et al., 2012; Sun et al., 2014b). However, there is also an active early release of HMGB1 during brain injury after SAH (Sun et al., 2014b). Both, the actively and the passively released HMGB1 have the potential of cytokine-like activity to trigger inflammation (Scaffidi et al., 2002). HMGB1 has been shown to be a late mediator of inflammation in sepsis and an early mediator of inflammatory response in cerebral ischemia (Wang et al., 1999; Qiu et al., 2008). It has been previously shown that HMGB1 leads to ischemic brain damage via activation and recruitment of peripheral macrophages (Muhammad et al., 2008) by binding to the receptor for advanced glycation end products (RAGE). A recent report showed that CSF of patients exhibited increased HGMB1 levels after SAH and that HMGB1 concentration in CSF correlated with unfavorable outcome (Nakahara et al., 2009; King et al., 2010). Increased blood brain barrier

permeability after brain injury allows the passively released HMGB1 to enter the systemic circulation (Muhammad et al., 2008), where it can induce an inflammatory response by binding to its receptors, including TLR4, TLR2 and RAGE. Our results suggest that early serum HMGB1 elevation could be due to its active release by peripheral bone marrow-derived cells (Fig. 7D) or it is being passively released from cells that were damaged during early brain injury. This is in agreement with experimental studies which confirmed early passively released HMGB1 from neurons after SAH (Sun et al., 2014b). Receptors of HMGB1 are expressed in a variety of cells, including monocytes and endothelial cells. Recently, experimental studies showed expression of HMGB1 and its receptors TLR4 and RAGE in brain tissue following SAH in animal models (Murakami et al., 2011; Li et al., 2013b; Sun et al., 2014b). The interaction between HMGB1 and its receptors leads to activation of nuclear factor kappa B (NF-κB) and expression of various pro-inflammatory genes, including IL-1β, TNFα and IL-6. In circulating monocytes/ macrophages, HMGB1 can induce its own synthesis in an active manner and enhance synthesis of other pro-inflammatory cytokines, including IL-6, IL-1β and TNF-α (Andersson et al., 2000; Agnello et al., 2002; Harris et al., 2012). We found elevated IL-6 in serum after aSAH (Fig. 19). Moreover, serum IL-6 levels showed a significant correlation with serum HMGB1 levels after aSAH (Fig. 7C). However, TNF-α can induce HMGB1 production (Rendon-Mitchell et al., 2003) suggesting the possibility of a vicious cycle of pro-inflammatory response.

Although it is difficult to investigate whether HMGB1 release precedes the increase of other cytokines in humans, it has, nevertheless, been proven in experimental settings (Sun et al., 2014b). Pro-inflammatory cytokines are damaging for neurovascular units, e.g. IL-1β and TNF-α induce apoptosis of endothelial cells (Kimura et al., 2003), whereas IL-6 can induce vasospasm in the cerebral artery (Hendryk et al., 2004). Interestingly, HMGB1 serum concentrations showed a significant correlation with serum IL-6 levels indicating the possibility of a pleiotropic effect of both molecules. The influence of systemic inflammatory cytokines suggests their importance in causing endothelial dysfunction, which, in turn, may contribute to development of CVS. Receptors of HMGB1, including TLRs and RAGE, are widely expressed on endothelial cells and are readily available for interaction with circulating HMGB1 (Li et al., 2013a; Shang et al., 2016). Pharmacological strategies blocking HMGB1 release revealed neuroprotection and attenuated CVS in an animal model of SAH (Chang et al., 2014; Sun et al., 2014a). CVS has been reported in around 70% of patients and it is the

main cause of delayed neurological decline (Carr et al., 2013). Systemic HMGB1 levels and their association with CVS may be of significant importance in the screening of patients at risk of CVS. The presented results clearly demonstrate the association of serum HMGB1 with CVS by showing that patients, who developed CVS, exhibited significantly higher HMGB1 levels than non-CVS patients (Fig. 4F) during the peak time of CVS development. Serum HMGB1 levels on day1 with a cut off value of 4.8 ng/ ml could predict CVS with a specificity of 72% and a sensitivity of 55% (Fig. 8A). Comparison of patients who were neurosurgically operated with patients treated with endovascular coiling did not find any difference of HMGB1, excluding the effect of craniotomy on HMGB1 release. Similarly, aneurysm localization and infection did not alter the HMGB1 significantly. The presented data demonstrate that HMGB1 might be involved directly or indirectly (via induction of other cytokines such as IL-6) in the pathophysiology of CVS. Sterile inflammation is a complex process, that is why single molecule targeted therapeutic options have not shown much success to date. It is important to find the source of molecular inflammation and identify its driving molecules. HMGB1 could be an early mediator and one of the driving molecules of post-aSAH inflammation giving rise to post-aSAH complications and delayed deterioration.

In conclusion**,** serum HMGB1 is differentially elevated after aSAH. Serum HMGB1 levels were elevated early after aSAH (day 1) and remained significantly high until day 13 in patients who developed CVS.

5.1.2. Mitochondrial DNA (mtDNA)

An array of different DAMPs molecules originating from different compartments of the cell undergoing stress, injury or necrosis have been discovered (Schaefer, 2014). Over the past, mitochondria have gained value as a potential host of different DAMPs. A great body of evidence supports the role of mtDNA as a DAMP mediating inflammation via different PRRs such as TLR-9, NLRP3-, NLRC4-, AIM2-inflammasome complex and cGAS-STING (Boyapati et al., 2017; West and Shadel, 2017). Hence, we aimed to investigate the temporal profile of systemic release of mtDNA after aSAH and assess its association with post-aSAH complications and clinical outcome.

The systemic levels of mtDNA were elevated in aSAH patients compared to healthy controls. Interestingly, mtDNA for D-Loop and COX-1 were significantly higher from day 1 until day 13 in aSAH patients, however, mt CytB levels were significantly elevated later on at day 7

(Fig. 9). This suggests that different mtDNA gene fragments are differentially released into systemic circulation after aSAH. Interestingly, all of investigated mtDNA gene fragments showed a secondary delayed increase with a peak at day 9, which coincides with the delayed deterioration phase. Our results are in agreement with the findings of Wang and coauthors who observed elevated mitochondrial ND2 levels in a small group of aSAH patients (Wang et al., 2013).

Further subgroup analysis was based on dichotomization of aSAH patients into two groups for different base line characters, development of different complications and clinical outcome. Interestingly, serum mtDNA levels of CytB and D-Loop were differently regulated in male and female aSAH patients (Fig. 10A, 11A and Table 4, 5). CytB and COX-1 mtDNA levels were sensitive to intracerebral bleeding in addition to primary subarachnoid bleed, but they were no more significant beyond the first day. There was no significant impact of infections on mtDNA levels. However, further subgrouping based on the type of infections revealed that mtDNA levels followed different trends and a significantly lower mt CytB and mt D-Loop levels were observed only at day 9 in patients with pneumonia infection, which is in contrast to the mtDNA levels in aSAH group. Another interesting trend was seen in CytB and COX-1 mtDNA levels where mtDNA levels were downregulated in patients who developed interventional CI as opposed to patients developing DCI or no CI. Whether this difference has some implications from immune paralysis may require further thorough investigations as immune depression is observed after aSAH and it is also known that mtDNA leads to immunosuppression via TLR-9 dependent mechanisms in cytotoxic T cells and deletion of cross presenting dendritic cells (Sarrafzadeh et al., 2011; Schafer et al., 2016). The aSAH patients experiencing seizures tended to have lower levels of both mt D-Loop and mt COX-1 levels, whereas in chronic hydrocephalus only mt D-Loop levels were downregulated. Another interesting difference, although significant at day 9, was seen in mt D-Loop levels where patients with poor clinical outcome (mRS 3-6) tended to have lower mt D-Loop levels compared to those with good outcome (mRS 0-2). However, this was in contrast to the findings of Wang et al., (2013) who found significant elevation of mtDNA at day 8 in poor outcome patients, but this difference does not exist anymore after controlling for the aneurysm treatment effects (Wang et al., 2013). Furthermore, the study of Wang et al. (2013) was comprised of a small population of patients (n = 21) with more patients in the

poor outcome group (n = 15), which might be the reason for divergence from the current findings.

The increasing levels of mtDNA in peripheral circulation may likely involve mtDNA release from necrotic cells or probably the impairment of the DNA clearance mechanisms owing to systemic inflammation mediated organ damage in critically ill patients (Tsai et al., 2011). Inflammation can lead to increased leucocyte counts (Neil-Dwyer and Cruickshank, 1974) and interestingly, mtDNA levels showed associations with leucocyte counts (Table 4). However, cumulative levels of CytB and D-Loop mtDNA were positively correlated with leucocyte count (Table 5), which is in agreement with previous findings (Tsai et al., 2011) and it suggests that mtDNA may probably lead to leukocytosis owing to its DAMP nature. A negative correlation was found at different days among mtDNA and CRP levels. It is already known that systemic DNA levels correlate with cerebral hematoma; however, we found a weak, but significant correlation among Fischer grade, cumulative mtDNA levels of CytB and COX-1 (Table 5) (Rainer et al., 2003). It was also noteworthy that the use of β-blockers and Ca2+ channel blockers was positively correlated with mtDNA levels and whether it was by chance or has some clinical significance may require further investigations.

It has already been mentioned that mtDNA levels are upregulated after CNS insult and TLR-9 is the major receptor mediating inflammatory effects of mtDNA (Boyapati et al., 2017). Therefore, TLR-9 represents an important target and different strategies based on oligodeoxynucleotides (ODN) aimed at antagonizing the inflammatory effects of TLR-9 activation are under development through preclinical or early clinical studies (Hennessy et al., 2010; Hoque et al., 2013; Savva and Roger, 2013). Another approach based on molecular scavenging of the free nucleic acids by nuclear acid binding polymers has been shown to limit the inflammation in preclinical studies (Holl et al., 2013; Holl et al., 2016). Therefore, further dissection of the inflammation associated with mtDNA and TLR-9 axis in animal models of SAH is warranted to unveil the therapeutic potential of this axis.

5.2. Systemic Cytokine response after aSAH

Circulating cytokines load play critical role in determining the health status of the individuals (Oke and Tracey, 2009). Cytokines mediate the immune or inflammatory response after injury and are also known to possess neuroregulatory properties with potential implications in various CNS diseases (Osuka et al., 1998). As already mentioned, inflammation plays an

indispensable role in early brain injury and also in the development of complications over the course of aSAH (Provencio, 2013; Miller et al., 2014; Moraes et al., 2015; Lucke-Wold et al., 2016). A great body of evidence supports the upregulation of different cytokines secreted by immune cells in aSAH (Fassbender et al., 2001; Takizawa et al., 2001; Hopkins et al., 2012). These inflammatory cytokines do not only exist in the CSF reflecting local response at the CNS level, rather are also increasingly documented in the systemic circulation and some of these cytokines have been associated with a late inflammatory response and poor outcome (Miller et al., 2014).

5.2.1. IL-23

IL-23 is a heterodimeric cytokine composed of p40 (shared with IL-12 p40) and p19 subunits and signals by binding to IL-23R and IL-12Rβ1 (Oppmann et al.; Parham et al., 2002). The p19 subunit of IL-23 shares structural homology with IL-6 and TNF-α (Oppmann et al., 2000). IL-23, released by activated monocytes and dendritic cells, plays a distinct role in Th17 cell polarization and amplifying IL-17 response (Uhlig et al., 2006; Lyakh et al., 2008; Ghoreschi et al., 2010). Serum IL-23 has been shown to be elevated in numerous inflammatory diseases (Ciprandi et al., 2012; Wen et al., 2012; Atwa et al., 2014; Chen et al., 2014; Du et al., 2014; Borovcanin et al., 2015; Fotiadou et al., 2015; Wendling et al., 2015). However, IL-23 has still not been investigated after aSAH in human subjects and to the best of our knowledge, this is the first study to investigate serum IL-23 levels in aSAH patients and find the association with post hemorrhagic complications and outcome.

We observed an early elevation of serum IL-23 after aSAH that persisted till day 7 (Fig. 13). It suggests that systemic inflammatory response is upregulated after aSAH and may contribute to the early brain injury and furthermore, in the pathophysiology of post-aSAH complications (Miller et al., 2014). Hence, we further analyzed IL-23 levels in different subgroups of patients after aSAH. Interestingly, serum IL-23 levels were downregulated in poor H&H and Fischer grades lately (Fig. 14A, Table 7) and in patients who developed seizures and at both days in other infections group (Fig 14D, F, Table 7). This might be due to immunodepression observed after aSAH and impaired capacity of the PBMCs to release cytokines under enhanced sympathetic activity due to ANS dysfunction (Kinoshita et al., 2007; Sarrafzadeh et al., 2011). Intracerebral bleeding, in addition to aSAH may present additional damage and is well known to be associated with poor outcome after aSAH,

therefore, may be leading to an early rise in serum IL-23 (Fig. 14B) (Rosengart et al., 2007). Endovascular coiling appeared to have less impact on IL-23 secretion as opposed to neurosurgical clipping (Fig. 14C, Table 7). Endovascular coiling is advocated to lead to better outcomes than neurosurgical clipping in small sized cohorts; and levels of CRP and S100B have been found to be higher postoperatively in aSAH patients undergoing neurosurgical clipping compared to endovascular coiling (Weiss et al., 2006; Jeon et al., 2012; Ayling et al., 2015; Taheri et al., 2015). Increased levels of IL-1RA were observed in CSF after surgery of poor H&H grade aSAH patients reflecting the contribution of surgical trauma to the measured cytokines (Mathiesen et al., 1997). However, are there any other differences in inflammatory response or immunologic markers such as IL-23, still warrants further investigations? Although, we did not find any significant increase of IL-23 in patients with cerebral ischemia, however, intriguingly serum IL-23 levels significantly upregulated promptly after aSAH in DCI patients and non-significantly sustained at day 7 in comparison to patients developing interventional CI, where elevation may have resulted from the drastic effects of aneurysm treatment (Fig. 14E, Table 7). DCI is a multifactorial phenomenon after aSAH and is a well established contributor to unfavourable clinical outcomes (Kiiski et al., 2017). However, serum IL-23 levels did not associate with the clinical outcome (Fig. 15).

IL-23 has been proposed as a surrogate marker for multiple sclerosis disease activity (Chen et al.). In an experimental acute encephalomyelitis model, anti-IL-23 p19 antibody reduced the serum IL-17, expression of other pro-inflammatory cytokines and CNS infiltration of myeloid and T cells (Konoeda et al., 2010). In ischemic stroke models, serum IL-23 has been shown to contribute to an inflammatory response and abolishing this response conferred neuroprotection and improved neurobehavioural outcomes (Shichita et al., 2009; Gelderblom et al., 2014). IL-23 gene deletion in mice has been shown to confer remarkable recovery in the setting of ischemia (Shichita et al., 2009). Konoeda et al. (2010) used anti- IL-23 p40 monoclonal antibody and JAK-kinase inhibitor to block the effects of IL-23 and its downstream signaling via JAK-STAT3 pathway respectively to demonstrate neuroprotection in ischemia/ reperfusion injury. At present, monoclonal antibodies targeting either IL-23 p40 or IL-23 p19 in various inflammatory diseases are being investigated in different phases of clinical trials (Gaffen et al., 2014; Teng et al., 2015). Therefore, IL-23 and its downstream signaling pathways represent potential modulatable therapeutic targets to treat various inflammatory diseases.

Until now, IL-23 and its role in aSAH has not been investigated in detail. Our data, although descriptive in nature, however, provide novel information in human subjects to further evaluate the pathophysiological role of IL-23 after aSAH.

5.2.2. IL-17

IL-17 or IL-17A is a signature cytokine for Th17 cells which express transcription factor RORγt (retinoic acid receptor-related orphan receptor-γt) and require IL-23 for maturation to an inflammatory phenotype (Gaffen et al., 2014). In addition to Th17 cells, IL-17 is also secreted by other innate immune cells such as γδ T cells, NK T cells and innate lymphoid cells (Gaffen et al., 2014). IL-17 signals mainly through heterodimeric complex of IL-17RA and IL-17RC and activates downstream pro-inflammatory pathways NFκB, MAPK and C/EBP (Korn et al., 2009; Gaffen et al., 2014). IL-17 can upregulate inflammation by inducing secretion of pro-inflammatory cytokines such as TNF-α, IL-1β, IL-6 and chemokines for recruiting neutrophils and macrophages (Mills, 2008). IL-17 plays a key role in many inflammatory autoimmune diseases such as psoriasis, inflammatory bowel disease, multiple sclerosis, rheumatoid arthritis and asthma (Korn et al., 2009; Gu et al., 2013). Shichita and co-authors (Shichita et al., 2009) have shown that IL-17 producing cells (mainly γδ T cells) mediate ischemic-reperfusion injury. IL-17 positive lymphocytes were also detected in post stroke autopsies and antibody mediated neutralization of IL-17 in experimental stroke reduced infarction and improved outcome (Gelderblom et al., 2012).

It is well established that IL-23 plays an indispensable role in the maturation of Th17 cells towards an inflammatory phenotype secreting IL-17 (Gaffen et al., 2014). In line with this, we found significant increase of IL-17 in aSAH compared to controls and the levels of IL-17 were significantly higher even at day 7 compared to day 1 in aSAH (Fig. 16). In contrast to serum IL-23 levels, severe H&H grade led to the upregulation of serum IL-17 (Table 7). A large number of patients develop anterior circulation aneurysms (D'Souza, 2015), the increased serum IL-17 in our study might be due to the greater population with anterior circulation aneurysms as compared to posterior circulation aneurysms (Fig. 17B). Interestingly, presence of both intraventricular and intracerebral hemorrhage led to significant downregulation of IL-17 initially and later on it was significantly upregulated (Fig. 17C), suggesting an initial neuroprotective anti-inflammatory response might be implicated to limit further damage, but later on uncontrolled inflammation led to soaring serum levels of IL-17.

Serum IL-17 levels showed decrease in DIND, while IL-23 in seizures (Fig. 17D). Interestingly, further subgroup analysis in the infarcts group showed that serum IL-17 levels were downregulated in DCI, while interventional CI induced increase in contrast to IL-23 (Fig. 14E, 17E, Table 7). In contrast to IL-23, serum IL-17 levels were upregulated in the patients in other infections group as compared to those who did not contract any infections and significant elevations in serum IL-17 were present in other infections group compared to only pneumonia or meningitis (Fig. 17F, 18A, B). IL-17 is well known to be upregulated under infections and since, other infections group represent aSAH patients with infections such as UTI, osteomyelitis or a combination with pneumonia and meningitis infections, so it may be likely that the greater burden of infections in this group led to significant upregulation of IL-17 secreting cells (Cua and Tato, 2010). These findings suggest that both cytokines were differentially regulated in systemic circulation under the development of different complications. The existence of association with some of aSAH complications and not with some others might be due to the pleiotropic nature of cytokines (Bukowski et al., 1994).

Several animal and human studies support the upregulation and involvement of IL-17 in cerebral ischemic injury (Kostulas et al., 1999; Li et al., 2005; Shichita et al., 2009; Gelderblom et al., 2012; Gelderblom et al., 2014). Shichita et al. (2009) have shown that IL-23 mediates early, while IL-17 is implicated in delayed damage due to ischemia and the source of IL-17 were γδ T cells. Neuroglial cells have also been shown to be the source of IL-17 in the ischemic brain damage (Li et al., 2005). At present, monoclonal antibodies targeting either IL-17 or IL-17RA in various inflammatory diseases are being investigated in different phases of clinical trials (Gaffen et al., 2014; Teng et al., 2015). Therefore, IL-17 represent potential modulatable therapeutic target to treat various inflammatory diseases.

A complex pathophysiology of aSAH involving brain, vasculature and immune cells preclude the pharmacological interventions in human subjects. Further evaluation of the role of IL-23/IL-17 axis in early brain injury and complications after aSAH is warranted by using neutralization monoclonal antibodies or genetic deletion in SAH animal models to provide valuable therapeutic options to treat aSAH.

5.2.3. IL-6

IL-6 represents a primary and key player in inflammation augmentation (Tang et al., 2014). IL-6 is a pleiotropic cytokine with hormone like activity that can influence vascular and

metabolic diseases (Bethin et al., 2000; Hodes et al., 2014; Kraakman et al., 2015). IL-6 signals via IL-6R (CD126, type 1 cytokine α-receptor subunit) and gp130 (CD130, β-receptor subunit) and involves downstream pathways such as GTPase Ras-Raf, MAPK and JAK-STAT (Scheller et al., 2011; Hunter and Jones, 2015). Three modes of IL-6 signaling have been identified: classical involving membrane bound IL-6R and gp130; trans-signaling dependent on soluble IL-6R whereby only gp130 expressing cells can gain response to IL-6-sIL-6R complex; and recently identified cluster signaling in which dendritic cells harboring IL-6-IL-6R complex in their membranes engage gp130 on the target cell membranes (Scheller et al., 2011; Hunter and Jones, 2015; Quintana, 2017). Depending on the context of the disease, IL-6 has both pro-inflammatory and anti-inflammatory effects (Hunter and Jones, 2015). In acute pathological conditions including aSAH, IL-6 stimulates the neuroinflammatory response (Suzuki et al., 2009) that may contribute to the disease progression. IL-6 levels in cerebrospinal fluid (CSF) of patients after aSAH have been shown to be associated with occurrence of cerebral vasospasm and clinical outcome (Osuka et al., 1998; Schoch et al., 2007; Sarrafzadeh et al., 2010; Helbok et al., 2015; Niwa and Osuka, 2016; Wu et al., 2016a; Zeiler et al., 2017). Moreover, elevated early serum IL-6 levels predict the unfavourable clinical outcome (Muroi et al., 2013; Hollig et al., 2015b; Hollig et al., 2015a; Kao et al., 2015).

IL-6 is one of the extensively investigated cytokine in the CSF after aSAH, but detailed investigations of systemic IL-6 during the course of different post-aSAH complications are still lacking. We have observed that systemic IL-6 levels were elevated starting from day of bleeding and remained high over the 2 weeks as compared to healthy controls (Fig. 19). Early brain injury is a complex row of events including elevation of intracranial pressure, reduction of cerebral blood flow, oxidative and metabolic disturbance with acute vascular reaction leading to transient global ischemia (Macdonald, 2014). Elevated IL-6 levels on admission might be the response of transient global ischemia during the early brain injury. In most of brain injuries including cerebral ischemia and SAH, the initial events can lead to secondary complications (Miller et al., 2014). Initially released cytokines link the later damage. The best example of cytokine mediated late damage is the High Mobility Group Box 1 (Wang et al., 1999; Tsung et al., 2005). It has been previously shown that cytokines released from necrotic cells of ischemic core mediate delayed brain damage in penumbra (Muhammad et al., 2008). Interestingly, IL-6 signaling is known to recruit neutrophils at the site of injury in initial

phase and proteolytic processing of IL-6R on neutrophils ultimately switches the IL-6 signaling to resident cells including cerebral vasculature cells (Jones, 2005). Furthermore, IL-6 can lead to polarization of naïve T cells to Th1 or Th2 cell subpopulations (Diehl et al., 2002; Diehl and Rincon, 2002). Both sub populations have distinct functions. Th1 type cells are pro-inflammatory in nature, but Th2 type cells have anti-inflammatory effects showing the anti-inflammatory side of IL-6.

Elevated IL-6 levels initially after aSAH may contribute to regulate vascular inflammation at later stages and hence, may contribute to post-aSAH complications. Occurrence of post-hemorrhagic complications is the key to determine clinical outcome of patients after aSAH. Our data demonstrate that the patients who developed cerebral vasospasm, delayed neurological deficits, hydrocephalus and symptomatic epilepsy showed elevated systemic IL-6 levels (Fig. 21C-F). Interestingly, pharmacological interventions to interrupt IL-6 signaling reversed vasospasm in rat femoral artery vasospasm model (Bowman et al., 2004; Bowman et al., 2006; Kooijman et al., 2014a). Furthermore, soluble gp130 antagonizing IL-6 signaling has been described to follow a parallel increase with IL-6 on day 1 after aSAH in CSF and then gradually declines, relieving IL-6 from regulatory check and paving the way to the development of vasospasm (Nakura et al., 2011). Elevated serum IL-6 in most of the post-aSAH complications seems to be a part of generalized inflammatory response rather than a cause of a specific post-aSAH complication (Miller et al., 2014). Similarly, the higher IL-6 in serum of poor grade aSAH patients (Fig. 20E) is in line with previous investigations (Savarraj et al., 2017b) and may reflect the unspecific upregulated inflammatory response due to tissue damage. The delayed elevation of IL-6 in serum of patients with cerebral ischemia (Fig. 22E) might be secondary to ischemia that is in line with literature from stroke research (Gertz et al., 2012). Nevertheless, elevated IL-6 levels showed association with poor clinical outcome (Fig. 23) confirming previously published findings (Hollig et al., 2015b; Hollig et al., 2015a). Our data suggest that IL-6 is not specific to predict post-aSAH complications, but could be a surrogate parameter of global inflammatory burden observed after aSAH (Miller et al., 2014). Interestingly, IL-6 has been regarded as the better predictor of disease activity than the most commonly used marker, C-reactive protein, because of its homeostatic basal regulation and rapid induction under different disease conditions (Panichi et al., 2004; Fraunberger et al., 2006; Mroczko et al., 2010). However, in line with the existing literature serum IL-6 levels is a predictor of clinical outcome.

Our study with human population has interesting findings, but with certain limitations. First of all, our patient population is very heterogeneous with wide age range, inclusion of both sexes and diverse grade of severity of subarachnoid hemorrhage with Hunt and Hess grad I-V. All these factors may lead to increase the variation as reflected by our data showing that patients with age over 55 years had higher serum IL-6 levels. Hence, due to the heterogeneity of aSAH population the data should be interpreted carefully for any implications in the clinical setting.

Moreover, in intubated patients the body temperature is artificially maintained during the intensive care. Elevated body temperature is known to be associated with increased IL-6 levels in systemic circulation (Herrmann et al., 2003). Hence, a controlled body temperature in intubated patients may confound the systemic IL-6 levels.

Furthermore, the assessment of clinical outcome with common test batteries including GOS and mRS are not sensitive and roughly reflects the neurological status and hence, the discrete changes in neurological status may be overlooked. Altogether the complex and pleiotropic nature of IL-6 biology and its elevation in multiple post-aSAH complications makes it an unspecific marker for post-aSAH complications.

5.2.4. IL-10

The neuronal injury and neurological outcome is based on a delicate balance between pro-inflammatory and anti-inflammatory mediators (Allan et al., 2005). IL-6 and IL-10 represent important players in the inflammatory cascade observed after infectious or inflammatory diseases of the CNS (Heep et al., 2004). Serum IL-6 levels have been already known to correlate with serum IL-10 levels after intracerebral bleeding and IL-6 can induce an anti-inflammatory response with upregulated IL-10 at cellular level via regulatory mechanisms (Dziedzic et al., 2002; Yasukawa et al., 2003). A very recent study has shown correlation among serum IL-6 and IL-10 under different conditions after aSAH (Savarraj et al., 2017a). Moreover, suppressed IL-10 expression has been shown in ruptured intracranial aneurysms and some SNPs in IL-10 gene have been identified to be associated with the formation of intracranial aneurysms (Jayaraman et al., 2005; Sathyan et al., 2015). However, comprehensive studies investigating the role of this pleiotropic immunomodulatory cytokine after aSAH are still lacking (Garcia et al., 2017). This prompted us to investigate serum IL-10

levels after aSAH and investigate its association with post-aSAH complications and clinical outcome.

A significant increase of serum IL-10 was recorded in aSAH patients at both days of assessment compared to healthy controls (Fig. 24). Serum IL-10 levels tended to be lower at day 7 compared to day 1, but were still significantly higher compared to controls and this upregulation of serum IL-10 after aSAH is in agreement with a previous study (Kinoshita et al., 2007). Most of the previous clinical studies have evaluated the CSF, extracellular fluid (by microdialysis) or serum IL-10 levels without any comparative controls (Dziurdzik et al., 2004; Mellergård et al., 2008; Mellergard et al., 2011; Hopkins et al., 2012; Savarraj et al., 2017a). Dziurdzik and coauthors have shown that serum IL-10 levels were significantly following a decreasing course with the passage of time in SAH and TBI patients and interestingly, serum IL-10 levels were higher compared to TBI patients and similar difference was revealed even on microdialysis representing local brain levels of IL-10 later on (Dziurdzik et al., 2004; Mellergård et al., 2008; Mellergard et al., 2011). Hopkins et al. (2012) did not find a huge separation between CSF and plasma levels of IL-10 after aSAH and Mellergard et al. (2011) reported an almost sustained IL-10 in microdialysates without any increasing or decreasing trend or fluctuation.

In subgroup analysis after dichotomization, no impact of patient's gender, aneurysm location or treatment modality on serum IL-10 levels were observed. Mellergard et al. (2011) while evaluating the course of IL-10 by microdialysis after aSAH and TBI also did not find any gender specific significant difference. A significantly marked elevation in serum IL-10 levels was observed at day 7 in aSAH patients with age $\geq$ 55 years, although IL-10 levels were higher at day 1 also (Fig. 25A). This rise might be reflecting parallel IL-10 upregulation in response to global inflammatory response after aSAH with advanced age, as increasing age independently predicts poor outcome at discharge and since, no such difference exists among healthy young and elderly human subjects in serum IL-10 levels and nor in healthy children or adults (Kim et al., 2011; Kleiner et al., 2013; Miller et al., 2014; Galea et al., 2017b). Peripheral IL-10 levels have already been shown to elevate significantly in poor grade aSAH patients (H&H $\geq$ 4) (Chamling et al., 2017; Savarraj et al., 2017a; Savarraj et al., 2017b). Although the levels of serum IL-10 were higher at day 1 and day 7 in our population of poor grade aSAH patients, yet they did not reach significant difference (Fig. 25B) and this might be due to the difference in H&H grades considered for dichotomy as they have considered

higher H&H grades to represent clinically severe aSAH patients. Interestingly, IL-10 levels were significantly increased at day 7 after IVH, but presence of both IVH and ICB led to an early significant increase in IL-10 at day 1 (Fig. 25C, D). Previous studies investigating the levels of IL-10 after intracerebral bleeding have consistently shown its significant upregulation and interestingly, IL-10 is linked to increase the expression of CD36 in microglia, thereby enhancing their erythrophagocytic capability and CD36 insufficiency led to increased pro-inflammatory cytokines and decreased IL-10 expression (Dziedzic et al., 2003; Oto et al., 2008; Wang et al., 2011a; Fang et al., 2014).

Serum IL-10 levels were already higher in aSAH patients who later on developed CVS and at day 7, serum IL-10 showed a very significant increase in CVS patients (Fig. 25E). This is in agreement with the findings of Li et al. (2017) who found significant upregulation of IL-10 expression in basilar artery showing decreased caliber and thickened walls in a rodent SAH model. Interestingly, increased IL-10 expression was associated with a parallel surge of pro-inflammatory cytokines (IL-1β, TNF-α and IL-6) and increased HMGB1 expression and glycyrrhizic acid supplementation, not only relieved vasospasm, but also abrogated the expression of pro-inflammatory factors and further enhanced IL-10 expression (Li et al., 2017). In the current study, a significant elevation of HMGB1 in aSAH patients presenting with CVS has also been recorded (Fig. 4F). HMGB1 is known to drive IL-10 release from M2-like macrophages through RAGE signaling selectively and also from PBMCs (Huber et al., 2016). Therefore, keeping in view these evidences it would be plausible to investigate the effects of glycyrrhizic acid clinically, since CVS is known to contribute majorly towards DCI and ultimately leading to poor clinical outcomes (Weidauer et al., 2007; Kruyt et al., 2010; Kooijman et al., 2014b; Macdonald, 2014; Garcia et al., 2017).

Serum IL-10 levels were also significantly raised at day 7 in patients requiring ventriculoperitoneal shunt mediated diversion of CSF due to development of chronic hydrocephalus (Fig. 25F). In normal pressure hydrocephalus, only CSF IL-10 levels have been shown to significantly rise and in the context of hemorrhagic stroke, hydrocephalus and plasma IL-10 are significantly associated with rebleeding and hematoma expansion with consequent adverse outcomes (Wang et al., 2011b; Sosvorova et al., 2014). Higher intracranial pressure is also known to elevate CSF IL-10 levels among other cytokines (Shiozaki et al., 2005). Serum IL-10 levels have not reflected any impact of cerebral ischemia/infarction. However, in patients with DCI serum IL-10 levels seemed to be higher

(Fig. 26E, F). Post-aSAH nosocomial infections are commonly reported and serum IL-10 levels showed significant elevation at day 7 (Fig. 26A) (Frontera et al., 2008; Sarrafzadeh et al., 2011). Further dissection of infections group showed that this significant surge in IL-10 at day 7 could be contributed by pneumonia or other infections (UTI, osteomyelitis or concomitant presence of these with pneumonia or meningitis) (Fig. 26B, C). Chamling et al. (2017) have also shown significant association of plasma IL-10 with pneumonia infection in aSAH patients. Furthermore, a significant increase at day 1 in serum IL-10 levels was observed in patients who developed pneumonia opposed to meningitis (Fig. 26D).

Finally, outcome assessment at discharge using GOS and mRS showed that serum IL-10 levels at both days of assessment were associated with poor clinical outcome (Fig. 27A, B). As Garcia et al. (2017) have already indicated that comprehensive and sophisticated studies investigating serum IL-10 post aSAH are lacking and also to the best of our knowledge, this is the first study indicating association of serum IL-10 with poor clinical outcome at discharge during the period of early brain injury (day 1) and delayed brain injury (day 7). Very recently, Savarraj et al. (2017a) have shown association of serum IL-10 measured within 48 hours of aSAH to be associated with clinical outcome at discharge with slightly different dichotomization of the mRS scale (Good outcome ≤ 3). These novel investigations showing upregulation of systemic IL-10 after aSAH, however, conforms to the previous investigations in ischemic stroke, intracerebral hemorrhage or traumatic brain injury (Shiozaki et al., 2005; Oto et al., 2008; Mellergard et al., 2011; Wang et al., 2011a; Garcia et al., 2017).

IL-10 represents an important anti-inflammatory cytokine secreted by almost all immune cells (Wang et al., 2017). A parallel increase in IL-10 levels is always associated with the elevation of pro-inflammatory cytokines (such as TNF-α, IL-1β, and IL-6) (Li et al., 2017; Savarraj et al., 2017a; Wang et al., 2017). Therefore, the significant elevation of IL-10 may be reflecting an upregulated inflammatory response set into play after aSAH (Kooijman et al., 2014b; Savarraj et al., 2017a). IL-10 is known to produce anti-inflammatory effects through various mechanisms such as inhibition of pro-inflammatory cytokine release and upregulation of antioxidant and radical scavenging enzymes and downregulation of ROS generating enzymes (Garcia et al., 2017). Microglial secreted IL-10 activates TGF-β secretion from astrocytes that blunts the pro-inflammatory cytokine response of the microglia in a feedback mechanism (Norden et al., 2014). IL-10 administration in stroke has been shown to be

neuroprotective, which could be the consequence of downregulation of NFκB, upregulated STAT3 signaling and inhibition of histone deacetylase resulting in Foxp3 expression by Tregs (de Bilbao et al., 2009; Liesz et al., 2013). Autonomic nervous system dysfunction after aSAH leading to increased sympathetic activity has been well known to trigger IL-10 release from peripheral blood mononuclear cells (PBMCs) and systemic IL-10 levels are attributed to be mainly derived from blood mononuclear cells (Pelidou et al., 1999; Kinoshita et al., 2007). Interestingly, IL-10 with LPS co-stimulation has been described to upregulate the expression of chemokine receptors (CCR1, CCR2, CCR5) and downregulate the CCR7 on dendritic cells, potentially hindering their maturation and migration capacity and the upregulated receptors sequester and scavenge pro-inflammatory chemokines such as RANTES/CCL5 produced at local inflammatory site (D'Amico et al., 2000). Thus, IL-10 promotes generation of functional decoy receptors on monocytes and dendritic cells to limit inflammatory chemokines (D'Amico et al., 2000). All these evidences highlight an indispensable role of IL-10 in inflammation after aSAH which may require further translational investigations and suggest that IL-10 has an important prognostic potential in aSAH associated complications and clinical outcome.

5.3. Chemokine response after aSAH

5.3.1. RANTES/CCL5

Chemokines represent small soluble mediators which play a critical role in the cell to cell communication and leucocyte trafficking (Zlotnik and Yoshie, 2000; Dorner et al., 2002). In contrast to the constitutively expressed chemokines with homeostatic role, several of the chemokines are induced during inflammation (Mantovani, 1999; Dorner et al., 2002). Regulated on activation, normal T cell expressed and secreted (RANTES) or CCL5 is a pro-inflammatory chemokine from class CC of chemokines and binds several of seven transmembrane GPCRs such as CCR5, CCR4, CCR3, CCR1, Syndecan (SDC)-4, SDC-4, and CD44 (Rollins, 1997; Xia and Hyman, 1999; Zlotnik and Yoshie, 2000; Suffee et al., 2017). CCL5 is secreted by T-lymphocytes, endothelial cells, epithelial cells, endometrial cells, smooth muscle cells, platelets, eosinophils, fibroblasts, glial cells and neurons (Appay and Rowland-Jones, 2001; Terao et al., 2008; Levy, 2009; Tokami et al., 2013). Elevated CCL5 has been regarded as a risk factor for stroke in asymptomatic subjects (Canouï-Poitrine et al., 2011). In numerous CNS related pathologies, CCL5 has been known to play an

inflammatory role (Simpson et al., 2000; Bartosik-Psujek and Stelmasiak, 2005; Cartier et al., 2005; Zaremba et al., 2006; Tang et al., 2014; Cerri et al., 2017). CCL5 expression has been shown to be upregulated in the rat cerebral aneurysm arterial walls (Aoki et al., 2008). Recent investigations in the context of SAH have demonstrated the involvement of CCL5 in ongoing inflammation (Smithason et al., 2012; Chang et al., 2015b). However, detailed clinical investigations of CCL5/RANTES have still not been performed. Here, we have evaluated the serum levels of CCL5/RANTES after aSAH and its association with post-aSAH complications and clinical outcome at discharge.

During the current analysis, systemic levels of CCL5 were higher in aSAH patients on early assessment at day 1 and later on at day 7 compared to controls (Fig. 28). This is in line with increased plasma levels of CCL5 observed after traumatic brain injury and ischemic stroke (Tokami et al., 2013; Albert et al., 2017). Analysis of multiple systemic cytokines after aSAH has already shown that CCL5 levels peaked 6-8 days after aSAH, but were the part of the cluster of platelet associated cytokines that were correlated at all the times of assessment after aSAH and included platelet derived growth factor (PDGF)-AA, PDGF-AB/BB, sCD40L, CXCL1P1 and TNF-α (Savarraj et al., 2017b). Interestingly, the CCL5 levels were shown to be negatively correlated with FLTL3 in less severe grade aSAH patients (Savarraj et al., 2017b). In an experimental SAH model, CCL5 levels were significantly upregulated in brain after 24 hours of SAH and more pronounced increase occurred if mice were pretreated with LPS and a very significant decrease was observed after myeloid cell depletion (Smithason et al., 2012). Interestingly, in another experimental SAH study, CCL5 upregulated along with adhesion molecules after SAH was attenuated by valproic acid supplementation and intrathecal administration of CCL5 reversed the valproic acid effects with increased adhesion molecules (ICAM-1, VCAM-1, E-selectin) expression and infiltration by CD45+ leucocytes (Chang et al., 2015b).

In the subgroup analysis after data dichotomization, it was interesting to note that the levels of CCL5 tended to be non-significantly lower in aSAH patients with higher age (Fig. 29A). However, higher age has been shown to be associated with upregulation of CCL5 levels in healthy subjects (Mansfield et al., 2012). Dichotomy of aSAH patients based on gender, aneurysm location, aneurysm treatment modality, severity of aSAH (H&H grades), CVS, DIND, seizures, cerebral ischemia and infections did not reveal any significant difference. Intriguingly, serum CCL5 levels were significantly downregulated under the development of

intracerebral bleeding, chronic hydrocephalus and pneumonia infection at day 7 in aSAH patients in the current study (Fig. 29B–D). Since, intracerebral bleeding represents additional damage, it may be likely that delayed release of CCL5 is restricted to limit further damage and may involve some immunosuppression phenomenon as CCL5 levels were non-significantly higher at day 1 (Sarrafzadeh et al., 2011). This is somehow in agreement with plasma CCL5 levels observed to be downregulated under severe head injury compared to mild to moderated head injury (Albert et al., 2017). Since, infections are associated with a downregulation in the levels of RANTES and also immunodepression is observed after aSAH, therefore, CCL5 levels were low in pneumonia affected aSAH patients (Sarrafzadeh et al., 2011; Albert et al., 2017).

The serum CCL5 levels were higher in good clinical outcome aSAH patients at day 1 and interestingly, at day 7 they were significantly higher compared to poor clinical outcome patients as assessed by GOS and mRS on discharge (Fig. 29E, F). Intriguingly, low levels of CCL5 have been established as predictors of mortality after myocardial infarction and cerebral malaria (John et al., 2006; Cavusoglu et al., 2007). As mentioned above, CCL5 levels tend to be lower in patients with severe head injury than those with mild to moderate head injury (Albert et al., 2017). However, in an experimental ischemic stroke model it was shown that knockout of RANTES was associated with relatively lower infarct volumes and reduced plasma levels of IL-6, IL-10 and IL-12 and furthermore, circulating blood cells as a potential source of RANTES that mediates BBB disruption, cerebral inflammation and infarction (Terao et al., 2008). In contrast to this, CCR5 knockouts had larger infarcts (Woiciechowsky et al., 1998). Tokami et al. (2013) have tried to answer this puzzling contradiction by suggesting an autocrine or paracrine role of neuron derived CCL5 which upregulates neuroprotective growth factors such as BDNF, EGF and VEGF and downregulates Caspase-3 in neurons through CCR5 and CCR3 ligation on neurons. Furthermore, they speculate that CCR1 expression by endothelial cells and by circulating blood cells may explain the acute detrimental effects of RANTES (Tokami et al., 2013). All these lines of evidence suggest that CCL5 which was found to be higher in good clinical outcome aSAH patients at discharge may have neuroprotective role. As to the best of our knowledge, this is the first study which investigates serum RANTES after aSAH and its association with clinical outcome at discharge, further investigations are strongly warranted to confirm these findings using experimental SAH models.

The CCL5 source during early brain injury after aSAH might be damaged neurons, glial cells, endothelial cells and infiltrating leucocytes as suggested by others in various CNS related pathologies (Pedrazzi et al., 2007; Terao et al., 2008; Dénes et al., 2010; Mirabelli-Badenier et al., 2011; Tokami et al., 2013). Pedrazzi et al. (2007) have shown that HMGB1 could lead to secretion of CCL5 from astrocytes and due to localization of astrocytes in close proximity to BBB, secreted CCL5 may play an important role in microglial and blood monocyte migration and activation, thus enhancing the brain damage. The systemic levels of HMGB1 have already been mentioned above to rise robustly after aSAH in our patient population (Fig. 2). Promotion of leucocyte infiltration at the inflammation site is a well established effect of RANTES (Appay and Rowland-Jones, 2001). CCL5 has been shown to mediate the brain damage through increasing the infiltration of mononuclear cells through BBB and lead to secondary brain injury via induction of potent inflammatory cytokines (Mirabelli-Badenier et al., 2011). Furthermore, CCL5 produced by DCs lead to a Th1 polarized response (Lebre et al., 2005; Ma et al., 2007). Interestingly, monoclonal antibody targeting of CCL5 has shown reduced leucocyte infiltration in CNS and also prevented neurological deficits in MS mouse model (Chang et al., 2015b). Therefore, further translational investigations using leucocyte or neuron specific knockout of RANTES or RANTES neutralization are highly encouraged to further understand the role of RANTES in the inflammation set into play by SAH.

5.4. Systemic immune cell response after aSAH

It is well known that DAMPs can activate the immune cells and trigger the production of numerous inflammatory mediators (Castellheim et al., 2009). Therefore, an upregulated DAMPs and cytokine response after aSAH may have underpinnings in the activation and polarization of immune cells. Hence, we have characterized different monocyte and CD4+ T helper cell subpopulations early after aSAH (during initial 72 hours) and later on during delayed brain injury phase (day 7) by polychromatic cell surface based flow cytometric immunophenotyping.

5.4.1. Systemic monocyte response after aSAH

Our data shows that total monocytes (CD45+) were significantly increased at day 7 compared to day 1 after aSAH and non-significantly elevated in comparison to controls ($p = 0.067$), suggesting an ongoing upregulated inflammation (Fig. 30A). However, monocytes expressed as CD14+ CD15- events did not show any significant difference among controls and aSAH

patients (Fig. 30B) and is in line with a previous study (Moraes et al., 2015). In subset analysis, no significant changes were evident in classical monocytes, which are mainly known to play a phagocytic role owing to higher peroxidase activity, enhanced IL-10 and diminished TNF-α response to LPS challenge (Geissmann et al., 2003; Cros et al., 2010). Moraes et al. (2015) have shown a significant decrease in intermediate monocytes compared to controls. However, we have only found a significant decrease at day 7 compared to day 1 after aSAH (Fig. 30D) and this might be due to their wider sampling time frame and comparatively more number of patients in the control group. However, we found a significant decrease in nonclassical monocytes at day 1 after aSAH compared to controls, which did not persist till day 7 after aSAH (Fig. 30E). Previous studies have assigned an inflammatory role to intermediate monocytes due to their increased IL-1β and TNF-α secretion upon LPS stimulation (Cros et al., 2010; Ziegler-Heitbrock et al., 2010; Ziegler-Heitbrock and Hofer, 2013; Guilliams et al., 2014). Whereas nonclassical monocytes are known to patrol the endothelium of vasculature and secrete IL-1β and TNF-α in response to nucleic acids such as DNA or RNA (Cros et al., 2010). A recent study has advocated nonclassical monocytes to be the main pro-inflammatory subtype and has shown the downregulation of CD16 expression during isolation procedures, likely mediating transition of nonclassical into intermediate monocytes (Mukherjee et al., 2015).

Chemokine receptors reflect the distinct maturity and migratory properties of the monocyte subsets, therefore, we have also assessed CCR2 and CX3CR1 expression on monocyte subsets. Interestingly, CX3CR1 expressing intermediate cells were significantly increased at day 1 in comparison to day 7 after aSAH, whereas nonclassical CX3CR1+ cells were significantly reduced immediately after aSAH compared to controls (Fig. 31B, C). The fractalkine receptor (CX3CR1) is intermediately expressed on intermediate monocytes, while highly expressed on nonclassical monocytes and by virtue of this receptor these cells crawl along the endothelia of the blood vessels and gain the name as patrolling monocytes (Cornwell et al., 2013). CX3CR1 expression is essential for monocyte homeostasis and survival due to inhibition of apoptosis (Landsman et al., 2009). Interestingly, the mice monocytes corresponding to the nonclassical human monocyte subset give rise to M2 or alternate tissue macrophages during inflammation (Cornwell et al., 2013; White et al., 2014). Conversely, CCR2 is highly expressed on classical monocytes and intermediate monocytes have characteristically intermediate expression and lowest on nonclassical subset.

Furthermore, CCR2 plays an important role in monocyte emigration from bone marrow and homing into sites of injury and differentiation into inflammatory macrophages (Geissmann et al., 2003; Tacke and Randolph, 2006; Cornwell et al., 2013). In line with this, CCR2+ classical monocytes were significantly increased after aSAH on day 1 compared to healthy controls (Fig. 31D), although no significant difference was found in classical monocytes among controls and aSAH patients. Similarly, CCR2+ intermediate monocytes were nonsignificantly higher at day 1 in aSAH patients as compared to controls and were significantly increased in comparison to day 7 after aSAH (Fig. 31E).

The monocyte activation marker HLA-DR represents an analog of MHC-II and is responsible for antigen presentation to T cells for paving the way to adaptive immune response (Palojärvi et al., 2012). Interestingly, HLA-DR expression has been shown to be upregulated during infection, but in sepsis and severe critical illness, downregulated HLA-DR expression on monocytes has been observed as a part of compensatory anti-inflammatory response syndrome which leads to immunosuppression (Kim et al., 2010; Palojärvi et al., 2012). Intriguingly, HLA-DR expressing classical monocytes were significantly decreased after aSAH at day 1 and day 7 as compared to controls; while HAL-DR+ intermediate cells showed decrease on day 7 compared to day 1 after aSAH; and nonclassical HLA-DR+ monocytes were significantly lower on day 1 after aSAH as compared to controls (Fig. 31G – I). These findings are in agreement with previous observation of reduced HLA-DR expression on monocytes and a prevalence of pneumonia infection among aSAH patients (Sarrafzadeh et al., 2011). The reduction in HLA-DR expression may stem from increased IL-10 and cortisol levels (Kim et al., 2010). Interestingly, we have found a significant increase in serum IL-10 after aSAH (Fig. 24) and the greater sensitivity of classical monocytes to HLA-DR downregulation is in concordance with a previous study, which suggested increased IL-10R expression on classical monocytes to be the likely mechanism (Kim et al., 2010).

To our knowledge, this is the first study in the context of aSAH analyzing monocyte subsets along with activation markers during early and delayed brain injury and showing differential expression of different monocyte subsets along with their activation markers.

5.4.2. Systemic CD4+ T cell response after aSAH

Over the past, different subsets of CD4+ T cells have been characterized, differentiating from naïve T cells under the influence of various cytokine microenvironments and expressing specific signature transcriptional factors, into Th1, Th2, Th17 and Treg cells (Murphy and Reiner, 2002; Acosta-Rodriguez et al., 2007; Sakaguchi et al., 2010). Th1 and Th17 cells represent with an inflammatory profile, while Th2 and Tregs promote anti-inflammatory responses (Murphy and Reiner, 2002; Acosta-Rodriguez et al., 2007; Boissier et al., 2008; Sakaguchi et al., 2010). A limited number of studies have investigated the major lymphocyte subsets such as CD4+ T cells, CD8+ T cells, and B cells after aSAH (Chrapusta et al., 2000; Sarrafzadeh et al., 2011; Moraes et al., 2015), but to date up to the best our knowledge, no study investigating specifically the subsets of CD4+ T cells based solely on the cell surface expression of different receptors and activation markers during early and delayed phase of aSAH has been performed.

Interestingly, we found significant decrease in lymphocytes and CD4+ T cells expressed as frequencies of CD45+ leucocytes after aSAH compared to controls (Fig. 32A, B). This lymphopenic response is in line with previous studies (Sarrafzadeh et al., 2011; Moraes et al., 2015). However, CD4+ T cells among lymphocyte population were outnumbered at day 1 and day 7 after aSAH as compared controls (Fig. 32C) which is in par with findings from (Moraes et al., 2015). The different subsets of CD4+ T cells showed some interesting significant differences and trends after aSAH. Th1 cells, which are pro-inflammatory in nature, were non-significantly lower at day 1 after aSAH ($p = 0.087$) compared to controls and increased non-significantly at day 7 compared to day 1 ($p = 0.092$) almost similar to that of controls (Fig. 33A). Notably, the Th2 cells were very slightly increased at day 1 after aSAH as compared to controls without significant difference, but this was followed by a significant decrease at day 7, which clearly represents an almost equal, but opposite behaviour of Th1/Th2 paradigm. Inhibition of Th1 response and augmentation of Th2 response has been shown to exert a neuroprotective role and improved outcomes in experimental models of ischemic stroke (Ayer et al., 2013). Similar to Th1 cells, Th17 cells were non-significantly lower at day 1 after aSAH as compared to healthy controls, but at day 7 after aSAH, Th17 cells significantly recovered to the levels almost similar to controls (Fig. 33C). Strikingly, Treg cells were significantly higher at day 1 after aSAH and increased further at day 7 with significant difference as compared to day 1 aSAH patients and healthy

controls (Fig. 33D). The pattern of Treg cells response seemed to parallel the inflammatory response of Th1 and Th17 subtypes. The increased Treg cells response seen after aSAH in our study is similar to that of observed after intracerebral hemorrhage (Shi et al., 2015). Zhang et al., have recently adopted a similar approach to identify helper T cell subsets and demonstrated a significant increase in Th17 and significant reduction in Th2 cells compared to healthy controls, which is in contrast to our findings as we have observed similar changes at day 7 as compared to day 1 in only aSAH patients. The plausible explanations for this difference might be due to inclusion of both ruptured and unruptured intracranial aneurysm patients and utilization of cryopreserved peripheral blood mononuclear cells. The chemokine receptor expression might be sensitive to temperature changes and density gradient separation techniques also modify surface expression of different receptors (Jalbert et al., 2013; Mukherjee et al., 2015).

Another peculiar aspect of our study of helper T cell subsets was the inclusion of permanent cell surface activation markers such as CD38 and HLA-DR as opposed to transient activation marker CD69 (Maecker et al., 2012). Assessment of CD38 and HLA-DR activation markers revealed that these markers are differentially expressed on different subsets of T helper cells (Fig. 34). CD38 expressing T cells have been shown to be larger, more granular and have reduced proliferative capacity, but enhanced cytokine production capability (Sandoval-Montes and Santos-Argumedo, 2005). Both HLA-DR and CD38 expression have been used as markers of activation of T cells and disease progression in various inflammatory diseases (Funderburg et al., 2013). The HLA-DR+ subset of Treg cells has been recognized as terminally activated effector Treg cells equipped with profound inhibition of proliferation of conventional T cells and prompt cytokine production compared to their HLA-DR- counterparts (Sakaguchi et al., 2010). Our results represent various novel findings with respect to different activation states of T helper cell subsets and suggest that polarization of these subsets is dynamic over the course of disease. However, the major limitation is the small sample size and further investigations are warranted to consolidate these findings in a large observational study.

6. Conclusion

Our data shows that damage associated molecular patterns including HMGB1 and mt DAMPs were elevated in the systemic circulation of patients with aSAH. Systemic HMGB1 was significantly associated with CVS and may have the potential to be a predictive biomarker for CVS. Furthermore, systemic cytokines including IL-17, IL-23, IL-6, IL-10 and RANTES have shown significant upregulation after aSAH and are involved in various complications after aSAH. Different subsets of monocytes and CD4+ T cells were differentially regulated during early and delayed phases of brain injury after aSAH. These findings altogether suggest an upregulation of systemic inflammation after aSAH, which may have diagnostic, prognostic and therapeutic implications and warrants further investigations using more sophisticated multicenter clinical studies and validation employing translational research.

7. Future Perspectives

Aneurysmal SAH is a complex disease involving a systemic inflammatory response, which is the mainstay of the current research. A plethora of DAMPs, cytokines and other molecular mediators may underlie this systemic inflammatory response which contributes to the development of different complications and delayed deterioration. The role of these pro- or anti-inflammatory molecules should be investigated through translational studies by exploiting genetic knockout techniques, administering monoclonal antibodies, aptamers and oligodeoxynucleotides, downregulating the expression through administration of miRNAs or by using pharmacological small molecule inhibitors.

Recently there is increasing evidence and renewed interest in the communication taking place at neuronal and immune interfaces with potential implications in modulating the pro-inflammatory or anti-inflammatory responses in the periphery (Chavan et al., 2017). Advancements in neuromodulation is uncovering new horizons to use "electrons" as therapeutics to modulate innate and adaptive immune responses in different diseases (Chavan et al., 2017). We have recently shown that the burst spinal cord stimulation (BSCS) not only leads to improvements in back pain in patients with failed back surgery syndrome (FBSS), but can also modulate the systemic levels of different cytokines and adipokines (Kinfe et al., 2017; Muhammad et al., 2017b; Muhammad et al., 2017a). We have found that BSCS increases the anti-inflammatory cytokine IL-10 systemic levels, which may underlie the improvements in pain and functional capacity in FBSS patients (Kinfe et al., 2017). Slavin and co-authors have studied the feasibility of cervical spinal cord stimulation (cSCS) over two weeks after aSAH for the management of CVS (Slavin et al., 2011). Neuromodulation represents an interesting field of research, though in infancy, has the potential to modulate the immune responses and may be exploited against systemic inflammation set into play after aSAH.

8. Summary

Aneurysmal subarachnoid hemorrhage (aSAH) is a dreadful disease with overwhelmingly high mortality and morbidity, although it accounts for only 5% of all strokes. Around half of the affectees are destined to death and it affects at relatively younger age. About 20% of the patients die before hospitalization and 40% - 60% within a month. Rupture of the intracranial aneurysm floods the subarachnoid space with blood and sometimes also involves brain ventricles and deeper brain parenchyma. Although, the obliteration of the bleeding aneurysms can be successfully achieved by neurosurgical clipping or endovascular coiling, but still a significant proportion of aSAH patients succumbs to life threatening complications such as CVS, DIND, seizures, chronic hydrocephalus, cerebral ischemia, infections and achieves poor clinical outcome. Failure of the CVS reversal paradigm to improve clinical outcome has led to reassess the role of inflammation in aSAH and its associated complications. Over the past, a role of systemic inflammation is well appreciated and the aim of our study was to assess systemic inflammation after aSAH and its associated complications.

Sterile inflammation is set into play after engagement of the DAMPs with PRRs on immune cells leading to their activation and polarization with the consequent release of inflammatory mediators such as cytokines. In order to characterize the systemic inflammation after aSAH, we have investigated the release of prototypical DAMPs members such as HMGB1, mitochondrial DNA, IL-1α and IL-33 after aSAH. Different pro-inflammatory and anti-inflammatory cytokines such as IL-23, IL-17, IL-6, IL-10 and CCL5 (RANTES) were analyzed at day 1 and day 7 after aSAH. The immune cells specifically monocyte subsets and CD4+ T helper subsets were analyzed by polychromatic cell surface based flow cytometry during early and delayed brain injury phases after aSAH.

Assessment of the DAMPs response showed significant elevation of serum HMGB1 after aSAH from day 1 until day 13. Interestingly, serum HMGB1 levels were significantly elevated in aSAH patients developing CVS early from day 1 until day 13. Hence, HMGB1 may have a prognostic potential for CVS after aSAH. Mitochondrial DNA gene fragments such as CytB, D-Loop and COX-1 were significantly elevated early after aSAH with exception of CytB, achieving significance at day 7. Serum mtDNA gene fragments showed differential associations with different aSAH patients' associated characters, complications and clinical outcome. However, IL-1α and IL-33 were rarely detectable in the systemic circulation after aSAH.

Among the cytokines, systemic IL-23 and IL-17 inflammatory axis was significantly upregulated after aSAH. However, subtle associations exist among subgroup analysis based on data dichotomization. The well-known acute pro-inflammatory cytokine, IL-6 was also evaluated after aSAH and serum IL-6 levels represented as an unspecific marker of aSAH associated complications and clinical outcome. The pro-inflammatory chemokine and cytokine CCL5 (RANTES) was also significantly elevated after aSAH, but CCL5 levels were significantly decreased at day 7 in patients who developed chronic hydrocephalus and pneumonia infection. Interestingly, CCL5 levels were significantly higher in good clinical outcome aSAH patients at day 7 after aSAH. Serum IL-10 levels were also significantly elevated and showed significant association with CVS, chronic hydrocephalus and infections at post-SAH day 7. Intriguingly, serum IL-10 levels were significantly elevated in poor clinical outcome patients at day 1 and day 7 after aSAH.

Monocytes were non-significantly increased after aSAH. Intermediate monocytes were significantly higher at post-SAH day 1 compared to day 7, while nonclassical monocytes were significantly decreased compared to healthy controls at day 1. The CX3CR1+ intermediate and nonclassical monocytes showed the similar significant differences as that of their parent populations. Intriguingly, classical CCR2+ monocytes significantly increased on post-SAH day 1 as compared to controls and intermediate CCR2+ monocytes compared to post-SAH day 7. Finally, HLA-DR+ classical monocytes were significantly reduced after aSAH at both day 1 and day 7 compared to controls, while intermediate and nonclassical HLA-DR+ monocytes showed significant differences as that of their parent populations. Interestingly, CD4+ T cells were significantly increased after aSAH. Interestingly, Th2 cells were significantly reduced at day 7, whereas Th17 cells increased compared to day 1 post-SAH. However, Treg cells were significantly increased at both assessment days compared to controls. These subtypes also revealed some interesting significant differences regarding their activation states assessed by CD38 and HLA-DR expression.

All these findings reflect an upregulated systemic inflammatory response after aSAH, which may underlie different post-aSAH complications and affect the clinical outcome. Moreover, the pro-inflammatory and anti-inflammatory factors are differentially regulated over time after aSAH during the development of complications. These investigations unveil the possible role of systemic inflammatory mediators as potential diagnostic and prognostic markers.

9. References

Abbas A, Gregersen I, Holm S, Daissormont I, Bjerkeli V, Krohg-Sørensen K, Skagen KR, Dahl TB, Russell D, Almås T, Bundgaard D, Alteheld LH, Rashidi A, Dahl CP, Michelsen AE, Biessen EA, Aukrust P, Halvorsen B, Skjelland M (2015) Interleukin 23 Levels Are Increased in Carotid Atherosclerosis: Possible Role for the Interleukin 23/Interleukin 17 Axis. Stroke 46:793-799.

Acosta-Rodriguez EV, Rivino L, Geginat J, Jarrossay D, Gattorno M, Lanzavecchia A, Sallusto F, Napolitani G (2007) Surface phenotype and antigenic specificity of human interleukin 17–producing T helper memory cells. Nature Immunology 8:639.

Agnello D, Wang H, Yang H, Tracey KJ, Ghezzi P (2002) HMGB-1, a DNA-binding protein with cytokine activity, induces brain TNF and IL-6 production, and mediates anorexia and taste aversion. Cytokine 18:231-236.

Aihara Y, Kasuya H, Onda H, Hori T, Takeda J (2001) Quantitative Analysis of Gene Expressions Related to Inflammation in Canine Spastic Artery After Subarachnoid Hemorrhage. Stroke 32:212-217.

Albert V, Subramanian A, Agrawal D, Bhoi SK, Pallavi P, Mukhopadhayay AK (2017) RANTES levels in peripheral blood, CSF and contused brain tissue as a marker for outcome in traumatic brain injury (TBI) patients. BMC Research Notes 10:139.

Allan SM, Tyrrell PJ, Rothwell NJ (2005) Interleukin-1 and neuronal injury. 5:629.

Andersson U, Tracey KJ (2011) HMGB1 Is a Therapeutic Target for Sterile Inflammation and Infection. Annual review of immunology 29:139-162.

Andersson U, Wang H, Palmblad K, Aveberger AC, Bloom O, Erlandsson-Harris H, Janson A, Kokkola R, Zhang M, Yang H, Tracey KJ (2000) High mobility group 1 protein (HMG-1) stimulates proinflammatory cytokine synthesis in human monocytes. J Exp Med 192:565-570.

Aoki T, Kataoka H, Ishibashi R, Nozaki K, Hashimoto N (2008) Gene expression profile of the intima and media of experimentally induced cerebral aneurysms in rats by laser-microdissection and microarray techniques. Int J Mol Med 22:595-603.

Aoki T, Frösen J, Fukuda M, Bando K, Shioi G, Tsuji K, Ollikainen E, Nozaki K, Laakkonen J, Narumiya S (2017) Prostaglandin E2–EP2–NF-κB signaling in macrophages as a potential therapeutic target for intracranial aneurysms. Science Signaling 10.

Appay V, Rowland-Jones SL (2001) RANTES: a versatile and controversial chemokine. Trends in Immunology 22:83-87.

Atwa MA, Emara AS, Youssef N, Bayoumy NM (2014) Serum concentration of IL-17, IL-23 and TNF-alpha among patients with chronic spontaneous urticaria: association with disease activity and autologous serum skin test. Journal of the European Academy of Dermatology and Venereology : JEADV 28:469-474.

Ayer RE, Ostrowski RP, Sugawara T, Ma Q, Jafarian N, Tang J, Zhang JH (2013) Statin-induced T-lymphocyte modulation and neuroprotection following experimental subarachnoid hemorrhage. Acta Neurochir Suppl 115:259-266.

Ayling OG, Ibrahim GM, Drake B, Torner JC, Macdonald RL (2015) Operative complications and differences in outcome after clipping and coiling of ruptured intracranial aneurysms. J Neurosurg 123:621-628.

Bartosik-Psujek H, Stelmasiak Z (2005) Correlations between IL-4, IL-12 levels and CCL2, CCL5 levels in serum and cerebrospinal fluid of multiple sclerosis patients. Journal of neural transmission (Vienna, Austria : 1996) 112:797-803.

Basil MC, Levy BD (2016) Specialized pro-resolving mediators: endogenous regulators of infection and inflammation. Nat Rev Immunol 16:51-67.

Bell JD, Rhind SG, Di Battista AP, Macdonald RL, Baker AJ (2017) Biomarkers of Glycocalyx Injury are Associated with Delayed Cerebral Ischemia Following Aneurysmal Subarachnoid Hemorrhage: A Case Series Supporting a New Hypothesis. Neurocrit Care 26:339-347.

Bethin KE, Vogt SK, Muglia LJ (2000) Interleukin-6 is an essential, corticotropin-releasing hormone-independent stimulator of the adrenal axis during immune system activation. Proceedings of the National Academy of Sciences 97:9317-9322.

Bianchi ME (2007) DAMPs, PAMPs and alarmins: all we need to know about danger. Journal of Leukocyte Biology 81:1-5.

Bianchi ME, Manfredi AA (2009) Dangers In and Out. Science 323:1683-1684.

Bianchi R, Kastrisianaki E, Giambanco I, Donato R (2011) S100B protein stimulates microglia migration via RAGE-dependent up-regulation of chemokine expression and release. J Biol Chem 286:7214-7226.

Boissier M-C, Assier E, Falgarone G, Bessis N (2008) Shifting the imbalance from Th1/Th2 to Th17/treg: The changing rheumatoid arthritis paradigm. Joint Bone Spine 75:373-375.

Boraschi D, Tagliabue A (2013) The interleukin-1 receptor family. Seminars in immunology 25:394-407.

Borovcanin M, Jovanovic I, Dejanovic SD, Radosavljevic G, Arsenijevic N, Lukic ML (2015) Increase systemic levels of IL-23 as a possible constitutive marker in schizophrenia. Psychoneuroendocrinology 56:143-147.

Bowman G, Dixit S, Bonneau RH, Chinchilli VM, Cockroft KM (2004) Neutralizing antibody against interleukin-6 attenuates posthemorrhagic vasospasm in the rat femoral artery model. Neurosurgery 54:719-725; discussion 725-716.

Bowman G, Bonneau RH, Chinchilli VM, Tracey KJ, Cockroft KM (2006) A novel inhibitor of inflammatory cytokine production (CNI-1493) reduces rodent post-hemorrhagic vasospasm. Neurocrit Care 5:222-229.

Boyapati RK, Rossi AG, Satsangi J, Ho GT (2016) Gut mucosal DAMPs in IBD: from mechanisms to therapeutic implications. Mucosal immunology 9:567-582.

Boyapati RK, Tamborska A, Dorward DA, Ho G-T (2017) Advances in the understanding of mitochondrial DNA as a pathogenic factor in inflammatory diseases. F1000Research 6:169.

Brandner S, Xu Y, Schmidt C, Emtmann I, Buchfelder M, Kleindienst A (2012) Shunt-Dependent Hydrocephalus Following Subarachnoid Hemorrhage Correlates with Increased S100B Levels in Cerebrospinal Fluid and Serum. In: Intracranial Pressure and Brain Monitoring XIV (Schuhmann UM, Czosnyka M, eds), pp 217-220. Vienna: Springer Vienna.

Broessner G, Lackner P, Fischer M, Beer R, Helbok R, Pfausler B, Schneider D, Schmutzhard E (2010) Influence of prophylactic, endovascularly based normothermia on inflammation in patients with severe cerebrovascular disease: a prospective, randomized trial. Stroke 41:2969-2972.

Bukowski RM, Olencki T, McLain D, Finke JH (1994) Pleiotropic effects of cytokines: clinical and preclinical studies. Stem cells (Dayton, Ohio) 12 Suppl 1:129-140; discussion 140-121.

Buryskova M, Pospisek M, Grothey A, Simmet T, Burysek L (2004) Intracellular interleukin-1alpha functionally interacts with histone acetyltransferase complexes. J Biol Chem 279:4017-4026.

Cahill J, Zhang JH (2009) Subarachnoid Hemorrhage: Is It Time for a New Direction? Stroke 40:S86-S87.

Cahill J, Calvert JW, Zhang JH (2006) Mechanisms of early brain injury after subarachnoid hemorrhage. J Cereb Blood Flow Metab 26:1341-1353.

Canouï-Poitrine F, Luc G, Mallat Z, Machez E, Bingham A, Ferrieres J, Ruidavets J-B, Montaye M, Yarnell J, Haas B, Arveiler D, Morange P, Kee F, Evans A, Amouyel P, Ducimetiere P, Empana J-P (2011) Systemic chemokine levels, coronary heart disease, and ischemic stroke events: The PRIME Study. Neurology 77:1165-1173.

Carr KR, Zuckerman SL, Mocco J (2013) Inflammation, Cerebral Vasospasm, and Evolving Theories of Delayed Cerebral Ischemia. Neurology Research International 2013:12.

Cartier L, Hartley O, Dubois-Dauphin M, Krause K-H (2005) Chemokine receptors in the central nervous system: role in brain inflammation and neurodegenerative diseases. Brain Research Reviews 48:16-42.

Castellheim A, Brekke OL, Espevik T, Harboe M, Mollnes TE (2009) Innate immune responses to danger signals in systemic inflammatory response syndrome and sepsis. Scand J Immunol 69:479-491.

Cavusoglu E, Eng C, Chopra V, Clark LT, Pinsky DJ, Marmur JD (2007) Low plasma RANTES levels are an independent predictor of cardiac mortality in patients referred for coronary angiography. Arterioscler Thromb Vasc Biol 27:929-935.

Cerri C, Caleo M, Bozzi Y (2017) Chemokines as new inflammatory players in the pathogenesis of epilepsy. Epilepsy Research 136:77-83.

Chackerian AA, Oldham ER, Murphy EE, Schmitz J, Pflanz S, Kastelein RA (2007) IL-1 receptor accessory protein and ST2 comprise the IL-33 receptor complex. J Immunol 179:2551-2555.

Chamling B, Gross S, Stoffel-Wagner B, Schubert GA, Clusmann H, Coburn M, Hollig A (2017) Early Diagnosis of Delayed Cerebral Ischemia: Possible Relevance for Inflammatory Biomarkers in Routine Clinical Practice? World Neurosurg 104:152-157.

Chang C-Z, Wu S-C, Kwan A-L, Lin C-L (2015a) 4′-O-β-d-glucosyl-5-O-methylvisamminol, an active ingredient of Saposhnikovia divaricata, attenuates high-mobility group box 1 and subarachnoid hemorrhage-induced vasospasm in a rat model. Behavioral and Brain Functions 11:1-13.

Chang C-Z, Lin C-L, Kassel NF, Kwan A-L, Howng S-L (2010) 6-Mercaptopurine attenuates adhesive molecules in experimental vasospasm. Acta Neurochirurgica 152:861-867.

Chang CZ, Lin CL, Wu SC, Kwan AL (2014) Purpurogallin, a natural phenol, attenuates high-mobility group box 1 in subarachnoid hemorrhage induced vasospasm in a rat model. Int J Vasc Med 2014:254270.

Chang CZ, Wu SC, Lin CL, Kwan AL (2015b) Valproic acid attenuates intercellular adhesion molecule-1 and E-selectin through a chemokine ligand 5 dependent mechanism and subarachnoid hemorrhage induced vasospasm in a rat model. J Inflamm (Lond) 12:27.

Chang CZ, Wu SC, Kwan AL, Lin CL (2016) Rhinacanthin-C, A Fat-Soluble Extract from Rhinacanthus nasutus, Modulates High-Mobility Group Box 1-Related Neuro-Inflammation and Subarachnoid Hemorrhage-Induced Brain Apoptosis in a Rat Model. World Neurosurg 86:349-360.

Chaudhry SR, Guresir E, Vatter H, Kinfe TM, Dietrich D, Lamprecht A, Muhammad S (2017) Aneurysmal subarachnoid hemorrhage lead to systemic upregulation of IL-23/IL-17 inflammatory axis. Cytokine 97:96-103.

Chavan SS, Pavlov VA, Tracey KJ (2017) Mechanisms and Therapeutic Relevance of Neuro-immune Communication. Immunity 46:927-942.

Chen GY, Nuñez G (2010) Sterile inflammation: sensing and reacting to damage. Nat Rev Immunol 10:826-837.

Chen JM, Jiang GX, Li QW, Zhou ZM, Cheng Q (2014) Increased serum levels of interleukin-18, -23 and -17 in Chinese patients with Alzheimer's disease. Dementia and geriatric cognitive disorders 38:321-329.

Chen T, Wang W, Li J-R, Xu H-Z, Peng Y-C, Fan L-F, Yan F, Gu C, Wang L, Chen G (2016) PARP inhibition attenuates early brain injury through NF-κB/MMP-9 pathway in a rat model of subarachnoid hemorrhage. Brain Research 1644:32-38.

Chen Y, Langrish CL, McKenzie B, Joyce-Shaikh B, Stumhofer JS, McClanahan T, Blumenschein W, Churakovsa T, Low J, Presta L, Hunter CA, Kastelein RA, Cua DJ Anti–IL-23 therapy inhibits multiple inflammatory pathways and ameliorates autoimmune encephalomyelitis. The Journal of Clinical Investigation 116:1317-1326.

Chou SH-Y, Feske SK, Atherton J, Konigsberg RG, De Jager PL, Du R, Ogilvy CS, Lo EH, Ning M (2012) Early Elevation of Serum Tumor Necrosis Factor-α Is Associated With Poor Outcome in Subarachnoid Hemorrhage. Journal of Investigative Medicine 60:1054-1058.

Chrapusta SJ, Gorski A, Mrowiec T, Grieb P, Andrychowski J, Ryba MS (2000) Immune abnormalities in aneurysmal subarachnoid haemorrhage patients: relation to delayed cerebral vasospasm. Scand J Immunol 51:400-407.

Chyatte D, Bruno G, Desai S, Todor DR (1999) Inflammation and intracranial aneurysms. Neurosurgery 45:1137-1146; discussion 1146-1137.

Ciprandi G, Cuppari C, Salpietro A, Tosca M, Grasso L, Rigoli L, La Rosa M, Marseglia GL, Miraglia Del Giudice M, Salpietro C (2012) Serum IL-23 in asthmatic children. Journal of biological regulators and homeostatic agents 26:S53-61.

Collins LV, Hajizadeh S, Holme E, Jonsson IM, Tarkowski A (2004) Endogenously oxidized mitochondrial DNA induces in vivo and in vitro inflammatory responses. J Leukoc Biol 75:995-1000.

Corbyn Z (2014) Statistics: a growing global burden. Nature 510:S2-3.

Cornwell W, Vega M, Rogers T (2013) Monocyte Populations Which Participate in Chronic Lung Inflammation. In: Smoking and Lung Inflammation (Rogers TJ, Criner GJ, Cornwell WD, eds), pp 29-58: Springer New York.

Couper KN, Blount DG, Riley EM (2008) IL-10: The Master Regulator of Immunity to Infection. The Journal of Immunology 180:5771-5777.

Cros J, Cagnard N, Woollard K, Patey N, Zhang S-Y, Senechal B, Puel A, Biswas SK, Moshous D, Picard C, Jais J-P, D'Cruz D, Casanova J-L, Trouillet C, Geissmann F (2010) Human CD14dim Monocytes Patrol and Sense Nucleic Acids and Viruses via TLR7 and TLR8 Receptors. Immunity 33:375-386.

Cua DJ, Tato CM (2010) Innate IL-17-producing cells: the sentinels of the immune system. Nat Rev Immunol 10:479-489.

D'Amico G, Frascaroli G, Bianchi G, Transidico P, Doni A, Vecchi A, Sozzani S, Allavena P, Mantovani A (2000) Uncoupling of inflammatory chemokine receptors by IL-10: generation of functional decoys. Nat Immunol 1:387-391.

D'Souza S (2015) Aneurysmal Subarachnoid Hemorrhage. Journal of Neurosurgical Anesthesiology 27:222-240.

Da Silva IRF, Gomes JA, Wachsman A, de Freitas GR, Provencio JJ (2017) Hematologic counts as predictors of delayed cerebral ischemia after aneurysmal subarachnoid hemorrhage. Journal of Critical Care 37:126-129.

David B. Kurland VG, J. Marc Simard (2015) DAMPs converging on Toll-like receptor 4 in hemorrhagic stroke, a Mini-Review. Current Neurobiology 6:4-8.

de Azua Lopez ZR, Egea-Guerrero JJ, Rivera-Rubiales G, Rodriguez-Rodriguez A, Vilches-Arenas A, Murillo-Cabezas F (2015) Serum brain injury biomarkers as predictors of mortality after severe aneurysmal subarachnoid hemorrhage: preliminary results. Clinical chemistry and laboratory medicine 53:e179-181.

de Bilbao F, Arsenijevic D, Moll T, Garcia-Gabay I, Vallet P, Langhans W, Giannakopoulos P (2009) In vivo over-expression of interleukin-10 increases resistance to focal brain ischemia in mice. Journal of neurochemistry 110:12-22.

de Rooij NK, Linn FH, van der Plas JA, Algra A, Rinkel GJ (2007) Incidence of subarachnoid haemorrhage: a systematic review with emphasis on region, age, gender and time trends. J Neurol Neurosurg Psychiatry 78:1365-1372.

Dénes Á, Humphreys N, Lane TE, Grencis R, Rothwell N (2010) Chronic systemic infection exacerbates ischaemic brain damage via a CCL5 (RANTES) mediated proinflammatory response in mice. The Journal of neuroscience : the official journal of the Society for Neuroscience 30:10086-10095.

Dengler J, Schefold JC, Graetz D, Meisel C, Splettstosser G, Volk HD, Schlosser HG (2008) Point-of-care testing for interleukin-6 in cerebro spinal fluid (CSF) after subarachnoid haemorrhage. Medical science monitor : international medical journal of experimental and clinical research 14:Br265-268.

Diehl S, Rincon M (2002) The two faces of IL-6 on Th1/Th2 differentiation. Mol Immunol 39:531-536.

Diehl S, Chow CW, Weiss L, Palmetshofer A, Twardzik T, Rounds L, Serfling E, Davis RJ, Anguita J, Rincon M (2002) Induction of NFATc2 expression by interleukin 6 promotes T helper type 2 differentiation. J Exp Med 196:39-49.

Dinarello CA, Simon A, van der Meer JWM (2012) Treating inflammation by blocking interleukin-1 in a broad spectrum of diseases. 11:633.

Dorner BG, Scheffold A, Rolph MS, Hüser MB, Kaufmann SHE, Radbruch A, Flesch IEA, Kroczek RA (2002) MIP-1α, MIP-1β, RANTES, and ATAC/lymphotactin function together with IFN-γ as type 1 cytokines. Proceedings of the National Academy of Sciences 99:6181-6186.

Downes CE, Crack PJ (2010) Neural injury following stroke: are Toll-like receptors the link between the immune system and the CNS? British Journal of Pharmacology 160:1872-1888.

Drake CG, Peerless SJ (1997) Giant fusiform intracranial aneurysms: review of 120 patients treated surgically from 1965 to 1992. J Neurosurg 87:141-162.

Du J, Li Z, Shi J, Bi L (2014) Associations between serum interleukin-23 levels and clinical characteristics in patients with systemic lupus erythematosus. The Journal of international medical research 42:1123-1130.

Dutra FF, Bozza MT (2014) Heme on innate immunity and inflammation. Frontiers in Pharmacology 5:115.

Dutra FF, Alves LS, Rodrigues D, Fernandez PL, de Oliveira RB, Golenbock DT, Zamboni DS, Bozza MT (2014) Hemolysis-induced lethality involves inflammasome activation by heme. Proceedings of the National Academy of Sciences 111:E4110-E4118.

Dziedzic T, Slowik A, Klimkowicz A, Szczudlik A (2003) Asymmetrical modulation of interleukin-10 release in patients with intracerebral hemorrhage. Brain, Behavior, and Immunity 17:438-441.

Dziedzic T, Bartus S, Klimkowicz A, Motyl M, Slowik A, Szczudlik A (2002) Intracerebral hemorrhage triggers interleukin-6 and interleukin-10 release in blood. Stroke 33:2334-2335.

Dziurdzik P, Krawczyk L, Jalowiecki P, Kondera-Anasz Z, Menon L (2004) Serum interleukin-10 in ICU patients with severe acute central nervous system injuries. Inflamm Res 53:338-343.

Eigenbrod T, Park JH, Harder J, Iwakura Y, Nunez G (2008) Cutting edge: critical role for mesothelial cells in necrosis-induced inflammation through the recognition of IL-1 alpha released from dying cells. J Immunol 181:8194-8198.

Etminan N, Rinkel GJ (2016) Unruptured intracranial aneurysms: development, rupture and preventive management. Nat Rev Neurol 12:699-713.

Fang H, Chen J, Lin S, Wang P, Wang Y, Xiong X, Yang Q (2014) CD36-Mediated Hematoma Absorption following Intracerebral Hemorrhage: Negative Regulation by TLR4 Signaling. The Journal of Immunology 192:5984-5992.

Fanizzi C, Sauerbeck AD, Gangolli M, Zipfel GJ, Brody DL, Kummer TT (2017) Minimal Long-Term Neurobehavioral Impairments after Endovascular Perforation Subarachnoid Hemorrhage in Mice. Scientific Reports 7:7569.

Fassbender K, Hodapp B, Rossol S, Bertsch T, Schmeck J, Schutt S, Fritzinger M, Horn P, Vajkoczy P, Kreisel S, Brunner J, Schmiedek P, Hennerici M (2001) Inflammatory cytokines in subarachnoid haemorrhage: association with abnormal blood flow velocities in basal cerebral arteries. J Neurol Neurosurg Psychiatry 70:534-537.

Fotiadou C, Lazaridou E, Sotiriou E, Gerou S, Kyrgidis A, Vakirlis E, Ioannides D (2015) IL-17A, IL-22, and IL-23 as Markers of Psoriasis Activity: A Cross-sectional, Hospital-based Study. Journal of cutaneous medicine and surgery 19:555-560.

Francoeur CL, Mayer SA (2016) Management of delayed cerebral ischemia after subarachnoid hemorrhage. Critical Care 20:277.

Fraunberger P, Wang Y, Holler E, Parhofer KG, Nagel D, Walli AK, Seidel D (2006) Prognostic value of interleukin 6, procalcitonin, and C-reactive protein levels in intensive care unit patients during first increase of fever. Shock 26:10-12.

Friedrich V, Flores R, Sehba FA (2012) Cell death starts early after subarachnoid hemorrhage. Neurosci Lett 512:6-11.

Frontera JA, Fernandez A, Schmidt JM, Claassen J, Wartenberg KE, Badjatia N, Parra A, Connolly ES, Mayer SA (2008) Impact of nosocomial infectious complications after subarachnoid hemorrhage. Neurosurgery 62:80-87; discussion 87.

Funderburg NT, Stubblefield Park SR, Sung HC, Hardy G, Clagett B, Ignatz-Hoover J, Harding CV, Fu P, Katz JA, Lederman MM, Levine AD (2013) Circulating CD4+ and CD8+ T cells are activated in inflammatory bowel disease and are associated with plasma markers of inflammation. Immunology 140:87-97.

Gaetani P, Tartara F, Pignatti P, Tancioni F, Rodriguez y Baena R, De Benedetti F (1998) Cisternal CSF levels of cytokines after subarachnoid hemorrhage. Neurol Res 20:337-342.

Gaffen SL, Jain R, Garg AV, Cua DJ (2014) The IL-23-IL-17 immune axis: from mechanisms to therapeutic testing. Nat Rev Immunol 14:585-600.

Galea J, Brough D (2013) The role of inflammation and interleukin-1 in acute cerebrovascular disease. Journal of Inflammation Research 6:121-128.

Galea J, Ogungbenro K, Hulme S, Patel H, Scarth S, Hoadley M, Illingworth K, McMahon CJ, Tzerakis N, King AT, Vail A, Hopkins SJ, Rothwell N, Tyrrell P (2017a) Reduction of inflammation after administration of interleukin-1 receptor antagonist following aneurysmal subarachnoid hemorrhage: results of the Subcutaneous Interleukin-1Ra in SAH (SCIL-SAH) study. J Neurosurg:1-9.

Galea JP, Dulhanty L, Patel HC (2017b) Predictors of Outcome in Aneurysmal Subarachnoid Hemorrhage Patients. Observations From a Multicenter Data Set.

Galluzzi L, Kepp O, Kroemer G (2012) Mitochondria: master regulators of danger signalling. Nat Rev Mol Cell Biol 13:780-788.

Garcia JM, Stillings SA, Leclerc JL, Phillips H, Edwards NJ, Robicsek SA, Hoh BL, Blackburn S, Doré S (2017) Role of Interleukin-10 in Acute Brain Injuries. Frontiers in Neurology 8.

Geissmann F, Jung S, Littman DR (2003) Blood monocytes consist of two principal subsets with distinct migratory properties. Immunity 19:71-82.

Gelderblom M, Arunachalam P, Magnus T (2014) gammadelta T cells as early sensors of tissue damage and mediators of secondary neurodegeneration. Front Cell Neurosci 8:368.

Gelderblom M, Weymar A, Bernreuther C, Velden J, Arunachalam P, Steinbach K, Orthey E, Arumugam TV, Leypoldt F, Simova O, Thom V, Friese MA, Prinz I, Hölscher C, Glatzel M, Korn T, Gerloff C, Tolosa E, Magnus T (2012) Neutralization of the IL-17 axis diminishes neutrophil invasion and protects from ischemic stroke.

Gertz K, Kronenberg G, Kälin RE, Baldinger T, Werner C, Balkaya M, Eom GD, Hellmann-Regen J, Kröber J, Miller KR, Lindauer U, Laufs U, Dirnagl U, Heppner FL, Endres M (2012) Essential role of interleukin-6 in post-stroke angiogenesis. Brain : a journal of neurology 135:1964-1980.

Ghoreschi K et al. (2010) Generation of pathogenic TH17 cells in the absence of TGF-[bgr] signalling. Nature 467:967-971.

Gladwin MT, Ofori-Acquah SF (2014) Erythroid DAMPs drive inflammation in SCD. Blood 123:3689-3690.

Grasso G, Alafaci C, Macdonald RL (2017) Management of aneurysmal subarachnoid hemorrhage: State of the art and future perspectives. Surgical Neurology International 8:11.

Greenhalgh AD, Brough D, Robinson EM, Girard S, Rothwell NJ, Allan SM (2012) Interleukin-1 receptor antagonist is beneficial after subarachnoid haemorrhage in rat by blocking haem-driven inflammatory pathology. Disease Models and Mechanisms 5:823-833.

Gruber A, Rossler K, Graninger W, Donner A, Illievich MU, Czech T (2000) Ventricular cerebrospinal fluid and serum concentrations of sTNFR-I, IL-1ra, and IL-6 after aneurysmal subarachnoid hemorrhage. J Neurosurg Anesthesiol 12:297-306.

Gu C, Wu L, Li X (2013) IL-17 family: cytokines, receptors and signaling. Cytokine 64:477-485.

Guilliams M, Ginhoux F, Jakubzick C, Naik SH, Onai N, Schraml BU, Segura E, Tussiwand R, Yona S (2014) Dendritic cells, monocytes and macrophages: a unified nomenclature based on ontogeny. Nat Rev Immunol 14:571-578.

Hanafy KA, Stuart RM, Khandji AG, Connolly ES, Badjatia N, Mayer SA, Schindler C (2010a) Relationship between brain interstitial fluid tumor necrosis factor-alpha and cerebral vasospasm after aneurysmal subarachnoid hemorrhage. Journal of clinical neuroscience : official journal of the Neurosurgical Society of Australasia 17:853-856.

Hanafy KA, Grobelny B, Fernandez L, Kurtz P, Connolly ES, Mayer SA, Schindler C, Badjatia N (2010b) Brain interstitial fluid TNF-alpha after subarachnoid hemorrhage. J Neurol Sci 291:69-73.

Hardemark HG, Almqvist O, Johansson T, Pahlman S, Persson L (1989) S-100 protein in cerebrospinal fluid after aneurysmal subarachnoid haemorrhage: relation to functional outcome, late CT and SPECT changes, and signs of higher cortical dysfunction. Acta Neurochir (Wien) 99:135-144.

Harris HE, Andersson U, Pisetsky DS (2012) HMGB1: a multifunctional alarmin driving autoimmune and inflammatory disease. Nat Rev Rheumatol 8:195-202.

Haruma J, Teshigawara K, Hishikawa T, Wang D, Liu K, Wake H, Mori S, Takahashi HK, Sugiu K, Date I, Nishibori M (2016) Anti-high mobility group box-1 (HMGB1) antibody attenuates delayed cerebral vasospasm and brain injury after subarachnoid hemorrhage in rats. Sci Rep 6:37755.

Hasan D, Chalouhi N, Jabbour P, Hashimoto T (2012) Macrophage imbalance (M1 vs. M2) and upregulation of mast cells in wall of ruptured human cerebral aneurysms: preliminary results. Journal of Neuroinflammation 9:1-7.

Hasan DM, Starke RM, Gu H, Wilson K, Chu Y, Chalouhi N, Heistad DD, Faraci FM, Sigmund CD (2015) Smooth Muscle Peroxisome Proliferator-Activated Receptor gamma Plays a Critical Role in Formation and Rupture of Cerebral Aneurysms in Mice In Vivo. Hypertension 66:211-220.

Hassan T, Nassar M, Elhadi SM, Radi WK (2012) Effect of magnesium sulfate therapy on patients with aneurysmal subarachnoid hemorrhage using serum S100B protein as a prognostic marker. Neurosurgical review 35:421-427; discussion 427.

Hawrylowicz CM, O'Garra A (2005) Potential role of interleukin-10-secreting regulatory T cells in allergy and asthma. Nat Rev Immunol 5:271-283.

Heep A, Stoffel-Wagner B, Bartmann P, Benseler S, Schaller C, Groneck P, Obladen M, Felderhoff-Mueser U (2004) Vascular Endothelial Growth Factor and Transforming Growth Factor-[bgr]1 Are Highly Expressed in the Cerebrospinal Fluid of Premature Infants with Posthemorrhagic Hydrocephalus. Pediatr Res 56:768-774.

Helbok R, Schiefecker AJ, Beer R, Dietmann A, Antunes AP, Sohm F, Fischer M, Hackl WO, Rhomberg P, Lackner P, Pfausler B, Thomé C, Humpel C, Schmutzhard E (2015) Early brain injury after aneurysmal subarachnoid hemorrhage: a multimodal neuromonitoring study. Critical Care 19:75.

Hendrix P, Foreman PM, Harrigan MR, Fisher WSR, Vyas NA, Lipsky RH, Lin M, Walters BC, Tubbs RS, Shoja MM, Pittet JF, Mathru M, Griessenauer CJ (2017) Impact of high-mobility group box-1 polymorphism on delayed cerebral ischemia following aneurysmal subarachnoid hemorrhage. World Neurosurg.

Hendryk S, Jarzab B, Josko J (2004) Increase of the IL-1 beta and IL-6 levels in CSF in patients with vasospasm following aneurysmal SAH. Neuro Endocrinol Lett 25:141-147.

Hennessy EJ, Parker AE, O'Neill LAJ (2010) Targeting Toll-like receptors: emerging therapeutics? Nat Rev Drug Discov 9:293-307.

Herrmann O, Tarabin V, Suzuki S, Attigah N, Coserea I, Schneider A, Vogel J, Prinz S, Schwab S, Monyer H, Brombacher F, Schwaninger M (2003) Regulation of Body Temperature and Neuroprotection by Endogenous Interleukin-6 in Cerebral Ischemia. Journal of Cerebral Blood Flow & Metabolism 23:406-415.

Heula AL, Sajanti J, Majamaa K (2015) Glycosaminoglycans in subdural fluid and CSF after meningeal injury. Acta Neurochir (Wien) 157:2105-2110; discussion 2110.

Hirashima Y, Nakamura S, Endo S, Kuwayama N, Naruse Y, Takaku A (1997) Elevation of Platelet Activating Factor, Inflammatory Cytokines, and Coagulation Factors in the Internal Jugular Vein of Patients with Subarachnoid Hemorrhage. Neurochemical Research 22:1249-1255.

Hirsiger S, Simmen H-P, Werner CML, Wanner GA, Rittirsch D (2012) Danger Signals Activating the Immune Response after Trauma. Mediators of Inflammation 2012:10.

Hodes GE et al. (2014) Individual differences in the peripheral immune system promote resilience versus susceptibility to social stress. Proceedings of the National Academy of Sciences 111:16136-16141.

Holl EK, Shumansky KL, Pitoc G, Ramsburg E, Sullenger BA (2013) Nucleic acid scavenging polymers inhibit extracellular DNA-mediated innate immune activation without inhibiting anti-viral responses. PLoS One 8:e69413.

Holl EK, Shumansky KL, Borst LB, Burnette AD, Sample CJ, Ramsburg EA, Sullenger BA (2016) Scavenging nucleic acid debris to combat autoimmunity and infectious disease. Proceedings of the National Academy of Sciences 113:9728-9733.

Hollig A, Thiel M, Stoffel-Wagner B, Coburn M, Clusmann H (2015a) Neuroprotective properties of dehydroepiandrosterone-sulfate and its relationship to interleukin 6 after aneurysmal subarachnoid hemorrhage: a prospective cohort study. Crit Care 19:231.

Hollig A, Remmel D, Stoffel-Wagner B, Schubert GA, Coburn M, Clusmann H (2015b) Association of early inflammatory parameters after subarachnoid hemorrhage with functional outcome: A prospective cohort study. Clin Neurol Neurosurg 138:177-183.

Hong CM, Tosun C, Kurland DB, Gerzanich V, Schreibman D, Simard JM (2014) Biomarkers as outcome predictors in subarachnoid hemorrhage – a systematic review. Biomarkers 19:95-108.

Hopkins SJ, McMahon CJ, Singh N, Galea J, Hoadley M, Scarth S, Patel H, Vail A, Hulme S, Rothwell NJ, King AT, Tyrrell PJ (2012) Cerebrospinal fluid and plasma cytokines after subarachnoid haemorrhage: CSF interleukin-6 may be an early marker of infection. J Neuroinflammation 9:255.

Hoque R, Farooq A, Malik A, Trawick BN, Berberich DW, McClurg JP, Galen KP, Mehal W (2013) A Novel Small Molecule Enantiomeric Analogue of Traditional (−)-morphinans has Specific TLR9 Antagonist Properties and Reduces Sterile Inflammation Induced Organ Damage. Journal of immunology (Baltimore, Md : 1950) 190:4297-4304.

Huang LT, Li H, Sun Q, Liu M, Li WD, Li S, Yu Z, Wei WT, Hang CH (2014) IL-33 Expression in the Cerebral Cortex Following Experimental Subarachnoid Hemorrhage in Rats. Cell Mol Neurobiol.

Huang M, Dong XQ, Hu YY, Yu WH, Zhang ZY (2010) High S100B levels in cerebrospinal fluid and peripheral blood of patients with acute basal ganglial hemorrhage are associated with poor outcome. World journal of emergency medicine 1:22-31.

Huang Q, Wang G, Hu YL, Liu JX, Yang J, Wang S, Zhang HB (2017) Study on the expression and mechanism of inflammatory factors in the brain of rats with cerebral vasospasm. European review for medical and pharmacological sciences 21:2887-2894.

Huber R, Meier B, Otsuka A, Fenini G, Satoh T, Gehrke S, Widmer D, Levesque MP, Mangana J, Kerl K, Gebhardt C, Fujii H, Nakashima C, Nonomura Y, Kabashima K, Dummer R, Contassot E, French LE (2016) Tumour hypoxia promotes melanoma growth and metastasis via High Mobility Group Box-1 and M2-like macrophages. 6:29914.

Hudson CA, Christophi GP, Gruber RC, Wilmore JR, Lawrence DA, Massa PT (2008) Induction of IL-33 expression and activity in central nervous system glia. Journal of Leukocyte Biology 84:631-643.

Hughes JT, Schianchi PM (1978) Cerebral artery spasm. A histological study at necropsy of the blood vessels in cases of subarachnoid hemorrhage. J Neurosurg 48:515-525.

Hunter CA, Jones SA (2015) IL-6 as a keystone cytokine in health and disease. Nat Immunol 16:448-457.

Iadecola C (2009) Bleeding in the brain: Killer waves of depolarization in subarachnoid bleed. Nature medicine 15:1131-1132.

Jakubzick CV, Randolph GJ, Henson PM (2017) Monocyte differentiation and antigen-presenting functions. Nat Rev Immunol 17:349-362.

Jalbert E, Shikuma CM, Ndhlovu LC, Barbour JD (2013) Sequential staining improves detection of CCR2 and CX3CR1 on monocytes when simultaneously evaluating CCR5 by multicolor flow cytometry. Cytometry Part A 83A:280-286.

Jayaraman T, Paget A, Shin YS, Li X, Mayer J, Chaudhry H, Niimi Y, Silane M, Berenstein A (2008) TNF-alpha-mediated inflammation in cerebral aneurysms: a potential link to growth and rupture. Vascular health and risk management 4:805-817.

Jayaraman T, Berenstein V, Li X, Mayer J, Silane M, Shin YS, Niimi Y, Kılıç T, Gunel M, Berenstein A (2005) Tumor Necrosis Factor α is a Key Modulator of Inflammation in Cerebral Aneurysms. Neurosurgery 57:558-564.

Jedrzejowska-Szypułka H, Larysz-Brysz M, Kukla M, Snietura M, Lewin-Kowalik J (2009) Neutralization of Interleukin-1β Reduces Vasospasm and Alters Cerebral Blood Vessel Density Following Experimental Subarachnoid Hemorrhage in Rats.

Jeon YT, Lee JH, Lee H, Lee HK, Hwang JW, Lim YJ, Park HP (2012) The postoperative C-reactive protein level can be a useful prognostic factor for poor outcome and symptomatic vasospasm in patients with aneurysmal subarachnoid hemorrhage. J Neurosurg Anesthesiol 24:317-324.

Jiang H-R, Milovanović M, Allan D, Niedbala W, Besnard A-G, Fukada SY, Alves-Filho JC, Togbe D, Goodyear CS, Linington C, Xu D, Lukic ML, Liew FY (2012a) IL-33 attenuates EAE by suppressing IL-17 and IFN-γ production and inducing alternatively activated macrophages. European Journal of Immunology 42:1804-1814.

Jiang Y, Liu D-W, Han X-Y, Dong Y-N, Gao J, Du B, Meng L, Shi J-G (2012b) Neuroprotective effects of anti-tumor necrosis factor-alpha antibody on apoptosis following subarachnoid hemorrhage in a rat model. Journal of Clinical Neuroscience 19:866-872.

John CC, Opika-Opoka R, Byarugaba J, Idro R, Boivin MJ (2006) Low levels of RANTES are associated with mortality in children with cerebral malaria. The Journal of infectious diseases 194:837-845.

Jones SA (2005) Directing transition from innate to acquired immunity: defining a role for IL-6. J Immunol 175:3463-3468.

Jung CS, Lange B, Zimmermann M, Seifert V (2013) CSF and Serum Biomarkers Focusing on Cerebral Vasospasm and Ischemia after Subarachnoid Hemorrhage. Stroke research and treatment 2013:560305.

Kang J-W, Kim S-J, Cho H-I, Lee S-M (2015) DAMPs activating innate immune responses in sepsis. Ageing Research Reviews 24:54-65.

Kao HW, Lee KW, Kuo CL, Huang CS, Tseng WM, Liu CS, Lin CP (2015) Interleukin-6 as a Prognostic Biomarker in Ruptured Intracranial Aneurysms. PLoS One 10:e0132115.

Kawaguchi M, Utada K, Yoshitani K, Uchino H, Takeda Y, Masui K, Sakabe T (2010) Effects of a short-acting [beta]1 receptor antagonist landiolol on hemodynamics and tissue injury markers in patients with subarachnoid hemorrhage undergoing intracranial aneurysm surgery. J Neurosurg Anesthesiol 22:230-239.

Keiichi Iseda, Shigeki Ono, Keisuke Onoda, Motoyoshi Satoh, Hiroaki Manabe, Mitsuhisa Nishiguchi, Kenji Takahashi, Koji Tokunaga, Kenji sugiu, Isao Date (2007) Antivasospastic and antiinflammatory effects of caspase inhibitor in experimental subarachnoid hemorrhage. Journal of Neurosurgery 107:128-135.

Kellermann I, Kleindienst A, Hore N, Buchfelder M, Brandner S (2016) Early CSF and Serum S100B Concentrations for Outcome Prediction in Traumatic Brain Injury and Subarachnoid Hemorrhage. Clin Neurol Neurosurg 145:79-83.

Kiiski H, Långsjö J, Tenhunen J, Ala-Peijari M, Huhtala H, Hämäläinen M, Moilanen E, Öhman J, Peltola J (2017) Time-courses of plasma IL-6 and HMGB-1 reflect initial severity of clinical presentation but do not predict poor neurologic outcome following subarachnoid hemorrhage. eNeurologicalSci 6:55-62.

Kim B, Lee Y, Kim E, Kwak A, Ryoo S, Bae SH, Azam T, Kim S, Dinarello CA (2013) The Interleukin-1α Precursor is Biologically Active and is Likely a Key Alarmin in the IL-1 Family of Cytokines. Frontiers in Immunology 4:391.

Kim HO, Kim H-S, Youn J-C, Shin E-C, Park S (2011) Serum cytokine profiles in healthy young and elderly population assessed using multiplexed bead-based immunoassays. Journal of translational medicine 9:113-113.

Kim OY, Monsel A, Bertrand M, Coriat P, Cavaillon J-M, Adib-Conquy M (2010) Differential down-regulation of HLA-DR on monocyte subpopulations during systemic inflammation. Critical Care 14:R61.

Kimura H, Gules I, Meguro T, Zhang JH (2003) Cytotoxicity of cytokines in cerebral microvascular endothelial cell. Brain Research 990:148-156.

Kinfe TM, Muhammad S, Link C, Roeske S, Chaudhry SR, Yearwood TL (2017) Burst Spinal Cord Stimulation Increases Peripheral Antineuroinflammatory Interleukin 10 Levels in Failed Back Surgery Syndrome Patients With Predominant Back Pain. Neuromodulation : journal of the International Neuromodulation Society 20:322-330.

King MD, Laird MD, Ramesh SS, Youssef P, Shakir B, Vender JR, Alleyne CH, Dhandapani KM (2010) Elucidating novel mechanisms of brain injury following subarachnoid hemorrhage: an emerging role for neuroproteomics. Neurosurg Focus 28:E10.

Kinoshita K, Yamaguchi J, Sakurai A, Ebihara T, Furukawa M, Tanjoh K (2007) Inhibition of lipopolysaccharide stimulated interleukin-1beta production after subarachnoid hemorrhage. Neurol Res 29:47-52.

Kleindienst A, Meissner S, Eyupoglu IY, Parsch H, Schmidt C, Buchfelder M (2010) Dynamics of S100B release into serum and cerebrospinal fluid following acute brain injury. Acta Neurochir Suppl 106:247-250.

Kleiner G, Marcuzzi A, Zanin V, Monasta L, Zauli G (2013) Cytokine Levels in the Serum of Healthy Subjects. Mediators of Inflammation 2013:6.

Konoeda F, Shichita T, Yoshida H, Sugiyama Y, Muto G, Hasegawa E, Morita R, Suzuki N, Yoshimura A (2010) Therapeutic effect of IL-12/23 and their signaling pathway blockade on brain ischemia model. Biochemical and Biophysical Research Communications 402:500-506.

Kooijman E, Nijboer CH, van Velthoven CT, Kavelaars A, Kesecioglu J, Heijnen CJ (2014a) The rodent endovascular puncture model of subarachnoid hemorrhage: mechanisms of brain damage and therapeutic strategies. Journal of Neuroinflammation 11:1-12.

Kooijman E, Nijboer CH, van Velthoven CTJ, Mol W, Dijkhuizen RM, Kesecioglu J, Heijnen CJ (2014b) Long-Term Functional Consequences and Ongoing Cerebral Inflammation after Subarachnoid Hemorrhage in the Rat. PLoS One 9:e90584.

Korherr C, Hofmeister R, Wesche H, Falk W (1997) A critical role for interleukin-1 receptor accessory protein in interleukin-1 signaling. Eur J Immunol 27:262-267.

Korja M, Kaprio J (2016) Controversies in epidemiology of intracranial aneurysms and SAH. Nat Rev Neurol 12:50-55.

Korn T, Bettelli E, Oukka M, Kuchroo VK (2009) IL-17 and Th17 Cells. Annu Rev Immunol 27:485-517.

Kostulas N, Pelidou SH, Kivisakk P, Kostulas V, Link H (1999) Increased IL-1beta, IL-8, and IL-17 mRNA expression in blood mononuclear cells observed in a prospective ischemic stroke study. Stroke 30:2174-2179.

Kraakman MJ et al. (2015) Blocking IL-6 trans-signaling prevents high-fat diet-induced adipose tissue macrophage recruitment but does not improve insulin resistance. Cell Metab 21:403-416.

Kruyt ND, Biessels GJ, DeVries JH, Luitse MJA, Vermeulen M, Rinkel GJE, Vandertop WP, Roos YB (2010) Hyperglycemia in aneurysmal subarachnoid hemorrhage: a potentially modifiable risk factor for poor outcome. Journal of Cerebral Blood Flow and Metabolism: Official Journal of the International Society of Cerebral Blood Flow and Metabolism 30:1577-1587.

Kubota T, Handa Y, Tsuchida A, Kaneko M, Kobayashi H (1993) The kinetics of lymphocyte subsets and macrophages in subarachnoid space after subarachnoid hemorrhage in rats. Stroke 24:1993-2000; discussion 2000-1991.

Kurowska-Stolarska M, Stolarski B, Kewin P, Murphy G, Corrigan CJ, Ying S, Pitman N, Mirchandani A, Rana B, van Rooijen N, Shepherd M, McSharry C, McInnes IB, Xu D, Liew FY (2009) IL-33 amplifies the polarization of alternatively activated macrophages that contribute to airway inflammation. J Immunol 183:6469-6477.

Kwon KY, Jeon BC (2001) Cytokine levels in cerebrospinal fluid and delayed ischemic deficits in patients with aneurysmal subarachnoid hemorrhage. Journal of Korean medical science 16:774-780.

Kwon MS, Woo SK, Kurland DB, Yoon SH, Palmer AF, Banerjee U, Iqbal S, Ivanova S, Gerzanich V, Simard JM (2015) Methemoglobin is an endogenous toll-like receptor 4 ligand-relevance to subarachnoid hemorrhage. International journal of molecular sciences 16:5028-5046.

Lai PM, Du R (2016) Association between S100B Levels and Long-Term Outcome after Aneurysmal Subarachnoid Hemorrhage: Systematic Review and Pooled Analysis. PLoS One 11:e0151853.

Landsman L, Bar-On L, Zernecke A, Kim KW, Krauthgamer R, Shagdarsuren E, Lira SA, Weissman IL, Weber C, Jung S (2009) CX3CR1 is required for monocyte homeostasis and atherogenesis by promoting cell survival. Blood 113:963-972.

Lebre MC, Burwell T, Vieira PL, Lora J, Coyle AJ, Kapsenberg ML, Clausen BE, De Jong EC (2005) Differential expression of inflammatory chemokines by Th1- and Th2-cell promoting dendritic cells: A role for different mature dendritic cell populations in attracting appropriate effector cells to peripheral sites of inflammation. Immunol Cell Biol 83:525-535.

Levy JA (2009) The Unexpected Pleiotropic Activities of RANTES. The Journal of Immunology 182:3945-3946.

Li G, Liang X, Lotze MT (2013a) HMGB1: The Central Cytokine for All Lymphoid Cells. Frontiers in Immunology 4:68.

Li GZ, Zhong D, Yang LM, Sn B, Zhong ZH, Yin YH, Cheng J, Yan BB, Li HL (2005) Expression of Interleukin-17 in Ischemic Brain Tissue. Scandinavian Journal of Immunology 62:481-486.

Li H, Wu W, Sun Q, Liu M, Li W, Zhang XS, Zhou ML, Hang CH (2013b) Expression and cell distribution of receptor for advanced glycation end-products in the rat cortex following experimental subarachnoid hemorrhage. Brain Res 1543:315-323.

Li H, Yue H, Hao Y, Li H, Wang S, Yu L, Zhang D, Cao Y, Zhao J (2016) Expression profile of long noncoding RNAs in human cerebral aneurysms: a microarray analysis. J Neurosurg:1-8.

Li Y, Sun F, Jing Z, Wang X, Hua X, Wan L (2017) Glycyrrhizic acid exerts anti-inflammatory effect to improve cerebral vasospasm secondary to subarachnoid hemorrhage in a rat model. Neurol Res:1-6.

Liesz A, Zhou W, Na SY, Hammerling GJ, Garbi N, Karcher S, Mracsko E, Backs J, Rivest S, Veltkamp R (2013) Boosting regulatory T cells limits neuroinflammation in permanent cortical stroke. J Neurosci 33:17350-17362.

Lu CH, Chang WN, Tsai NW, Chuang YC, Huang CR, Wang HC (2010) The value of serial plasma nuclear and mitochondrial DNA levels in adult community-acquired bacterial meningitis. QJM : monthly journal of the Association of Physicians 103:169-175.

Lucke-Wold BP, Logsdon AF, Manoranjan B, Turner RC, McConnell E, Vates GE, Huber JD, Rosen CL, Simard JM (2016) Aneurysmal Subarachnoid Hemorrhage and Neuroinflammation: A Comprehensive Review. International journal of molecular sciences 17.

Lyakh L, Trinchieri G, Provezza L, Carra G, Gerosa F (2008) Regulation of interleukin-12/interleukin-23 production and the T-helper 17 response in humans. Immunol Rev 226:112-131.

Ma C, Zhou W, Yan Z, Qu M, Bu X (2015) Toll-like receptor 4 (TLR4) is correlated with delayed cerebral ischemia (DCI) and poor prognosis in aneurysmal subarachnoid hemorrhage. J Neurol Sci 359:67-71.

Ma K, Xu W, Shao X, Yanyue, Hu L, Xu H, Yuan Z, Zheng X, Xiong S (2007) Coimmunization with RANTES plasmid polarized Th1 immune response against hepatitis B virus envelope via recruitment of dendritic cells. Antiviral research 76:140-149.

Ma S, Zhong D, Chen H, Zheng Y, Sun Y, Luo J, Li H, Li G, Yin Y (2013) The immunomodulatory effect of bone marrow stromal cells (BMSCs) on interleukin (IL)-23/IL-17-mediated ischemic stroke in mice. Journal of Neuroimmunology 257:28-35.

Macdonald RL (2014) Delayed neurological deterioration after subarachnoid haemorrhage. Nat Rev Neurol 10:44-58.

Macdonald RL, Weir BK (1991) A review of hemoglobin and the pathogenesis of cerebral vasospasm. Stroke 22:971-982.

Macdonald RL, Schweizer TA (2017) Spontaneous subarachnoid haemorrhage. The Lancet 389:655-666.

Macdonald RL, Diringer M, Citerio G (2014) Understanding the disease: aneurysmal subarachnoid hemorrhage. Intensive Care Med:1-4.

Macedo SK, de Siqueira CP, de Siqueira SBP, Nuss RM, Dias LC, Souza AC, Pereira GVR (2010) Frequency/prevalence analysis of risk factors on aneurysmal subarachnoid hemorrhage. Critical Care 14:P337.

Maecker HT, McCoy JP, Nussenblatt R (2012) Standardizing immunophenotyping for the Human Immunology Project. Nat Rev Immunol 12:191-200.

Mansfield AS, Nevala WK, Dronca RS, Leontovich AA, Shuster L, Markovic SN (2012) Normal ageing is associated with an increase in Th2 cells, MCP-1 (CCL1) and RANTES (CCL5), with differences in sCD40L and PDGF-AA between sexes. Clinical and Experimental Immunology 170:186-193.

Mantovani A (1999) The chemokine system: redundancy for robust outputs. Immunology Today 20:254-257.

Masakazu Takayasu, Masato Shibuya, Masahiko Kanamori, Yoshio Suzuki, Koichiro Ogura, Naoki Kageyama, Hayato Umekawa, Hiroyoshi Hidaka (1985) S-100 protein and calmodulin levels in cerebrospinal fluid after subarachnoid hemorrhage. Journal of Neurosurgery 63:417-420.

Mathew A, Lindsley TA, Sheridan A, Bhoiwala DL, Hushmendy SF, Yager EJ, Ruggiero EA, Crawford DR (2012) Degraded mitochondrial DNA is a newly identified subtype of the damage associated molecular pattern (DAMP) family and possible trigger of neurodegeneration. J Alzheimers Dis 30:617-627.

Mathiesen T, Edner G, Ulfarsson E, Andersson B (1997) Cerebrospinal fluid interleukin-1 receptor antagonist and tumor necrosis factor-alpha following subarachnoid hemorrhage. J Neurosurg 87:215-220.

Matzinger P (1994) Tolerance, Danger, and the Extended Family. Annual Review of Immunology 12:991-1045.

McKeating EG, Andrews PJ (1998) Cytokines and adhesion molecules in acute brain injury. Br J Anaesth 80:77-84.

McMahon CJ, Hopkins S, Vail A, King AT, Smith D, Illingworth KJ, Clark S, Rothwell NJ, Tyrrell PJ (2013) Inflammation as a predictor for delayed cerebral ischemia after aneurysmal subarachnoid haemorrhage. Journal of neurointerventional surgery 5:512-517.

Mellergard P, Aneman O, Sjogren F, Saberg C, Hillman J (2011) Differences in cerebral extracellular response of interleukin-1beta, interleukin-6, and interleukin-10 after subarachnoid hemorrhage or severe head trauma in humans. Neurosurgery 68:12-19; discussion 19.

Mellergård P, Åneman O, Sjögren F, Pettersson P, Hillman J (2008) Changes in extracellular concentrations of some cytokines, chemokines, and neurotrophic factors after insertion of intracerebral microdialysis catheters in neurosurgical patients. Neurosurgery 62:151-158.

Miller BA, Turan N, Chau M, Pradilla G (2014) Inflammation, Vasospasm, and Brain Injury after Subarachnoid Hemorrhage. BioMed Research International 2014:16.

Mills CD, Kincaid K, Alt JM, Heilman MJ, Hill AM (2000) M-1/M-2 macrophages and the Th1/Th2 paradigm. J Immunol 164:6166-6173.

Mills KH (2008) Induction, function and regulation of IL-17-producing T cells. Eur J Immunol 38:2636-2649.

Mirabelli-Badenier M, Braunersreuther V, Viviani GL, Dallegri F, Quercioli A, Veneselli E, Mach F, Montecucco F (2011) CC and CXC chemokines are pivotal mediators of cerebral injury in ischaemic stroke. Thrombosis and haemostasis 105:409-420.

Moore KW, de Waal Malefyt R, Coffman RL, O'Garra A (2001) Interleukin-10 and the interleukin-10 receptor. Annu Rev Immunol 19:683-765.

Moraes L, Grille S, Morelli P, Mila R, Trias N, Brugnini A, N LL, Biestro A, Lens D (2015) Immune cells subpopulations in cerebrospinal fluid and peripheral blood of patients with Aneurysmal Subarachnoid Hemorrhage. SpringerPlus 4:195.

Moreth K, Iozzo RV, Schaefer L (2012) Small leucine-rich proteoglycans orchestrate receptor crosstalk during inflammation. Cell Cycle 11:2084-2091.

Moritz S, Warnat J, Bele S, Graf BM, Woertgen C (2010) The prognostic value of NSE and S100B from serum and cerebrospinal fluid in patients with spontaneous subarachnoid hemorrhage. J Neurosurg Anesthesiol 22:21-31.

Mroczko B, Groblewska M, Gryko M, Kedra B, Szmitkowski M (2010) Diagnostic usefulness of serum interleukin 6 (IL-6) and C-reactive protein (CRP) in the differentiation between pancreatic cancer and chronic pancreatitis. Journal of clinical laboratory analysis 24:256-261.

Muhammad S, Roeske S, Chaudhry SR, Kinfe TM (2017a) Burst or High-Frequency (10 kHz) Spinal Cord Stimulation in Failed Back Surgery Syndrome Patients With Predominant Back Pain: One Year Comparative Data. Neuromodulation : journal of the International Neuromodulation Society 20:661-667.

Muhammad S, Chaudhry SR, Yearwood TL, Krauss JK, Kinfe TM (2017b) Changes of Metabolic Disorders Associated Peripheral Cytokine/Adipokine Traffic in Non-Obese Chronic Back Patients Responsive to Burst Spinal Cord Stimulation. Neuromodulation : journal of the International Neuromodulation Society.

Muhammad S, Barakat W, Stoyanov S, Murikinati S, Yang H, Tracey KJ, Bendszus M, Rossetti G, Nawroth PP, Bierhaus A, Schwaninger M (2008) The HMGB1 Receptor RAGE Mediates Ischemic Brain Damage. The Journal of Neuroscience 28:12023-12031.

Mukherjee R, Kanti Barman P, Kumar Thatoi P, Tripathy R, Kumar Das B, Ravindran B (2015) Non-Classical monocytes display inflammatory features: Validation in Sepsis and Systemic Lupus Erythematous. Scientific Reports 5:13886.

Munoz-Guillen NM, Leon-Lopez R, Tunez-Finana I, Cano-Sanchez A (2013) From vasospasm to early brain injury: new frontiers in subarachnoid haemorrhage research. Neurologia 28:309-316.

Murakami K, Koide M, Dumont TM, Russell SR, Tranmer BI, Wellman GC (2011) Subarachnoid Hemorrhage Induces Gliosis and Increased Expression of the Pro-inflammatory Cytokine High Mobility Group Box 1 Protein. Transl Stroke Res 2:72-79.

Muroi C, Frei K, El Beltagy M, Cesnulis E, Yonekawa Y, Keller E (2008) Combined therapeutic hypothermia and barbiturate coma reduces interleukin-6 in the cerebrospinal fluid after aneurysmal subarachnoid hemorrhage. J Neurosurg Anesthesiol 20:193-198.

Muroi C, Burkhardt JK, Hugelshofer M, Seule M, Mishima K, Keller E (2012) Magnesium and the inflammatory response: potential pathophysiological implications in the management of patients with aneurysmal subarachnoid hemorrhage? Magnesium research 25:64-71.

Muroi C, Hugelshofer M, Seule M, Tastan I, Fujioka M, Mishima K, Keller E (2013) Correlation Among Systemic Inflammatory Parameter, Occurrence of Delayed Neurological Deficits, and Outcome After Aneurysmal Subarachnoid Hemorrhage. Neurosurgery 72:367-375.

Muroi C, Fujioka M, Mishima K, Irie K, Fujimura Y, Nakano T, Fandino J, Keller E, Iwasaki K, Fujiwara M (2014) Effect of ADAMTS-13 on cerebrovascular microthrombosis and neuronal injury after experimental subarachnoid hemorrhage. Journal of Thrombosis and Haemostasis 12:505-514.

Murphy KM, Reiner SL (2002) The lineage decisions of helper T cells. Nature Reviews Immunology 2:933.

Murray KN, Parry-Jones AR, Allan SM (2015) Interleukin-1 and acute brain injury. Frontiers in Cellular Neuroscience 9.

Nakahara T, Tsuruta R, Kaneko T, Yamashita S, Fujita M, Kasaoka S, Hashiguchi T, Suzuki M, Maruyama I, Maekawa T (2009) High-mobility group box 1 protein in CSF of patients with subarachnoid hemorrhage. Neurocrit Care 11:362-368.

Nakura T, Osuka K, Inukai T, Takagi T, Takayasu M (2011) Soluble gp130 regulatess interleukin-6 in cerebrospinal fluid after subarachnoid haemorrhage. J Neurol Neurosurg Psychiatry 82:952-954.

Nam DH, Kim JS, Hong SC, Lee WH, Lee JI, Shin HJ, Park K, Eoh W, Han DH, Kim JH (2001) Expression of interleukin-1 beta in lipopolysaccharide stimulated monocytes derived from patients with aneurysmal subarachnoid hemorrhage is correlated with cerebral vasospasm. Neurosci Lett 312:41-44.

Neil-Dwyer G, Cruickshank J (1974) THE BLOOD LEEUCOCYTE COUNT AND ITS PROGNOSTIC SIGNIFICANCE IN SUBARACHNOID HæMORRHAGE. Brain : a journal of neurology 97:79-86.

Niwa A, Osuka K (2016) Interleukin-6, MCP-1, IP-10, and MIG are sequentially expressed in cerebrospinal fluid after subarachnoid hemorrhage. 13:217.

Norden DM, Fenn AM, Dugan A, Godbout JP (2014) TGFβ produced by IL-10 redirected astrocytes attenuates microglial activation. Glia 62:881-895.

O'Neill LAJ, Golenbock D, Bowie AG (2013) The history of Toll-like receptors [mdash] redefining innate immunity. Nat Rev Immunol 13:453-460.

Oke SL, Tracey KJ (2009) The Inflammatory Reflex and the Role of Complementary and Alternative Medical Therapies. Annals of the New York Academy of Sciences 1172:172-180.

Olmos G, Llad, #xf3, J, #xf2, nia (2014) Tumor Necrosis Factor Alpha: A Link between Neuroinflammation and Excitotoxicity. Mediators of Inflammation 2014:12.

Oppmann B et al. (2000) Novel p19 Protein Engages IL-12p40 to Form a Cytokine, IL-23, with Biological Activities Similar as Well as Distinct from IL-12. Immunity 13:715-725.

Ordovas-Montanes J, Rakoff-Nahoum S, Huang S, Riol-Blanco L, Barreiro O, von Andrian UH (2015) The Regulation of Immunological Processes by Peripheral Neurons in Homeostasis and Disease. Trends in Immunology 36:578-604.

Ostrowski RP, Colohan AR, Zhang JH (2006) Molecular mechanisms of early brain injury after subarachnoid hemorrhage. Neurological research 28:399-414.

Osuka K, Suzuki Y, Tanazawa T, Hattori K, Yamamoto N, Takayasu M, Shibuya M, Yoshida J (1998) Interleukin-6 and Development of Vasospasm after Subarachnoid Haemorrhage. Acta Neurochirurgica 140:943-951.

Oto J, Suzue A, Inui D, Fukuta Y, Hosotsubo K, Torii M, Nagahiro S, Nishimura M (2008) Plasma proinflammatory and anti-inflammatory cytokine and catecholamine concentrations as predictors of neurological outcome in acute stroke patients. Journal of Anesthesia 22:207-212.

Palojärvi A, Petäjä J, Siitonen S, Janér C, Andersson S (2012) Low monocyte HLA-DR expression as an indicator of immunodepression in very low birth weight infants. Pediatric Research 73:469.

Panichi V, Maggiore U, Taccola D, Migliori M, Rizza GM, Consani C, Bertini A, Sposini S, Perez-Garcia R, Rindi P, Palla R, Tetta C (2004) Interleukin-6 is a stronger predictor of total and cardiovascular mortality than C-reactive protein in haemodialysis patients. Nephrology, dialysis, transplantation : official publication of the European Dialysis and Transplant Association - European Renal Association 19:1154-1160.

Parham C et al. (2002) A receptor for the heterodimeric cytokine IL-23 is composed of IL-12Rbeta1 and a novel cytokine receptor subunit, IL-23R. J Immunol 168:5699-5708.

Pedrazzi M, Patrone M, Passalacqua M, Ranzato E, Colamassaro D, Sparatore B, Pontremoli S, Melloni E (2007) Selective Proinflammatory Activation of Astrocytes by High-Mobility Group Box 1 Protein Signaling. The Journal of Immunology 179:8525-8532.

Pelidou S-H, Kostulas N, Matusevicius D, Kivisäkk P, Kostulas V, Link H (1999) High levels of IL-10 secreting cells are present in blood in cerebrovascular diseases. European Journal of Neurology 6:437-442.

Pera J, Korostynski M, Golda S, Piechota M, Dzbek J, Krzyszkowski T, Dziedzic T, Moskala M, Przewlocki R, Szczudlik A, Slowik A (2013) Gene expression profiling of blood in ruptured intracranial aneurysms: in search of biomarkers. J Cereb Blood Flow Metab 33:1025-1031.

Pereira AR, Sanchez-Pena P, Biondi A, Sourour N, Boch AL, Colonne C, Lejean L, Abdennour L, Puybasset L (2007) Predictors of 1-year outcome after coiling for poor-grade subarachnoid aneurysmal hemorrhage. Neurocrit Care 7:18-26.

Perez-Santiago J, Schrier RD, de Oliveira MF, Gianella S, Var SR, Day TR, Ramirez-Gaona M, Suben JD, Murrell B, Massanella M, Cherner M, Smith DM, Ellis RJ, Letendre SL, Mehta SR (2016) Cell-free mitochondrial DNA in CSF is associated with early viral rebound, inflammation, and severity of neurocognitive deficits in HIV infection. Journal of neurovirology 22:191-200.

Persson L, Hårdemark HG, Gustafsson J, Rundström G, Mendel-Hartvig I, Esscher T, Påhlman S (1987) S-100 protein and neuron-specific enolase in cerebrospinal fluid and serum: markers of cell damage in human central nervous system. Stroke 18:911-918.

Petzold A, Keir G, Lim D, Smith M, Thompson EJ (2003) Cerebrospinal fluid (CSF) and serum S100B: release and wash-out pattern. Brain Res Bull 61:281-285.

Piazza M, Damore G, Costa B, Gioannini TL, Weiss JP, Peri F (2011) Hemin and a metabolic derivative coprohemin modulate the TLR4 pathway differently through different molecular targets. Innate immunity 17:293-301.

Podlesniy P, Vilas D, Taylor P, Shaw LM, Tolosa E, Trullas R (2016a) Mitochondrial DNA in CSF distinguishes LRRK2 from idiopathic Parkinson's disease. Neurobiology of disease 94:10-17.

Podlesniy P, Llorens F, Golanska E, Sikorska B, Liberski P, Zerr I, Trullas R (2016b) Mitochondrial DNA differentiates Alzheimer's disease from Creutzfeldt-Jakob disease. Alzheimer's & dementia : the journal of the Alzheimer's Association 12:546-555.

Podlesniy P, Figueiro-Silva J, Llado A, Antonell A, Sanchez-Valle R, Alcolea D, Lleo A, Molinuevo JL, Serra N, Trullas R (2013) Low cerebrospinal fluid concentration of mitochondrial DNA in preclinical Alzheimer disease. Annals of Neurology 74:655-668.

Probert L (2015) TNF and its receptors in the CNS: The essential, the desirable and the deleterious effects. Neuroscience 302:2-22.

Provencio JJ (2013) Inflammation in subarachnoid hemorrhage and delayed deterioration associated with vasospasm: A review. Acta neurochirurgica Supplement 115:233-238.

Qiu J, Nishimura M, Wang Y, Sims JR, Qiu S, Savitz SI, Salomone S, Moskowitz MA (2008) Early release of HMGB-1 from neurons after the onset of brain ischemia. J Cereb Blood Flow Metab 28:927-938.

Quintana FJ (2017) Old dog, new tricks: IL-6 cluster signaling promotes pathogenic TH17 cell differentiation. Nat Immunol 18:8-10.

Rainer TH, Wong LKS, Lam W, Yuen E, Lam NYL, Metreweli C, Lo YMD (2003) Prognostic Use of Circulating Plasma Nucleic Acid Concentrations in Patients with Acute Stroke. Clinical Chemistry 49:562-569.

Raman D, Sobolik-Delmaire T, Richmond A (2011) Chemokines in health and disease. Experimental Cell Research 317:575-589.

Recinos PF, Pradilla G, Thai Q-A, Perez M, Hdeib AM, Tamargo RJ (2006) Controlled release of lipopolysaccharide in the subarachnoid space of rabbits induces chronic vasospasm in the absence of blood. Surgical Neurology 66:463-469.

Rendon-Mitchell B, Ochani M, Li J, Han J, Wang H, Yang H, Susarla S, Czura C, Mitchell RA, Chen G, Sama AE, Tracey KJ (2003) IFN-gamma induces high mobility group box 1 protein release partly through a TNF-dependent mechanism. J Immunol 170:3890-3897.

Rollins BJ (1997) Chemokines. Blood 90:909-928.

Rosengart AJ, Schultheiss KE, Tolentino J, Macdonald RL (2007) Prognostic Factors for Outcome in Patients With Aneurysmal Subarachnoid Hemorrhage. Stroke 38:2315-2321.

Ryba M, Grieb P, Pastuszko M, Węgier-Filipiuk B, Mrowiec E, Andrychowski J, Konopka L (1993) Impaired in vitro proliferative response of suppressor lymphocytes in patients with subarachnoid haemorrhage from ruptured intracranial aneurysm. Acta Neurochirurgica 122:240-243.

Sabat R, Grutz G, Warszawska K, Kirsch S, Witte E, Wolk K, Geginat J (2010) Biology of interleukin-10. Cytokine Growth Factor Rev 21:331-344.

Sakaguchi S, Miyara M, Costantino CM, Hafler DA (2010) FOXP3+ regulatory T cells in the human immune system. Nat Rev Immunol 10:490-500.

Sanchez-Pena P, Pereira AR, Sourour NA, Biondi A, Lejean L, Colonne C, Boch AL, Al Hawari M, Abdennour L, Puybasset L (2008) S100B as an additional prognostic marker in subarachnoid aneurysmal hemorrhage. Crit Care Med 36:2267-2273.

Sanchez-Pena P, Nouet A, Clarencon F, Colonne C, Jean B, Le Jean L, Fonfrede M, Aout M, Vicaut E, Puybasset L (2012) Atorvastatin decreases computed tomography and S100-assessed brain ischemia after subarachnoid aneurysmal hemorrhage: a comparative study. Crit Care Med 40:594-602.

Sarrafzadeh A, Schlenk F, Gericke C, Vajkoczy P (2010) Relevance of cerebral interleukin-6 after aneurysmal subarachnoid hemorrhage. Neurocrit Care 13:339-346.

Sarrafzadeh A, Schlenk F, Meisel A, Dreier J, Vajkoczy P, Meisel C (2011) Immunodepression after aneurysmal subarachnoid hemorrhage. Stroke 42:53-58.

Sasaki T, Kasuya H, Onda H, Sasahara A, Goto S, Hori T, Inoue I (2004) Role of p38 Mitogen-Activated Protein Kinase on Cerebral Vasospasm After Subarachnoid Hemorrhage. Stroke 35:1466-1470.

Sathyan S, Koshy LV, Srinivas L, Easwer HV, Premkumar S, Nair S, Bhattacharya RN, Alapatt JP, Banerjee M (2015) Pathogenesis of intracranial aneurysm is mediated by proinflammatory cytokine TNFA and IFNG and through stochastic regulation of IL10 and TGFB1 by comorbid factors. Journal of Neuroinflammation 12:1-10.

Savarraj J, Parsha K, Hergenroeder G, Ahn S, Chang TR, Kim DH, Choi HA (2017a) Early Brain Injury Associated with Systemic Inflammation After Subarachnoid Hemorrhage. Neurocrit Care.

Savarraj JPJ, Parsha K, Hergenroeder GW, Zhu L, Bajgur SS, Ahn S, Lee K, Chang T, Kim DH, Liu Y, Choi HA (2017b) Systematic model of peripheral inflammation after subarachnoid hemorrhage. Neurology.

Savva A, Roger T (2013) Targeting Toll-Like Receptors: Promising Therapeutic Strategies for the Management of Sepsis-Associated Pathology and Infectious Diseases. Frontiers in Immunology 4:387.

Scaffidi P, Misteli T, Bianchi ME (2002) Release of chromatin protein HMGB1 by necrotic cells triggers inflammation. Nature 418:191-195.

Schaefer L (2014) Complexity of Danger: The Diverse Nature of Damage-associated Molecular Patterns. The Journal of Biological Chemistry 289:35237-35245.

Schafer ST, Franken L, Adamzik M, Schumak B, Scherag A, Engler A, Schonborn N, Walden J, Koch S, Baba HA, Steinmann J, Westendorf AM, Fandrey J, Bieber T, Kurts C, Frede S, Peters J, Limmer A (2016) Mitochondrial DNA: An Endogenous Trigger for Immune Paralysis. Anesthesiology.

Schallner N, Pandit R, LeBlanc R, III, Thomas AJ, Ogilvy CS, Zuckerbraun BS, Gallo D, Otterbein LE, Hanafy KA (2015) Microglia regulate blood clearance in subarachnoid hemorrhage by heme oxygenase-1. The Journal of Clinical Investigation 125:2609-2625.

Scheller J, Chalaris A, Schmidt-Arras D, Rose-John S (2011) The pro- and anti-inflammatory properties of the cytokine interleukin-6. Biochimica et Biophysica Acta (BBA) - Molecular Cell Research 1813:878-888.

Schneider UC, Schiffler J, Hakiy N, Horn P, Vajkoczy P (2012) Functional analysis of Pro-inflammatory properties within the cerebrospinal fluid after subarachnoid hemorrhage in vivo and in vitro. Journal of Neuroinflammation 9.

Schoch B, Regel JP, Wichert M, Gasser T, Volbracht L, Stolke D (2007) Analysis of intrathecal interleukin-6 as a potential predictive factor for vasospasm in subarachnoid hemorrhage. Neurosurgery 60:828-836; discussion 828-836.

Sedger LM, McDermott MF (2014) TNF and TNF-receptors: From mediators of cell death and inflammation to therapeutic giants – past, present and future. Cytokine & Growth Factor Reviews 25:453-472.

Sen J, Belli A (2007) S100B in neuropathologic states: The CRP of the brain? Journal of Neuroscience Research 85:1373-1380.

Shang D, Peng T, Gou S, Li Y, Wu H, Wang C, Yang Z (2016) High Mobility Group Box Protein 1 Boosts Endothelial Albumin Transcytosis through the RAGE/Src/Caveolin-1 Pathway. 6:32180.

Shi L, Qin J, Song B, Wang QM, Zhang R, Liu X, Liu Y, Hou H, Chen X, Ma X, Jiang C, Sun X, Gong G, Xu Y (2015) Increased frequency of circulating regulatory T cells in patients with acute cerebral hemorrhage. Neuroscience Letters 591:115-120.

Shichita T, Sugiyama Y, Ooboshi H, Sugimori H, Nakagawa R, Takada I, Iwaki T, Okada Y, Iida M, Cua DJ, Iwakura Y, Yoshimura A (2009) Pivotal role of cerebral interleukin-17-producing [gamma][delta]T cells in the delayed phase of ischemic brain injury. Nature medicine 15:946-950.

Shiozaki T, Hayakata T, Tasaki O, Hosotubo H, Fuijita K, Mouri T, Tajima G, Kajino K, Nakae H, Tanaka H, Shimazu T, Sugimoto H (2005) Cerebrospinal fluid concentrations of anti-inflammatory mediators in early-phase severe traumatic brain injury. Shock 23:406-410.

Simpson J, Rezaie P, Newcombe J, Cuzner ML, Male D, Woodroofe MN (2000) Expression of the β-chemokine receptors CCR2, CCR3 and CCR5 in multiple sclerosis central nervous system tissue. Journal of Neuroimmunology 108:192-200.

Sims JE, March CJ, Cosman D, Widmer MB, MacDonald HR, McMahan CJ, Grubin CE, Wignall JM, Jackson JL, Call SM, et al. (1988) cDNA expression cloning of the IL-1 receptor, a member of the immunoglobulin superfamily. Science 241:585-589.

Singh N, Hopkins SJ, Hulme S, Galea JP, Hoadley M, Vail A, Hutchinson PJ, Grainger S, Rothwell NJ, King AT, Tyrrell PJ (2014) The effect of intravenous interleukin-1 receptor antagonist on inflammatory mediators in cerebrospinal fluid after subarachnoid haemorrhage: a phase II randomised controlled trial. J Neuroinflammation 11:1.

Slavin KV, Vannemreddy PSSV, Goellner E, Alaraj AM, Aydin S, Eboli P, Mlinarevich N, Watson KS, Walters LE, Amin-Hanjani S, Deveshwar R, Aletich V, Charbel FT (2011) Use of Cervical Spinal Cord Stimulation in Treatment and Prevention of Arterial Vasospasm after Aneurysmal Subarachnoid Hemorrhage:Technical Details. The Neuroradiology Journal 24:131-135.

Smithason S, Moore SK, Provencio JJ (2012) Systemic administration of LPS worsens delayed deterioration associated with vasospasm after subarachnoid hemorrhage through a myeloid cell-dependent mechanism. Neurocrit Care 16:327-334.

Sokol B, Wozniak A, Jankowski R, Jurga S, Wasik N, Shahid H, Grzeskowiak B (2015) HMGB1 Level in Cerebrospinal Fluid as a Marker of Treatment Outcome in Patients with Acute Hydrocephalus Following Aneurysmal Subarachnoid Hemorrhage. Journal of stroke and cerebrovascular diseases : the official journal of National Stroke Association 24:1897-1904.

Sondheimer N, Zollo O, Van Deerlin V, Trojanowski JQ (2014) Analysis of cerebrospinal fluid mitochondrial DNA levels in Alzheimer disease. Ann Neurol 75:458-460.

Song JN, Zhang M, Li DD, Li M, An JY, Cheng MF, Guo XY (2014) Dynamic expression of the suppressor of cytokine signaling-3 and cytokines in the cerebral basilar artery of rats with subarachnoid hemorrhage, and the effect of acetylcholine. Acta Neurochir (Wien) 156:941-949; discussion 949.

Sorci G, Bianchi R, Riuzzi F, Tubaro C, Arcuri C, Giambanco I, Donato R (2010) S100B Protein, a Damage-Associated Molecular Pattern Protein in the Brain and Heart, and Beyond. Cardiovascular Psychiatry and Neurology 2010.

Sosvorova L, Vcelak J, Mohapl M, Vitku J, Bicikova M, Hampl R (2014) Selected pro- and anti-inflammatory cytokines in cerebrospinal fluid in normal pressure hydrocephalus. Neuro Endocrinol Lett 35:586-593.

Sozen T, Tsuchiyama R, Hasegawa Y, Suzuki H, Jadhav V, Nishizawa S, Zhang JH (2009) Role of Interleukin-1β in Early Brain Injury after Subarachnoid Hemorrhage in Mice. Stroke; a journal of cerebral circulation 40:2519-2525.

Starke RM, Chalouhi N, Jabbour PM, Tjoumakaris SI, Gonzalez LF, Rosenwasser RH, Wada K, Shimada K, Hasan DM, Greig NH, Owens GK, Dumont AS (2014) Critical role of TNF-α in cerebral aneurysm formation and progression to rupture. Journal of Neuroinflammation 11:77-77.

Stranjalis G, Korfias S, Psachoulia C, Kouyialis A, Sakas DE, Mendelow AD (2007) The prognostic value of serum S-100B protein in spontaneous subarachnoid haemorrhage. Acta Neurochir (Wien) 149:231-237; discussion 237-238.

Strle K, Zhou JH, Shen WH, Broussard SR, Johnson RW, Freund GG, Dantzer R, Kelley KW (2001) Interleukin-10 in the brain. Critical reviews in immunology 21:427-449.

Suarez JI, Tarr RW, Selman WR (2006) Aneurysmal Subarachnoid Hemorrhage. New England Journal of Medicine 354:387-396.

Subramaniam S, Stansberg C, Cunningham C (2004) The interleukin 1 receptor family. Developmental and comparative immunology 28:415-428.

Suffee N, Le Visage C, Hlawaty H, Aid-Launais R, Vanneaux V, Larghero J, Haddad O, Oudar O, Charnaux N, Sutton A (2017) Pro-angiogenic effect of RANTES-loaded polysaccharide-based microparticles for a mouse ischemia therapy. Scientific Reports 7:13294.

Sun Q, Wang F, Li W, Hu YC, Li S, Zhu JH, Zhou M, Hang CH (2014a) Glycyrrhizic acid confers neuroprotection after subarachnoid hemorrhage via inhibition of high mobility group box-1 protein: a hypothesis for novel therapy of subarachnoid hemorrhage. Med Hypotheses 81:681-685.

Sun Q, Wu W, Hu YC, Li H, Zhang D, Li S, Li W, Li WD, Ma B, Zhu JH, Zhou ML, Hang CH (2014b) Early release of high-mobility group box 1 (HMGB1) from neurons in experimental subarachnoid hemorrhage in vivo and in vitro. J Neuroinflammation 11:106.

Suzuki S, Tanaka K, Suzuki N (2009) Ambivalent aspects of interleukin-6 in cerebral ischemia: inflammatory versus neurotrophic aspects. J Cereb Blood Flow Metab 29:464-479.

Tacke F, Randolph GJ (2006) Migratory fate and differentiation of blood monocyte subsets. Immunobiology 211:609-618.

Taheri Z, Harirchian MH, Ghanaati H, Khoshnevisan A, Salamati P, Miri M, Firouznia K, Saeednejad M, Shakiba M, Rahimi-Movaghar V (2015) Comparison of endovascular coiling and surgical clipping for the treatment of intracranial aneurysms: A prospective study. Iranian Journal of Neurology 14:22-28.

Takeuchi O, Akira S (2010) Pattern Recognition Receptors and Inflammation. Cell 140:805-820.

Takizawa T, Tada T, Kitazawa K, Tanaka Y, Hongo K, Kameko M, Uemura KI (2001) Inflammatory cytokine cascade released by leukocytes in cerebrospinal fluid after subarachnoid hemorrhage. Neurol Res 23:724-730.

Tang P, Chong L, Li X, Liu Y, Liu P, Hou C, Li R (2014) Correlation between Serum RANTES Levels and the Severity of Parkinson’s Disease. Oxidative Medicine and Cellular Longevity 2014:4.

Teng MWL, Bowman EP, McElwee JJ, Smyth MJ, Casanova J-L, Cooper AM, Cua DJ (2015) IL-12 and IL-23 cytokines: from discovery to targeted therapies for immune-mediated inflammatory diseases. Nature medicine 21:719-729.

Terao S, Yilmaz G, Stokes KY, Russell J, Ishikawa M, Kawase T, Granger DN (2008) Blood cell-derived RANTES mediates cerebral microvascular dysfunction, inflammation and tissue injury following focal ischemia-reperfusion. Stroke; a journal of cerebral circulation 39:2560-2570.

Thornberry NA, Bull HG, Calaycay JR, Chapman KT, Howard AD, Kostura MJ, Miller DK, Molineaux SM, Weidner JR, Aunins J, et al. (1992) A novel heterodimeric cysteine protease is required for interleukin-1 beta processing in monocytes. Nature 356:768-774.

Tokami H, Ago T, Sugimori H, Kuroda J, Awano H, Suzuki K, Kiyohara Y, Kamouchi M, Kitazono T (2013) RANTES has a potential to play a neuroprotective role in an autocrine/paracrine manner after ischemic stroke. Brain Research 1517:122-132.

Tsai NW, Lin TK, Chen SD, Chang WN, Wang HC, Yang TM, Lin YJ, Jan CR, Huang CR, Liou CW, Lu CH (2011) The value of serial plasma nuclear and mitochondrial DNA levels in patients with acute ischemic stroke. Clin Chim Acta 412:476-479.

Tsung A, Sahai R, Tanaka H, Nakao A, Fink MP, Lotze MT, Yang H, Li J, Tracey KJ, Geller DA, Billiar TR (2005) The nuclear factor HMGB1 mediates hepatic injury after murine liver ischemia-reperfusion. J Exp Med 201:1135-1143.

Uhlig HH, McKenzie BS, Hue S, Thompson C, Joyce-Shaikh B, Stepankova R, Robinson N, Buonocore S, Tlaskalova-Hogenova H, Cua DJ, Powrie F (2006) Differential Activity of IL-12 and IL-23 in Mucosal and Systemic Innate Immune Pathology. Immunity 25:309-318.

van Dijk BJ, Vergouwen MDI, Kelfkens MM, Rinkel GJE, Hol EM (2016) Glial cell response after aneurysmal subarachnoid hemorrhage — Functional consequences and clinical implications. Biochimica et Biophysica Acta (BBA) - Molecular Basis of Disease 1862:492-505.

van Gijn J, Kerr RS, Rinkel GJE (2007) Subarachnoid haemorrhage. The Lancet 369:306-318.

Varhaug KN, Vedeler CA, Myhr KM, Aarseth JH, Tzoulis C, Bindoff LA (2016) Increased levels of cell-free mitochondrial DNA in the cerebrospinal fluid of patients with multiple sclerosis. Mitochondrion.

Vecchione C, Frati A, Di Pardo A, Cifelli G, Carnevale D, Gentile MT, Carangi R, Landolfi A, Carullo P, Bettarini U, Antenucci G, Mascio G, Busceti CL, Notte A, Maffei A, Cantore GP, Lembo G (2009) Tumor necrosis factor-alpha mediates hemolysis-induced vasoconstriction and the cerebral vasospasm evoked by subarachnoid hemorrhage. Hypertension 54.

Veiga-Fernandes H, Mucida D (2016) Neuro-Immune Interactions at Barrier Surfaces. Cell 165:801-811.

Wang H, Bloom O, Zhang M, Vishnubhakat JM, Ombrellino M, Che J, Frazier A, Yang H, Ivanova S, Borovikova L, Manogue KR, Faist E, Abraham E, Andersson J, Andersson U, Molina PE, Abumrad NN, Sama A, Tracey KJ (1999) HMG-1 as a late mediator of endotoxin lethality in mice. Science 285:248-251.

Wang HC, Yang TM, Lin WC, Lin YJ, Tsai NW, Liou CW, Kwan AL, Lu CH (2013) The value of serial plasma and cerebrospinal fluid nuclear and mitochondrial deoxyribonucleic acid levels in aneurysmal subarachnoid hemorrhage. J Neurosurg 118:13-19.

Wang KC, Tang SC, Lee JE, Li YI, Huang YS, Yang WS, Jeng JS, Arumugam TV, Tu YK (2017) Cerebrospinal fluid high mobility group box 1 is associated with neuronal death in subarachnoid hemorrhage. J Cereb Blood Flow Metab 37:435-443.

Wang KW, Cho CL, Chen HJ, Liang CL, Liliang PC, Tsai YD, Wang HK, Lu K (2011a) Molecular biomarker of inflammatory response is associated with rebleeding in spontaneous intracerebral hemorrhage. Eur Neurol 66:322-327.

Wang Z, Wang KY, Wu Y, Zhou P, Sun XO, Chen G (2010) Potential role of CD34 in cerebral vasospasm after experimental subarachnoid hemorrhage in rats. Cytokine 52:245-251.

Wang Z, Zuo G, Shi X-Y, Zhang J, Fang Q, Chen G (2011b) Progesterone administration modulates cortical TLR4/NF-κB signaling pathway after subarachnoid hemorrhage in male rats. Mediators of inflammation 2011.

Weidauer S, Lanfermann H, Raabe A, Zanella F, Seifert V, Beck J (2007) Impairment of cerebral perfusion and infarct patterns attributable to vasospasm after aneurysmal subarachnoid hemorrhage: a prospective MRI and DSA study. Stroke 38:1831-1836.

Weiss N, Sanchez-Pena P, Roche S, Beaudeux JL, Colonne C, Coriat P, Puybasset L (2006) Prognosis value of plasma S100B protein levels after subarachnoid aneurysmal hemorrhage. Anesthesiology 104:658-666.

Wen S-R, Liu G-J, Feng R-N, Gong F-C, Zhong H, Duan S-R, Bi S (2012) Increased levels of IL-23 and osteopontin in serum and cerebrospinal fluid of multiple sclerosis patients. Journal of Neuroimmunology 244:94-96.

Wendling D, Abbas W, Godfrin-Valnet M, Kumar A, Guillot X, Khan KA, Vidon C, Coquard L, Toussirot E, Prati C, Herbein G (2015) Dysregulated serum IL-23 and SIRT1 activity in peripheral blood mononuclear cells of patients with rheumatoid arthritis. PLoS One 10:e0119981.

Werman A, Werman-Venkert R, White R, Lee JK, Werman B, Krelin Y, Voronov E, Dinarello CA, Apte RN (2004) The precursor form of IL-1alpha is an intracrine proinflammatory activator of transcription. Proc Natl Acad Sci U S A 101:2434-2439.

West AP, Shadel GS (2017) Mitochondrial DNA in innate immune responses and inflammatory pathology. Nat Rev Immunol 17:363-375.

White GE, McNeill E, Channon KM, Greaves DR (2014) Fractalkine promotes human monocyte survival via a reduction in oxidative stress. Arteriosclerosis, Thrombosis, and Vascular Biology 34:2554-2562.

Wiesmann M, Missler U, Hagenstrom H, Gottmann D (1997) S-100 protein plasma levels after aneurysmal subarachnoid haemorrhage. Acta Neurochir (Wien) 139:1155-1160.

Woiciechowsky C, Asadullah K, Nestler D, Eberhardt B, Platzer C, Schöning B, Glöckner F, Lanksch WR, Volk H-D, Döcke W-D (1998) Sympathetic activation triggers systemic interleukin-10 release in immunodepression induced by brain injury. Nature medicine 4:808.

Wostrack M, Reeb T, Martin J, Kehl V, Shiban E, Preuss A, Ringel F, Meyer B, Ryang YM (2014) Shunt-dependent hydrocephalus after aneurysmal subarachnoid hemorrhage: the role of intrathecal interleukin-6. Neurocrit Care 21:78-84.

Wu W, Guan Y, Zhao G, Fu X-J, Guo T-Z, Liu Y-T, Ren X-L, Wang W, Liu H-R, Li Y-Q (2016a) Elevated IL-6 and TNF-α Levels in Cerebrospinal Fluid of Subarachnoid Hemorrhage Patients. Molecular Neurobiology 53:3277-3285.

Wu Y, Zhao XD, Zhuang Z, Xue YJ, Cheng HL, Yin HX, Shi JX (2010) Peroxisome proliferator-activated receptor gamma agonist rosiglitazone attenuates oxyhemoglobin-induced Toll-like receptor 4 expression in vascular smooth muscle cells. Brain Res 1322:102-108.

Wu Y, Pang J, Peng J, Cao F, Vitek MP, Li F, Jiang Y, Sun X (2016b) An apoE-derived mimic peptide, COG1410, alleviates early brain injury via reducing apoptosis and neuroinflammation in a mouse model of subarachnoid hemorrhage. Neurosci Lett 627:92-99.

Xia M, Hyman BT (1999) Chemokines/chemokine receptors in the central nervous system and Alzheimer's disease. Journal of neurovirology 5:32-41.

Yamada Y, Sakuma J, Takeuchi I, Yasukochi Y, Kato K, Oguri M, Fujimaki T, Horibe H, Muramatsu M, Sawabe M (2017) Identification of six polymorphisms as novel susceptibility loci for ischemic or hemorrhagic stroke by exome-wide association studies. International Journal of Molecular Medicine.

Yang TM, Lin YJ, Tsai NW, Lin WC, Ho JT, Chang WN, Cheng BC, Kung CT, Lee TH, Huang CC, Wang HC, Lu CH (2012) The prognostic value of serial leukocyte adhesion molecules in post-aneurysmal subarachnoid hemorrhage. Clin Chim Acta 413:411-416.

Yasukawa H, Ohishi M, Mori H, Murakami M, Chinen T, Aki D, Hanada T, Takeda K, Akira S, Hoshijima M, Hirano T, Chien KR, Yoshimura A (2003) IL-6 induces an anti-inflammatory response in the absence of SOCS3 in macrophages. Nat Immunol 4:551-556.

Yoshimoto Y, Tanaka Y, Hoya K (2001) Acute Systemic Inflammatory Response Syndrome in Subarachnoid Hemorrhage. Stroke 32:1989-1993.

You W, Zuo G, Shen H, Tian X, Li H, Zhu H, Yin J, Zhang T, Wang Z (2016) Potential dual role of nuclear factor-kappa B in experimental subarachnoid hemorrhage-induced early brain injury in rabbits. Inflammation Research 65:975-984.

Zaremba J, Ilkowski J, Losy J (2006) Serial measurements of levels of the chemokines CCL2, CCL3 and CCL5 in serum of patients with acute ischaemic stroke. Folia neuropathologica 44:282-289.

Zeiler FA, Thelin EP, Czosnyka M, Hutchinson PJ, Menon DK, Helmy A (2017) Cerebrospinal Fluid and Microdialysis Cytokines in Aneurysmal Subarachnoid Hemorrhage: A Scoping Systematic Review. Front Neurol 8:379.

Zhang H-F, Zhao M-G, Liang G-B, Yu C-Y, He W, Li Z-Q, Gao X (2015) Dysregulation of CD4+ T Cell Subsets in Intracranial Aneurysm. DNA and Cell Biology 35:96-103.

Zhang Q, Raoof M, Chen Y, Sumi Y, Sursal T, Junger W, Brohi K, Itagaki K, Hauser CJ (2010) Circulating mitochondrial DAMPs cause inflammatory responses to injury. Nature 464:104-107.

Zhao XD, Mao HY, Lv J, Lu XJ (2016) Expression of high-mobility group box-1 (HMGB1) in the basilar artery after experimental subarachnoid hemorrhage. Journal of clinical neuroscience : official journal of the Neurosurgical Society of Australasia 27:161-165.

Zhou C, Xie G, Wang C, Zhang Z, Chen Q, Zhang L, Wu L, Wei Y, Ding H, Hang C, Zhou M, Shi J (2015) Decreased progranulin levels in patients and rats with subarachnoid hemorrhage: a potential role in inhibiting inflammation by suppressing neutrophil recruitment. Journal of Neuroinflammation 12:200.

Zhou Y, Jiang Y, Peng Y, Zhang M (2017) The Quantitative and Functional Changes of Postoperative Peripheral Blood Immune Cell Subsets Relate to Prognosis of Patients with Subarachnoid Hemorrhage: A Preliminary Study. World Neurosurg 108:206-215.

Zhu X-D, Chen J-S, Zhou F, Liu Q-C, Chen G, Zhang J-M (2012) Relationship between plasma high mobility group box-1 protein levels and clinical outcomes of aneurysmal subarachnoid hemorrhage. Journal of Neuroinflammation 9:1-12.

Ziegler-Heitbrock L, Hofer TP (2013) Toward a refined definition of monocyte subsets. Front Immunol 4:23.

Ziegler-Heitbrock L, Ancuta P, Crowe S, Dalod M, Grau V, Hart DN, Leenen PJM, Liu Y-J, MacPherson G, Randolph GJ, Scherberich J, Schmitz J, Shortman K, Sozzani S, Strobl H, Zembala M, Austyn JM, Lutz MB (2010) Nomenclature of monocytes and dendritic cells in blood.

Zlotnik A, Yoshie O (2000) Chemokines: A New Classification System and Their Role in Immunity. Immunity 12:121-127.

10. Appendices

10.1. List of tables

10.2. List of figures

10.3. Composition of solutions used

10x Tris EDTA (TE) pH 7.4

100 mM Tris-Cl (pH 7.4)

10 mM EDTA (pH 8.0)

Solutions were sterlized by autoclaving for 20 minutes at 15 psi on liquid cycle. Stored the buffer at room temperature

10.4. List of antibodies along with their catalog numbers and clones

Sr. #	Product	Clone	Catalog no.	Company
1	Anti-Human CD127 FITC	HIL-7R-M21	560549	Pharmingen™ BD Biosciences
2	Anti-Human CD183 (CXCR3) APC	1C6	550967	Pharmingen™ BD Biosciences
3	Anti-Human CD196 (CCR6) BUV737	11A9	564377	Horizon™ BD Biosciences
4	Anti-Human CD25 PerCP-Cy5.5	M-A251	560503	Pharmingen™ BD Biosciences
5	Anti-Human HLA-DR BV421	G46-6	562804	Horizon™ BD Biosciences
6	Anti-Human CD4 BV605	RPA-T4	562658	Horizon™ BD Biosciences
7	Anti-Human CD3 PE-Cy7	UCHT1	563423	Pharmingen™ BD Biosciences
8	Anti-Human HLA-DR PE-Cy7	L243(G46-6)	560651	Pharmingen™ BD Biosciences
9	Anti-Human CD16 APC	B73.1	561304	Pharmingen™ BD Biosciences
10	Anti-Human CD15 PerCP-Cy5.5	HI98	560828	Pharmingen™ BD Biosciences
11	Anti-Human CD192 (CCR2) BV421	48607	564067	Horizon™ BD Biosciences
12	Anti-Human CD45 APC-H7	2D1	560178	Pharmingen™ BD Biosciences
13	Anti-Human CD38 PE	HIT2	555460	Pharmingen™ BD Biosciences
14	Anti-Human CD14 FITC	M5E2	555397	Pharmingen™ BD Biosciences
15	Anti-Human CX3CR1 PE	2A9-1	12-6099-42	Affymetrix eBioscience™

10.5. Gating strategy for monocytes

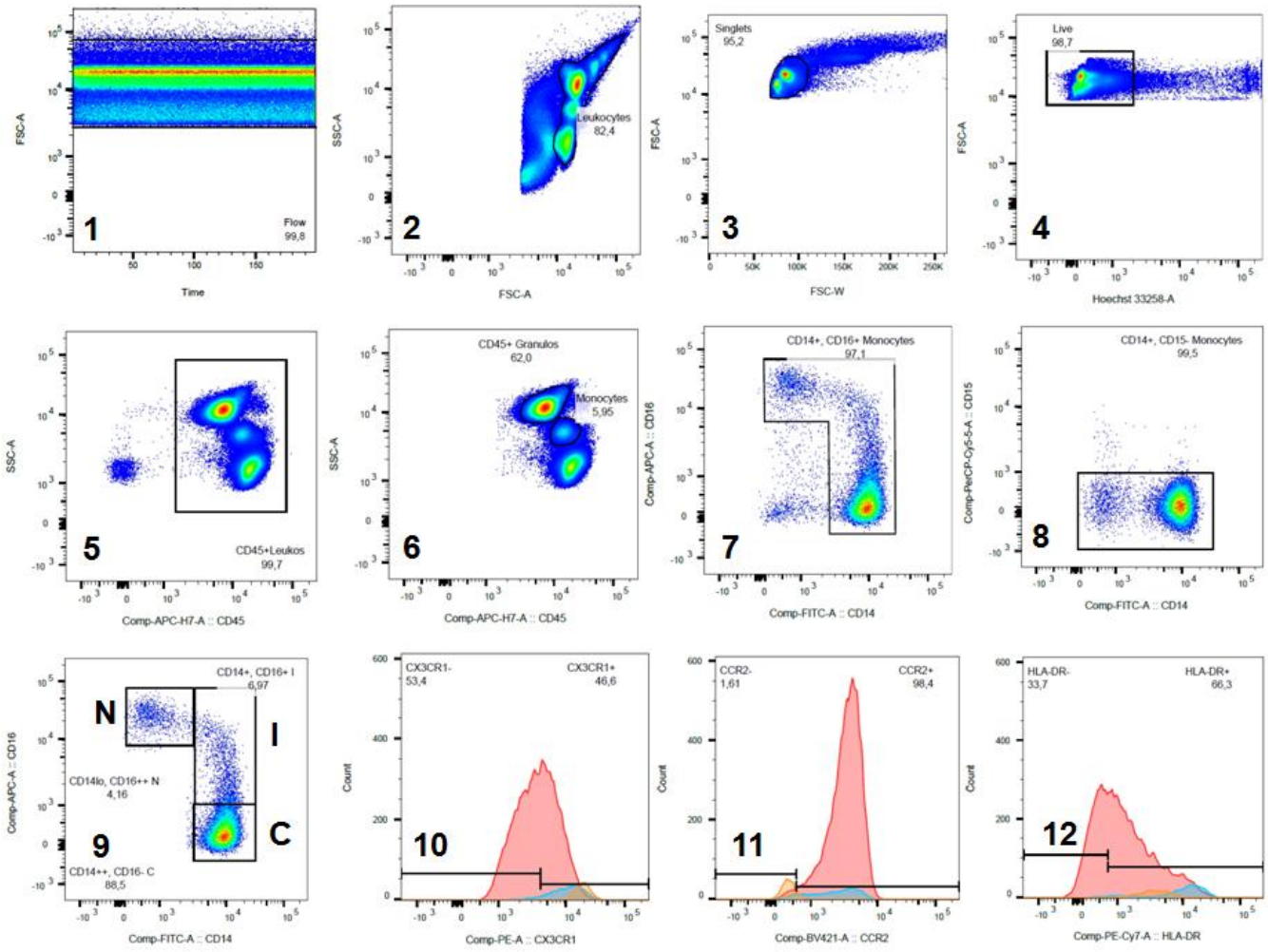

The initial gate was made on the events with consistent flow by bivariate plot of Forward Scatter (FSC) and time **(1)**. Then, these events were shown as FSC and side scatter (SSC) plot and a global gate was used to select leucocytes excluding erythrocytes, platelets and debris **(2)**. Next doublets were excluded based on FSC-A vs FSC-W **(3)**. Subsequently, dead cells were excluded based on their Hoechst 33258 staining **(4)**. Then, a bivariate plot of SSC vs CD45 was used to select the CD45+ leucocytes **(5)**. Further, these events were displayed once again on a bivariate plot of SSC vs CD45 and then, monocytes were selected based on their intermediate SSC and CD45 expression **(6)**. Monocytes were then displayed as CD14 vs CD16 plot and a global gate was placed around CD14+ CD16+ events **(7)**. Further, CD14+CD16+ events were displayed as CD14 vs CD15 plot and CD15+ events were excluded to purify monocytes from left over granulocytes **(8)**. Once again, CD14+CD15- events were displayed as a bivariate plot of CD14 vs CD16 **(9)**. Then, three subsets of monocytes were identified such as classical CD14++CD16- **(C)**, intermediate CD14+CD16+ **(I)** and nonclassical CD14-CD16++ **(N)**. The expression of chemokine receptors CX3CR1 **(10)**, CCR2 **(11)** and HLA-DR **(12)** was determined on all these three subsets by employing respective FMO controls on histogram plots.

10.6. Gating strategy for CD4+ T cell subsets

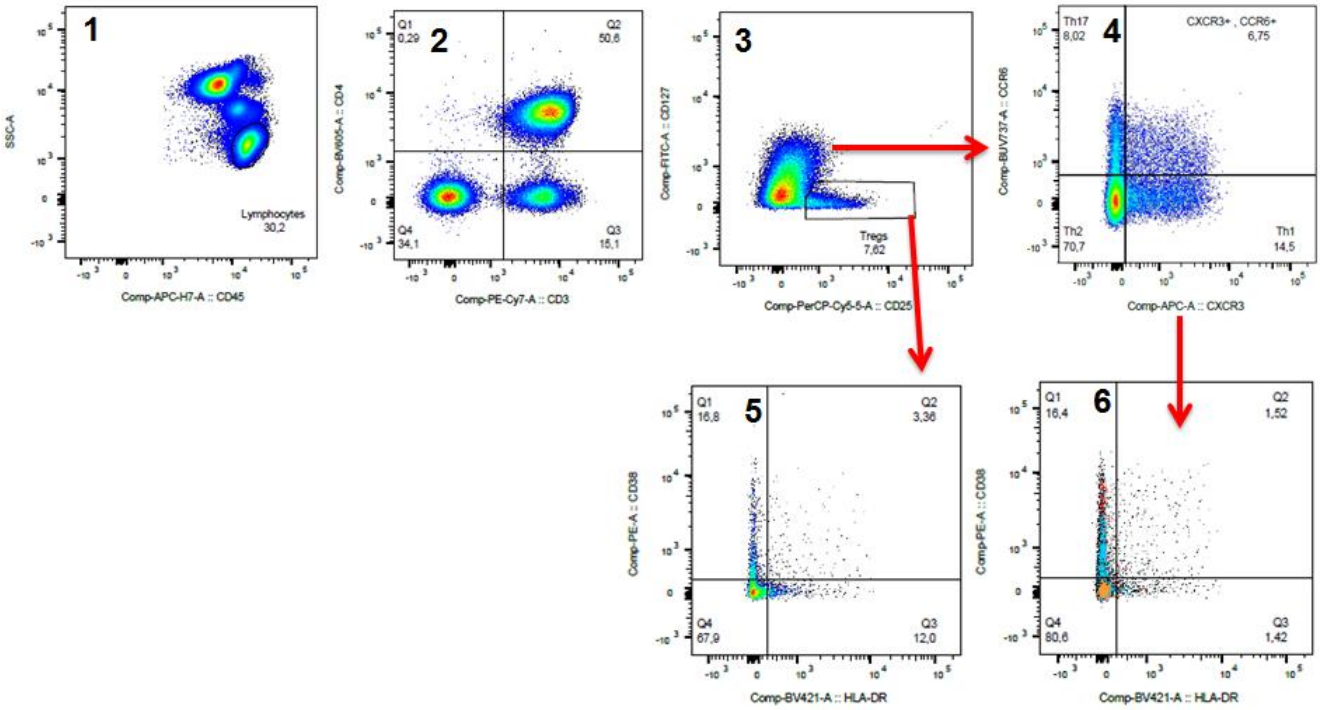

Gating strategy was similar to monocytes until the identification of CD45+ leucocytes. Lymphocytes were selected from these CD45+ events by their low side scatter and high CD45 expression **(1)**. These lymphocytes were then displayed as CD3 vs CD4 plot and a quadrant gate was applied **(2)**. Then, from this quadrant gate CD3+ CD4+ events were selected as CD4+ T cells. CD4+ T cells were then displayed on a CD25 vs CD127 plot and CD25hiCD127lo events were gated as Tregs and this gating strategy was based on CD25 FMO control **(3)**. Then, by applying a NOT gating function, events other than Tregs were selected and were named as Th cells. These Th cells were further displayed on a bivariate plot of CXCR3 vs CCR6 **(4)**. Then, a quadrant gate was used based on FMO controls for CXCR3 and CCR6 to identify CXCR3+ CCR6- cells as Th1, CXCR3- CCR6- cells as Th2 and CXCR3- CCR6+ Th17 cells. Then, HLA-DR+ and CD38+ cells were identified among these subsets such as Tregs **(5)**, Th1, Th2, and Th17 cells **(6)** by using FMO controls and applying a quadrant gate.

List of Publications underlying thesis

Chaudhry, SR., Güresir, E., Vatter, H., Kinfe, TM., Dietrich, D., Lamprecht, A., Muhammad, S. Aneurysmal Subarachnoid Hemorrhage lead to systemic upregulation of IL-23/IL-17 inflammatory axis. Cytokine, 2017, 97: 96 – 103.

Chaudhry, SR., Stoffel-Wagner, B., Kinfe, TM., Güresir, E., Vatter, H., Dietrich, D., Lamprecht, A., Muhammad, S. Elevated systemic IL-6 levels in patients with aneurysmal subarachnoid hemorrhage is an unspecific marker for post-SAH complications. International Journal of Molecular Sciences, 2017, 18: 2580, doi: 10.3390/ijms18122580.

Muhammad, S*., **Chaudhry, SR*.**, Güresir, A., Stoffel-Wagner, B., Fimmers, R., Kinfe, TM., Dietrich, D., Lamprecht, A., Vatter, H., Güresir, E. Systemic HMGB1, a novel predictive biomarker for cerebral vasospasm in Subarachnoid Hemorrhage. Critical Care Medicine (Submitted). *Equally contributed.

Kinfe, TM., Muhammad, S., Link, C., Roeske, S., **Chaudhry, SR.**, Yearwood, TL. Burst Spinal Cord stimulation increases peripheral antineuroinflammatory Interleukin 10 levels in Failed Back Surgery Syndrome patients with predominant back pain. Neuromodulation, 2017, DOI: 10.1111/ner.12586.

Muhammad, S., **Chaudhry, SR**., Yearwood, T., Krauss, J., Kinfe, TM. Changes of metabolic disorders associated peripheral cytokine/adipokine traffic in non-obese chronic back patients responsive to burst spinal cord stimulation. Neuromodulation, 2017, DOI: 10.1111/ner.12708.

Chaudhry, SR., Dietrich, D., Vatter, H., Lamprecht, A., Muhammad, S. A review on the role of danger associated molecular pattern molecules (DAMPs) in aSAH. (In preparation).

Chaudhry, S., Frede, S., Seifert, G., Vatter, H., Dietrich, D., Lamprecht, A., Muhammad, S. Temporal profile of serum mitochondrial DNA (mtDNA) in patients with aneurysmal Subarachnoid Hemorrhage (aSAH). (In preparation).

Curriculum Vitae (CV)

Shafqat Rasul Chaudhry

List of publications

Review: **Chaudhry, SR.**, Muhammad, S., Eidens, M., Klemm, M., Khan, D., Efferth, T., Weisshaar, MP. Pharmacogenetic prediction of individual variability in drug response based on CYP2D6, CYP2C9 and CYP2C19 genetic polymorphisms. Current Drug Metabolism, 2014, 15 (7): 711-718.

Chaudhry, SR., Akram, A., Aslam, N., Asif, M., Wajid, M., Kinfe, TM., Jabeen, Q., Muhammad, S. Antidiabetic and antidyslipidemic effects of *Heliotropium strigosum* in rat models of type I and type II diabetes. Acta Poloniae Pharmaceutica – Drug Research, 2016, 73 (6): 1575 – 1586.

Kinfe, TM., Muhammad, S., Link, C., Roeske, S., **Chaudhry, SR.**, Yearwood, TL. Burst Spinal Cord stimulation increases peripheral antineuroinflammatory Interleukin 10 levels in Failed Back Surgery Syndrome patients with predominant back pain. Neuromodulation, 2017, DOI: 10.1111/ner.12586.

Muhammad, S., Roeske, S., **Chaudhry, SR.**, Kinfe, TM. Burst or high frequency (10 kHz) spinal cord stimulation in failed back surgery syndrome patients with predominant back pain: one year comparative data. Neuromodulation, 2017, DOI:10.1111/ner.12611.

Chaudhry, SR., Akram, A., Aslam, N., Wajid, M., Iqbal, Z., Nazir, I., Jabeen, Q., Muhammad, S. Antidiabetic and antidyslipidemic potential of *Echinops echinatus* Roxb. in rat models of type I and type II diabetes. Pakistan Journal of Pharmaceutical Sciences, 2018 (accepted).

Chaudhry, SR., Güresir, E., Vatter, H., Kinfe, TM., Dietrich, D., Lamprecht, A., Muhammad, S. Aneurysmal Subarachnoid Hemorrhage lead to systemic upregulation of IL-23/IL-17 inflammatory axis. Cytokine, 2017, 97: 96 – 103.

Muhammad, S., **Chaudhry, SR.**, Yearwood, T., Krauss, J., Kinfe, TM. Changes of metabolic disorders associated peripheral cytokine/adipokine traffic in non-obese chronic back patients responsive to burst spinal cord stimulation. Neuromodulation, 2017, DOI: 10.1111/ner.12708.

Muhammad, S*., **Chaudhry, SR*.**, Güresir, A., Stoffel-Wagner, B., Fimmers, R., Kinfe, TM., Dietrich, D., Lamprecht, A., Vatter, H., Güresir, E. Systemic HMGB1, a novel predictive biomarker for cerebral vasospasm in Subarachnoid Hemorrhage. Critical Care Medicine (Submitted). *Equally contributed.

Chaudhry, SR., Stoffel-Wagner, B., Kinfe, TM., Güresir, E., Vatter, H., Dietrich, D., Lamprecht, A., Muhammad, S. Elevated systemic IL-6 levels in patients with aneurysmal subarachnoid hemorrhage is an unspecific marker for post-SAH complications. International Journal of Molecular Sciences, 2017, 18: 2580, doi: 10.3390/ijms18122580.

Boström, A., Scheele, D., Roeske, S., Stoffel-Wagner, B., Hoenig, F., Muhammad, S., **Chaudhry, SR.**, Hurlemann, R., Krauss, J., Kinfe, TM. Inter-ictal saliva oxytocin and interleukin IL-1β signaling in therapy-resistant migraine patients responsive to adjunctive cervical non-invasive vagus nerve stimulation: The MOXY feasibility study. Neuromodulation (submitted).

Chaudhry, SR., Dietrich, D., Vatter, H., Lamprecht, A., Muhammad, S. A review on the role of danger associated molecular pattern molecules (DAMPs) in aSAH. (In preparation).

Chaudhry, S., Frede, S., Seifert, G., Vatter, H., Dietrich, D., Lamprecht, A., Muhammad, S. Temporal profile of serum mitochondrial DNA (mtDNA) in patients with aneurysmal Subarachnoid Hemorrhage (aSAH). (In preparation)

Posters

Shafqat Rasul Chaudhry, Stilla Frede, Gerald Seifert, Rolf Fimmers, Dirk Dietrich, Alf Lamprecht, Erdem Güresir, Hartmut Vatter and Sajjad Muhammad. Temporal profile of mitochondrial DNA (mtDNA) in the serum of patients with aneurysmal Subarachnoid Hemorrhage (aSAH). 5th Venusberg meeting on Neuroinflammation, Bonn, Germany, 2017.

Shafqat Rasul Chaudhry, Erdem Güresir, Dirk Dietrich, Alf Lamprecht, Hartmut Vatter and Sajjad Muhammad. Aneurysmal Subarachnoid Hemorrhage leads to elevated systemic levels of proinflammatory cytokine IL-23. 68th Annual Meeting of the German Society of Neurosurgery; 7th Joint Meeting with the Society of British Neurological Surgeons, Magdeburg, Germany, 2017.

Sajjad Muhammad, **Shafqat Rasul Chaudhry**, Jasmin Scorzin, Birgit Stoffel Wagner, Rolf Fimmers, Hartmut Vatter, Erdem Güresir. Danger Signal Molecule HMGB1 is differentially regulated in patients with Aneurysmal Subarachnoid Hemorrhage developing Cerebral Vasospasm. 7th Int. Symposium on DAMPS and HMGB1, Bonn, Germany, 2015.

Maria Weisshaar, Eslam Shehata, Shadi Amin, Stephan Irsen, Julio Reinecke, Peter Wehling and **Shafqat Rasul Chaudhry**. Comparison of the traditional ultracentrifugation techniques and PEG precipitation for isolating exosomes from ACS (autologous conditioned serum): a kinetic study. 4th Int. Meeting of ISEV, Washington, USA, 2015.

Conferences:

5th Venusberg Meeting on "Neuroinflammation". Privileged or not: basic, translational and clinical aspects of immune activation in the brain. Bonn, 11 – 13 May, 2017.

4th Venusberg Meeting on "Neuroinflammation": Privileged or not: basic, translational and clinical aspects of immune activation in the brain. Bonn, 7– 9 May, 2015.

Declaration

I hereby declare that the work presented in the current thesis is my own work except where explicitly stated otherwise in the text or in the bibliography. The current thesis has not been submitted as a whole or in a part for obtaining the doctoral degree to any other university except the University of Bonn.

Bonn, 08.01.2018
Shafqat Rasul Chaudhry